FLUORESCENCE AS A PROBE TO STUDY SELF-ORGANIZATION IN METHACRYLATE POLYMERS AND THE DESIGN OF NOVEL HIERARCHICAL ARCHITECTURES

THESIS SUBMITTED TO THE

UNIVERSITY OF PUNE

FOR THE DEGREE OF
DOCTOR OF PHILOSOPHY

IN CHEMISTRY

BY

KAUSHLENDRA KUMAR

RESEARCH SUPERVISOR
DR. S. K. ASHA

POLYMER SCIENCE AND ENGINEERING DIVISION
CSIR-NATIONAL CHEMICAL LABORATORY
PUNE-411008
INDIA

OCTOBER 2013

……………………………...DEDICATED TO

To my Parents, Grandmother and Wife

DECLARATION

I hereby declare that the research work embodied in the thesis entitled "**FLUORESCENCE AS A PROBE TO STUDY SELF-ORGANIZATION IN METHACRYLATE POLYMERS AND THE DESIGN OF NOVEL HIERARCHICAL ARCHITECTURES**" has been carried out by me at Polymer Science and Engineering Division of CSIR-National Chemical Laboratory, Pune under the supervision of Dr. S. K. Asha. I also affirm that this work is original and has not been submitted in part or full, for any other degree or diploma to this or any other University or Institution.

Date: Kaushlendra Kumar

Dr. S. K. Asha
Scientist

CERTIFICATE

This is to certify that the work embodied in the thesis entitled **"FLUORESCENCE AS A PROBE TO STUDY SELF-ORGANIZATION IN METHACRYLATE POLYMERS AND THE DESIGN OF NOVEL HIERARCHICAL ARCHITECTURES"** has been carried out by **Mr. Kaushlendra Kumar** under my supervision at Polymer Science and Engineering Division of CSIR-National Chemical Laboratory, Pune and the same has not been submitted elsewhere for any other degree.

Dr. S. K. Asha

(Research Supervisor)

ACKNOWLEDGEMENT

I also want to thank my college teachers who have encouraged me to do well in life. Dr. P. P. Sinha, Dr. D. A. Harrison, and Dr. Nisheeth Rastogi always deserve a special mention in my life.

I would also take this opportunity to show my sincere thanks to those who have immensely helped me at some point of time during my research. S. Menon Sir, D. Doble Mam, Ms. Poorvi, Mr. Saroj have helped me in GPC characterization. Ketan (SEM analysis), Naren, Anuj, Pandiaraj, Shravani, Pankaj (TEM analysis) and Ms. Pooja (AFM) are also acknowledged.

I also want to thank all members of PSE division and D-wing PAML for giving me all the good times.

It is always tough to walk alone. Any journey of life becomes difficult, when we do not have the support of friends and well-wishers. I wish to thanks my present and former labmates and friends both from NCL and IISER. When I joined the lab, Dr. Deepak V.D. and Rekha Narayan were already a part of that and they welcomed me with arms open and provided me full support. On the way, it was joined by Dr. Jancy, Dr. Amrutha, Dr. Anil, Dr. Jinish, Mahima, Ghanashyam, Nagesh, Chinmay, Shekhar, Balamurugan, Nisha, Senthil, Saibal, Prajitha, Swapnil, Sandeep, Jeena, Harpreet, Smita, Pramod, Ananthraj, Bapu, Narsimha, Rajendra, Bhagyashree, Anuj, Vivek and Uma and the journey kept on becoming smoother and smoother with no hassles.

My stay at GJ hostel has made the life more relaxing after hectic lab chores. The extra co curricular activities in the hostel premises have always helped to bridge the gap between regional disparities and share leisure time with friends with full throttle. I thank Dayanand, Majid and Manish (my roommates and friends of different times) for being with them and sharing the good times at hostel. I will like to convey my heartfelt thanks to Anand, Jitendra, Ajit, Umesh, Krunal, Sanjay, Adheesh, Raviraj with whom I had all the fun on dining table and roaming across the Pune. Ajit and Priyanka (Ajit's wife) helped and supported me at most crucial time. I also like to thank all the members of my cricket team DD specially Mishraji, Krunal, Sanjay, Varun, Mandeep, Somesh, Shakeel, Nishant and all others who have given me most memorable times away from research. I will not forget my TT matches with many players such as Dr. Kannan, Dr. Umesh, Dr. Ambarish, Dr. Anurag, Ramireddy and others. I wish to thank them for all the fun we had on the TT board.

My special mention goes to few more friends namely Tutu bhaiya, Gaurav (my best friend), Tukaram, Vijay Thorat, Malviyaji, Tamas, Subhadeep, Dr. Gobinda (Prof.) for giving me the best times of my life at some point of time. Tutu bhaiya and Gaurav require a special mention for making me believe in, what I am today.

The ride of life becomes more smooth and easy going when we have the blessings of all of them who matters the most in life. I am lucky to have very supportive family members, who have provided me all the best facilities at all time. I owe my sincere and heartfelt gratitude to my Grand Mother, parents and my wife. I dedicate my thesis to all of them for their constant encouragement.

Kaushlendra

CONTENTS

Chapter-4. Microstructural Reorganization and Cargo Release from Dye Encapsulated Pyrene Urethane Methacrylate Copolymer Hollow Capsules.   **121-149**

Chapter 5: H-bonding vs Non-H bonding in 100% Pyrene Labeled Methacrylate Comb Polymers: TRES and Temperature Dependent Fluorescence.   **150-180**

Abbreviations and Symbols

$\chi 2$	Chi-square
τ	Decay time
Đ	Polydispersity index
α	Pre-exponential factor
Q	Quantum yield
T_g	Glass transition temperature
AFM	Atomic force microscopy
ATRP	Atom transfer radical polymerization
bipy	Bipyridyl
BPO	Benzoyl peroxide
Cu(I)Br	Copper(I) bromide
$CDCl_3$	Deuterated chloroform
DAPI	4'-6-Diamidino-2-phenylindole
DBTDL	Dibutyltin dilaurate
DCM	Dichloromethane
DLS	Dynamic light scattering
DMAP	Dimethyl amino pyridine
DMF	N,N-Dimethyl formamide
DSC	Differential scanning calorimetry
EDCl	1-Ethyl-3-(3-dimethylaminopropyl)carbodiimide hydrochloride
FAB-MS	Fast atom bombardment-mass spectrometry
FET	Field effect transistors

FTIR	Fourier transform infrared
GPC	Gel permeation chromatography
HCl	Hydrochloric acid
HEMA	2-Hydroxyethyl methacrylate
hr	hour
HMDI	Hexamethylene diisocyanate
HPLC	High performance liquid chromatography
HR-TEM	High resolution transmission electron microscopy
HPC-Py	Pyrene labeled hydroxypropyl cellulose polymers
IEMA	2-Isocyanatoethyl methacrylate
IPDI	Isophorone Diisocyanate
KBr	Potassium bromide
KJ	Kilo Joule
L	Litre
LCST	Lower critical solution temperature
LED	Light emitting diode
MALDI-TOF	Matrix-assisted laser desorption ionization-time of flight
M_n	Number average molecular weight
M_w	Weight average molecular weight
mg	Milligram
mL	Millilitre
mol	Mole
mmol	Millimole
NMR	Nuclear magnetic resonance

ns-TRES	Nanosecond Time-resolved emission spectra
PAAMePy	Pyrene labeled Poly(acrylic acid)
PDMA	Poly(N,N-dimethylacrylamide)
PDP	3-Pentadecyl phenol
PEGMA	Poly(ethylene glycol) methacrylate
PMDETA	N,N,N′,N′,N″-Pentamethyldiethylenetriamine
PMMA	Polymethyl methacrylate
PNIPAM	Poly(N-isopropyl acrylamide)
PS	Polystyrene
Py	Pyrene
RB	Round bottom
RFP	Red Fluorescent Protein
RhB	Rhodamine B
SEM	Scanning electron microscopy
SiN	Silicon Nitride
TCSPC	Time-correlated single photon counting
TEM	Transmission electron microscopy
TGA	Thermal gravimetric analysis
THF	Tetrahydrofuran
TMS	Tetramethylsilane
TRES	Time-resolved emission spectra

PREFACE

Understanding the process of self-assembly in polymeric systems has been one of the toughest challenges for the researchers across the globe. The spontaneous formation of well-defined architecture via non-covalent interactions has been used by nature to assemble the large functional biomolecules such as DNA, proteins etc. Due to the multi dimensional applications in the areas of biology, chemistry, or physics, the process of self-assembly have helped in bridging the gap among the various disciplines of science. Our group has been working on a unique polymer design with side-chain urethane methacrylate polymers with bulky pendant units. The different morphology depending on the solvents from which it was drop casted has immensely helped in understanding the structure-property relationship of these systems. Introduction of pyrene as a bulky pendant unit helped to understand the self-assembly by photophysical studies. The excimer formation in the polymers at very low concentrations by intra chain interactions have shown the potential in 100% pyrene loaded systems to be photophysically rich as compared to traditionally studied pyrene labeled polymers.

The aim of the present work is to study the self assembling behaviour of various pyrene labeled polymers having different architecture like block, and random copolymers, where the pyrene labeling was varied from 1-100%. The photophysical properties were studied using various fluorescence techniques like steady-state and life time decay analysis as well as time resolved emission spectra (TRES). The applicative aspect of the pyrene labeled polymers was shown by rhodamine dye encapsulation and release studies as a function of temperature and its temperature triggered release was also used as a handle to understand the microstructural changes inside the polymer microcapsule.

Thus, the thesis analyses the following important aspects:

1. Exploration of fundamental aspects of the self assembly of different pyrene labeled polymers like block, random or homopolymers by the detailed photophysical analyses

2. Applicative aspects of the pyrene labeled polymers: probed by rhodamine B encapsulation and release.

3. Self assembly behavior in H-bonded versus non-H-bonded polymers at very dilute concentrations: differences and similarities.

4. Architectural differences among the polymers: probed by TRES and temperature dependent fluorescence.

The thesis is divided into 6 chapters. Chapter 1 deals with the literature survey and introduction of pyrene photophysics. It also discusses the basics of different techniques which were used to study the photophysical studies of the polymers. Finally, few specific examples where pyrene photophysics has helped in understanding the systems, were also discussed.

Chapter 2 deals with the effect of polymer architecture upon self-assembly. Four well-defined hierarchical architectures having pyrene-labeled side-chain urethane methacrylate polymers were synthesized. The two homopolymers with short 'ethyleneoxy' and long 'polyethyleneoxy' segment and random and block copolymer of short chain polymer with polystyrene were synthesized. The polymerization techniques adopted in this work are free radical polymerization for homo and random copolymers and atom transfer radical polymerization (ATRP) for block. The self-assembly of these polymer architectures were explored by steady state emission studies and the pyrene excimer formation have brought out the structural differences and similarities in these polymers.

Out of the various architectures studied in chapter 2, random copolymer architecture with varying amount of pyrene was preferred to study the self-organization in chapter 3. The second unit in the random system was carefully selected so that the self-assembly did not get disrupted and hence 3-pentadecyl phenol (PDP) was chosen as the other suitable comonomer. A series of random copolyurethane methacrylate comb polymers with 1-100% pyrene loading were prepared by free radical polymerization. The SEM and TEM studies showed that all the polymers had a tendency to form spheres in DMF and THF and pores in $CHCl_3$ irrespective of the varying pyrene incorporation. The excimer emission of these copolymers were studied as a function of both time and temperature using time resolved emission spectra (TRES) experiments and variable temperature steady-state fluorescence and lifetime measurements. The nature of emitting species was extensively explored by the time- resolved emission spectra (TRES) studies conducted at room temperature as well as higher temperature. The presence of ground state aggregates were unequivocally proven by lifetime and TRES studies.

Chapter 4 shows the applicative aspects of these random copolymers by rhodamine encapsulation and release studies. A new approach to bridge the gap between solid and solution phase morphology was developed by dialyzing the THF solution of dye and polymer against water. The rhodamine B (RhB) was chosen for encapsulation studies and the structural changes happening to the comb polymer as a function of temperature was probed by changes in FRET induced RhB emission. It was shown that, on heating the capsules beyond 50 ^{o}C, the dye released completely and the polymer underwent irreversible microstructural organization.

Chapter 5 addresses a very fundamentally challenging task by photophysical investigations. The importance of hydrogen bonding interactions provided by the urethane linkage in directing the self assembly of pendant pyrenes were compared to analogous 100 % pyrene polymer lacking the hydrogen bonding interaction. A series of 100 % pyrene labeled polymers differing from one another in terms of presence or absence of hydrogen bondable units, or the length as well as nature (linear vs kink) of the spacer segment linking the pendant pyrene units from the methacrylate backbone was developed. The photophysical properties were analyzed as regards to the nature of excimer emission –static vs dynamic excimer, to obtain information regarding the chain organization in each of the polymers. The variable temperature (heating & cooling) emission studies significantly showed the difference in the chain interactions of H-bonded vs non-H-bonded polymers.

Finally, chapter 6 highlights the overall outcome of the thesis.

Chapter 1:

Introduction and Literature Survey

1.1. Introduction

The spontaneous formation of well-defined architectures via non-covalent interactions through a process called self-assembly has been an interesting area of research for researchers worldwide. The concept of self-assembly for the synthesis of supramolecules from small molecules has been mimicked from nature, as nature has used it for millions of years to assemble large functional biological molecules such as DNA, proteins etc. Self-assembled polymeric structures find increasing application in a wide range of areas from biology to materials; for example, in drug delivery and optoelectronics.[1-5] For the effective utilization of these self-assembled polymeric materials, it is very crucial to control the forces of self-assembly into generating well-defined architectures. Well-defined organization of donors and acceptors is a requirement for the device efficiency in photovoltaic and optoelectronic applications. Self assembling tools like non-covalent interactions are incorporated into the structural design of materials so that the self organized material may function effectively as the electron /hole transport layers or as the main donor or acceptor active layers.[6-10] The various non-covalent interactions involved in directing the well-defined organizations are H-bonding, π-π interactions, electrostatic forces, Vander waal's forces etc.[11-15] Various instrumentation techniques are used to obtain the information of polymer self-organization like the nuclear magnetic resonance (NMR) spectroscopy,[16, 17] Light Scattering techniques (such as static and dynamic),[18, 19] microscopic techniques such as scanning electron microscopy (SEM),[20] transmission electron microscopy[21, 22] (TEM) and atomic force microscopy (AFM),[23, 24] and photophysical techniques such as absorbance and fluorescence spectroscopy.[25-29] Compared to techniques like NMR spectroscopy, fluorescence spectroscopy allows studies to be carried out under much more dilute conditions. Fluorescence can be used at concentrations as low as 10^{-7} M also where essentially only intramolecular interactions predominate.[29] Among the various fluorophores, the unique properties of pyrene like its strong excimer formation, long fluorescence lifetime values for monomer as well as excimers, large Stoke's shift and molar extinction coefficient, high fluorescence quantum yield, the vibrational fine structures of the fluorescence emission spectra that shows strong solvent polarity dependence etc. makes it an interesting choice to study the interactions among molecules as well as polymer chains.[29-36] The excimer formation kinetics of pyrene has been studied since 1960s. Birks studied the solution kinetics of isolated pyrene

molecules for the first time in 1963.[30] Since then, pyrene has been used to study different kind of architectures. It has been applied to label chain ends of alkyl chains, where the excimer formation has provided the knowledge of ring closure.[37] This concept was further extended to study the cyclization of polymeric chains by putting the pyrene at the chain ends of the low polydisperse polymers and these studies have provided information regarding the effect of molecular weight on the cyclization constant.[38] Significant progress has been made in understanding the photophysical properties of various simple as well as complex molecules, such as small molecules and macromolecules labeled with pyrene at specified positions and complex polymers randomly labeled with pyrenes.[37, 39, 40] Traditionally, pyrene has been used to study EEC (End-to-End cyclization) experiments.[38, 39, 41, 42] The chain dynamics of the polymers have also been studied by pyrene photophysics. Nowadays focus has shifted towards the studies of more complex architectures such as dendrimers, lipids, peptides or amino acids labeled with pyrenes etc.[43-51] Few of the specific examples of pyrene labeled polymers will be discussed in detail in the subsequent sections. A major breakthrough in the investigation of chain dynamics of the polymers randomly labeled with pyrene came with the extensive application of various photophysical techniques such as steady-state emission studies, fluorescence decay studies and time resolved emission spectra (TRES).[38-40, 52-58] Time Resolved Emission Spectra (TRES) studies provide significant information regarding the origin of emitting species as a function of time.[56-58] The three-dimensional time-intensity-wavelength contour plot constructed by collecting fluorescence decays at different wavelengths and the 2D emission spectra that can be constructed from this data can give insight regarding the nature of emitting species, their origin and decay profile etc., which can subsequently give an overall picture of the polymer chains.[30, 32, 56, 59] These photophysical investigations have contributed significantly towards bringing about a better understanding of the structure-property relationship among the various architectures.

1.2. Pyrene as a fluorescent probe

Pyrene has been one of the most studied fluorophores because of its numerous unique photophysical properties. The excimer formation tendency of pyrene and its derivatives has been widely used for probing the self assembling properties of macromolecules or polymeric systems.[29] The Figure-1.1 illustrates the excimer formation process via aggregation between an excited and ground state pyrene (i.e. dynamic process), or direct

excitation of ground state aggregates of the same chromophores (i.e. static process). The static excimer formation is more commonly observed in aqueous media where hydrophobic and pi-stacking interactions between the fluorophores are prevalent even at low concentrations or in organic solvents where the macromolecules contain the pyrene moieties in constrained environment.[29] The presence of ground state aggregates could be readily detected by absorption spectrum: **a)** decrease in molar extinction of the fluorophore, **b)** broadening of the absorption bands and **c)** small red-shift in the peaks. It could also be traced by comparing the excitation spectra collected for the monomer vs excimer emission bands.[29, 60]
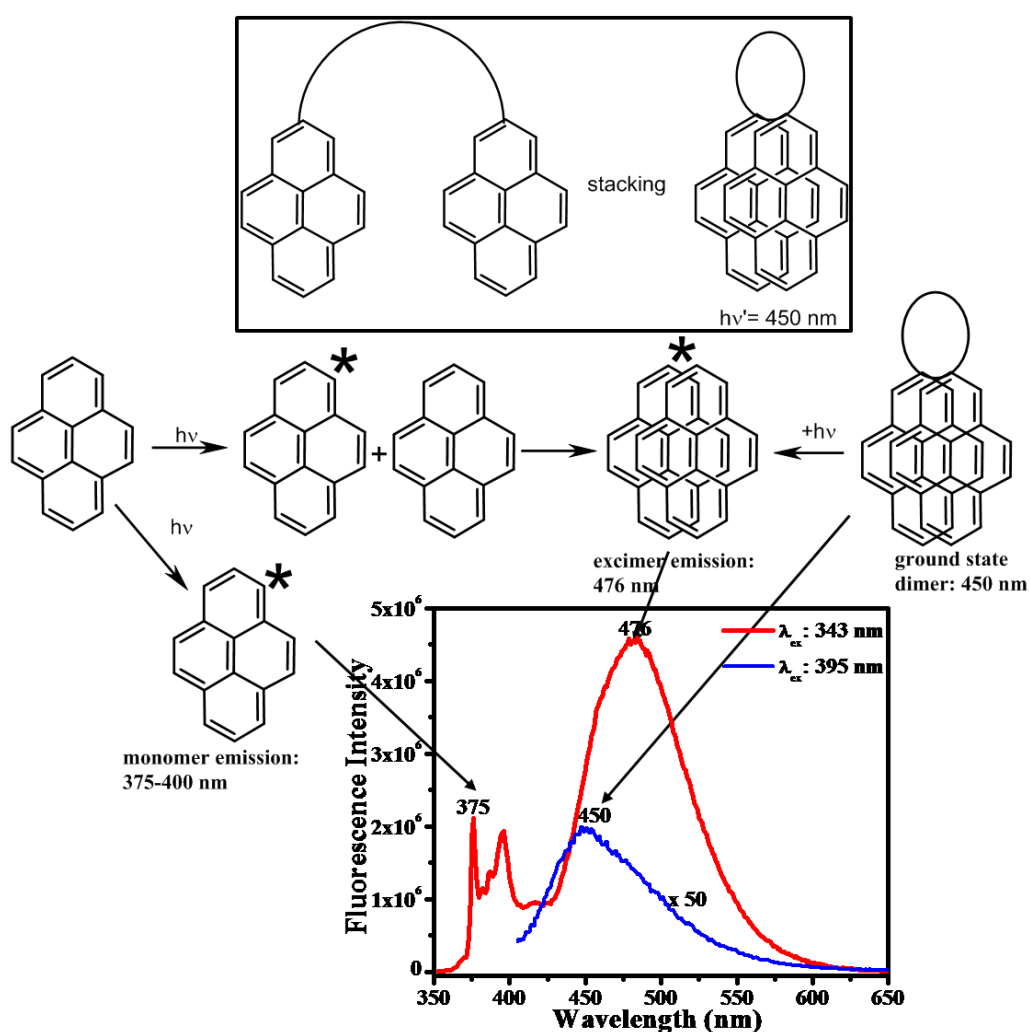
Figure-1.1: Mechanism of excimer formation: Dynamic vs Static.

Apart from its excimer formation tendency, the most noticeable property of pyrene is its large molar extinction coefficient and large quantum yield, which enables the easy detection of pyrene even at very low concentrations.[30, 31] The

unique properties of pyrene which make it an interesting and most studied fluorophore are summarized in the Figure-1.2.
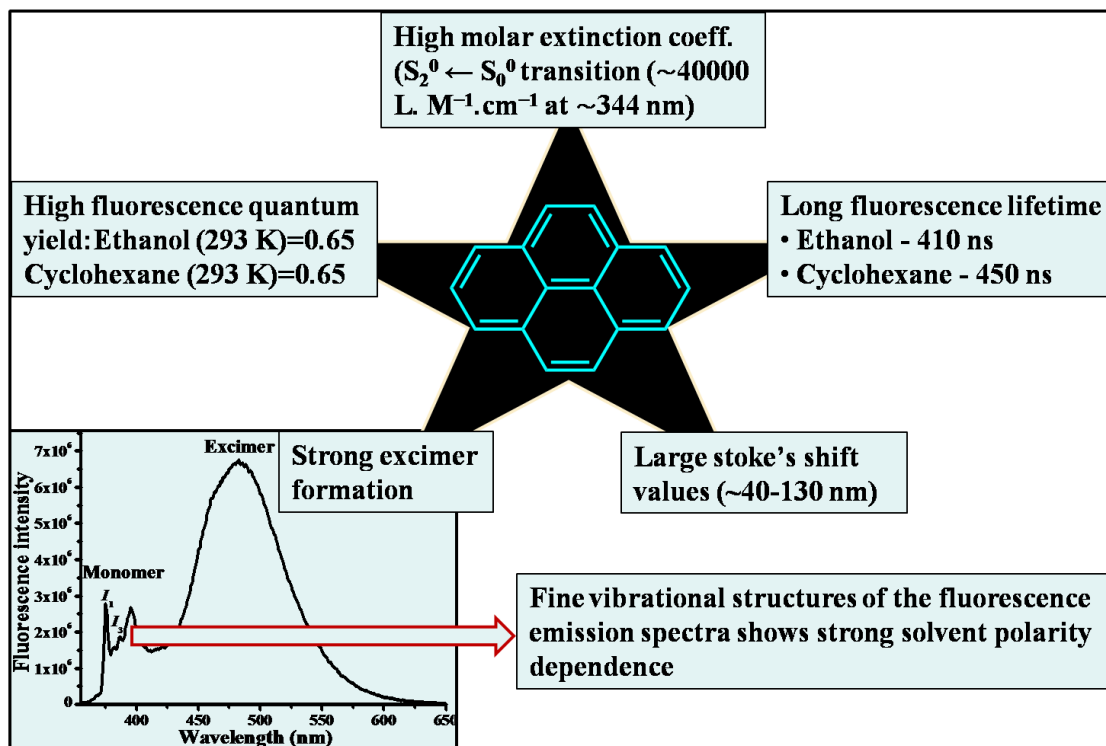
Figure-1.2: Some of the unique properties of pyrene.

1.2.1. I_E/I_M and I_1/I_3 ratio

A ground state pyrene can be excited by irradiation with UV light (~340 nm). The absorbance spectrum of a pyrene molecule exhibits several bands. The S1 ←S0 transition is symmetry forbidden and it displays very weak band.[35, 36, 61] The pyrene is excited at the S2 ←S0 transition peak using an excitation wavelength between 335-350 nm depending on the different pyrene derivatives as well as the solvent used. Figure-1.3 shows the normalized absorbance and fluorescence emission spectra of a typical pyrene labeled polymer for 0.1 OD in DMF. From the figure, it is evident that the pyrene monomer fluorescence showed sharp peaks in the 370-425 nm range, and the pyrene excimer fluorescence is displayed by broad structureless emission centred around 460-490 nm region. The quantitative information regarding the excimer formation could be obtained from the ratio of the intensity of the excimer (I_E) to that of the monomer (I_M) in the emission spectrum (I_E/I_M ratio). The monomer (I_M) intensity can be obtained by

integrating the fluorescence spectra in the first monomer peak between 372-378 nm and the excimer (I_E) intensity can be obtained by integrating the region 500-530 nm.[62] The complete monomer and excimer region are not integrated to avoid the overlap between the monomer and excimer peak intensities. Another significant information that can be obtained from the steady state spectrum is regarding the polarity of the medium. The I_1/I_3 ratio, which is obtained by the intensity ratio between the first (I_1) and the third (I_3) vibronic bands of the monomeric emission, is dependent on the dielectric constant of the solvent and thus can provide information regarding the microenvironment of the polymer.[29, 35, 63, 64] However, a direct comparison of the I_1/I_3 ratio with the solvent is rather difficult as the interaction of the solvents may disturb the symmetry of pyrene fluorophore.[60, 65] The I_1/I_3 ratio varies between 0.6 to 1.8 for the most hydrophobic environment to most hydrophilic environment around pyrene.
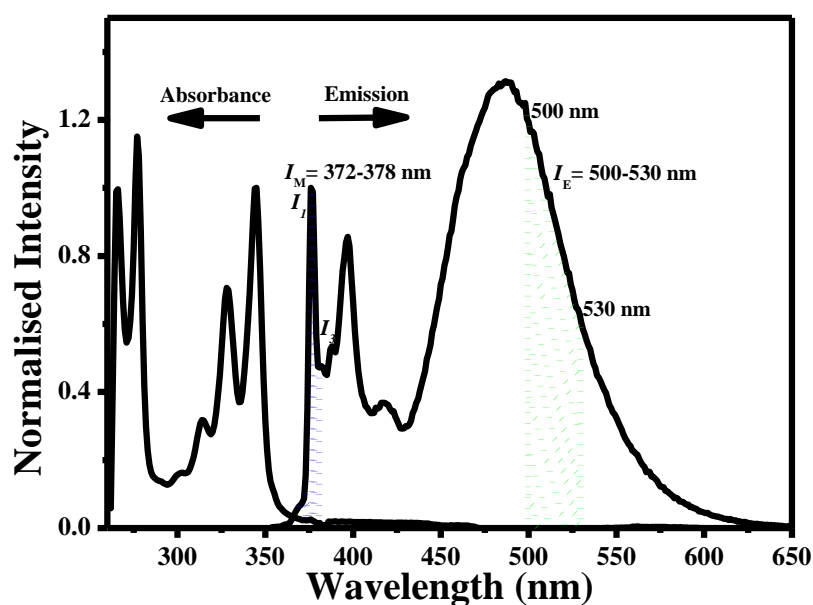
Figure-1.3: The normalized absorbance and fluorescence emission spectra of a typical pyrene labeled urethane methacrylate polymer having 0.1 OD in DMF.

1.2.2. The fluorescence decay

The fluorescence decay studies of the pyrene labeled polymers provide important information about the dynamics of the polymers. The rate constant of excimer formation can be determined by carefully analyzing the fluorescence decay of the monomer species.[30, 38] The rate of excimer formation in polymer randomly labeled with pyrene is time dependent; as the distance between the pyrene pairs is increased, the excimer formation slows down. Another important aspect that could be extracted from

the excimer decay curves is the presence or absence of rise time. Figure-1.4 compares the typical decay curves of a pyrene labeled polymer collected at the monomer (375 nm) and excimer (500 nm) emission wavelength. The excimer formation through diffusion encounters is characterized by the presence of rise curve as the excimer formation is delayed relative to initial excitation. The excimers formed by the direct excitation of ground stated aggregated species do not show the rise curve since they are instantaneously formed.
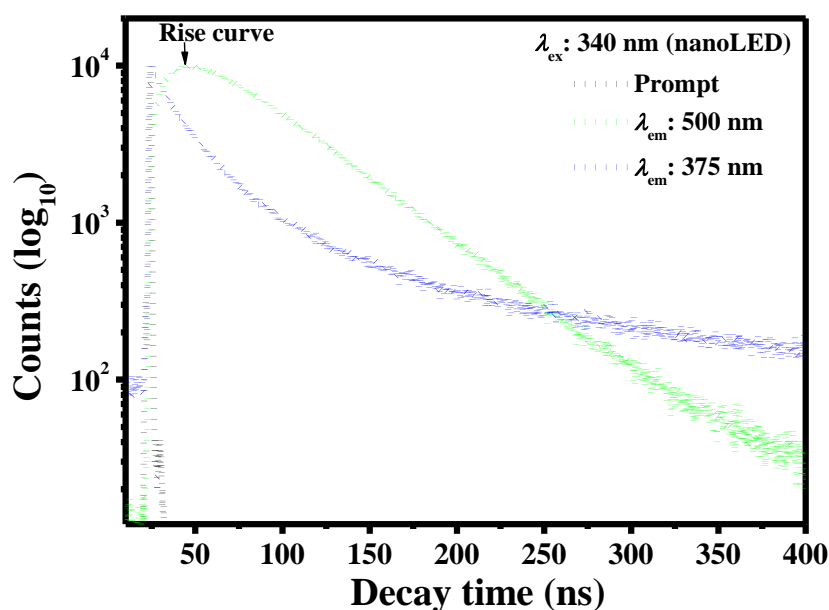
Figure-1.4: The monomer (375 nm) and excimer (500 nm) fluorescence decays of pyrene labeled polymer obtained by exciting at 340 nm.

1.3. Spectroscopic techniques used

1.3.1. Steady State Fluorescence

Fluorescence is one of the most sensitive techniques. It is sensitive enough to detect even a single molecule in some cases. The fluorescent species whose emission spectrum exhibits well defined vibronic bands such as polyaromatic hydrocarbons can be identified via fluorescence. The emission and excitation spectra are recorded using a spectrofluorometer and the light source is generally high pressure xenon arc lamp with constant photon flow.

1.3.1.1. Emission Spectra

The emission spectrum is the characteristic of a given compound and it reflects the distribution of the probability of the various transitions from the lowest vibrational level

of the excited state S_1 to the various vibrational levels of the ground state S_0. The energy distribution of the emitted photons could be expressed as steady state fluorescence intensity per absorbed photon and it could be represented as a function of the wavelength of the emitted photons. The fluorescence intensity is proportional to the concentration for low absorbances but it reduces when the concentration of the fluorophores is high due to the inner filter effect. The quantum yield calculation is always done for the very dilute solutions having optical density (OD) < 0.1.

1.3.1.2. Excitation Spectra

The excitation spectrum is defined by the variation in fluorescence intensity as a function of excitation wavelength for a fixed emission wavelength. The excitation spectrum is identical to the absorbance spectrum in shape, if there is a single species in the ground state. If there are more species or the species in different form, the excitation spectra and absorbance are not superimposable. Thus the comparison of absorption and excitation spectra provides significant information regarding the ground state species whether they are present in isolated form or aggregated form or some other conformation etc.

1.3.1.3. Stoke's shift

It provides information on the excited states and is defined by the gap between the maximum of the first absorption band and the maximum of the emission spectrum. The polarity of the fluorescent probes could be estimated by this. If the fluorescent molecule possess high dipole moment in the excited state than in the ground state, the stoke's shift increases with the solvent polarity.

1.3.2. Fluorescence lifetime

The fluorescence lifetime is one of the most crucial and peculiar characteristic of a fluorescent molecule because it provides information of dynamic nature of species and also the duration of the interaction of the fluorophore with its surroundings. Moreover, the lifetime of a fluorophore signifies for how long it has remained in the excited state and how much distance and volume it covered before decaying. During this period the fluorophore undergoes conformational changes and it is also subjected to various possible interactions with the environment. In short, the fluorescence lifetime depends on concentration, which makes it sensitive to trace the various emitting species on the

basis of the variations in the lifetime. Information regarding aggregation could be obtained by the reduction in the lifetime. The energy transfer processes taking place via collisional quenching, FRET etc. could be studied extensively with the analysis of the lifetime of the species.[32, 66]

The fluorescence lifetime (τ) of a fluorophore can be used to probe the microenvironment and illustrated by its dependence on the rates of competing decay pathways i.e. radiative rate constant (k_r) and the radiationless rate constant (k_{nr}).

$$\tau = \frac{1}{k_r + k_{nr}}$$

An excited fluorophore can return to the ground state through several interactions such as fluorophore-fluorophore interaction, fluorophore-solvent interaction etc. If the only way of returning to the ground state is through radiative process, the lifetime is called radiative lifetime (in preference to natural lifetime) and denoted by τ_r.[66] The Strickler-Berg relation predicts the radiative lifetime theoretically from the absorption and fluorescence spectra.[67] When the contribution of radiationless processes increases as compared to radiative processes, the fluorescence quantum yield (Q), the ratio of radiative rate constant to the sum of all rate constants) decreases.[66]

$$Q = \frac{k_r}{k_r + k_{nr}}$$

The fluorescence lifetime is greatly affected by the presence of molecular oxygen, as it quenches the fluorescence through collisional process via diffusional encounters with the fluorophore. The effect of quenching on the lifetime and quantum yield depends on the nature of the fluorophore and the medium. The flurophores in high viscous media is least affected by the oxygen quenching. The oxygen quenching affects mostly the fluorophores of long lifetimes such as pyrene, naphthalene and it could be avoided by the proper purging with nitrogen or argon. The most effective way to remove dissolved oxygen is through freeze-thaw process.[66]

1.3.3. Time-resolved emission spectra (TRES)

The excited state kinetics and heterogeneity of the emissive species among the macromolecules is ambiguous due to its complex architecture. The more appropriate information regarding the kinetics and the contribution of emissive species could be

traced by wavelength dependence of fluorescence decays. Figure-1.5 shows the wavelength dependent lifetime and the reconstructed TRES plot.
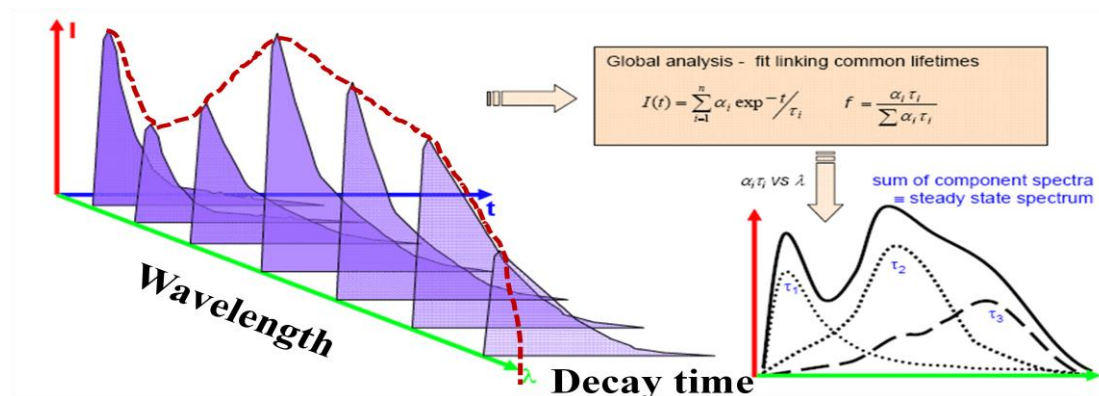
Figure-1.5: Schematic representation of wavelength dependent lifetime and the reconstructed TRES. *Adapted from reference 68.*

The time-resolved emission spectra (TRES), plotted as intensity vs wavelength $I(\lambda, t)$ is constructed using the following equation.[56, 69]

$$I(\lambda, t) = I_{ss}(\lambda) \left(\sum_j \alpha_j(\lambda) \, e^{-t/\tau_j(\lambda)} \Big/ \sum_j \alpha_j(\lambda) \, \tau_j(\lambda) \right)$$

where $I_{ss}(\lambda)$ is the steady state fluorescence intensity, $\alpha_j(\lambda)$ is the amplitude pre-exponential factor and $\tau_j(\lambda)$ is the decay times. The number of emitting species in a system could be traced by the presence of an iso-emissive point in the reconstructed time resolved emission spectrum.[56, 58] An iso-emissive point in the emission spectrum is analogous to the isosbestic point in the absorption spectroscopy and it is defined by the wavelength at which the intensity does not vary with time.[58] The presence of one iso-emissive point in the spectrum indicates the two emitting species in the system. In general, the number of emitting species is given by n+1, where n is the number of iso-emissive points in the system. Along with the presence of iso-emissive point, another significant information could be obtained by the amplitude values for a decay constant. The negative amplitude for a decay constant at a wavelength (long emission wavelength) provides an additional support of the kinetically coupledness of the emissive species.[56, 58]
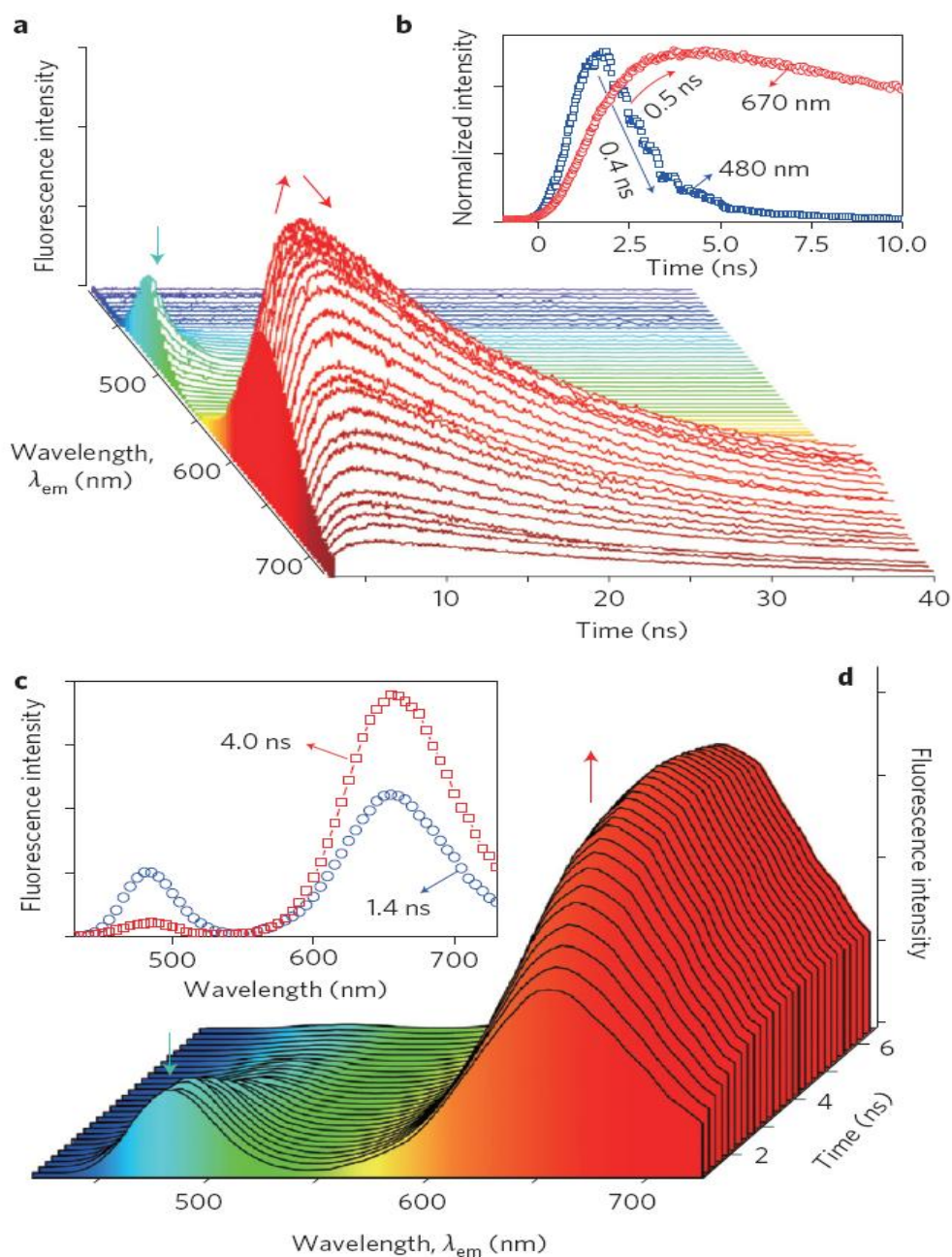
Figure-1.6: Time-resolved fluorescence spectra of donor-loaded polymerized vesicles in aqueous solution. **a)** Fluorescence decay curves in the emission wavelength (λ_{em}) range of 420 nm to 720 nm in 5 nm steps for donor-loaded polymerized vesicles in aqueous solution at pH 10.4. **b)** Fluorescence decay curves of donor-loaded polymerized vesicles at emission wavelengths of 480 nm and 670 nm. **c)** Time-resolved emission spectra of donor-loaded polymerized vesicles at 1.4 ns (blue circles) and 4.0 ns (red squares) in aqueous solution at pH 10.4. **d)** Time-resolved emission spectra of donor-loaded polymerized vesicles in aqueous solution at pH 10.4 for the time range 1.2 ns to 6.4 ns in 0.2 ns steps. *Adapted from reference 70.*

Figure-1.6 shows the wavelength dependent lifetime spectrum of the pyrene-perylene donor-acceptor system where the Forster resonance energy transfer (FRET) occurs at pH 10.4 and the regenerated time resolved emission spectra (TRES) in the time range of 1.2 ns to 6.4 ns. Figure-1.6 (**a, b**) shows the wavelength dependent lifetime studies in the wavelength range 420 to 720 nm and at specific wavelength of 480 and 670 nm respectively for pyrene loaded perylene vesicles where as the TRES are given in the figure-1.6 (**c, d**) in the time range of 1.2 to 6.4 ns with an interval of 0.2 ns. This example highlights the significance of wavelength dependent lifetime studies for studying the time evolution of the FRET occuring between donor and acceptor species. The regenerated TRES provides information regarding the nature of emitting species in the donor-acceptor system.

1.4. Specific Examples: Fluorescently labeled Polymers

The significance of the statement regarding the usefulness of pyrene as a hydrophobic probe *"by far the most frequently used dye in fluorescence studies of labeled polymers"* made by Winnik[29] nearly two decades ago still holds true. The excimer formation process between an excited pyrene and ground state pyrene has provided innumerable insight into the dynamical and structural features of macromolecules as well as self-assembling behaviour of the molecules. The seminal work by the pioneers in the area of photophysics has exploited pyrene's unique photophysical properties for understanding the microstructure and dynamics of polymer chains. Due to the uniqueness of the photophysical properties, pyrene as the fluorescent probe has attained the worth of gold standard. Table-1.1 displays the brief history of pyrene and its use for understanding various processes.

The excimer formation tendency of pyrene has often been used to understand the various processes involved with polymers such as end-to-end cyclization of polymers,[38, 39, 41] polymer chain dynamics,[40, 80] polymer coil-to-globule transitions,[19, 81] association between polymers and surfactants[78, 82, 83] etc. which have been extensively investigated using pyrene photophysics. Figure-1.7 shows the schematic representation of pyrene-labeled species such as end-labeled polymers, vinyl polymers, associative polymers, dendrimers, lipids etc. which have been extensively investigated for its self-assembling behaviour by fluorescence.[84] Some of the specific examples of pyrene-labeled polymers are discussed here.

Table-1.1: History of pyrene and its exploration as a probe.

Sl. No.	Year	Contributor (Scientist)	Progress	Reference
1	1837	Laurent, A.	Discovery of pyrene	71
2	1954	Forster, T. and Kasper, K.	Intermolecular excimer formation in solution	72
3	1963	Birks, J. B.	Pyrene Excimer formation through diffusion (reversible).	73
4	1976	Zachariasse, A.	Intramolecular excimer formation (EEC in short-chain, end-labeled molecules)	37
5	1977	Cuniberti, C. and Perico, A.	EEC in monodisperse polymers	41
6	1977	Kalyanasundaram and Thomas	Sensitivity towards solvent environment (I_3/I_1)	35
7	1980	Winnik, M. A.	Importance of time-resolved measurements to probe internal dynamics of polymers	38
8	1980	Winnik, M. A.	Quantitative characterization of internal dynamics	38
9	1987	Winnik, F. M.	Photophysics of randomly labeled polymer	74
10	1993	Duhamel, J. et al.	Polymer chain dynamics: Blob Model	75
10	1998	Lee, S. et al.	hydrophobic interaction: Sequential Model (SM)	76
11	1999	Mathew, H. et al.	Chain dynamics of randomly labeled polymers: Fluorescence Blob Model	77

			(FBM)	
12	2004	Siu, H. et al.	Interaction between HMPs and surfactants	78
13	2011	Chen, S et al.	EEC revisited by FBM	79
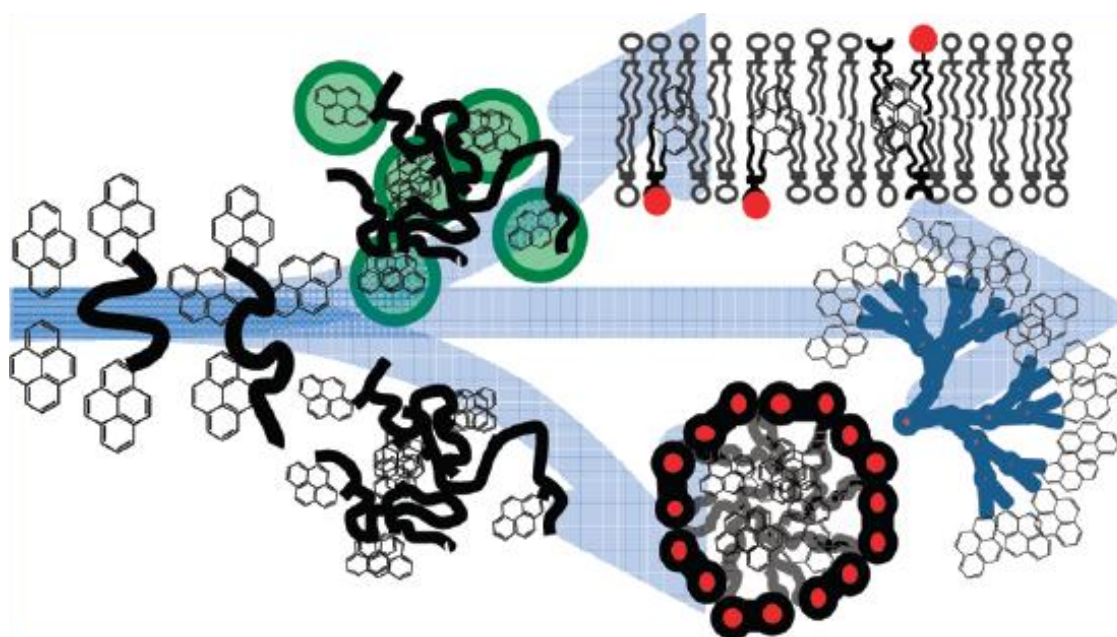
Figure-1.7: Schematic representation of various pyrene-labeled macromolecules studied so far. Adapted from *reference 84.*

1.4.1. Pyrene End-labeled Polymers: End-to-End Cyclization (EEC)

Cyclization of polymer chains has been of significant interest to the polymer community. The properties of polymers such as nylon and silicone rubbers are affected by cyclization. Pyrene labeled DNA to probe cyclization is the most widely studied biopolymer. There are 3 important parameters that must be met for studies on the cyclization dynamics of the polymers.[84] 1) suitable functionality at the chain ends for pyrene-labeling, 2) The monodispersity of polymer chains since the cyclization rate constant (k_{cyc}) depends on polymer chain length and 3) relatively short polymer chains are required to accurately monitor the cyclization rate.

The study of cyclization of polymers can be done by observing the changes in the spectroscopic properties of the system when the end-substituents (or fluorophores) of the polymer chains show some close proximity. Making use of this approach, Sisido's group in Japan have labeled the poly(N-methyl)glycine chain ends with a dinitrobenzoate at one end and a dimethylanilino derivative at the other end and the cyclization was studied by donor-acceptor complex formation between the end groups.[85] The pyrene end-labeled macromolecules have been extensively investigated for evaluating the cyclization rates to gather information regarding chain dynamics. The early studies were focussed on the short chain alkanes labeled with pyrene at the ends. Zachariasse, in 1976 studied a series of molecules having the structure 1-pyrene-$(CH_2)_n$-1-pyrene varying the values of n between 1 and 32.[37] The most significant outcome of his constant strive over several years was the observation that the extent of excimer formation depends on the conformational and the dynamic properties of the alkyl chains with strong inhibition of intramolecular excimer formation for n= 5 to 8.[37, 86, 87] The intramolecular excimer formation in end-labeled alkyl chains through steady state fluorescence was extensively studied and provided the information on the ring closure by way of excimer formation. The end-to-end cyclization (EEC) in the polymers has also been studied by making use of intramolecular excimer formation process.

In 1974, Willemski and Fixman studied the end-to-end cyclization of monodisperse polymers theoretically and gave the idea that the cyclization can be described by a single rate constant k_{cy}.[88, 89] In 1977, Cuniberti and Perico was the first to recognize the value of pyrene excimer formation to study the end-to-end cyclization dynamics of polymers and as a consequence, prepared a series of pyrene end-labeled poly(ethyleneoxide) polymers.[41] The end-to-end cyclization was studied by steady state emission and a correlation was developed as a consequence of chain length with excimer formation which elaborated that as the chain length increased, the EEC decreased between the pyrene end groups as they were separated by a longer chain. However, the most significant work on the EEC studies has come through the seminal work of Winnik through a series of research papers over the years.[36, 38, 39] In 1980, Winnik studied the cyclization dynamics of polymers by time-resolved fluorescence.[38] Figure-1.8 shows: **A)** the chemical structure of polystyrene end-labeled with pyrene whose number average molecular weight (M_n) varied from 3900 to 27000, and **B)** schematic representation of the kinetic scheme followed for the determination of

cyclization rate constant. A series of pyrene-labeled monodisperse polystyrenes were synthesized by anionic polymerization and cyclization rate constant has been obtained through time resolved fluorescence. He could also quantitatively characterize the internal dynamics of the macromolecules through the study of pyrene excimer formation. From these studies he was able to demonstrate that k_{cy} depended strongly on the polymer chain length and scaled as $N^{-\gamma}$ where N was the number of monomer units and γ was the scaling factor dependent on solvent–polymer interaction. γ has been found to be -1.62 for PS-Py$_2$ in cyclohexane at 34.5 $^{\circ}$C.
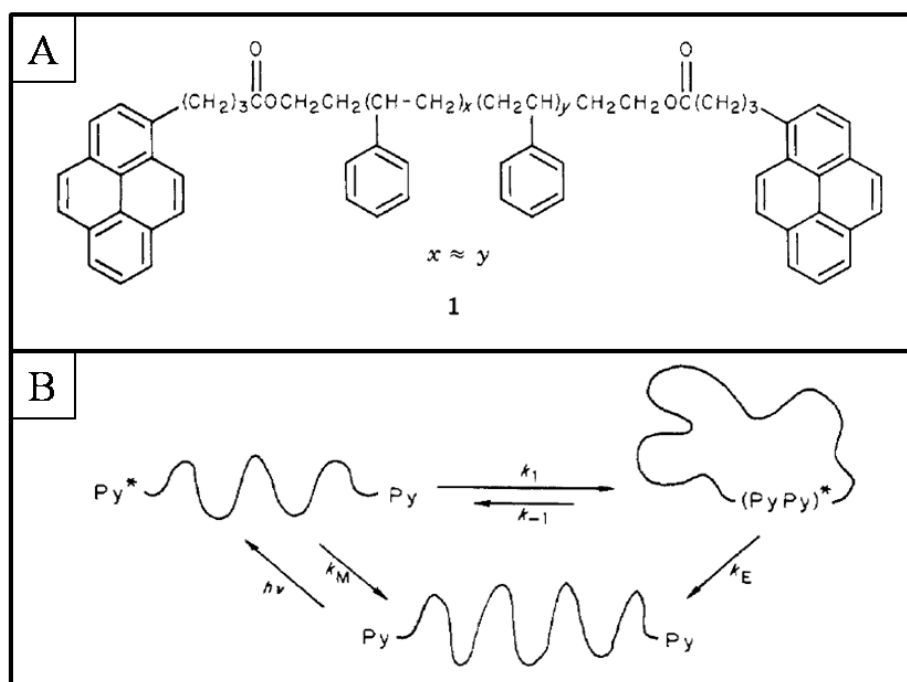
Figure-1.8: **A)** The chemical structure of the pyrene-labeled polystyrene and **B)** The kinetic scheme followed for determination of cyclization rate constant. *Adapted from reference 38.*

Some of the other polymer backbones that have been investigated for cyclization dynamics include poly(N-isopropylacrylamides),[90-92] poly(dimethylsiloxane),[93-95] poly(tetrahydrofuran),[96] poly(ε-caprolactone),[97] poly(ethyleneoxide),[98-100] polycarbonates[101, 102] etc. The cyclization studies have also been carried out for polymers where the pyrene is attached at fixed and specified positions of the polymeric chains apart from the chain ends.[103] Recently, Duhamel's group has relooked pyrene end-labeled polymers such as polyethyleneoxide (PEO)

having different M_n values.[104] In this report, they have studied pyrene-labeled PEO with M_n values between 2 to 16.5 kDa and the effect of chain length and polymer concentration on the kinetics and the level of pyrene association by time-resolved fluorescence.

The labeling of the broad spectrum of the polymers at the chain ends are difficult to functionalize and furthermore, it is rather difficult to obtain the quantitative information of the internal dynamics of the polymers if the polymers were labeled with more than two pyrenes and these labels were not separated by a fixed distance. Another limitation of this end to end cyclization was the polymer chain length; beyond a certain chain length, the increase in the chain length decreased the excimer formation manifold as a consequence of which the internal dynamics could not be studied. Such limitations have to be overcome to study the internal dynamics of the polymer chains by labeling at specific positions which are close to each other.

1.4.2. Pyrene labeled Random Copolymers

Designing of new polymers for improved performance requires an extensive and detailed understanding of structure-property relationship. Here few pyrene labeled random copolymers from the literature will be described in detail to understand their properties on the basis of pyrene photophysics.

1.4.2.1. Hydrophobically modified Polymers

Hydrophobically modified polymers are an important class of industrial polymers. They are used as viscosity and rheology modifiers in water soluble paints and in fluids for coating applications, as flocculating agents in water treatment and as surface active agents in personal care products.[105-108] These are also used as frictional drag reducing agents in turbulent flow, improved oil recovery (IOR) in oil industry etc.[108] Partially hydrolysed polyacrylamide (HPAM) and biopolymers such as xanthan gum are used commercially in the oil industry.[109] The associative thickeners which have influenced the paint industry are hydrophobically-modified cellulose derivatives such as hydroxyethylcellulose (HMHEC), telechelic hydrophobically-modified ethoxylated urethane (HEUR), and alkali-swellable emulsion (HASE) polymers.[105] These modified polymers are almost similar to water soluble polymers except few hydrophobic groups incorporated into its backbone which significantly change the polymer properties even with less than 1 mol% incorporation. Figure-1.9 shows the effect of concentration on

the HMPs and the formation of network structure. The sphere-shaped micelles formed by the hydrophobes constitute the cross-link points in the network, two neighbouring micelles being connected by the hydrophilic part of one thickener molecule. These aggregates or networks can be disrupted by application of shear and are reversible in nature i.e. when the shear is removed the disrupted network reforms again. At higher shear rate rearrangement in the network formation occurs and the intermolecular associations among the polymer chains which were holding the hydrophobic molecules rearrange as a consequence of shear thinning and the intramolecular associations holds the network structure.

c: Concentration of polymer
CMC: Critical micelle concentration
C*: Critical aggregation concentration
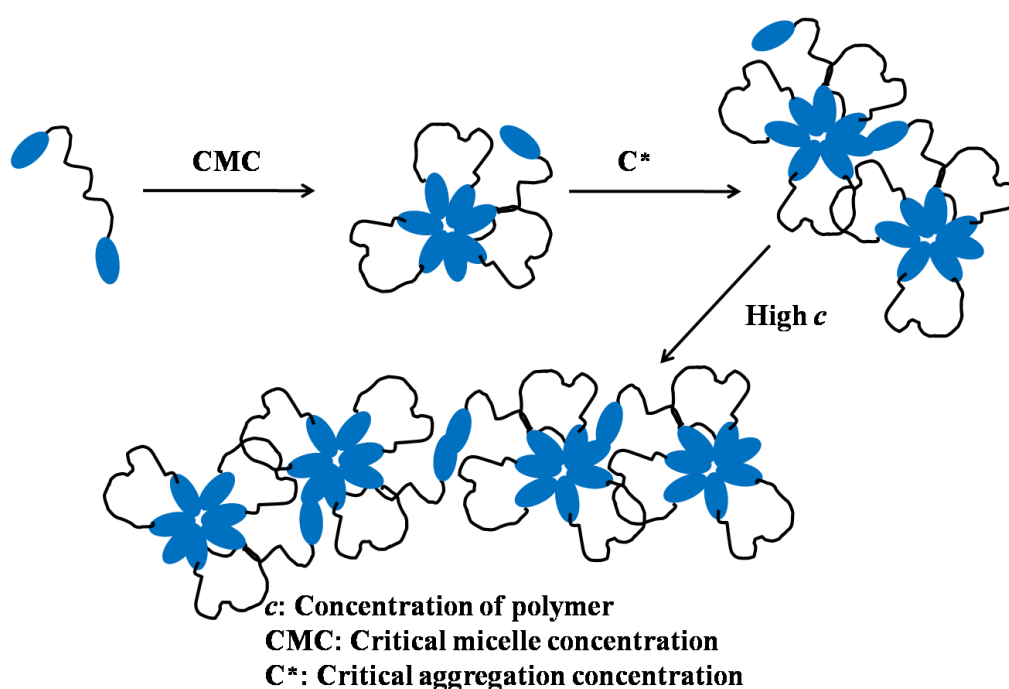
Figure-1.9: Effect of concentration on the HMPs. *Adapted from reference 110.*

These water soluble polymers are modified by covalently attaching hydrophobic dyes such as pyrene. The presence of two or more hydrophobic functionalities facilitates network formation by micellization.[110] By monitoring the photophysics of pyrene fluorophore, the self-aggregating behaviour of such complex structures can be easily understood. Some of the initial studies by fluorescence on the hydrophobically modified cellulose ethers such as (hydroxypropyl)cellulose and (hydroxyethyl)cellulose labeled by a fluorophore were conducted by Winnik's group.[111-113] In one of the initial reports, the interpolymeric association in water in fluorescently labeled (hydroxypropyl)cellulose was studied by non-radiative energy transfer between chromophores attached to different polymer chains. These two

polymers were the pyrene and fluorene-labeled (hydroxypropyl)cellulose.[113] The structure of the polymers is given in the figure-1.10. The pyrene-labeled polymer contained on an average 0.5 pyrene per chain and the fluorene-labeled polymer contained on an average 3 fluorene groups per chain.
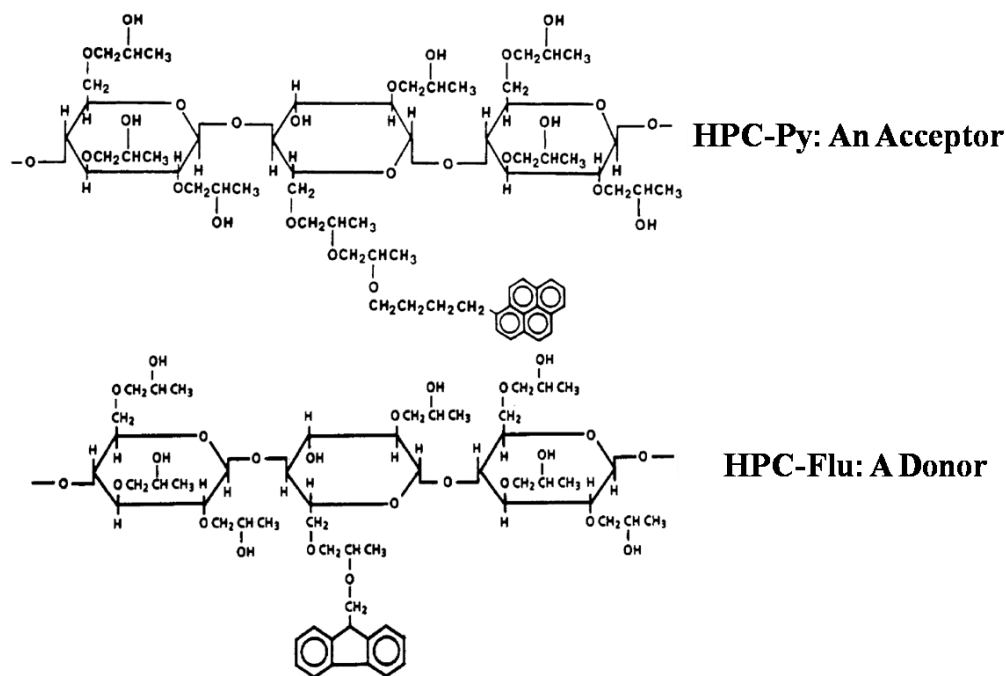
Figure-1.10: Chemical structure of pyrene and fluorene- labeled (hydroxypropyl)cellulose HPC-Py and HPC-Flu. *Adapted from reference 113.*

The energy transfer between the pyrene-fluorene donor-acceptor pair was made use of to study the interactions. The energy transfer between the donor, fluorene-labeled polymer and the acceptor, pyrene labeled polymer took place in the aqueous solution for total polymer concentration as low as 0.02 g L^{-1}. In methanol, no energy transfer occurred. Figure-1.11 shows the emission spectra of HPC-Py and HPC-Flu and the mixture of two polymers at the same concentration in water. It was observed that the pyrene emission was enhanced in the presence of HPC-Flu. The strong interpolymeric mutual attraction between the chromophores in water, resulted in the formation of interchain aggregates at very low concentrations, where as in good solvents like methanol and dioxane, no such interaction occurred. Thus, the non-radiative energy transfer between pyrene and fluorene labeled (hydroxypropyl)cellulose helped in understanding the interpolymeric association in water at very low concentrations.
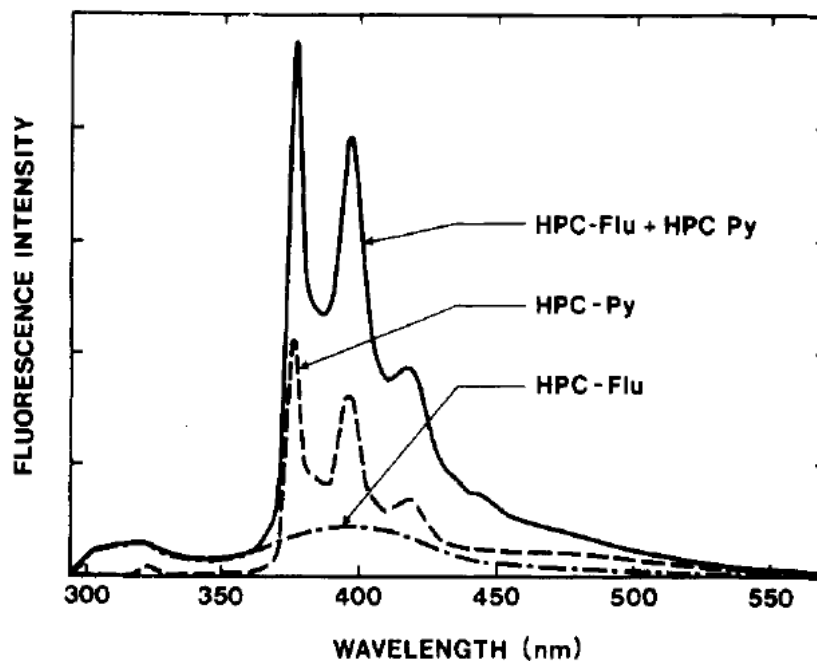
Figure-1.11: Fluorescence spectra of aqueous solutions of fluorene-labeled (hydroxypropyl)cellulose (HPC-Flu/33, 0.05 g L^{-1}), pyrene-labeled ((hydroxypropyl)cellulose (HPC-Py/33, 0.15 g L^{-1}) and a mixture of the two polymers [HPC-Flu/33, (0.05 g L^{-1}) and HPC-Py/33, (0.15 g L^{-1})]; λ_{exc}: 290 nm. *Adapted from reference 113.*
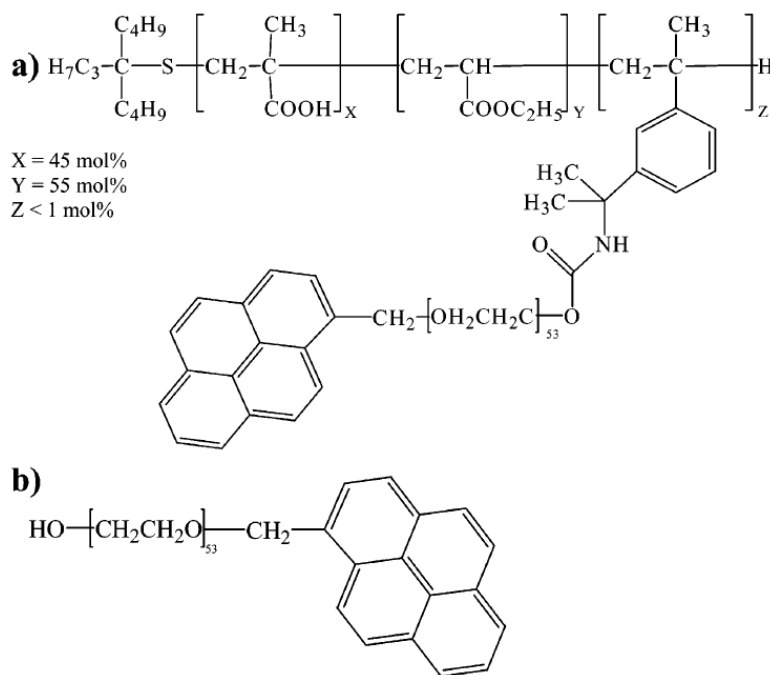
Figure-1.12: Chemical structure of (a) Py-HASE and (b) Py-PEO surfactant. *Adapted from reference 114.*

Another recent example to study the association behaviour using fluorescence was the pyrene-labeled hydrophobically modified alkali swellable emulsion copolymer (Py-HASEs) (Figure-1.12), whose interaction with sodium dodecyl sulphate was studied.[114] The aggregation of Py-HASEs resulting in the high pyrene concentration in aqueous solutions facilitated excimer formation on a rapid time scale, which was extensively studied by time-resolved fluorescence. The macroscopic viscoelastic behaviour of such systems could be easily understood by these studies. This example thus highlights the use of fluorescence techniques to support the enhancement in viscosity of the associative polymer solution upon addition of the surfactant.

1.4.2.2. Pyrene labeling to understand Coil-to-globule Transition

The lower critical solution temperature (LCST) behaviour of thermosensitive polymers such as poly(N-isopropylacrylamide) PNIPAM was made use of to study the coil-to-globule transition by labeling the polymer with suitable dye and following the emission behaviour as a function of stimuli response. PNIPAM displays a coil-to-globule conformational transition beyond a certain temperature called LCST.[115] These conformational transitions in a polymer chain depend on the properties of solvent as well as the polymer and are a consequence of interplay between various intermolecular and intramolecular interactions. Such polymers play a major role in drug delivery, peptide separation, surface modification, tissue engineering etc.[116] External stimuli such as pH, temperature etc. plays a major role on these studies.[117] Smart polymer interface materials such as PNIPAM have attracted a lot of attention due to the excellent control over surface properties in response to external stimuli as a mimic to important biological behaviour.

Coil-to-globule transitions have been studied through various techniques such a calorimetry,[118] light scattering,[119, 120] NMR,[121] IR spectroscopy,[121] intrinsic viscosity measurement[122] etc. But these techniques are not sensitive enough to study the polymer chains of low molecular weight at very low concentrations. Fluorescence has been used to study the conformational changes in the solution. It is useful in monitoring the changes in chain mobility even for very dilute solutions where intramolecular effects could be explored. Making use of the pyrene photophysics, literature reports the coil-to-globule conformational transitions for many pyrene-labeled polymers such as poly(N-

isopropylacrylamide),[123, 124] poly(sulphamethoxinemethacrylamide),[125] poly(dimethylacrylamide),[19, 126] polystyrene,[81] poly(N-vinylcaprolactam),[127] Poly(ε-caprolactone),[128] poly(ethyleneoxide),[129] etc. One of the earlier examples of the coil-to-globule transition by fluorescence was studied by Liu et al. for polystyrene chains labeled with phenanthrene and anthracene.[130] Polymer globules were formed by mixing the labeled polymer with unlabeled polystyrene matrix in benzene and rapid freezing of the solution followed by sublimation. The changes in the energy transfer from phenanthrene (donor) to anthracene (acceptor) on heating above the T_g was monitored by emission studies. Winnik was one of the pioneer investigator to study coil-to-globule transition using pyrene.[124] Pyrene-labeled poly(N-isopropylacrylamides) (PNIPAM/Py) was investigated below and above the LCST by fluorescence in methanol as well as aqueous solutions. In methanol, the fluorescence spectra exhibited the spectrum of typical random-coil polymers, where as in aqueous solutions, strong excimer emission attributed to ground-state pyrene aggregates was observed. On heating the polymer solutions above their LCST, the disruption of pyrene aggregates took place as evidenced by an increase of pyrene monomer emission at the expense of excimer emission.
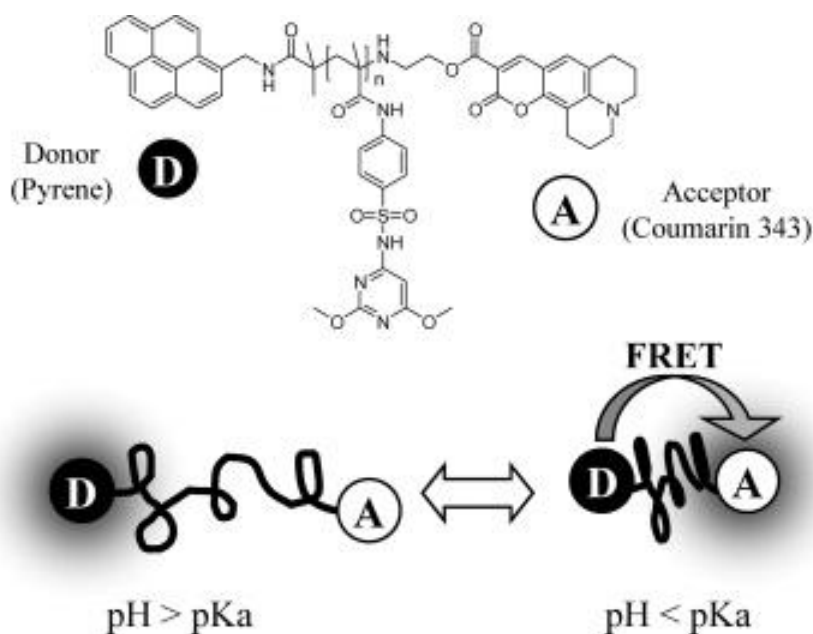
Figure-1.13: Chemical structure of P-PSDM-C and the schematic representation of the mechanism of FRET under change of pH. *Adapted from reference 125.*

Figure-1.13 shows an example where the pH induced coil-to-globule transition explored on the basis of FRET between the pyrene (donor) and coumarin (acceptor) attached at the ends of polysulfadimethoxine mathacrylamide.[125] When the transition occured as a function of pH change, the distance between the donor and acceptor changed influencing the FRET efficiency.

1.4.3. Pyrene labeling in Biological systems

Fluorescence has proved to be a vital technique in understanding the self-assembly behaviour of biological molecules. The fundamental problem related to many biological phenomena such as chain folding of proteins, nature of biomembranes involving lipids and carbohydrates, assembling of polypeptides, polynucleic acids, packing of DNA molecules, enzymatic activity as well as phenomena like the collapse of gel-network, complexation between two polymer chains etc. could be studied.[34, 80, 131-136] Here, one such example from the biological system will be discussed where the pyrene photophysics has helped in understanding the presence of TERRA RNA (telomeric repeat–containing RNA) in living cells of mammalian body. A light-switching pyrene probe was designed and used to investigate the G-quadruplexes formation by its fluorescence from monomer to excimer emission.[137] Figure-1.14 (A and B) shows the schematic representation of excimer formation to probe the G-quadruplex structure and fluorescence spectra for pyrene-modified oligonucleotide probes. The pyrene molecules exhibit monomeric blue emission (400 nm), but when G-quadruplexes are formed, pyrene excimer formation occurs as a consequence of which green light (∼480 nm) is emitted after photoexcitation.
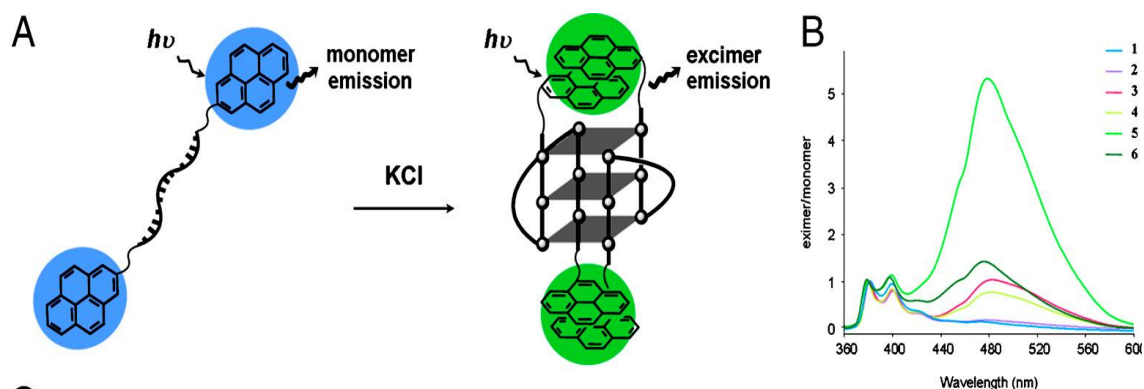
Figure-1.14: (A) The pyrene excimer formation to probe G-quadruplex structure. (B) Fluorescence spectra for pyrene-modified oligonucleotide probes. *Adapted from reference 137.*
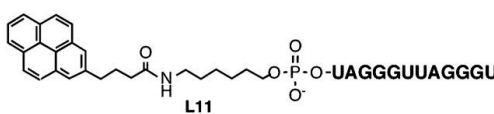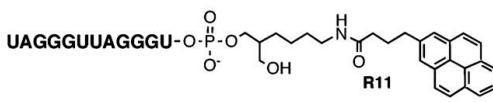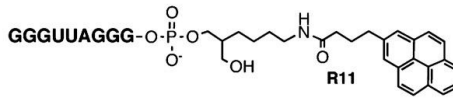
Figure-1.15: Chemical structures of pyrene probes with different linker lengths (L and R), RNA chain sequences, and numbers of pyrenes. E/M is the excimer/monomer fluorescence intensity ratio (E at 480, M at 380). *Adapted from reference 137.*

A series of oligonucleotide probes having human TERRA RNA sequence were designed and synthesized which possess pyrene moieties at their 5′ and/or 3′ termini. The probes had varied linker lengths, RNA chain sequences, and numbers of pyrenes. Figure-1.15 shows the chemical structures of pyrene-modified oligonucleotide probes with different linker lengths that were explored to probe G-quadruplex structure. A long list of probes was explored to take advantage of the distance dependence of excimer formation with pyrene, which could be used as a unique excimer signalling device for detecting G-quadruplex structure. This study provided an insight into TERRA RNA structure in living cells.

1.4.4. Pyrene-labeled Dendrimers

In the series of various fascinating pyrene-labeled architectures, the dendrimers are an important class of macromolecules which have attracted a lot of attention recently and their internal dynamics have been studied by pyrene excimer formation.[43] Dendrimers are monodisperse polymers and their exquisitively controlled molecular architectures have attracted the researchers to understand their internal dynamics for applications in many areas such as catalysis, biomedical fields such as drug delivery, sensing, light harvesting devices etc.[138] Apart from their synthetically challenging architecture, the understanding of their internal dynamics has also been challenging. Figure-1.16 shows the schematic representation of pyrene-labeled dendrimer.[43]
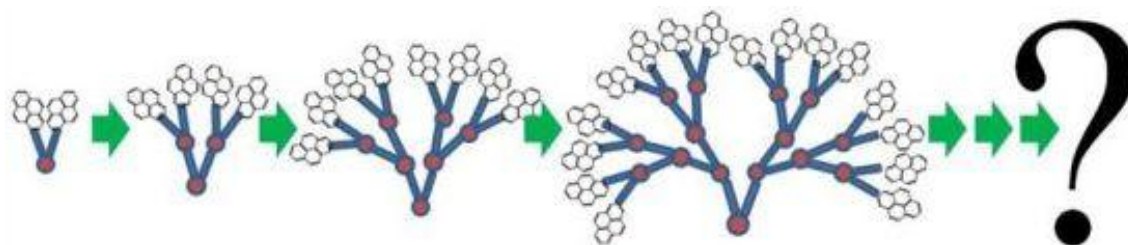
Figure-1.16: Schematics of pyrene-labeled dendrimers with various generations.
Adapted from reference 43.

Their internal dynamics have been explored by NMR,[139] molecular and Brownian dynamics computation,[140] neutron scattering,[141] rheology,[142] dielectric relaxation spectroscopy,[143] fluorescence anisotropy[144] etc. which provided the information that the mobility of the chain ends was more than that of the internal segments. Literature reports the synthesis of an array of pyrene-labeled dendrimers, where the internal dynamics were investigated through fluorescence. The internal segmental dynamics was explored for dendrimers having flexible segments such as poly(amido amine) (PAMAM dendrimers), polyamide, poly(2,2-bis(hydroxymethyl)-propionic acid, poly(benzyl ester), poly(benzyl ether), poly(propylene amine) etc.[145-150] Two processes were investigated mostly to study the dynamics: 1) energy transfer processes such as fluorescence resonance energy transfer (FRET), energy hopping or migration, electron transfer between a donor and an acceptor, 2) excimer formation between pyrene pendants. The internal dynamics have been mostly probed for dendrimers having an acceptor at the focal point with pyrenyl-pendants at the periphery. However, the excimer formation between the pyrenyl moieties attached at the chain

ends of the dendrimers were investigated in very few reports.[43] Investigation of pyrene-labeled poly(benzyl ether) dendrimers for the pyrene excimer formation, in particular via the (I_E/I_M) ratio is one such report.[149] A recent review on the investigation of dynamics of dendritic molecules by pyrene excimer formation by Duhamel has highlighted the challenges faced by the investigators in studying the dynamics of the dendritic molecules.[43]

1.5. Aim of the Present Investigation

This thesis highlights the relevance of fluorescence techniques for understanding self-assembly in polymeric systems. Our research group has been studying the self assembly of a unique class of side chain urethane methacrylate polymers possessing bulky pendant unit, which exhibited different morphologies depending on the solvent from which it was drop cast. Incorporation of pyrene as the pendant bulky unit enabled the self assembly to be traced in dilute solution using fluorescence spectroscopy. Photophysical studies showed that the polymers formed excimers even at very low concentrations due to intra chain interactions whereas at higher concentrations pyrene dimers and aggregates were observed due to inter chain interactions. Structure-property studies involving alkyl and ethyleneoxy spacer segments indicated that several parameters like hydrogen bonding, hydrophilic/hydrophobic interaction etc. were at play in defining the self assembling characteristics of these polymers. These earlier studies also brought to focus the fact that in contrast to the generally studied pyrene end- labeled polymers, a 100% pyrene labeled polymer was a photophysically rich system with unique characteristics which could provide in-depth understanding of the polymer dynamics.

The aim of the present work is to study the self assembling behaviour of various pyrene labeled polymers having different architecture like block, and random copolymers, where the pyrene labeling was varied from 1-100%. The challenging task of identifying the role of hydrogen bonding alone in presence of other interactions like π-π interactions or hydrophilic/hydrophobic interactions towards the self-organization process is also addressed by designing tailor-made pyrene labeled polymers without hydrogen bonding functionalities and comparing their photophysical properties with that of analogous systems which could also self assemble by hydrogen bonding. The photophysical properties of these diverse polymers were studied using various

fluorescence techniques like steady-state and life time decay analysis as well as time resolved emission spectra (TRES). The self assembly of the pyrene labeled polymers was also utilized to encapsulate Rhodamine dye as a model compound and its temperature triggered release was used as a handle to understand the microstructural changes inside the polymer microcapsule.

Thus, the thesis analyses the following important aspects:

5. Fundamental aspects of the self assembly of different pyrene labeled polymers by the detailed photophysical analyses highlighting their differences and similarities.

6. Exploration of various pyrene labeled polymers with different architectures like block, random copolymers to understand their photophysics.

7. The applicative aspects of the pyrene labeled polymers probed by rhodamine encapsulation and release.

8. Differences in self assembly behaviour in H-bonded versus non H-bonded polymers at very dilute concentrations.

9. The architectural differences among the H-bonded homopolymers probed by TRES and temperature dependent fluorescence.

1.6. Thesis Outline

The overall findings of the thesis are distributed in 6 chapters. Chapter 1 is the literature survey on pyrene as a fluorescence probe in understanding the self-assembly of various pyrene-labeled macromolecules such as end-labeled polymers, randomly labeled polymers, dendrimer, pyrene-labeled biomolecules such as peptides, lipids, DNA etc. Chapter 2 focuses on exploration of self-assembly of pyrene-labeled polymers with different architectures like block, random copolymers based on their excimer formation. In chapter 3, the random copolymer architecture with varying amount of pyrene content is extensively investigated. The pyrene incorporation was varied from 1 to 100% and TRES studies at RT and 70 $^{\text{o}}$C were conducted to understand various emitting species. The chapter 4 highlights the applicative aspects of these random copolymers by rhodamine encapsulation and release as a function of temperature in water medium. Chapter 5 addresses fundamentally challenging question - the self-assembling nature of H-bonded versus non-H-bonded polymers at very dilute

concentrations explored by steady state fluorescence, fluorescence decay studies as well as TRES studies. This chapter also covers the chain dynamics of H-bonded homopolymers with small differences in the side chains carrying pyrene pendents attached to the methacrylate backbone. And finally, the chapter 6 gives the overall conclusion of the thesis.

1.7. References

1) Nurmawati, M. H.; Renu, R.; Ajikumar, P. K.; Sindhu, S.; Cheong, F. C.; Sow, C. H.; Valiyaveettil, S. *Adv. Funct. Mater.* **2006**, *16*, 2340-2345.

2) Wang, J.; Tang, F.; Li, F.; Lin, J.; Zhang, Y.; Du, Linfang; Zhao, X. *J. Nanomat.* **2008,** 1-8.

3) Yu, G.; Yokoyama, M.; Okano, T.; Sakurai, Y.; Kataoka, K. *J. Control. Release* **1993**, *29*, 17-23.

4) Gou, P. F.; Zhu, W. P.; Shen, Z. Q.; *Biomacromolecules* **2010,** *11*, 934-943.

5) Kazunori, K.; Glenn S. K.; Masayuki, Y.; Teruo, O.; Yasuhisa, S. *J. Control. Release* **1993**, *24*, 119-132.

6) Wu, K. C.; Ku, P. J.; Lin, C. S.; Shih, H. T., Wu, F. I.; Huang, M. J.; Lin, J. J.; Chen, I. C.; Cheng, C. H. *Adv. Funct. Mater.* **2008**, *18*, 67-75.

7) Schmidt-Mende, L.; Fechtenkotter, A.; Mullen, K.; Moons, E.; Friend, R. H.; MacKenzie, J. D. *Science* **2001,** *293*, 1119-1122.

8) Ikkala, O.; Brinke, G. T. *Chem. Commun.* **2004**, *19*, 2131-2137.

9) Kowollik, C. B.; Dalton, H.; Davis, T. P.; Stenzel, M. H. *Angew. Chem. Int. Ed.* **2003**, *42*, 3664-3668.

10) Heischkel, Y.; Schmidt, H. W. *Macromol. Chem. Phys.* **1998**, *199*, 869-880.

11) Forster, S. *Polymer Vesicles. In Encyclopaedia of Polymer Science and Technology*; John Wiley & Sons: New York, **2005**.

12) Antonietti, M.; Forster, S. *Adv. Mater.* **2003**, *15*, 1323-1333.

13) Brunsveld, L.; Folmer, B. J. B.; Meijer, E. W.; Sijbesma, R. P. *Chem. Rev.* **2001**, *101*, 4071-4098.

14) Nagai, A.; Kokado, K.; Miyake, J.; Chujo, Y. *Macromolecules* **2009**, *42*, 5446-5452.

15) Wang, C.; Wang, Z.; Zhang, X. *Acc. Chem. Res.* **2012**, *45*, 618-625.

16) Kimmich, R.; Fatkullin, N. *Adv. Polym. Sci.* **2004**, *170*, 1-113.

17) Spiess, H. W. *Macromol. Chem. Phys*. **2003**, *204*, 340-346.

18) Thuresson, K.; Soderman, O.; Hansson, P.; Wang, G. *J. Phys. Chem.* **1996**, *100*, 4909-4918.

19) Picarra, S.; Relogio, P.; Afonso, C. A. M.; Martinho, J. M. G.; Farinha, J. P. S. *Macromolecules* **2003**, *36*, 8119-8129.

20) Yan, X.; Li, S.; Pollock, J. B.; Cook, T. R.; Chen, J.; Zhang, Y.; Ji, X.; Yu, Y.; Hunag, F.; Stang, P. J. *Proc. Natl. Acad. Sci.USA* **2013**, *110*, 15585-15590.

21) Cauchin, D.; Candau, F.; Zana, R.; Talmon, Y. *Macromolecules* **1992**, *25*, 4220-4223.

22) Zana, R.; Kaplan, A.; Talmon, Y. *Langmuir* **1993**, 9, 1948-1950.

23) Kawakami, M.; Byrne, K.; Brockwell, D. J.; Radford, S. E.; Smith, D. A. *Biophys. J. Biophys. Lett.* **2006**, *91*, L16-L18.

24) Mitsui, K.; Hara, M.; Ikai, A. *FEBS Lett.* **1996**, *385*, 29-33.

25) Perkins, T. T.; Quake, S. R.; Smith, D. E.; Larson, R. G.; Chu, S. *Science* **1995**, *268*, 83-87.

26) Horinaka, J.; Amano, S.; Funada, H.; Ito, S.; Yamamoto, M. *Macromolecules* **1998**, *31*, 1197-1201.

27) Ha, T.; Ting, A. Y.; Liang, J.; Caldwell, W. B.; Deniz, A. A.; Chemla, D. S.; Schultz, P. G.; Weiss, S. *Proc. Natl. Acad. Sci. USA* **1999**, *96*, 893-898.

28) Duhamel, J. in *Molecular Interfacial Phenomena of Polymers and Biopolymers* Editor: P. Chen, Woodhead Publishing Limited, Cambridge, **2005**, *214-248*.

29) Winnik, F. M.; *Chem. Rev.* **1993**, *93*, 587-614.

30) Birks, J. B. *Photophysics of Aromatic Molecules; Wiley/Interscience*; New York, **1970**.

31) Berlman, I. B. *Handbook of Fluorescence Spectra of Aromatic* Molecules, Academic Press N. Y., **1971**.

32) Lakowicz, J. R. *Principles of Fluorescence Spectroscopy*, 2nd ed.; Kluwer Academics/Plenum Publisher: New York, **1999**.

33) Birks, J. B.; Dyson, D. J. *Proc. Roy. Soc.* **1963**, *275*, 135-148.

34) Conlon, P.; Yang, C. J.; Wu, Y.; Chen, Y.; Martinez, K.; Kim, Y.; Stevens, N.; Marti, A. A.; Jockusch, S.; Turro, N. J.; Tan, W. *J. Am. Chem. Soc.* **2008**, 130, 336-342.

35) Kalyanasundaram, K.; Thomas, J. K. *J. Am. Chem. Soc.* **1977**, *99*, 2039-2044.

36) Dong, D. C.; Winnik, M. A. *Can. J. Chem.* **1984**, *62*, 2560-2565.

37) Zachariasse, K.; Kuhnle, W. *Z. Phys. Chem. Neue F* **1976**, *101*, 267-276.

38) Winnik, M. A.; Redpath, T.; Richards, D. H. *Macromolecules* **1980**, *13*, 328−335.

39) Winnik, M. A. *Acc. Chem. Res.* **1985**, *18*, 73−79.

40) Duhamel, J. *Acc. Chem. Res.* **2006**, *39*, 953−960.

41) Cuniberti, C.; Perico, A. *Eur. Polym. J.* **1977**, *13*, 369−374.

42) Cuniberti, C.; Perico, A. *Prog. Polym. Sci.* **1984**, *10*, 271-316.

43) Duhamel, J. *Polymers* **2012**, *4*, 211−239.

44) Figueira-Duarte, T.M.; Simon, S.C.; Wagner, M.; Druzhinin, S.I.; Zachariasse, K.A.; Müllen, K. *Angew. Chem. Int. Ed.* **2008**, *47*, 10175–10178.

45) Stewart, G. M.; Fox, M. A. *J. Am. Chem. Soc.* **1996**, *118*, 4354–4360.

46) Bondurant, B.; Last, J. A.; Waggoner, T. A.; Slade, A.; Sasaki, D.Y. *Langmuir* **2003**, *19*, 1829−1837.

47) Goedeweeck, R.; Vanderauweraer, M.; Deschryver, F. C. *J. Am. Chem. Soc.* **1985**, *107*, 2334.

48) Sahoo, D.; Weers, P. M. M.; Ryan, R. O.; Narayanaswami, V. *Mol. Biol.* **2002**, *321*, 201.

49) Keyes-Baig, C.; Mathew, M.; Duhamel, J. *J. Am. Chem. Soc.* **2012,** *134*, 16791-16797.

50) Siddique, B.; Duhamel, J. *Langmuir* **2011**, *27*, 6639–6650.

51) Ollmann, M.; Schwarzmann, G.; Sandhoff, K.; Galla, H. J. *Biochemistry* **1987**, *26*, 5943.

52) Yekta, A.; Xu, B.; Duhamel, J.; Adiwidjaja, H.; Winnik, M. A. *Macromolecules* **1995**, *28*, 956-966.

53) Evertsson, H.; Nilsson, S. *Carbohydr. Polym.* **1999**, *40*, 293-298.

54) Maiti, S.; Jayachandran, K. N.; Chatterji, P. R. *Polymer* **2001**, *42*, 7801-7808.

55) Picarra, S.; Duhamel, J.; Fedorov, A.; Martinho, J. M. G. *J. Phys. Chem. B* **2004**, *108*, 12009-12015.

56) Koti, A. S. R.; Krishna, M. M. G.; Periasamy, N. *J. Phys. Chem. A* **2001**, *105,* 1767-1771.

57) Ware, W. R.; Chow, P.; Lee, S. K. *Chem. Phys. Lett.* **1968**, *2*, 356-358.

58) Koti, A. S. R.; Periasamy, N. *J. Chem. Phys.* **2001**, *115*, 7094–7099.

59) Costa, T.; De Melo, J. S. S.; Castro, C. S.; Gago, S.; Pillinger, M.; Goncalves, I. S. *J. Phys. Chem. B* **2010**, *114*, 12439−12447.

60) De Melo, J. S. S.; Costa, T.; Miguel, M. d. G.; Lindman, B.; Schillen, K. *J. Phys. Chem. B* **2003**, *107*, 12605−12621.

61) Nakajima, A. *J. Lumin.* **1976**, *11*, 429-432.

62) Prazeres, T. J. V.; Beingessner, R.; Duhamel, J.; Olesen, K.; Shay, G.; Bassett, D. R. *Macromolecules* **2001**, *34*, 7876-7884.

63) Dong, D. C.; Winnik, M. A. *Can. J. Chem.-Re. Can. Chim.* **1984**, *62*, 2560-2565.

64) Karpovich, D. S.; Blanchard, G. J. *J. Phys. Chem.* **1995**, *99*, 3951-3958.

65) Winnik, F. M.; Winnik, M. A.; Ringsdorf, H.; Venzmer, J. *J. Phys.Chem.* **1991**, *95*, 2583-2587.

66) Valeur, B. *Molecular Fluorescence: Principles and Applications*. Wiley-VCH, **2001**.

67) Strickler, S, J.; Berg, R. A. *J. Chem. Phys.* **1962**, *37*, 814-822.

68) *Time-Resolved Fluorescence Technical Note TRFT-4*: By Horiba Scientific.

69) Easter, J. H.; DeToma R. P.; Brand, L. *Biophys. J.* **1976**, *16*, 571-583.

70) Zhang, X.; Rehm, S.; Safont-Sempere, M. M.; Wurthner, F. *Nature Chem.* **2009**, *1*, 623-629.

71) Laurent, A. *Ann. Chim. Phys.* **1837**, *66*, 136-137.

72) Forster, T.; Kasper, K. *Z. Physik. Chem.* **1954**, 1, 19-23.

73) Birks, J. B.; Dyson, D. J.; Munro, H. *Proc. R. Soc. A* **1963**, *275*, 575-588.

74) Winnik, F. M. *Macromolecules*, **1987**, *20*, 2475-2750.

75) Duhamel, J.; Yekta, A.; Winnik, M. A.; Jao, T. C.; Mishra, M. K., Rubin, I. D. *J. Phys. Chem.* **1993**, *97*, 13708-13712.

76) Lee, S.; Duhamel, J. *Macromolecules* **1998**, *31*, 9193-9200.

77) Mathew, A. K.; Siu, H.; Duhamel, J. *Macromolecules* **1999**, *32*, 7100-7108.

78) Siu, H.; Duhamel, J. *Macromolecules* **2004**, *37*, 9287-9289.

79) Chen, S.; Duhamel, J.; Winnik, M. A. *J. Phys. Chem. B* **2011**, *115*, 3289-3302.

80) Duhamel, J.; Kanagalingam, S.; O'Brien, T.; Ingratta, M. *J. Am. Chem. Soc.* **2003**, *125*, 12810-12822.

81) Picarra, S.; Duhamel, J.; Fedorov, A.; Martinho, J. M. G. *J. Phys. Chem. B* **2004**, *108*, 12009-12015.

82) Siu, H.; Duhamel, J. *Macromolecules* **2005**, *38*, 7184-7186.

83) Siu, H.; Duhamel, J. *J. Phys. Chem. B* **2005**, *109*, 1770-1780.

84) Duhamel, J. *Langmuir* **2012**, *28*, 6527-6538.

85) Sisido, M.; Imanishi, Y.; Hagashimura, T. *Macromolecules* **1976**, *9*, 316-319.

86) Zachariasse, K. A.; Duveneck, G.; Busse, R. *J. Am. Chem. Soc.* **1984**, *106*, 1045−1051.

87) Zachariasse, K. A.; Busse, R.; Duveneck, G.; Kuhnle, W. *J. Photochem.* **1985**, *28*, 237-253.

88) Willemski, G.; Fixman, M. *J. Chem. Phys.* **1974**, *60*, 866-877.

89) Willemski, G.; Fixman, M. *J. Chem. Phys.* **1974**, *60*, 878-890.

90) Segui, F.; Qiu, X.-P.; Winnik, F. M. *J. Polym. Sci., Part A: Polym. Chem.* **2008**, *46*, 314-326.

91) Yip, J.; Duhamel, J.; Qiu, X.-P.; Winnik, F. M. *Can. J. Chem.* **2011**, *89*, 163-172.

92) Rao, J.; Xu, J.; Luo, S.; Liu, S. *Langmuir* **2007**, *23*, 11857-11865.

93) Gardinier, W. E.; Bright, F. V. *J. Phys. Chem. B* **2005**, *109*, 14824-14829.

94) Kim, S. D.; Torkelson, J. M. *Macromolecules* **2002**, *35*, 5943-5952.

95) Kane, M. A.; Pandey, S.; Baker, G. A. Perez, S. A.; Bukowski, E. J.; Hoth, D. C.; Bright, F. V. *Macromolecules* **2001**, *34*, 6831-6838.

96) Slomkowski, S.; Winnik, M. A. *Macromolecules* **1986**, *19*, 500.

97) Picarra, S.; Gomes, P. T.; Martinho, J. M. G. *Macromolecules* **2000**, *33*, 3947-3950.

98) Cheung, S.-T.; Winnik, M. A.; Redpath, A. E. C. *Makromol. Chem.* **1982**, *183*, 1815-1824.

99) Char, K.; Frank, C. W.; Gast, A. P. *Macromolecules* **1989**, *22*, 3177-3180.

100) Duhamel, J.; Yekta, A.; Hu, Y. Z.; Winnik, M. A. *Macromolecules* **1992**, *25*, 7024-7030.

101) Boileau, S.; Mechin, F.; Martinho, J. M. G.; Winnik, M. A. *Macromolecules* **1989**, *22*, 215-220.

102) Duhamel, J.; Khaykin, Y.; Hu, Y. Z.; Winnik, M. A.; Boileau, S.; Mechin, F. *Eur. Polym. J.* **1994**, *30*, 129-134.

103) Lee, S.; Winnik, M. A. *Macromolecules* **1997**, *30*, 2633-2641.

104) Chen, S.; Duhamel, J. *Langmuir* **2013**, *29*, 2821-2834.

105) Winnik, M. A.; Yekta, A. *Curr. Opin. Colloid Interface Sci.* **1997**, *2*, 424-436.

106) El-Sherbiny, S.; Xiao, H. *Ind. Eng. Chem. Res.* **2005**, *44*, 9875-9883.

107) Goddard, E. D.; Gruber, J. V. *Principles of Polymer Science and Technology in Cosmetics and Personal Care. Cosmetic science and technology V. 22.* Eastern Hemisphere Distribution, Marcel Dekker AG, Basel, Switzerland, **1999**.

108) Anwari, F. M.; Schwab, F. G. *In Polymers in Aqueous Media. Performance Through Association:* Glass, J. E., Ed.; American Chemical Society Washington, DC, **1989**.

109) Wever, D. A. Z.; Picchioni, F.; Broekhuis, A. A. *Prog. Polym. Sci.* **2011**, *36*, 1558–1628.

110) Chen, S. *Quantitative Characterization of Pyrene-Labeled Macromolecules in Solution by Global Analysis of Fluorescence Decays*. Ph.D. Thesis, Waterloo, **2012**, pp 5-9.

111) Winnik, F. M.; Regismond, S.T.A.; Anghel, D.F. *Associative Polymers in Aqueous Media*, Glass, J.E., Ed.; ACS Symposium Series 765; American Chemical Society: Washington, DC, **2000**, 286–302.

112) Nishikawa, K.; Yekta, A.; Pham, H. H.; Winnik, M. A.; Sau, A. C. *Langmuir* **1998**, *14*, 7119-7129.

113) Winnik, F. M. *Macromolecules* **1989**, *22*, 734-742.

114) Siu, H.; Duhamel, J. *Macromolecules* **2006,** *39,* 1144-1155.

115) Heskins, M.; Guillet, J. E. *J. Macromol. Sci.: Part A – Chem.* **1968***, 2,* 1441-1455.

116) Chandaroy, P., Sen, A., and Hui, S.W. *J. Control. Release* **2001**, *76*, 27-37.

117) Kitano, H., Maeda, Y., Takeuchi, S., Ieda, K., and Aizu, Y. *Langmuir* **1994**, *10*, 403-406.

118) Vshivkov, S. A.; Safronov, A. P. *Macromol. Chem. Phys.* **1997**, *198*, 3015-3023.

119) Sun, S.-T.; Nishio, I.; Swislow, G.; Tanaka, T. *J. Chem. Phys.* **1980**, 73, 5971-5975.

120) Wu, C.; Shuigin, Z. *Macromolecules* **1995**, *28*, 8381-8387.

121) Maeda, Y.; Higuchi, T.; Ikeda, I. *Langmuir* **2000**, *16*, 7503-7509.

122) Zhu, P. W. *Chem. Phys. Lett.* **1993**, *215*, 627-630.

123) Ringsdorf, H.; Simon, J.; Winnik, F. M. *Macromolecules* **1992**, *25*, 7306-7312.

124) Winnik, F. M. *Macromolecules* **1990**, *23*, 233-242.

125) Hong, S. W.; Kim, K. H.; Huh, J.; Ahn, C.-H.; Jo, W. H. *Chem. Mater.* **2005**, *17*, 6213-6215.

126) Irondi, K.; Zhang, M.; Duhamel, J. *J. Phys. Chem. B* **2006**, *110*, 2628-2637.

127) Laukkanen, A.; Winnik, F. M.; Tenhu, H. *Macromolecules* **2005**, 38, 2439-2448.

128) Picarra, S.; Martinho, J. M. G. *Macromolecules* **2001**, *34*, 53-58.

129) Farinha, J. P. S.; Picarra, S.; Miesel, K.; Martinho, J. M. G. *J. Phys. Chem. B* **2001**, *105*, 10536-10545.

130) Liu, C.–Y.; Morawetz, H. *Macromolecules* **1988**, *21*, 515-518.

131) Duhamel, J.; Kanyo, J.; Dinter-Gottlieb, G.; Lu, P. *Biochemistry* **1996**, *35*, 16687-16697.

132) Bains, G.; Patel, A. B.; Narayanaswami, V. *Molecules* **2011**, *16*, 7909-7935.

133) Zhang, R.; Tang, D.; Lu, P.; Yang, X.; Liao, D.; Zhang, Y.; Zhang, M.; Yu, C.; Yam, V. W. W. *Org lett* **2009**, *11*, 4302-4305.

134) Pownall, H. J.; Smith, L. C. *Chem. Phys. Lipids* **1989**, *50*, 191-211.

135) Wu, C.; Wang, C.; Yan, L.; Yang, C. J. *J. Biomed. Nanotechnol.* **2009**, *5*, 495-504.

136) Paris, P. L.; Langenhan, J. M. Kool, E. T. *Nucleic Acids Res.* **1998**, *26*, 3789-3793.

137) Xu, Y.; Suzuki, Y.; Ito, K.; Komiyama, M. *Proc. Natl. Acad. Sci.USA* **2010**, *33*, 14579-14584.

138) Astruc, D.; Boisselier, E.; Ornelas, C. *Chem. Rev.* **2010**, *110*, 1857-1959.

139) Meltzer, A. D.; Tirrell, D. A.; Jones, A. A.; Inglefield, P. T. *Macromolecules* **1992**, *25*, 4549–4552.

140) Gorman, C. B.; Smith, J. C. *Polymer* **2000**, *41*, 675–683.

141) Stark, B.; Stühn, B.; Frey, H.; Lach, C.; Lorenz, K.; Frick, B. *Macromolecules* **1998**, *31*, 5415-5423.

142) Uppuluri, S.; Morrison, F. A.; Dvornic, P. R. *Macromolecules* **2000**, *33*, 2551-2560.

143) Emran, S. K.; Newkome, G. R.; Weis, C. D.; Harmon, J. P. *J. Polym. Sci. B* **1999**, *37*, 2025-2038.

144) Aumanen, J.; Kesti, T.; Sundström. V.; Teobaldi, G.; Zerbetto, F.; Werner, N.; Richardt, G.; van Heyst, J.; Vögtle, F.; Korppi-Tommola, J. *J. Phys. Chem. B* **2010**, *114*, 1548-1558.

145) Wang, B.-B.; Zhang, X.; Jia, X.-R.; Li, Z.-C.; Ji, Y.; Yang, L.; Wei, Y. *J. Am. Chem. Soc.* **2004**, *126*, 15180–15194.

146) Wang, B.-B.; Zhang, X.; Yang, L.; Jia, X.-R.; Ji, Y.; Li, W.-S.; Wei, Y. *Polym. Bull.* **2006**, *56*, 63–74.

147) Yip, J.; Duhamel, J.; Bahun, G. J.; Adronov, A. *J. Phys. Chem. B* **2010**, *114*, 10254–10265.

148) Wilken, R.; Adams, J. *Macromol. Rapid. Commun.* **1997**, *18*, 659-665.

149) Stewart, G. M.; Fox, M. A. *J. Am. Chem. Soc.* **1996**, *118*, 4354–4360.

150) Baker, L. A.; Crooks, R. M. *Macromolecules* **2000**, *33*, 9034–9039.

Chapter 2:

Correlation of Architecture with Excimer Emission in Hierarchical Self-Assembled Polymers

2.1. Abstract

This chapter describes the self organization behavior of various hierarchical architectures having pyrene as a pendant. Pyrene was incorporated as pendant unit to side-chain urethane methacrylate polymers having a short ethyleneoxy or a long polyethyleneoxy spacer segment. The short-spacer pyrene urethane methacrylate was also incorporated either as block or random copolymer (1:9) along with polystyrene. The excimer emission was observed to be different for different polymers with the random copolymer exhibiting the lowest efficiency. But, the total quantum yield was highest (Q= 0.58) for random copolymer due to the high emission coefficient of monomer compared to that of excimer. The polymers were compared by steady state emission for their excimer formation in THF and THF/water solvent mixture and films. The evolution of excimeric emission centered ~430 or ~480 nm as a function of temperature was also studied in THF/water. The I_E/I_M ratio for the λ_{343} nm excitation exhibited steady increase with temperature with the block copolymer exhibiting the highest ratio and highest rate of increase; whereas, the random copolymer had the lowest I_E/I_M ratios.

This Chapter has been adapted from the corresponding paper:

2.2. Introduction

Mimicking nature for constructing well-organized architectures from small molecules or macromolecules through the non-covalent forces has bridged the gap between various disciplines of science such as chemistry, physics, biology etc.[1-6] These well-defined architectures are constructed by a process called self-assembly.[6] Controlling the forces of self-assembly into generating well-defined architectures is very crucial for the effective utilization of the polymeric materials for multifarious applications ranging from drug delivery to optoelectronics and device fabrication etc.[7-9] In photovoltaic and optoelectronic devices, not only are they utilized as the main donor or acceptor active layers, but they find application as the electron transport or hole transport layers etc. [10-12] The potential of a material as an useful candidate for these devices depends not only upon the inherent molecular property of the material but also on how it organizes in the solid state. Whether it forms sandwich stacks which will quench the fluorescence or whether it can stack in a manner that will promote better electron or hole transport determines the polymer's fate as a potential device material.[13] This requires understanding and controlling the supramolecular organization of the material as a function of various parameters like concentration, thickness, temperature, solvent used as well as architecture of the polymer – block, random, star, rod-coil etc.

Several groups of researchers have conducted studies on pyrene randomly or end labeled polymers to unravel different modes of associations.[14-23] For instance, in covalently linked systems pyrene moieties have been found to exist in pre-associated ground state aggregates. If these ground state aggregates are in the appropriate conformation (sandwich) they exhibit excimer emission (~ 470 nm) by light absorption through a static mechanism.[24] To complicate things further, when the ground state aggregates are not in the preferred sandwich configuration, but are partially overlapped then they give rise to blue shifted excimer emission (~ 440 nm).[25, 26] These two states (partially overlapped dimer and sandwich type dimer) can be interconverted both in ground state as well as in excited state.[27]

One of the recent example where random labeling of pyrene through various ways such as short or long, flexible linker or rigid linker and labeling by different routes is discussed here.[28] Figure-2.1 shows the schematic representation of pyrene-labeled polymer via different linker and its representative steady state emission spectrum and also the structures of the polymers used for study.[28] These polymers were extensively

investigated by steady state emission and time-resolved fluorescence experiments in various solvents of varying viscosities. It was demonstrated that the polymers with long and flexible linker (GrE-PS and CoE-PS) formed excimer more efficiently than the short and rigid linker polymer (CoA-PS). Another significant finding from these studies has been on the extent of excimer formation by the polymers having identical chemical structure but different method of incorporation of pyrene i.e by grafting onto reaction or copolymerization. The polymers GrE-PS (by grafting) and CoE-PS (by copolymerization) have same chemical structure but different method of incorporation and the association of pyrene was found to be higher for GrE-PS than CoE-PS. These studies have provided significant insights into the randomly incorporated pyrene-labeled polymers.
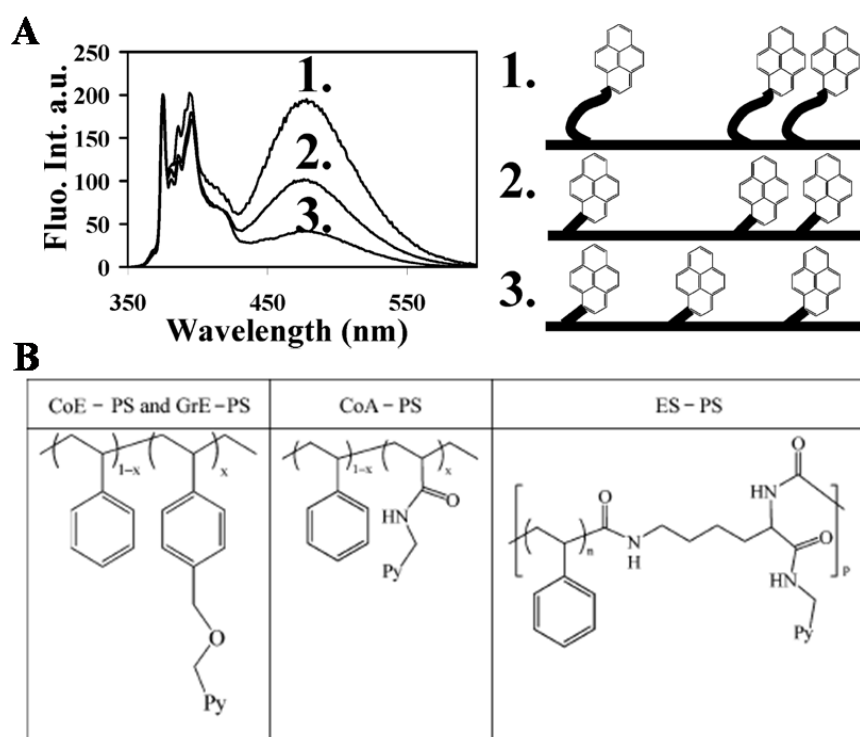
Figure-2.1: **A**) Schematic representation of pyrene labeled polymers with different linker type and **B**) Structures of the polymers used for the study. *Adapted from reference 28.*

The consequence of incorporating pyrene labels on all repeating units of a polymer, on its solution properties like self assembly is a very challenging task to address. You et al. compared the self-assembly behavior of a random versus diblock methacrylate copolymer incorporating pyrene pendant units by following their excimer emission.[29] Figure-2.2 show the structures of pyrene labeled random and block

copolymers synthesized by atom transfer radical polymerization approach. As per our knowledge, this is the first reference where 100% loaded pyrene polymer has been reported. However, the article focused on the improvement in self-assembly (as evidenced by their morphology) in thin films upon thermal annealing and they did not report the detailed photophysical studies as a consequence of the varied polymer architecture. Figure-2.3 shows the schematic representation of excimer intensity control by temperature and the generation of well-ordered pyrene structures from block copolymers.[29]
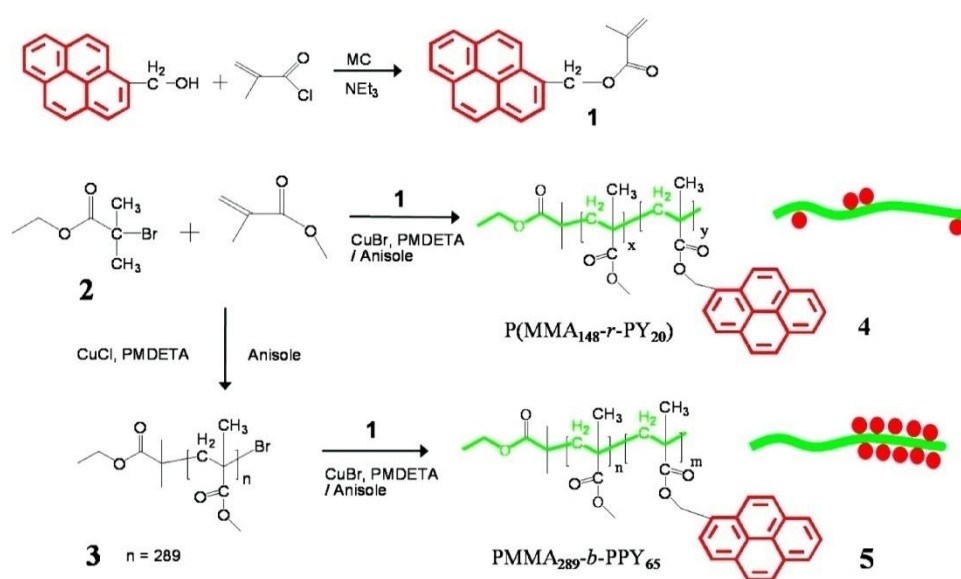
Figure-2.2: Structures of pyrene labeled random and block copolymers synthesized by ATRP. *Adapted from reference 29.*

In 100% labeled pyrene polymers the possibility of simultaneous existence of various emitting species like the isolated monomers which decay by monomer emission, monomers that can give rise to excimer emission and those which are held in conformation that are unfavorable for excimer formation can complicate the analysis of time resolved fluorescence data. For instance, the possibility of ground state pyrene association is very high when they are incorporated on every pendant chain of a side chain polymer. Analyzing the photophysical data, which is rich in information regarding orientation, distribution etc., can lead to a better understanding of the polymer self organization.
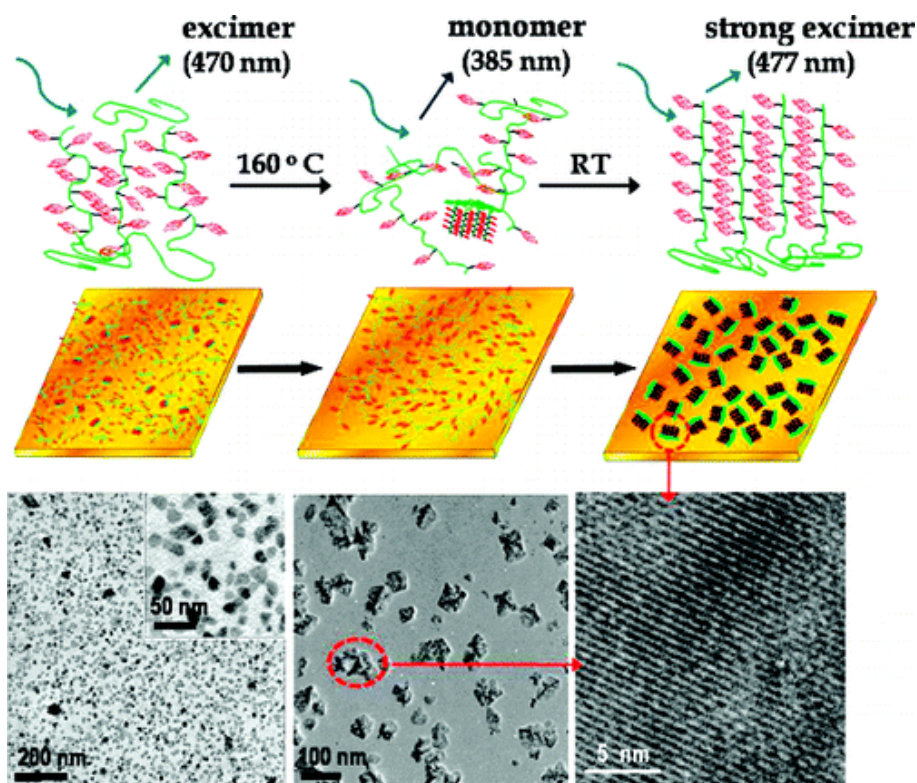
Figure-2.3: Schematic representation of the mechanism of excimer intensity control by temperature and the generation of well-ordered pyrene structure. *Adapted from reference 29.*

In this chapter we have addressed the question of influence of different hierarchical polymer architectures such as the one having different spacer lengths like short "ethyleneoxy" or long "polyethyleneoxy" unit attached to pendant pyrene via urethane linkage and the short spacer incorporated as block or random copolymer with styrene. These polymers were explored for their photophysical as well as morphological characteristics. The effect of this varied structure design on their emission characteristics were studied using steady state temperature dependent fluorescence measurements. The significant difference and similarities among the hierarchical polymeric architecture have been brought out by the extensive photophysical insights provided by pyrene labeling in different ways.

2.3. Experimental Section

2.3.1. Materials

Isophorone diisocyanate (IPDI), 2-hydroxyethyl methacrylate (HEMA), poly(ethyleneglycol) methacrylate (M_n ~ 350, n ~ 6; determined from ^{1}H NMR), 1-pyrenemethanol, dibutyltin dilaurate (DBTDL), ethyl 2-bromopropionate, 2,2'-bipyridine (bipy), N,N,N′,N′,N″-pentamethyldiethylenetriamine (PMDETA) were purchased from Sigma Aldrich and used as such. Styrene was purchased from Aldrich and purified using standard procedures prior to use.[30] Benzoyl peroxide was purchased from Sigma Aldrich and recrystallized from methanol. CuBr (99%, Aldrich) was stirred in glacial acetic acid overnight, filtered, and then it was washed with ethanol and dried under vacuum at 60 ^{o}C overnight. N,N-dimethylformamide (DMF) was purified by keeping it for 72 hours over calcium sulfate followed by decanting and vacuum distilling. Tetrahydrofuran (THF) and chloroform (both HPLC grade) were purchased from Merck, India and used as such.

2.3.2. Measurements

^{1}H and ^{13}C NMR spectra of monomer and polymers were recorded using 200-MHz and 400-MHz Bruker NMR spectrophotometer in CDCl$_3$ containing small amounts of tetramethylsilane (TMS) as internal standard. Infrared spectra were recorded using a Perkin Elmer, Spectrum one FT-IR spectrophotometer. The liquid samples or dilute solution of the solid samples in THF were spread over KBr plates and their spectra were recorded. IR spectra were recorded in the range of 4000 - 400 cm^{-1}. The molecular weights of the polymers were determined by gel permeation chromatography (GPC) (supplied by THERMO GPC SYSTEM) using RI detector in chloroform calibrated by 39 polystyrene standards of the molecular weight range 1.62 x 10^2 to 4.29 x 10^6. The columns used were Waters HT Styragel columns (10 micron) HT-2, HT-3, HT-4, HT-5, HT-6 and guard column. The flow rate of the chloroform was maintained as 1 mL/min throughout the experiments. Thermal gravimetric analysis (TGA) of all the polymers was performed using Perkin Elmer Pyris-6 instrument. Differential scanning calorimetry (DSC) measurements were performed on a TA Q20 Differential Scanning Calorimeter at a heating rate of 10 ^{o}C/min under nitrogen atmosphere. Typically, 4-5 mg of samples was placed in an aluminum pan, sealed properly, and scanned from -30 to 200 ^{o}C. The instrument was calibrated with indium standards before measurements.

Photophysical studies

Absorption Spectra were recorded using Perkin Elmer Lambda 45 UV – spectrophotometer. Steady State Fluorescence studies were performed using Horiba Jobin Yvon Fluorolog 3 spectrophotometer having 450-W Xenon lamp. For steady state emission as well as excitation and concentration dependent fluorescence measurements, samples were dissolved in THF. Variable temperature analysis was carried out in a solvent mixture of THF/water (9:1). Films were also prepared by spin-coating from THF on to quartz slides with a constant rotation of 2200 rpm for ~ 2 min. All measurements were made at 90° positions for solutions and 22.5^o in front face for films. The emission as well as excitation slit width was maintained at 1 nm throughout the experiments and the data was obtained in 'S_1/R_1' mode (to account for the variations in lamp intensity). Temperature dependent fluorescence was recorded using Peltier sample compartment having Peltier Sample Cooler F-3004 attached with Thermoelectric Temperature Controller (Model No. LFI-3751) with autotune PID supplied by Wavelength Electronics. The temperature was set manually for each reading and it was equilibrated for 10 min at each temperature before recording the spectrum. The tolerance range for each set temperature was maintained 0.5 ^{o}C. The samples were prepared by making the optical density 0.1 ± 0.05 at excitation wavelength (λ_{ex}~ 343 nm) in THF as well as THF/water (9:1). All samples were deoxygenated by purging it with gentle flow of nitrogen. All experiments were performed under identical conditions.

Scanning Electron Microscopy

SEM images were recorded using FEI, QUANTA 200 3D Scanning Electron Microscope with tungsten filament as electron source and the samples were provided with a thin gold/palladium (90:10) coating of 5 nm thickness using an Emitech Sputter Coater. The sample preparation method adopted was as follows. A solvent/nonsolvent combination of THF/water was first mixed in a 9:1 ratio, and then 10 mg of polymer was dissolved in 1 mL of this mixture resulting in a stable and clear polymer solution. 20 µL of this solution was placed on a glass slide and the solution was allowed to evaporate at room temperature in air. All films were prepared at atmospheric pressure without air flow.

Transmission Electron Microscopy

TEM images were recorded using a JEOL-JEM-3010 instrument at 80 KV. For TEM measurements, a drop of the polymer solution (10^{-4} M in THF/water (9:1) mixture) was deposited directly on Formvar coated copper grid. No staining treatment was performed for the measurement. A JEOL JEM-3010 electron microscope operating at 300 kV (Cs=0.6 mm, resolution 1.7 A°) was used for HR-TEM sample observation. A Gatan digital camera (model 794, Gatan 1024 x 1024 pixels, pixel size 24 x 24 μm) at 15000-80000 x magnifications was used to record micrographs.

2.3.3. Synthesis of short chain monomer (<u>I</u>sophoronediisocyanate – <u>H</u>ydroxyethyl - <u>P</u>yrene: IHP)

In a 50 mL two necked round bottom flask, isophorone diisocyanate (IPDI) (1 g, 4.5 x 10^{-3} mol) in 6 mL dry dimethylformamide (DMF) was taken and the contents were cooled with ice. 2-hydroxyethyl methacrylate (0.59 g, 4.5 x 10^{-3} mol) was added drop wise under nitrogen atmosphere over a period of 0.5 hr. The reaction was allowed to proceed under ice cold conditions for further 0.5 hr and then left stirring at room temperature for 2 hr. 2-3 drops dibutyltin dilaurate (DBTDL) was added as catalyst followed by drop wise addition of 1-pyrenemethanol (1.04 g, 4.5 x 10^{-3} mol) solution in DMF (5mL) to the reaction mixture under ice cold conditions within 0.5 hr and then slowly heated to 60 °C for 6 hr. The contents were poured into 300 mL water and extracted with dichloromethane. The extract was washed with plenty of water and then dried over anhydrous sodium sulphate. The solvent was removed under reduced pressure and dried in vacuum oven at 60 °C for 2 hr. Yield: 2.35 g (90 %). ^{1}H NMR (200 MHz, CDCl$_3$) δ ppm: 8.45-7.85 (m, 9H, Ar-**H**), 6.13, 5.58 (2s, 2H, **CH**$_2$=C), 5.78 (s, 2H, O**CH**$_2$ next to pyrene ring), 4.80-4.50 (m, N**H**), 4.29 (s, 4H, O-**CH**$_2$-**CH**$_2$-O of HEMA), 3.24, 2.86 (b, 3H, -**CH**-NH-COO and -**CH**$_2$-NH-COO of IPDI), 1.93 (s, 3H, -**CH**$_3$ of HEMA), 1.65-0.86 (other aliphatic protons). ^{13}C NMR (400 MHz, CDCl$_3$, δ ppm):166.17, 161.56, 155.94, 154.71, 134.87, 133.17, 130.45, 129.53, 128.32, 126.96, 126.58, 125.01, 124.30, 124.08, 123.49,121.93, 64.04, 62.28, 61.88, 61.53, 61.33, 53.75, 46.50, 45.82, 45.01, 43.54, 40.50, 35.21, 33.87, 30.63, 28.54, 26.49, 22.06, 17.23. FT-IR (cm^{-1}): 3331, 3043, 2955, 2916, 1718, 1637, 1530, 1456, 1386, 1307, 1299, 1233, 1168, 1058, 1027, 944, 896, 844, 813, 708. (MW: 584) FAB HRMS: 585.05 (M+1)

2.3.4. Synthesis of long chain monomer (Isophoronediisocyanate – PolyEthyleneGlycol -Pyrene: IPEGP)

Isophorone diisocyanate (IPDI) (1 g, 4.5×10^{-3} mol) in 6 ml dry DMF was taken in a 50 ml two necked round bottom flask and the contents were cooled with ice. Polyethyleneglycol methacrylate (1.62 g, 4.5×10^{-3} mol) was added drop wise under nitrogen atmosphere over a period of 0.5 hr. The reaction was allowed to proceed under ice cold conditions for further 0.5 hr and then left stirring at room temperature for 2 hr. 2-3 drops dibutyltin dilaurate (DBTDL) was added as catalyst followed by drop wise addition of 1-pyrenemethanol (1.04 g, 4.5×10^{-3} mol) to the reaction mixture under ice cold condition within 0.5 hr and then slowly heated to 60 ^{o}C for 6 hr. The contents were poured into 300 ml water and extracted with dichloromethane. The extract was washed with plenty of water and then dried over anhydrous sodium sulphate. The solvent was removed under reduced pressure and dried in vacuum oven at 60 ^{o}C for 12 hours. Yield: 3.10 g (84 %). ^{1}H NMR (200 MHz, CDCl$_3$) δ ppm: 8.39-7.78 (m, 9H, Ar-**H**), 6.10, 5.54 (2s, 2H, C**H**$_2$=C), 5.72 (s, 2H, OC**H**$_2$ next to pyrene ring), 5.02-4.73 (b, N**H**), 4.26 (s, 4H, O-C**H**$_2$-C**H**$_2$-O near to double bond), 3.70-3.58 (m, 20H, other O-C**H**$_2$-C**H**$_2$-O protons), 3.22, 2.82 (b, 3H, -C**H**-NH-COO and -C**H**$_2$-NH-COO of IPDI), 1.91 (s, 3H, -C**H**$_3$ of HEMA), 1.62-0.80 (other aliphatic protons). ^{13}C NMR (400 MHz, CDCl$_3$, δ ppm): 167.37, 156.94, 155.75, 136.09, 134.26, 131.55, 131.11, 130.61, 129.42, 128.04, 127.67, 127.31, 125.99, 125.91, 125.81, 125.34, 125.15, 124.56, 122.99, 72.71, 70.48, 69.58, 69.08, 63.86, 46.84, 46.12, 44.58, 36.28, 34.98, 31.74, 27.58, 23.22, 18.31. FT-IR (cm^{-1}): 3327, 3047, 2951, 2903, 1718, 1641, 1530, 1460, 1381, 1351, 1298, 1241, 1169, 1115, 1038, 951, 848, 810, 772, 716. (MW: 804) FAB-HRMS: 805.34 (M+1).

2.3.5. Free Radical Polymerization of IHP (PIHP)

IHP-monomer (1 g, 1.23×10^{-3} mol) and benzoyl peroxide (BPO) (0.009 g, 3.69×10^{-5} mol) were taken in DMF (5 mL) in a 10 mL round bottom (RB) flask provided with a water condenser. The reaction mixture was purged with nitrogen for 0.5 hr. The polymerization was carried out by stirring the contents at 65 ^{o}C for 20 hr. The viscous liquid was cooled and precipitated in methanol. Yield: 0.67 g (67 %). THF GPC: M_n=1.60x10^{4}, Đ=2.02. ^{1}H-NMR (200 MHz, CDCl$_3$) δ ppm: 8.01-7.94 (m, 9H, Ar-**H**), 5.69 (b, 2H, OC**H**$_2$ next to pyrene ring), 4.30 (b, N**H**), 4.12-3.71 (b, 4H, O-C**H**$_2$-OC**H**$_2$-O of HEMA), 2.89-0.86 (aliphatic protons of IPDI). ^{13}C NMR (400MHz, CDCl$_3$, δ

ppm): 156.89, 155.68, 131.64, 131.15, 130.69, 129.52, 128.11, 127.72, 126.02, 125.38, 124.63, 123.08, 67.97, 65.21, 64.97, 54.86, 46.91, 46.17, 44.68, 41.72, 36.40, 34.96, 31.79, 29.66, 27.61, 25.61, 23.28, 18.29. FT-IR (cm^{-1}): 3379, 3043, 2955, 1718, 1530, 1465, 1386, 1356, 1302, 1237, 1137, 1110, 1058, 1023, 896, 844, 800, 770, 708, 682.

2.3.6. Free Radical Polymerization of IPEGP (PIPEGP)

IPEGP (1g, 1.23 x 10^{-3} mol) and benzoyl peroxide (0.009 g, 3.69 x 10^{-5} mol) were taken in THF (5ml) in a 10 ml round bottom flask provided with a water condenser. The reaction mixture was purged with nitrogen for 10 min. The polymerization was carried out by stirring the contents at 65 $^{\circ}$C for 12 hr. The viscous liquid was cooled and precipitated in methanol. Yield: 0.61g (61%). CHCl$_3$ GPC: M$_n$=1.45x10^{4}, Đ=1.6. ^{1}H NMR (200 MHz, CDCl$_3$) δ ppm: 8.37-7.87 (m, 9H, Ar-**H**), 5.80 (s, 2H, O**CH$_2$** next to pyrene ring), 5.02-4.73 (b, N**H**), 4.16, 3.61 (b, 24H, O-**CH$_2$**-**CH$_2$**-O protons), 3.23, 2.91 (b, 3H, -**CH**-NH-COO and -**CH$_2$**-NH-COO of IPDI), 1.82-0.86 (other aliphatic protons). ^{13}CNMR (400 MHz, CDCl$_3$, δ ppm):177.36, 156.95, 155.74, 131.57, 131.17, 130.66, 129.47, 128.12, 127.73, 127.37, 126.05, 125.43, 124.65, 123.09, 72.76, 71.48, 69.60, 68.55, 64.89, 63.86, 61.50, 54.93, 53.85, 46.91, 46.18, 44.72, 41.74, 36.39, 35.04, 31.80, 27.61, 23.26. FT-IR (cm^{-1}): 3376, 2952, 1727, 1535, 1464, 1386, 1351, 1306, 1242, 1110, 1036, 953, 843, 777, 713.

2.3.7. Synthesis of random copolymer PS-r-PIHP

IHP (0.47 g, 8 x 10^{-4} mol), styrene (0.75 g, 7.2 x 10^{-3} mol) and benzoylperoxide (0.06 g, 2.5 x 10^{-5} mol) were taken in THF (3 mL) in a 10 mL round bottom flask provided with a water condenser. The reaction mixture was purged with nitrogen for 10 min. The polymerization was carried out by stirring the contents at 65 $^{\circ}$C for 15 hr. The viscous liquid was cooled and precipitated into methanol. Yield: 0.72 g (60%). CHCl$_3$ GPC: M$_n$=14700, Đ=1.89. ^{1}H NMR (200 MHz, CDCl$_3$) δ ppm: 8.37-7.88 (b, 9H, Ar-**H** of pyrene), 7.22-6.25 (b, 5H, Ar-**H** of styrene), 5.81 (s, 2H, -O**CH$_2$** next to pyrene ring), 4.30 (s, N**H**), 3.74 (b, 4H, O-**CH$_2$**-**CH$_2$**-O of HEMA), 3.38, 2.89 (b, 3H, -**CH**-NH-COO and -**CH$_2$**-NH-COO of IPDI), 1.93-0.50 (other aliphatic protons). ^{13}C NMR (400 MHz, CDCl$_3$) δ ppm: 176.24, 156.92, 155.72, 145.28, 131.67, 131.19, 130.71, 129.53, 128.13, 127.75, 126.05, 125.46, 124.66, 123.09, 67.98, 65.24, 65.01, 62.98, 62.23, 54.87, 53.96, 46.93, 46.20, 44.71, 41.74, 40.39, 38.88, 36.41, 35.05, 31.80, 29.67, 27.62, 23.28,

18.34. FT-IR (cm^{-1}): 3415, 3058, 3027, 2926, 2851, 1725, 1602, 1515, 1454, 1387, 1369, 1304, 1229, 1115, 1031, 909, 849, 759, 701, 539.

2.3.8. Synthesis of polystyrene macroinitiator by ATRP

Ethyl 2-bromo propionate (0.1 g, 5.5 x 10^{-4} mol) and styrene (2.87 g, 2.76 x 10^{-2} mol) were taken in a 10 mL round bottom flask. It was sealed by rubber septum and purged with nitrogen for 15 min. The reaction mixture was transferred to a schlenk flask containing Cu(I)Br (0.079 g, 5.5 x 10^{-4} mol), bipyridine (0.26 g, 1.7 x 10^{-3} mol) by degassed syringe. Further the schlenk flask was evacuated by three freeze-pump-thaw cycles. Then it was heated in an oil bath at 85 ^{o}C for 4 hr under nitrogen atmosphere. The viscous liquid was dissolved in THF and was passed through an alumina column to remove the copper catalyst, and then was concentrated and precipitated in methanol. Yield: 2.60 g (90 %). CHCl$_3$ GPC: M$_n$=3.50x10^3. Đ=1.18.

2.3.9. Synthesis of block copolymer PS-b-PIHP

Polystyrene macroinitiator (0.035 g, 1 x 10^{-5} mol) and IHP (0.59 g, 1 x 10^{-3} mol) was dissolved in 2mL dry DMF in 10 mL round bottom flask fully stoppered with rubber septum. It was then purged with nitrogen for 15 min. This mixture was transferred to Schlenk tube containing Cu(I)Br (0.0015 g, 1 x 10^{-5} mol) and PMDETA (0.0021 g, 1 x 10^{-5} mol). It was then evacuated by 3 freeze-pump-thaw cycles. Slowly the reaction mixture was heated upto 85-90 ^{o}C. Then the reaction continued at this temperature for 20 hr with continuous stirring. The viscous liquid was precipitated in methanol. Yield: 0.400 g (65 %). CHCl$_3$ GPC: M$_n$=1.02x10^4, Đ=1.86. ^{1}H NMR (200 MHz, CDCl$_3$) δ ppm: 8.37-7.88 (b, 9H, Ar-**H** of pyrene), 7.22-6.25 (b, 5H, Ar-**H** of styrene), 5.71 (s, 2H, -OC**H**$_2$ next to pyrene ring), 4.32 (b, N**H**), 4.10-3.73 (b, 4H, O-C**H**$_2$-C**H**$_2$-O of HEMA), 3.38, 2.86 (b, 3H, -C**H**-NH-COO and -C**H**$_2$-NH-COO of IPDI), 1.93-0.50 (other aliphatic protons). ^{13}C NMR (400 MHz, CDCl$_3$) δ ppm: 177.48, 157.07, 155.82, 145.22, 131.50, 131.10, 130.58, 129.44, 128.06, 127.67, 126.04, 125.41, 124.56, 122.93, 67.98, 65.01, 63.72, 61.61, 54.87, 46.93, 46.01, 44.72, 41.74, 40.42, 36.43, 35.09, 31.76, 29.71, 27.61, 25.61, 23.25, 18.31. FT-IR (cm^{-1}): 3401, 3028, 2951, 2925, 1722, 1859, 1606, 1522, 1456, 1384, 1370, 1335, 1306, 1236, 1155, 1061, 1031, 975, 850, 769, 677.

2.4. Results and Discussions

2.4.1. Synthesis and Characterization

Two methacrylate monomers incorporating the fluorophore pyrene at the terminal was used for the study – one having a short ethyleneoxy unit and the other a longer polyethyleneglycol spacer segment connecting the polymerizable methacrylate with the pyrene through hydrogen bondable urethane linkage. The monomers were named **IHP** (**I**PDI-**H**EMA-**P**yrene) and **IPEGP** (**I**PDI-**P**oly**E**thylene**G**lycol-**P**yrene) respectively, highlighting the varying spacer length. The synthesis of the monomer **IHP** is given in scheme-2.1. The synthesis involved the one-pot coupling of one equivalent of isophorone diisocyanate (IPDI) with one equivalent respectively of hydroxyethyl methacrylate (HEMA) for **IHP** or polyethyleneglycol methacrylate (PEGMA) for **IPEGP**, followed by reacting with one equivalent of 1-pyrenemethanol in dry DMF.[31]
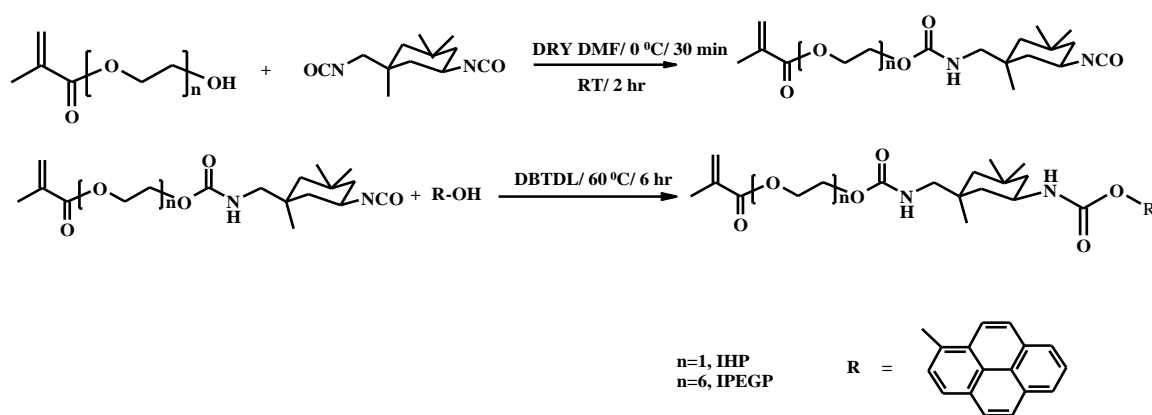
Scheme-2.1: Synthesis of monomers.

The two monomers were polymerized using 3 mol % benzoyl peroxide (BPO) as initiator in tetrahydrofuran (THF) as solvent as shown in scheme-2.2. Apart from the variation of the spacer length connecting the fluorophore to the polymer backbone, the architecture of incorporation of the pyrene in the polymer was also varied by synthesizing a random copolymer **PS-r-PIHP** (scheme-2.2) as well as a block copolymer **PS-b-PIHP** of **IHP** with styrene (scheme-2.3). The feed ratio of styrene to **IHP** was 9:1 for the random copolymer **PS-r-PIHP** which was polymerized under identical conditions as that for the homopolymers. The block copolymer **PS-b-PIHP** of **IHP** was synthesized using polystyrene macroinitiator via ATRP route using PMDETA as ligand and Cu(I)Br as catalyst.
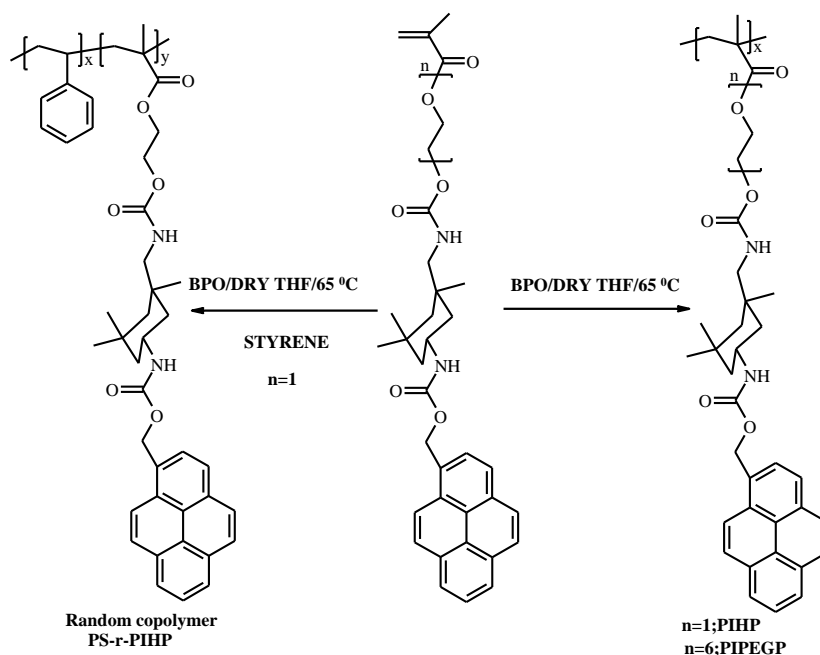
Scheme-2.2: Polymerization procedure for homo and random copolymers.
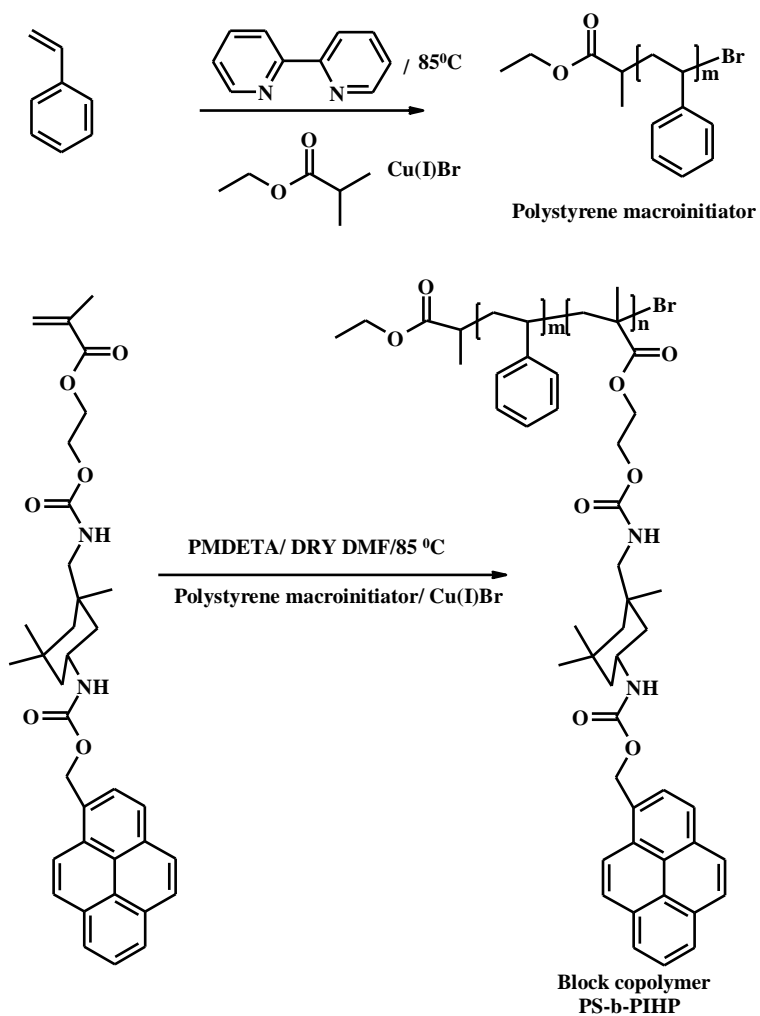
Scheme-2.3: Synthesis of block copolymer **PS-b-PIHP**.
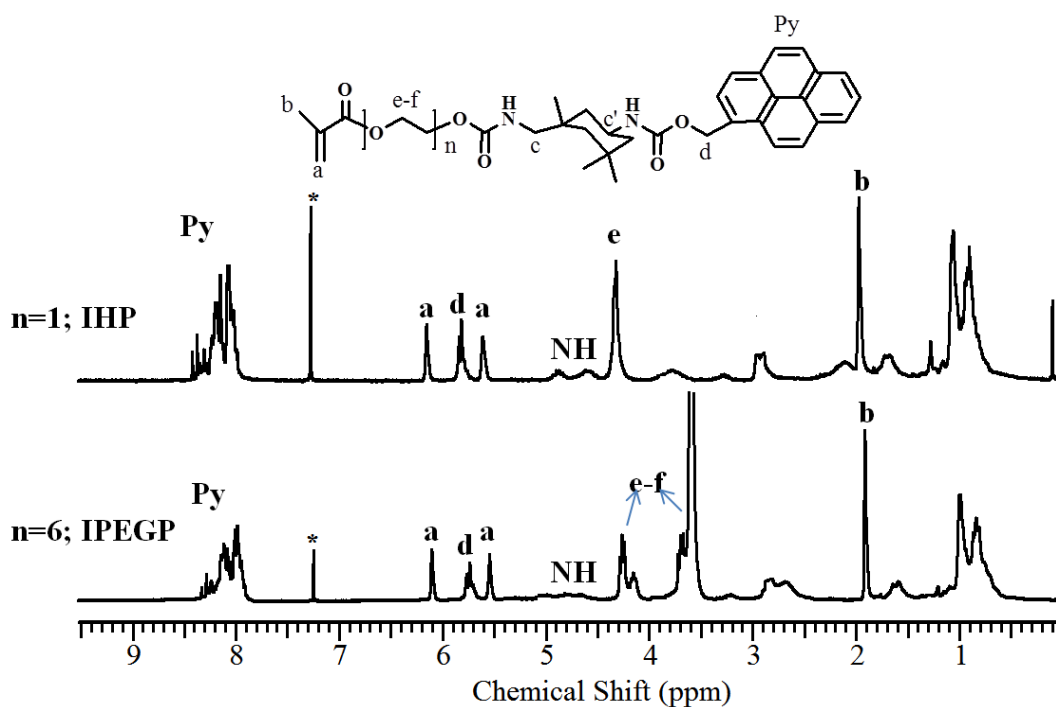
Figure-2.4: ^{1}H NMR spectra of short chain monomer **IHP** and long chain monomer **IPEGP**.

The monomers and polymers were structurally characterized by ^{1}H-NMR, ^{13}C-NMR, FTIR and mass spectroscopy. Figure- 2.4 compares the proton NMR spectra of the monomers **IHP** and **IPEGP**. Figure-2.5 compares the proton NMR spectra of the homo and copolymers. The peaks at ~6.10 and 5.54 ppm in the ^{1}H-NMR spectra corresponded to the methacrylic protons and the complete disappearance of these peaks confirmed the formation of polymers. ^{13}C NMR spectra of all polymers are given in figure-2.6. In the random **PS-r-PIHP** and block **PS-b-PIHP** copolymers, the peaks at 7.22-6.25 ppm corresponded to aromatic protons of styrene and peaks at 8.37-7.88 ppm corresponded to aromatic protons of pyrene. The incorporation of styrene and pyrene units in the random copolymer **PS-r-PIHP** was calculated by integrating the peak at 8.37-7.88 corresponding to the 9 aromatic protons of pyrene and the peak at 7.22-6.25 corresponding to the 5 aromatic protons of styrene. From the integration an incorporation of styrene and **IHP** was found to be ~9.24:0.76 (9:1). The number of repeating units of the **IHP** block in block copolymer **PS-b-PIHP** was calculated using the ^{1}H NMR spectra of the block copolymer **PS-b-PIHP** as well as the M_n value of the polystyrene macroinitiator (PS-macro).

52
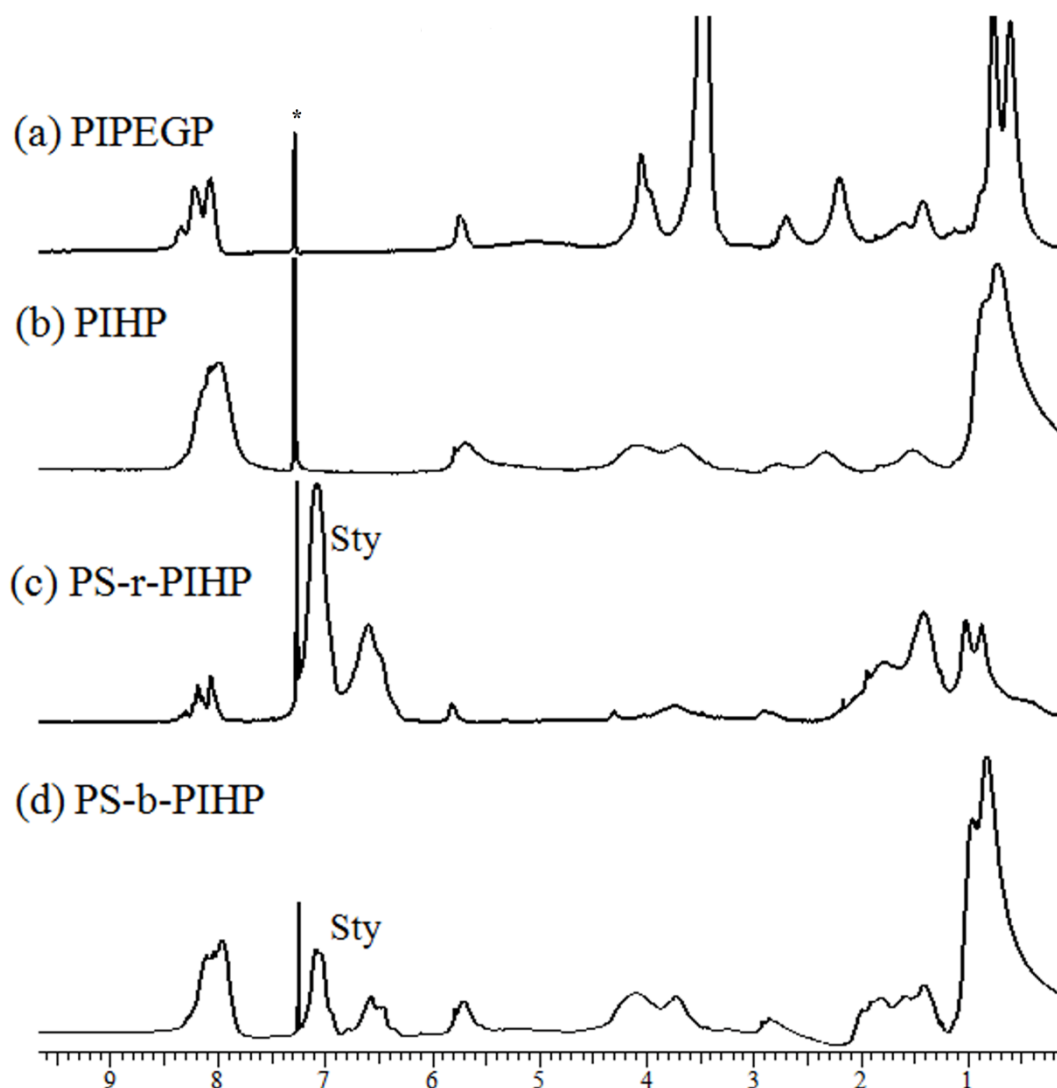
Figure-2.5: ^{1}H NMR spectra of the polymers (a) **PIPEGP** (b) **PIHP** (c) **PS-r-PIHP** and (d) **PS-b-PIHP**.

Table-2.1 gives the molecular weight details obtained from GPC and the chromatograms are shown in figure-2.7. The details of the calculation are as follows. The repeating unit of the polystyrene macroinitiator calculated based on the GPC molecular weight measurements was ~33. The block copolymer **PS-b-PIHP** had molecular weight (M_n) 1.02×10^4 with polydispersity in the range 1.86. The integral value for the nine aromatic protons of pyrene was 9 and that for five aromatic protons of styrene in the styrene block was 7.36. So the ratio of the integral for one proton of pyrene in **IHP** block to that in styrene block was 0.679. The degree of polymerization (DP) of the pyrene block in **[PS$_{33}$-b-PIHP$_x$]** was a factor of 0.679 times that of the polystyrene block. Knowing the DP of polystyrene as 33, the DP of pyrene block was

calculated using the equation DP of pyrene block = [DP of Pyrene/DP of PS] (from NMR data) x [DP of PS] (from GPC data). (0.679 x 33 = 22.42). Therefore the degree of polymerization of the **IHP** block in the **[PS-b-PIHP]** was found to be ~22. So the block copolymer could be represented as **[PS$_{33}$-b-PIHP$_{22}$].** This is an approximate representation only since the hydrodynamic volume of polystyrene will be different from that of urethane methacrylate segment containing the pyrene pendant unit.
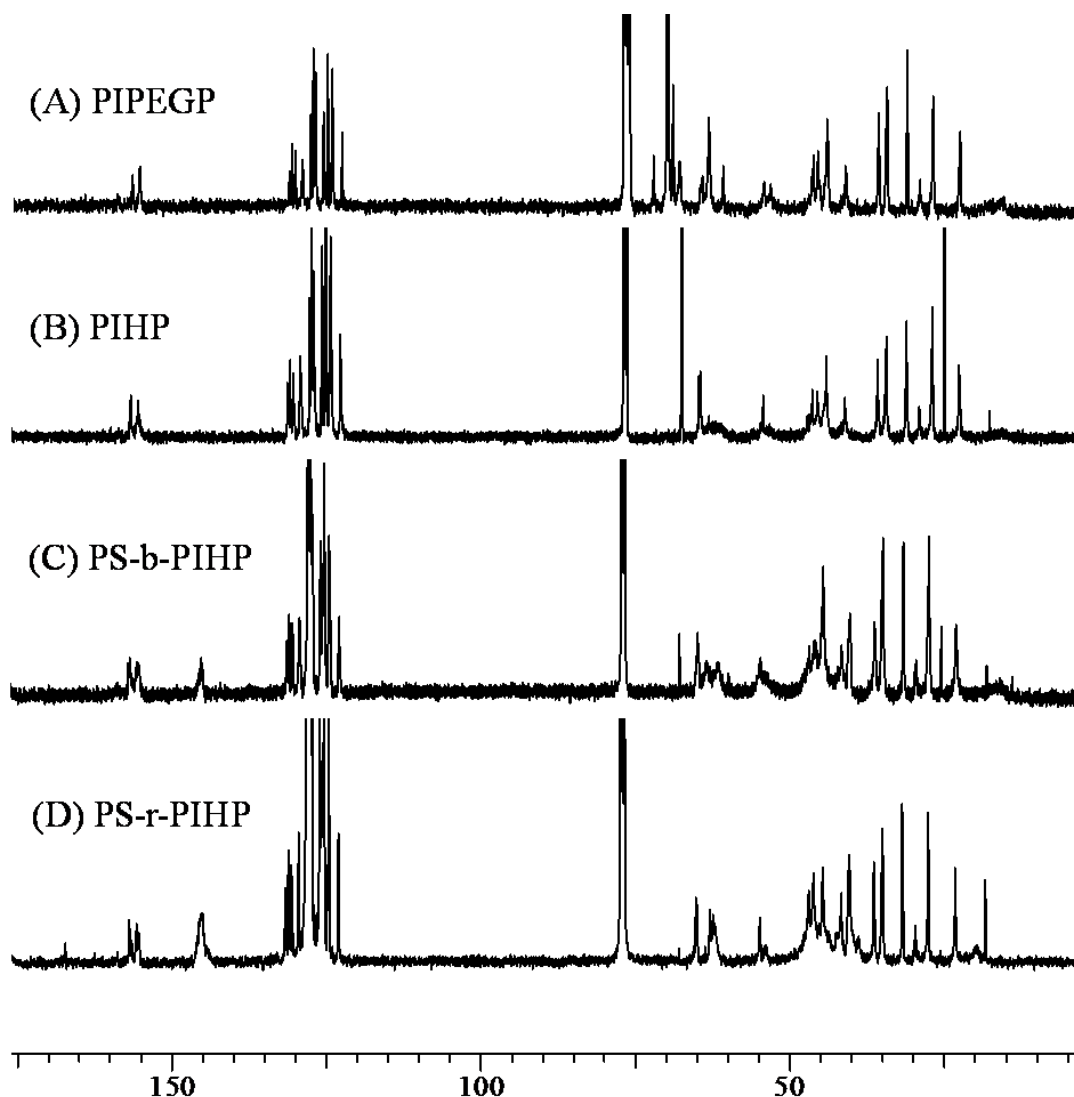
Figure-2.6: ^{13}C NMR spectra the polymers (a) **PIPEGP** (b) **PIHP** (c) **PS-r-PIHP** and (d) **PS-b-PIHP**.
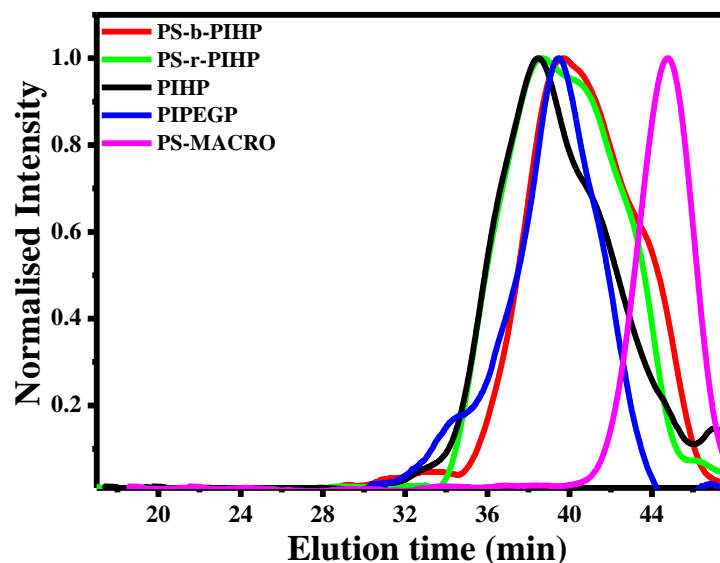
Figure-2.7: GPC chromatogram of all polymers.

Table-2.1: Molecular weight, Polydispersity indices (Đ), thermal data, yield etc

Sample	M_n	M_w	Đ	Yield (%)[a]	10 Wt. % Loss (°C)[b]	T_g (°C)[c]
PIHP	1.60×10^4	3.26×10^4	2.02	67	275	128
PIPEGP	1.45×10^4	2.40×10^4	1.65	61	285	39
PS-macroinitiator	3.45×10^3	4.07×10^4	1.18	90	346	79
PS-b-PIHP	1.02×10^4	1.90×10^4	1.86	65	299	83, 153
PS-r-PIHP	1.47×10^4	2.78×10^4	1.89	60	301	110

a. Final yield of the reprecipitated polymer
b. Temperature represents 10 % weight loss in TGA measurements at heating rate of 10 °C/min under nitrogen
c. Determined by DSC analysis

The thermal properties of the polymers were studied using TGA and DSC. Table-2.1 gives the 10 wt % loss temperature obtained from TGA and the thermograms are given in figure 2.8.
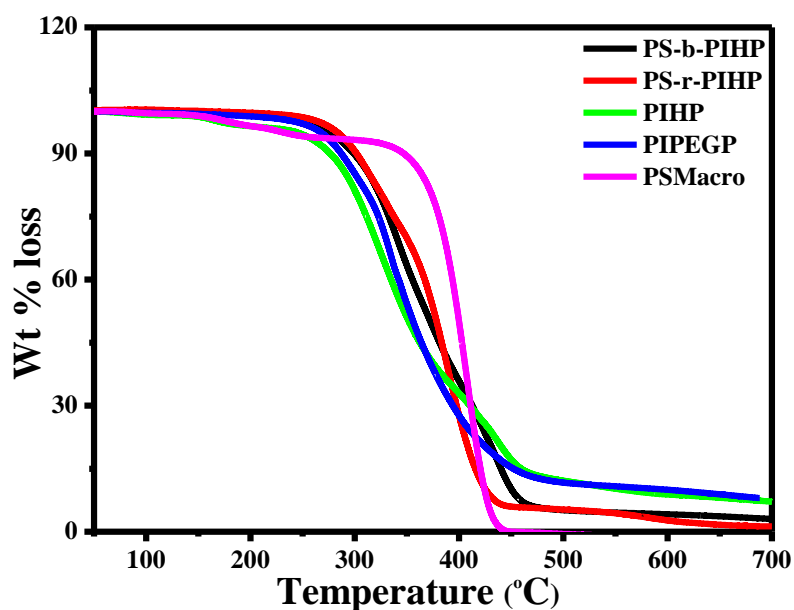
Figure-2.8: TGA Plot of all polymers.
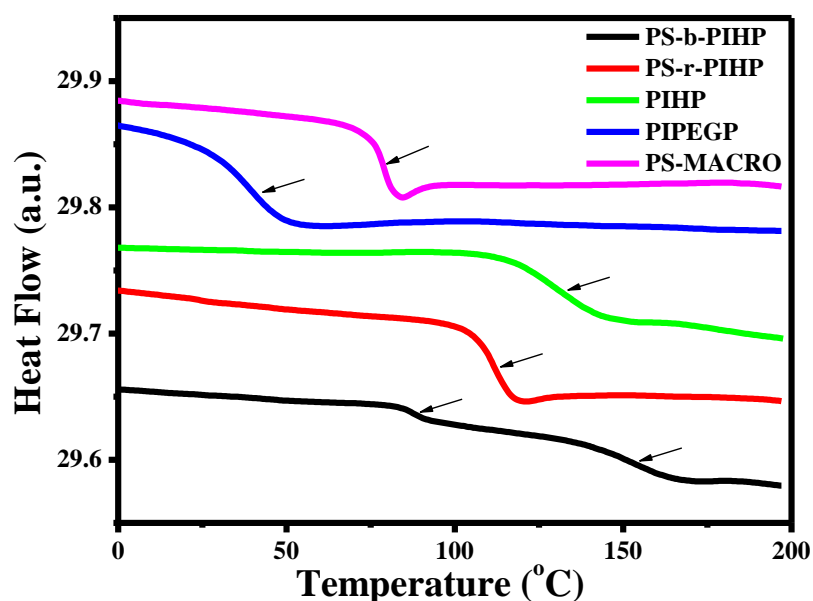
Figure-2.9: DSC thermogram of all polymers.

The DSC plots of all the polymers are given in the figure-2.9. The PS macroinitiator had a T_g ~79 ^{o}C. Normally the T_g for PS is ~100 ^{o}C; however the low molecular weight of the macroinitiator resulted in low T_g value. The DSC thermograms showed that the polymers were all amorphous with the short chain homopolymer **PIHP** exhibiting a T_g at 128 ^{o}C while the long chain homopolymer **PIPEGP** had T_g ~39 ^{o}C. The incorporation of the highly flexible polyethyleneglycol units reduced the T_g drastically by ~90 ^{o}C for **PIPEGP** compared to **PIHP.** The random copolymer **PS-r-**

PIHP exhibited a single T_g at 110 ^{o}C, which was between that for the two individual components. This was slightly higher than the calculated value for T_g which was 102 ^{o}C. Increased rigidity (afforded by the rigid hydrogen bonding as well as by the pyrene units) has been known to increase the T_g of the system above the calculated value.[32, 33] On the other hand, the block copolymer **PS-b-PIHP** showed two T_g – one at 83 ^{o}C corresponding to that of PS and the other at 153 ^{o}C corresponding to that of pyrene urethane methacrylate. The existence of two T_g as against a single T_g for the random copolymer **PS-r-PIHP** also confirmed the formation of block **PS-b-PIHP** consisting of PS and pyrene urethane methacrylate blocks. However, the T_g values for both the blocks were higher than that for the individual blocks observed in their corresponding homopolymers (PS macroinitiator and PIHP). This could be due to higher rigidity afforded by the phase separation of the blocks in the block copolymer **PS-b-PIHP** at higher temperatures.

2.4.2. Photophysical studies

The photophysical studies of all the polymers were recorded in THF at a slit width of 1 nm. Figure-2.10 shows the absorption (normalized) and emission spectra of the polymers recorded by exciting at the λ_{max} of 343 nm for 0.1 OD solutions. The absorption spectra of all the polymers showed the three peaks at 312, 326 and 343 nm corresponding to the characteristic vibronic transitions of pyrene.[23, 24] The emission spectra of the polymers showed characteristic peaks at 375-395 nm regions corresponding to the pyrene monomer emission and a broad red shifted peak around 480 nm corresponding to pyrene excimer emission.[34] The absorption and emission λ_{max} values for the four polymers are compared along with their quantum yields in table-2. The quantum yields were measured by a relative method using quinine sulfate as the standard (Q_r= 0.546 in 0.1M H_2SO_4) for nitrogen purged polymer samples. The quantum yield was calculated using the following equation.[35]

$$Q_s= Q_r \,[F_s \, A_r \,/\, F_r \, A_s] \,(n_s/n_r)^2$$

Where Q_s is the fluorescence quantum yield of the sample, F is the area of the emission peak, n is the refractive index of solution, and A is the absorbance of the solution at the exciting wavelength. The subscripts r and s denote reference and sample respectively.
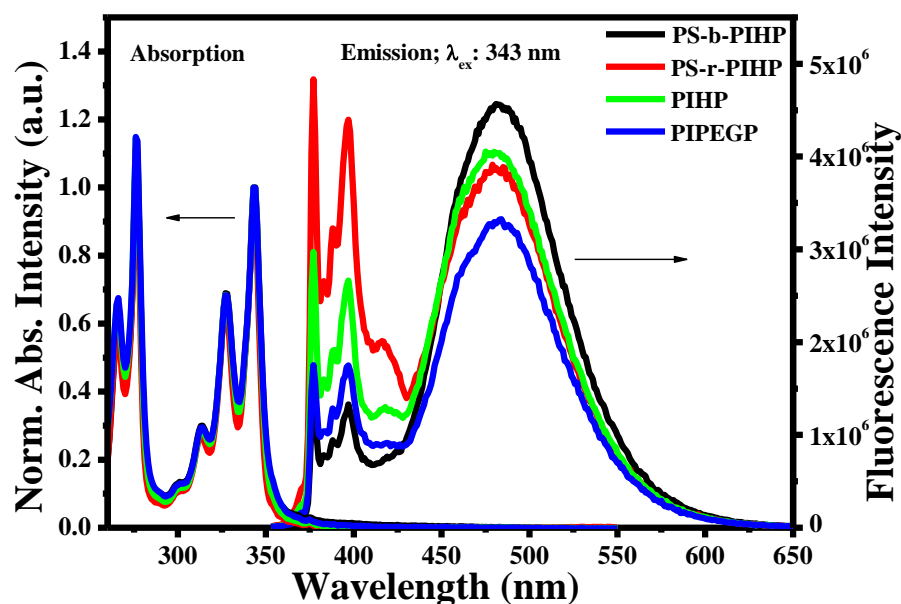
Figure-2.10: Combined plot for the UV-Vis Absorption (normalised) and emission spectra (λ_{ex}-343) for 0.1 OD solution in THF for all polymers.

       From table-2.2 it can be seen that, the random copolymer **PS-r-PIHP** which had very low pyrene loading, had the highest quantum yield of Q= 0.58. The short chain homopolymer **PIHP** and its block copolymer with styrene **PS-b-PIHP** had similar quantum yields of 0.52 and 0.50 respectively and the lowest quantum yield was that for the long chain homopolymer **PIPEGP** (Q= 0.4). The high total emission quantum yield for the random copolymer **PS-r-PIHP** was due to the fact that (1) the total emission was very much quenched in the other polymers, although they had higher excimer emission and (2) the random copolymer **PS-r-PIHP** had higher intensity for the monomer emission in the region 370-420 nm which has higher coefficient of emission than the excimer emission. In fact, the methacrylate monomers for the long and short chain polymers (i.e. **IHP** and **IPEGP**) had much higher quantum yields compared to their respective polymers again for the same reason of monomeric emission being of higher intensity. Upon polymerization, their pyrene monomer emission was very much quenched. The amplitude of excimer emission at 480 nm was different for the four polymers; the relative efficiency of the excimer fluorescence is usually expressed by the ratio I_E/I_M (the ratio of the integrated area of excimer region (500-530 nm) and monomer emission region (372-378 nm). These values are also given in table-2.2.

Table -2.2: Photophysical properties of Polymers in THF ~0.1 OD and in film (given in brackets).

Sample	Absorbance λ_{max} (nm) [Film]	Emission λ_{max}^a (nm) [Film]	Q_{FL}^b	I_E/I_M^c (Film)
PIHP	343 (351)	377, 383, 388, 397, 419, 480 (475)	0.52	8.02 (38.2)
PIPEGP	343 (348)	377, 383, 388, 396, 415, 484 (378, 384, 390, 399, 460)	0.40	11.5 (17.5)
PS-b-PIHP	344 (351)	377, 383, 388, 396, 413, 483 (378, 389, 396, 460)	0.50	20.4 (23.5)
PS-r-PIHP	343 (351)	377, 383, 388, 397, 413, 480 (377, 385, 390, 397, 418, 454)	0.58	4.81 (3.92)

a. Excitation wavelength is 343 nm in THF and film.

b. Calculated using 0.1 OD quinine sulphate solution as standard. Excitation wavelength is 343 nm in THF as solvent.

c. I_E/I_M determined by taking the integrated area of excimer (500-530 nm) and monomer (372-378 nm) emission

The random copolymer **PS-r-PIHP** had the lowest excimer efficiency, which was not surprising since the labeling of pyrene was very low (9:1 PS:Pyrene) and the probability of locating a properly oriented pyrene in the neighbourhood to form the excimer configuration was lower. This is also in conformation with the observation from the proton NMR spectra which showed well-resolved peaks for the aromatic protons of the pyrene in the random copolymer **PS-r-PIHP** which indicated less interaction between the pyrene units. The block copolymer **PS-b-PIHP** exhibited higher excimer emission efficiency than even its own homopolymer **PIHP**, which was rather surprising. Their total emission quantum yields were similar but **PIHP** had an I_E/I_M of 8.01 whereas the corresponding value for the block **PS-b-PIHP** was 20.4. They also show that the block **PS-b-PIHP** had lower monomer emission as well as higher excimer

emission, both factors contributing to the overall higher I_E/I_M value for the latter. The reason for this could be attributed to the presence of the rigid polystyrene segment in the block copolymer **PS-b-PIHP** leading to higher tendency of pyrene aggregation in solution. Similarly comparing the two homopolymers, **PIHP** and **PIPEGP** the latter had very low emission quantum yields but its excimer emission efficiency was higher compared to the former. Here also the origin of the higher excimer emission could lie in the higher tendency of aggregation of the hydrophobic pyrene units in presence of the highly hydrophilic polyethyleneglycol segment. However, these effects were totally different in the solid state as will be explained in the following section.
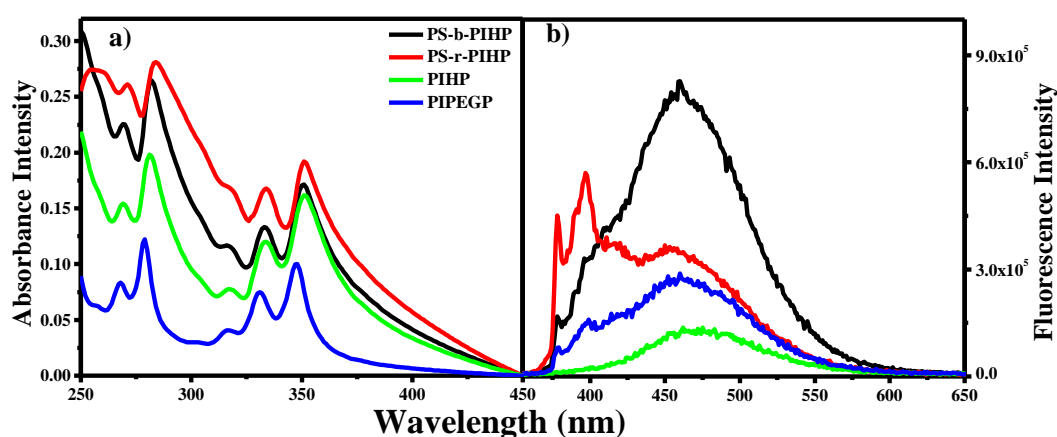
Figure-2.11: Combined plot for the (**a**) UV-Vis Absorption and (**b**) emission spectra (λ_{ex}-343) for polymers in the solid state.

Figure-2.11 shows the UV-Vis absorption and emission spectra of thin spin coated films of the four polymer samples. The films were prepared by spin-coating 60 micro litres of 2.5×10^{-3} M solution from THF onto quartz slides and the OD was in the range of 0.1 to 0.2. The absorption peak maxima was red shifted by 5-8 nm and the onset of absorption also was red shifted for all the films compared to that in THF indicating the presence of ground state aggregates. Figure-2.11b shows the emission spectra of the film samples upon excitation at 343 nm and the peak maxima values are given in table-2.2. The short chain homopolymer **PIHP** exhibited only excimer emission, albeit slightly blue shifted (475 nm) compared to that in its THF solution (480 nm). The monomer emission in the 370-420 nm was completely quenched. The random copolymer **PS-r-PIHP** represented the other extreme situation with more monomer emission than excimer emission and also the excimer emission peak maxima was blue shifted by 26 nm from 480 nm in THF to 456 nm in the solid state. The block **PS-b-PIHP** and the long chain homopolymer **PIPEGP** had very small monomer emission

peaks which appeared as shoulders to the excimer emission with peak maxima at 460 nm. A clear difference could be observed in the emission behaviour of the block **PS-b-PIHP** and **PIHP** homopolymer in that the emission was much more quenched in **PIHP** than that in the block even though both the films had almost same OD in absorption. It suggested a shielding of the IHP block by the styrene block from concentration quenching. Also, unlike the I_E/I_M values in THF, in the solid state **PIHP** had the highest I_E/I_M value as there was no monomer emission in this case. Normally it has been suggested that pyrene moieties that are in parallel or sandwich orientation brought about either during diffusional interaction (in solution) or from ground state aggregates give rise to emission in the 470 nm and beyond.[24] On the other hand, pyrene moieties that are constrained as in a film or adsorbed on surfaces do not attain an energy minimum sandwich orientation but are slightly displaced and they emit in the 440 nm range. These are known as the dimeric emitting species.[25, 36] The blue shift observed in the emission of the film samples is due to contribution from these type of blue emitting dimeric species also. The extent of dimeric emitting species differed in the different polymer architectures. For instance, the blue shift was maximum in the random copolymer **PS-r-PIHP**. This could be understood to be due to the presence of styrene units which prevent the favourable orientation of the pyrenes and unlike in solution this orientation is frozen-in in the solid state. **PIHP** had the lowest blue shift indicating that the pyrene aggregates in this sample were in the correct (sandwich) orientation for excimer emission; however their emission intensity was reduced due to concentration quenching.

Figure-2.12 shows the variable concentration absorbance spectra of all the polymers. The short chain homopolymer **PIHP** exhibited a new red shifted peak at 395 nm at higher concentrations corresponding to the presence of ground state aggregates.[31] A similar effect was observed for long chain homopolymer **PIPEGP**, random copolymer **PS-r-PIHP** and block copolymer **PS-b-PIHP** also. Figure-2.13 shows the variable concentration emission spectrum. The total emission (monomer + excimer) increased initially followed by concentration quenching. A plot of I_E/I_M remained invariant until a concentration of ~ 10^{-4} M and showed a drastic change thereafter indicating that at lower concentrations (<10^{-4} M) the excimer emission was due to intramolecular interactions whereas at higher concentrations (>10^{-4} M) intermolecular interactions also became predominant. A representative plot of the I_E/I_M as a function of

log of the concentration for the random polymer **PS-r-PIHP** is given in the inset of figure-2.13 highlighting this aspect.
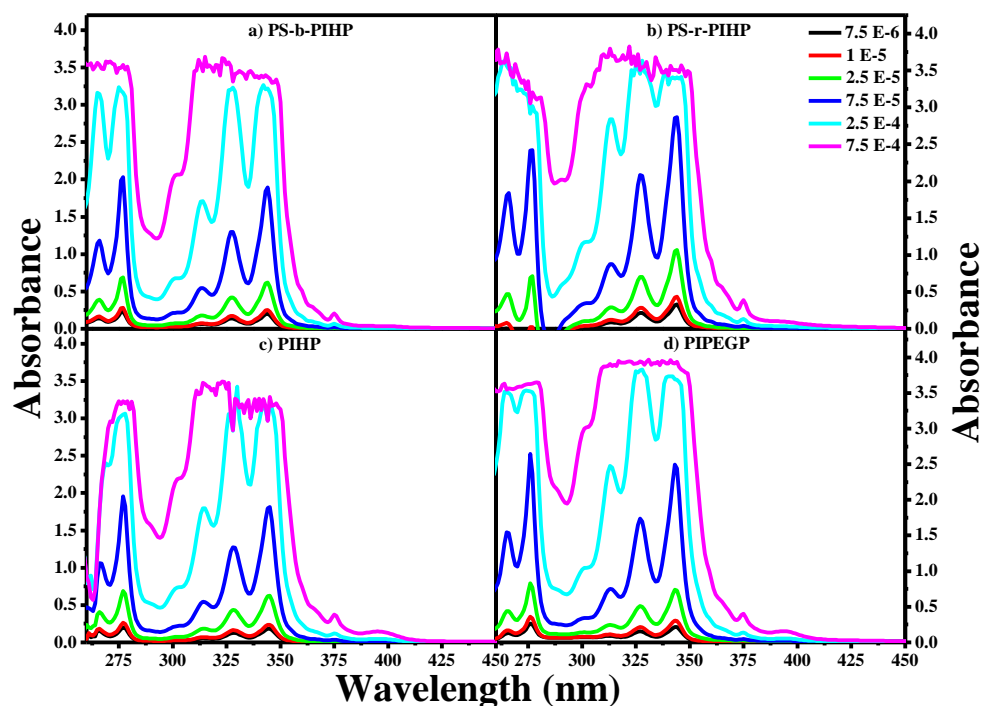
Figure-2.12: Variable concentration absorption spectra of all polymers in THF in the oncentration range of 7.5 x 10^{-4} to 1 x 10^{-6} M.

Figure-2.13: Variable concentration emission spectra of all polymers in THF in the concentration range of 7.5 x 10^{-4} to 1 x 10^{-6} M.

2.4.3. Variable Temperature Studies

Variable temperature emission was recorded in THF/water (9:1) as solvent by varying the temperature from -10 to 50 °C and at two different excitation wavelengths – 343 nm and 395 nm. (These measurements were carried out in THF alone as solvent also and the observation was similar to that in the THF/water (9:1) mixture. Since all polymers exhibited interesting morphologies – as will be discussed later, in THF/water (9:1) combination, the variable temperature measurement in this solvent mixture is reported here). Figure-2.14 shows the variable temperature (-10 to 50 °C) emission spectrum of the polymers obtained upon exciting at 343 nm. The lowest and the highest temperature plots are shown in bold lines. A blue shift of ~ 2-8 nm (485 – 477 nm) was observed in the emission λ_{max} as the temperature was increased from -10 to 50 °C. From the figure it can be seen that the total emission (monomer + excimer) decreased for all polymers with increase of temperature, although the rate of decrease of the monomer and excimer emission was different at different temperatures for the four polymers.

Figure-2.15 (a-c) compares the integrated area of excimer region (I_E: 500-530 nm), integrated area of monomer region (I_M: 372-378 nm) and I_E/I_M values as a function of temperature for the 343 nm excitation. The dotted lines are for guidance of the eye only. The I_E values showed a slight increase initially with temperature and then decreased steadily whereas the I_M values showed a steady decrease with a slow levelling off at higher temperature. The I_E/I_M ratio reflected this behavior as an initial steady increase followed by a levelling off at higher temperature (beyond 30 °C). The emission spectra were also recorded upon excitation at 395 nm as a function of temperature and the plots are given in the figure-2.16. The variable temperature measurements are very useful in distinguishing between the excimer emission having a diffusional origin with those having its origin from ground state aggregates. As it has been discussed in literature,[27] the former decreases in intensity at low temperature whereas the latter is stabilized at low temperature and therefore its emission intensity is enhanced. The 343 nm excitation excites both "monomer" emission in the 370-420 nm region as well as "excimer" emission in the 430-550 nm region. The excimer band itself has been shown to have two regions – the 470-490 nm region (true excimer emission) as well as the 430-460 nm region (excitation of dimers formed in the ground state). The 395 nm excitation preferentially excites the excimer emitting in the 440-460 nm region. Figure-2.15 (d) compares the integrated area of the emission beyond 420 nm as a function of

temperature for 395 nm excitation for the four polymers. The emission at ~ 440 nm was highest at the lowest temperature of -10 °C and this emission intensity decreased steadily with increase in temperature for all polymers. This was in contrast with the initial increase (increased excimer emission due to increased collisional encounter) followed by decrease for the I_E values. At low temperatures the excimer emission has more contribution from ground state aggregates since these are more stabilized and the collisional encounters of excited monomer with ground state monomers are low.[27] Upon increasing the temperature, diffusional encounters increase; therefore, the excimeric emission in the 470-490 nm region increases, at the expense of the emission in the 440-460 nm region. Since the 343 nm excitation excites both the monomer emission as well as the excimer emission, the effect of increase in the temperature is an increase in the I_E/I_M ratio (the monomer intensity I_M is highest at low temperature). However at still higher temperatures (> 30 °C) the dissociation of pyrene excimer results in a levelling off of the I_E/I_M value.
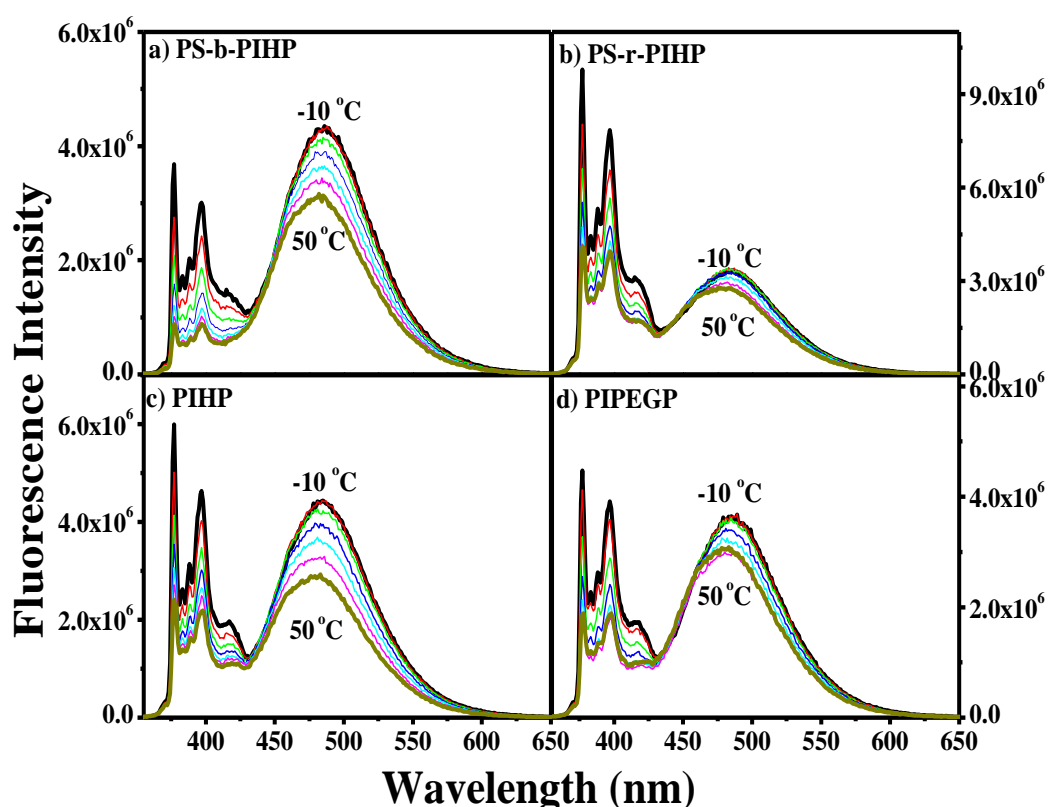
Figure-2.14: Emission spectra of the polymers (λ_{ex}-343 nm) as a function of temperature (-10 to 50 °C) recorded in THF/water (9:1).
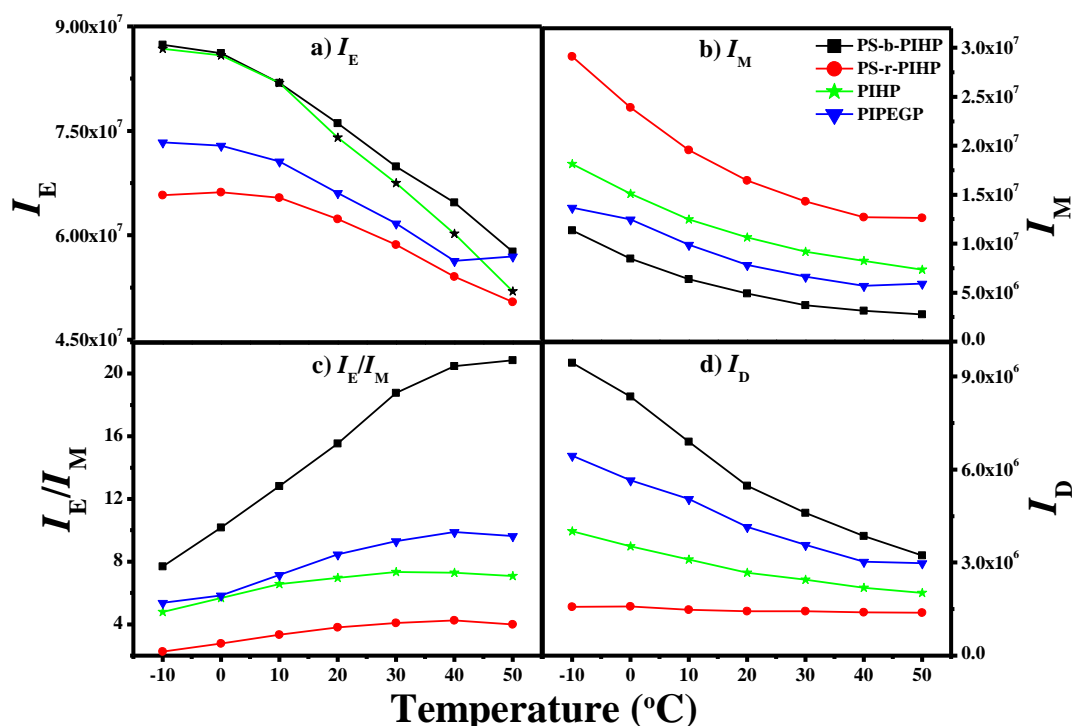
Figure-2.15: Plot of **(a)** Integrated area of excimer region (500-530 nm) (I_E) **(b)** Integrated area of monomer region (372-378 nm) (I_M) and **(c)** I_E/I_M obtained from emission spectrum by excitation at 343 nm and **(d)** Integrated area of dimer region (> 420 nm) obtained from emission spectrum by excitation at 395 nm as a function of temperature in THF/water for all polymers.

The 395 nm excitation, on the other hand excites the ground state aggregates whose intensity increases upon cooling. Upon increasing the temperature, the 440 nm emission steadily decreases since the aggregates are not stable at high temperature. The 440 nm emission also exhibited a slowing or levelling off at >30 °C. This was probably due to contribution from a different emitting species with emission centered ~ 450 nm region at higher temperatures (figure-2.16). Although the overall trend was similar for the polymers there was distinct difference in the absolute values as well as in the rate of change of the I_E/I_M value for the different polymer architectures. For instance, the rate of the initial increase in the I_E/I_M value for the 343 nm excitation was highest for the block copolymer **PS-b-PIHP**. Higher temperature augments the aggregation which drives the pyrene to conformations favourable for excimer emission to a greater extent in the block copolymer **PS-b-PIHP** compared with its own homopolymer **PIHP**. Similarly the two homopolymers, **PIHP** and **PIPEGP** exhibit almost identical

behaviour at low temperature but at higher temperature the aggregation of the hydrophobic pyrene units versus the hydrophilic polyethyleneglycol segment results in higher I_E/I_M value in the later.
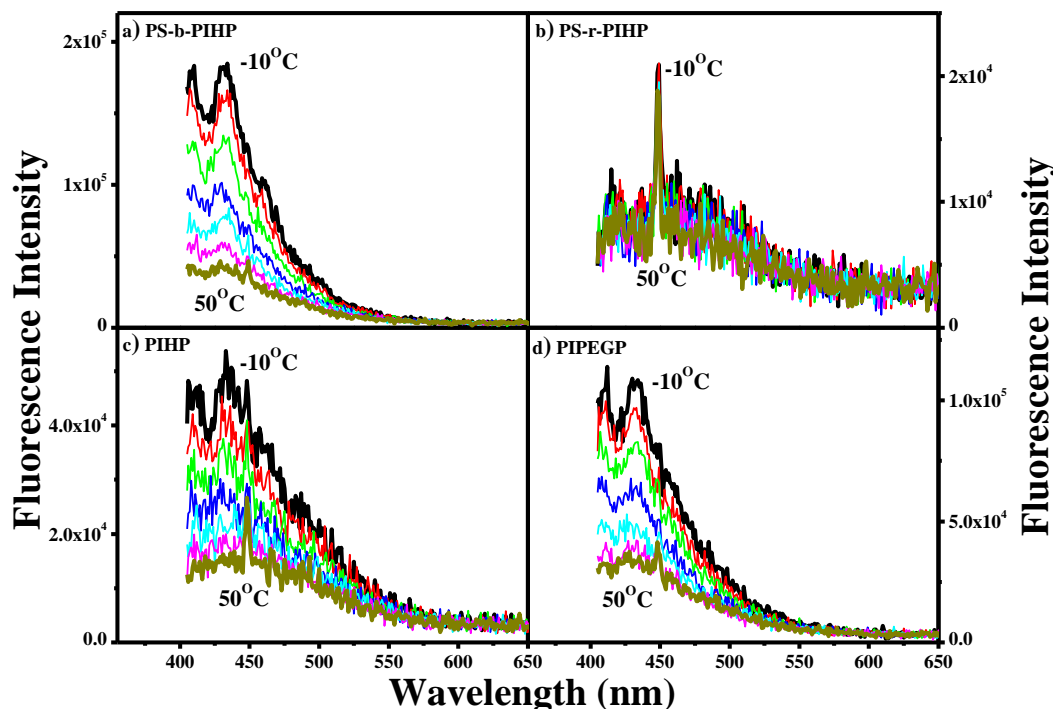
Figure-2.16: Emission spectra of polymers (λ_{ex}-395 nm) as a function of temperature (-10 to 50 ^{o}C) recorded in THF/water.

2.4.4. Morphology

The solvent induced self-organization behaviour of drop-casted films were studied for all the polymers. The short chain homopolymer **PIHP** was shown to exhibit spherical particle morphology upon drop casting from THF/water (9:1) solvent combination onto glass slides.[31] SEM and TEM studies were in agreement with each other and both showed the formation of spherical particles. The block copolymer **PS-b-PIHP** exhibited identical morphology upon drop casting a 10^{-2} M sample from a solvent combination of THF/water (9:1) in which it formed spheres in the size range of 1.5 to 0.5 µm. The SEM image for the block copolymer **PS-b-PIHP** is given in figure-2.17a. The polystyrene macroinitiator films prepared under identical condition did not exhibit any morphology. To further understand the nature of spheres formed whether they were hollow or rigid, TEM measurements were carried out. The polymer film for TEM measurements were prepared by dropcasting 10^{-4} M solution of the block copolymer **PS-b-PIHP** on to formvar coated copper grids without any special staining applied and

the images are given in figure-2.17b. The TEM image of the block copolymer **PS-b-PIHP** also showed spheres of diameter ranging from 1.7 to 0.7 µm (nearly similar to the observation from SEM measurements). The block copolymer **PS-b-PIHP** exhibited more uniform spheres ranging from 1.5 to 1.1 µm upon dropcasting from DMF/water (99:1) as shown in the SEM images in figure-2.17c.

However, the random copolymer **PS-r-PIHP** which had mostly PS exhibited pore formation in THF with diameter ranging from 2.5 to 0.9 µm (figure-2.17d). The long chain homopolymer **PIPEGP** did not exhibit any characteristic morphology under identical conditions or upon drop casting from a variety of other solvent and solvent combination (figure-2.17). The formation of pores or spherical particles in these side chain polyurethane methacrylates could be attributed to a combination of solvent induced breath figure formation as well as to self assembly brought about by the rigid/flexible segments of variable solubility incorporated into the polymer design. The pore morphology of the random copolymer **PS-r-PIHP** is mainly a solvent driven phase separation which has been well-studied in PS based systems. But the spherical morphology in the block **PS-b-PIHP** or homo polymer **PIHP** has its origin in the phase separation of the segments of different solubility in the solvent used.[37, 38] The length of blocks play very important role in deciding the morphology.[39] Block copolymers with hydrophilic/hydrophobic blocks exhibit a tendency to self-organize the hydrophobic block into microspheres.[40] However, when the long hydrophilic polyethyleneoxy spacer is used in **PIPEGP**, it takes the upperhand and increases the solubility much more compared to the hydrophobic methacrylic backbone as well as the pendant pyrene moiety. The overall increased solubility reduces tendencies for phase separation resulting in absence of characteristic morphology.

Here it should be mentioned that the above-discussed solid state morphology of the different polymer architectures does not find any correlation with their respective photophysical studies either in the solvents like THF or THF/water (9:1) combination or in solvent cast films. For instance, although the photophysical studies (either in solvent or in solid state) clearly demonstrated the ability of the long chain homopolymer **PIPEGP** to form excimer emission, the solvent cast films of **PIPEGP** did not exhibit any characteristic morphology either upon drop casting from THF or THF/water (9:1). Also, the short chain homopolymer **PIHP**, exhibited different morphologies like pores upon drop casting from THF alone or spheres upon drop casting from THF/water (9:1)

as observed by SEM. However, the photophysical studies like the fluorescence lifetime decay or variable temperature measurements did not show any pronounced difference in THF and THF/water (9:1). This does not mean that the polymer **PIPEGP** was not capable of self-organization or that **PIHP** behaved differently in THF and THF/water (9:1). On the contrary, it points to the fact that the observation of morphology in solvent cast polymer films is a phenomenon that occurs due to phase separation during solvent evaporation and the different polymer architecture reacts differently (produces different morphology) to different amounts of a solvent-non solvent presence.
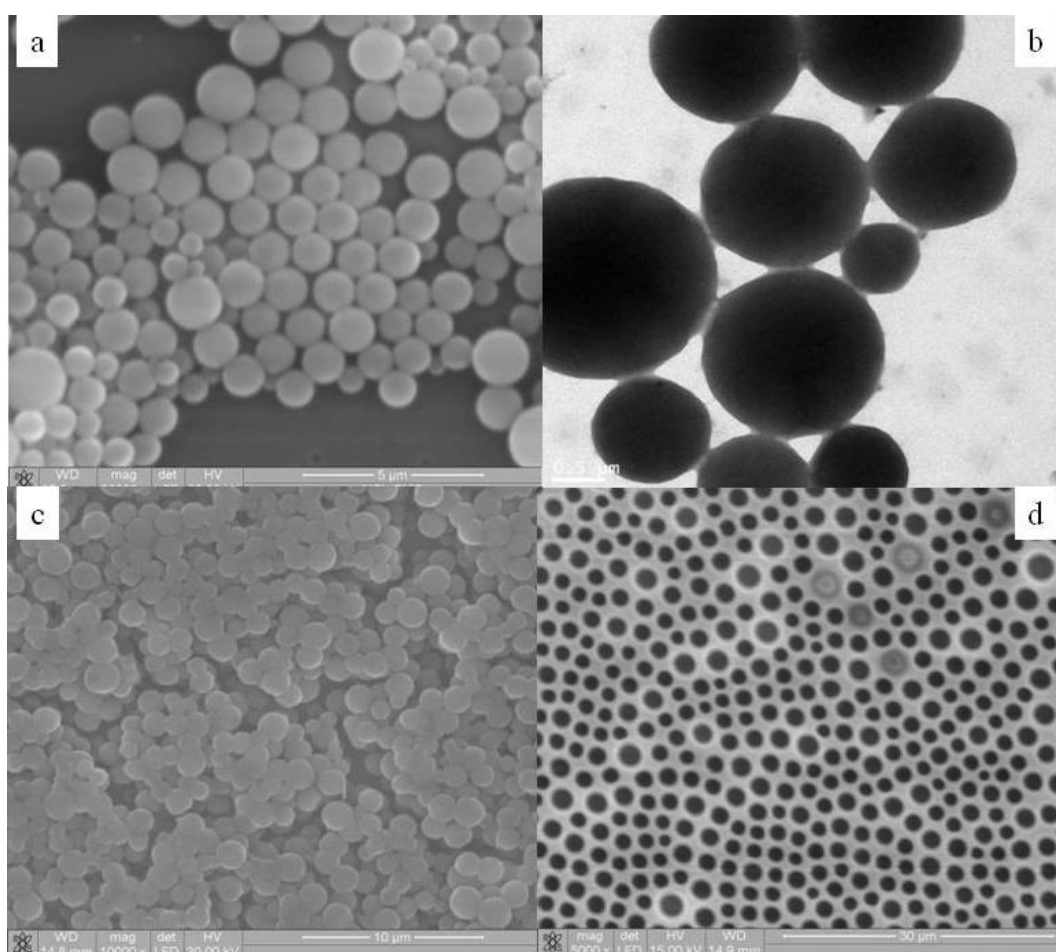
Figure-2.17. (**a**) SEM image of block copolymer **PS-b-PIHP** in THF/H$_2$O (9:1) (**b**) TEM image of block copolymer **PS-b-PIHP** in THF/H$_2$O (9:1) (**c**) SEM image of block copolymer **PS-b-PIHP** in DMF/ H$_2$O (99:1) (**d**) SEM image of random copolymer **PS-r-PIHP** in THF.
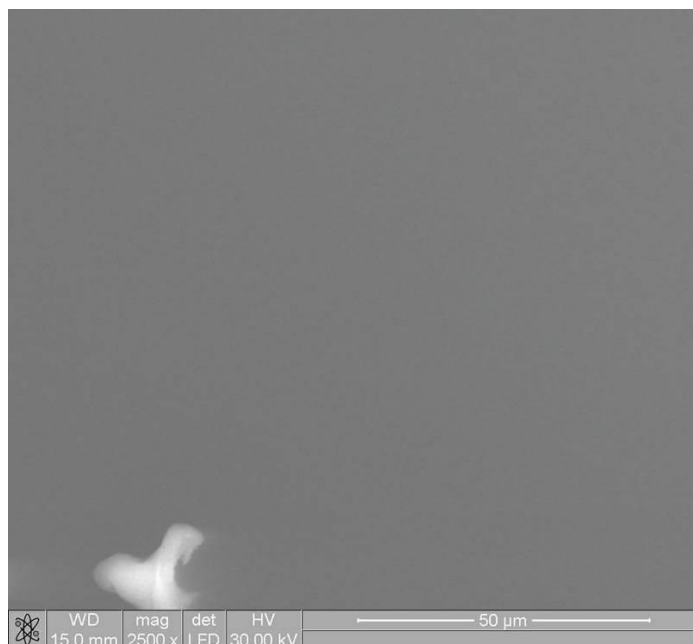
Figure-2.18: SEM image of **PIPEGP** in THF/H$_2$O (9:1).

2.5. Conclusions

This chapter focused on the effect of polymer architecture upon self-assembly. The self-assembly of four well-defined hierarchical architectures having pyrene labeled side chain urethane methacrylate polymers in – (a) short (ethyleneoxy) chain homopolymer with pyrene moieties hanging from every side chain of a urethane methacrylate backbone (**PIHP**), (b) long chain homopolymer with a long flexible polyethylenoxy unit in place of the short ethyleneoxy unit (**PIPEGP**), (c) block copolymer of the short chain pyrene urethane methacrylate (IHP) with polystyrene (**PS-b-PIHP**) and (d) random copolymer of **IHP** with PS (**PS-r-PIHP**) were explored. The pyrene excimer formation by steady state emission studies is compared for the four architectures in solution in THF/water (9:1) as well as in the solid state. The overall conclusions based on these different experimental measurements are summarized below.

1) The four different polymer architectures had varied influence on the excimer emission efficiency with the poorly pyrene labeled random copolymer **PS-r-PIHP** having the lowest excimer emission efficiency and the block copolymer **PS-b-PIHP** exhibiting the highest excimer emission efficiency in THF as well as in THF/water (9:1) as evidenced by I_E/I_M values.

2) In the solid state, the polymers exhibited almost only excimer emission with the exception of the random copolymer **PS-r-PIHP** which had strong monomer emission also. The solid state emission of all polymers also showed a pronounced blue shift due to more contribution from partially overlapped aggregated species.

3) The variable temperature steady state fluorescence studies in THF/water (9:1) indicated a continuous increase in the I_E/I_M values for the λ_{343} nm excitation with increase in temperature followed by a slow levelling off at higher temperatures. The block copolymer **PS-b-PIHP** exhibited the highest ratio as well as largest rate of increase which could be the result of increased aggregation of the polystyrene and pyrene units at higher temperatures.

4) The evolution of the dimer emission centred ~430 nm upon excitation at the λ_{395} nm; on the other hand, exhibited a steady decrease with temperature, indicating their better stability at low temperature.[26]

5) All the polymers exhibited interesting morphologies as observed under SEM either from THF or THF/water (9:1) solvent combination. However, no correlation was observed for the self-assembly in solution as traced by the photophysical studies with the solvent-driven solid state morphology.

2.6. References

1) Lehn, J.-M. *Supramolecular Chemistry: Concepts and Perspectives* (VCH, Weinheim, Germany, **1995**).

2) Philp, D.; Stoddart, J. F. *Angew. Chem. Int. Ed. Engl.* **1996**, *35*, 1154 – 1196.

3) Szostak, J. W.; Bartel, D. P.; Luisi, P. L. *Nature* **2001**, *409*, 387–390.

4) Whitesides, G. M.; Grzybowski, B. *Science* **2002**, *295*, 2418 – 2421.

5) Xu, X.; Yuan, H.; Chang, J.; He, B.; Gu, Z. *Angew. Chem. Int. Ed.* **2012**, *51*, 3130–3133.

6) Lehn, J.-M. *Science* **2002**, *295*, 2400-2403.

7) Yu, G.; Yokoyama, M.; Okano, T.; Sakurai, Y.; Kataoka, K. *J. Control. Release* **1993**, *29*, 17-23.

8) Ikkala, O.; Brinke, G. T. *Science* **2002**, *295*, 2407-2409.

9) Schmidt-Mende, L.; Fechtenkotter, A.; Mullen, K.; Moons, E.; Friend, R. H.; MacKenzie, J. D. *Science* **2001,** *293*, 1119-1122.

10) Kowollik, C. B.; Dalton, H.; Davis, T. P.; Stenzel, M. H. *Angew. Chem. Int. Ed.* **2003**, 42, 3664-3668.

11) Wu, K. C.; Ku, P. J.; Lin, C. S.; Shih, H. T., Wu, F. I.; Huang, M. J.; Lin, J. J.; Chen, I. C.; Cheng, C. H. *Adv. Funct. Mater.* **2008**, *18*, 67-75.

12) Heischkel, Y.; Schmidt, H. W. *Macromol. Chem. Phys.* **1998**, *199*, 869-880.

13) Bullock, J. E.; Carmieli, R.; Mickley, S. M.; Vura-Weis, J.; Michael R.; Wasielewski, M. R. *J. Am. Chem. Soc.* **2009**, *131*, 11919-11929.

14) Cuniberti, C.; Perico, A. *Eur. Polym. J.* **1977**, *13*, 369-374.

15) Winnik, M. A.; Redpath, T.; Richards, D. H. *Macromolecules* **1980**, *13*, 328-335.

16) Duhamel, J. *Acc. Chem. Res.* **2006**, *39*, 953-960.

17) Duhamel, J.; Yekta, A.; Hu, Y. Z.; Winnik, M. A. *Macromolecules* **1992**, *25*, 7024–7030.

18) Picarra, S.; Duhamel, J.; Fedorov, A.; Martinho, J. M. G. *J. Phys. Chem. B* **2004**, *108*, 12009-12015.

19) Costa, T.; De Melo, J. S. S.; Castro, C. S.; Gago, S.; Pillinger, M.; Goncalves, I. S. *J. Phys. Chem. B* **2010**, *114*, 12439−12447.

20) Picarra, S.; Relogio, P.; Afonso, C. A. M.; Martinho, J. M. G.; Farinha, J. P. S. *Macromolecules* **2003**, *36*, 8119-8129.

21) Winnik, M. A. *Acc. Chem. Res.* **1985**, *18*, 73-79.

22) Castanheira, E. M. S.; Martinho, J. M. G.; Duracher, D.; Charreyre, M. T.; Elaissari, A.; Pichot, C. *Langmuir* **1999**, *15*, 6712–6717.

23) Prado, E. A.; Yamaki, S. B.; Atvars, T. D. Z.; Zimerman, O. E.; Weiss, R. G. *J. Phys. Chem. B* **2000**, *104*, 5905–5914.

24) Winnik, F. M. *Chem. Rev.* **1993**, *93*, 587–614.

25) Sluch, M. I.; Vitukhnovsky, A. G.; Petty, M. C. *Thin Solid Films* **1996**, *284*, 622–626.

26) Zilberstein, J.; Bromberg, A.; Berkovic, G. *J. Photochem. Phototobiol. A* **1994**, *77*, 69–81.

27) Zimerman, O. E.; Weiss, R. G. *J. Phys. Chem. A* **1998**, *102*, 5364–5374.

28) Ingratta, M.; Duhamel, J. *Macromolecules* **2007**, *40*, 6647-6657.

29) You, J.; Yoon, J. A.; Kim, J.; Huang, C. F.; Matyjaszewski, K.; Kim, E. *Chem. Mater.* **2010**, *22*, 4426–4434.

30) Tyman, J. H. P. *J. Chromatogr.* **1975**, *111*, 277–284.

31) Deepak, V. D.; Asha, S. K. *J. Phys. Chem. B* **2009**, *113*, 11887–11897.

32) Matsumoto, A.; Mizuta, K.; Otsu, K. J. *J. Polym. Sci. Part A: Polym. Chem.* **1993**, *31*, 2531–2539.

33) Hadjichristidis, N.; Touloupis, C.; Fetters, L. *Macromolecules* **1981**, *14*, 128–130.

34) Birks, J. B. *Photophysics of Aromatic Molecules*. Wiley/Interscience: New York, 1970.

35) Eaton, D. F. *Pure Appl. Chem.* **1988**, *60*, 1107–1114.

36) Matsui, J.; Mitsuishi, M.; Miyashita, T. *J. Phys. Chem. B* **2002**, *106*, 2468–2473.

37) Yu, Y., Zhang, L.; Eisenberg, A. *Langmuir* **1997**, *13*, 2578–2581.

38) Zhang, L.; Shen, H.; Eisenberg, A. *Macromolecules* **1997**, *30*, 1001–1011.

39) Zhang, L.; Eisenberg, A. *Science* **1995**, 268, 1728–1731.

40) Discher, D. E.; Ahmed, F. *J. Control. Release* **2004**, 96,37–53.

Chapter 3:

Random Pyrene Urethane Methacrylate Copolymers with high Pyrene Incorporation: Variable Temperature TRES

3.1. Abstract

Among the various architectures studied in chapter 2, the random copolymer architecture was chosen to trace self assembly by varying the pyrene incorporation. For this, a series of random copolyurethane methacrylate comb polymers with pyrene (Py) and 3-pentadecyl phenol (PDP) as pendant units were prepared by free radical polymerization. The PDP monomer was carefully chosen for copolymerization with pyrene urethane metahcrylate so that the self-organization tendency of the pyrene moieties was not disrupted. The pyrene incorporation was varied from 1 to 100 mol %. All the copolymers formed spheres upon drop casting from DMF. Hence DMF was chosen as a solvent of choice to conduct photophysical studies in dilute conditions. The excimer emission of these copolymers were studied as a function of both time and temperature using time resolved emission spectra (TRES) experiments and variable temperature steady-state fluorescence measurements. Variable temperature steady-state as well as decay experiments showed that the contribution from excimers via diffusional encounters increased at the cost of pyrene monomer as temperature increased until ~ 50 °C; beyond which non-radiative losses predominated. The TRES collected at 25 °C and 70 °C were compared to study the nature of emitting species as a function of pyrene loading. TRES at 25 °C clearly indicated the presence of ground state pyrene dimers with emission centred ~ 435 nm which soon gave way to emission centred ~ 465 and 485 nm in the time gated spectra collected at higher time intervals. In the TRES collected at 70 °C, excimer emission centred ~ 465 and 485 nm was very high even at short time scales. The lowest pyrene loaded polymer **PIHPDP-1Py** did not exhibit excimer emission in the TRES collected at 25 °C as well as 70 °C.

3.2. Introduction

Understanding the self-assembly of complex polymeric architectures have thrown a unique challenge to the scientific community across the globe. The significant problem lies in exploring the nature of self-assembly at the molecular level. The photophysical studies have provided unique opportunities in understanding the self-organization processes at very low concentrations.[1] The photophysics of pyrene is the most studied and well understood among the fluorophores used to explore the self-organization by way of excimer formation.[1-10] Pyrene as a fluorophore has long been used due to several of its advantageous characteristics like long fluorescence life time, large quantum yield, large stoke's shift and molar absorption coefficient etc.[1, 10-15] The advancement in fluorescence analysis have significantly contributed in gaining the detailed molecular information of various complex molecules.[16] For instance, acrylic and methacrylic polymers having small loading of pyrene as pendant fluorophores have been studied by various groups.[17, 18] PNIPAM systems incorporated with varying amounts of pyrene have been extensively investigated to understand their LCST behaviour.[19] The association behavior in good or bad solvents of hydrophobically modified water soluble polymers such as polyacrylic acids with small labeling of pyrene have been thoroughly investigated and their self-organization at the molecular level studied.[20-22] Another interesting system making use of the pyrene photophysics is the amphiphilic copolymers encapsulating pyrene to study their micellization behaviour.[23] Pyrene aggregates have also been investigated for calculation of the molar absorbance coefficient in pyrene-labeled systems such as poly(N,N-dimethylacrylamide)s (Py-PDMA) with different amount of pyrene labeling or poly(ethylene oxide) capped at a single end with pyrene.[24, 25]

Compared to systems with low pyrene incorporation a 100 % pyrene labeled linear polymer where every side chain is labeled with a pendant pyrene unit presents a challenging task as an interesting case study. Even under extreme dilute conditions one can expect that there will be regions where pyrene labels are crowded together into poorly stacked arrangements resulting in pyrene dimers which have a characteristic lifetime different from that of pyrene excimers.[26, 27] There has so far been no detailed report on fully pyrene labeled polymers where the contribution from different types of pyrene excimers and monomers were analyzed. The hydrogen bonding of the urethane linkage as well as the varying solubility of the rigid/flexible parts of the polymer

resulted in various self assembled structures like pores, spheres, vesicles etc. from different solvents like THF and THF/water mixtures.[28, 29, 30] Steady-state fluorescence measurements and concentration dependent studies had shown the presence of blue shifted dimer emission centered around 445 nm.[18] These studies have prompted us to explore the nature and origin of emitting species in the polymers in great details with pyrene incorporation varying from 1 to 100%.

Time Resolved Emission Spectra (TRES) experiments where fluorescence decays are collected at different wavelengths and then used to construct the three-dimensional time-intensity-wavelength contour plot of the emission spectra can give valuable information regarding the nature of emitting species, their origin and decay.[12, 31] In one of the early reports of TRES studies in polymeric systems, pyrene labeled hydroxypropyl cellulose polymers (HPC-Py) were investigated to understand the origin of emission band with maxima at 420 and 470 nm.[32] Figure-3.1 shows the time-resolved emission spectra of two pyrene labeled hydroxypropyl cellulose having a single pyrene species per 56 glucose units (HPC-Py/56) and 438 glucose (HPC-Py/438) units respectively. It could be clearly seen from the figure that in HPC-Py/56, significant changes in the spectrum have been observed on going from the picoseconds to the nanosecond time region. Whereas in HPC-Py/438, where the density of pyrene is lower, the monomer band is dominant and the excimer fluorescence and the excimer contribution is very low. In yet another interesting study pyrene was immobilized on quartz plate surface and used to study the sensing of dicarboxylic acids.[33] TRES studies were conducted on these solid samples to gather information of various emitting species as a function of various time-gated spectra.

Recently, TRES studies was reported on poly(acrylic acid) labeled with up to 10% pyrene, where picosecond time resolved emission studies were also conducted to understand the dynamics of dimer formation.[34] Figure-3.2 shows schematic representation of the nature of emitting species of pyrene labeled poly(acrylic acid) which demonstrates 10 mol % of pyrene loading (corresponding to 10 monomer units per pyrene chromophore). It is one of the first literature report where the presence of excimer formation through the excitation of preassociated dimers have been demonstrated for high pyrene loaded (10 mol%) polymers.
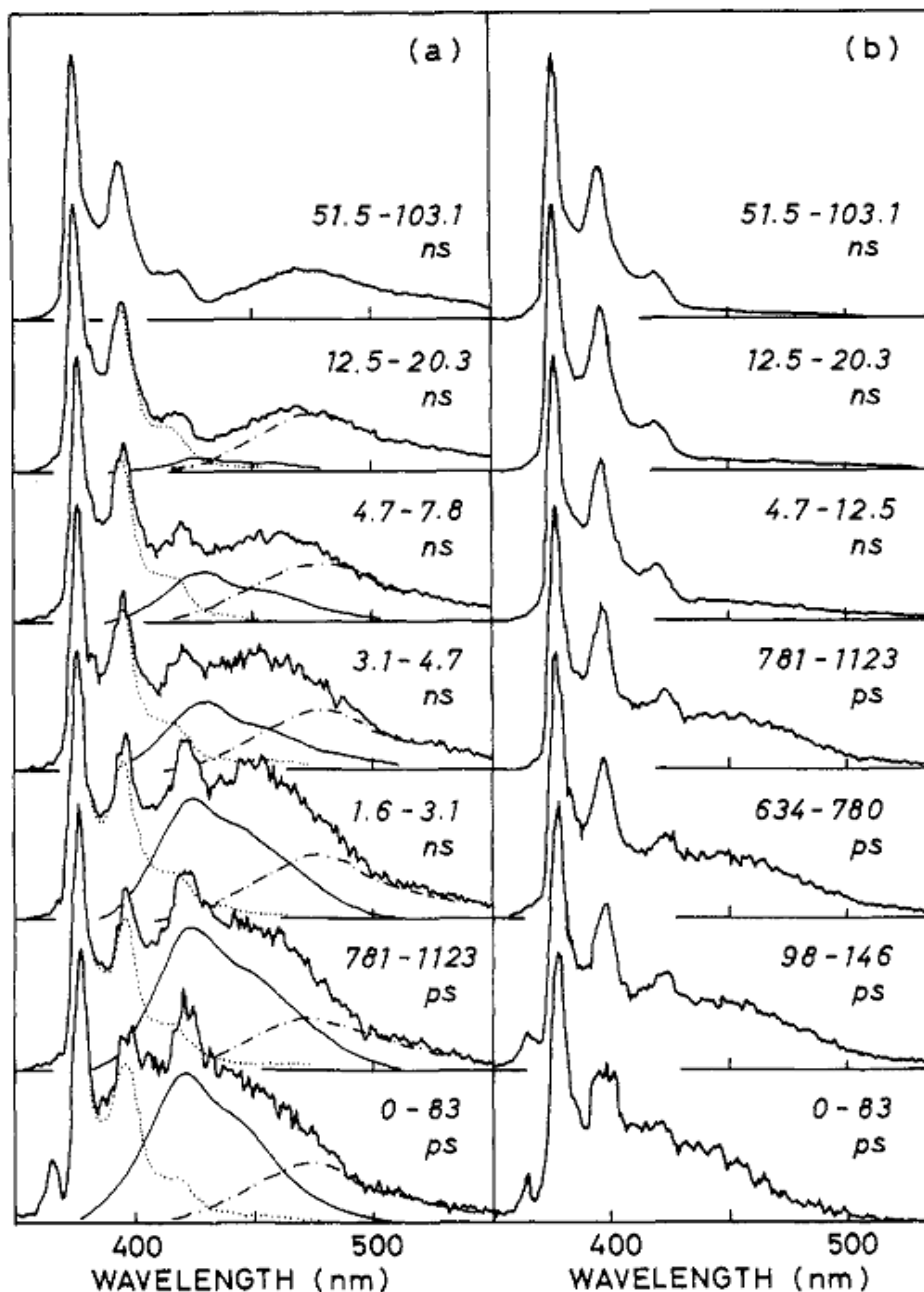
Figure-3.1: Normalised TRES (at maximum intensity) of pyrene labeled hydroxypropyl cellulose, (a) HPC-Py/56 and (b) HPC-Py/438 in water. *Adapted from reference 32.*

Figure-3.3 shows the nanosecond time-resolved emission spectra (ns-TRES) of PAAMePy (450)11 where the lifetime was studied in the wavelength range 375 to 545 nm at an interval of 10 nm and the regenerated spectrum was constructed. The TRES spectra were found to change with time, exhibiting the emission contribution from two species.
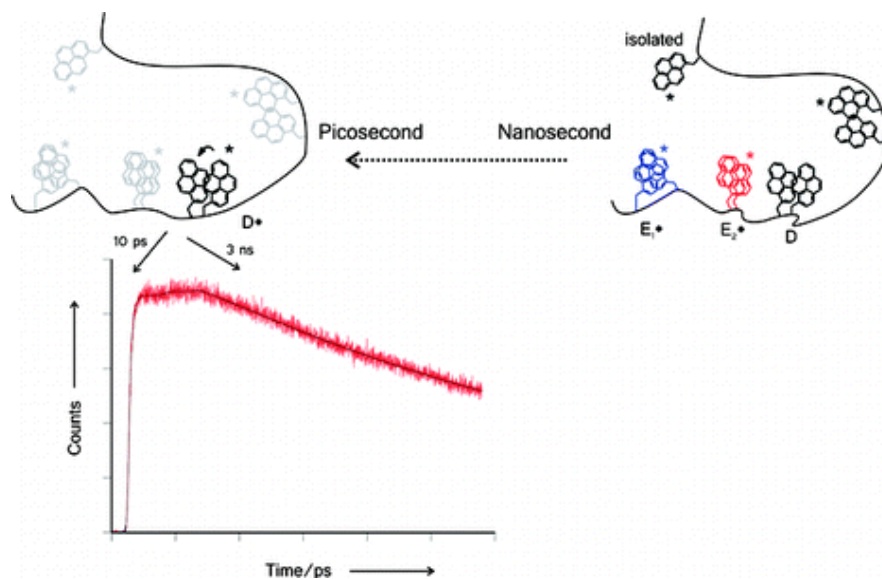
Figure-3.2: Schematic representation of nature of emitting species exhibited by pyrene labeled Poly(acrylic acid) referred to as PAAMePy(450)11. *Adapted from reference 34.*
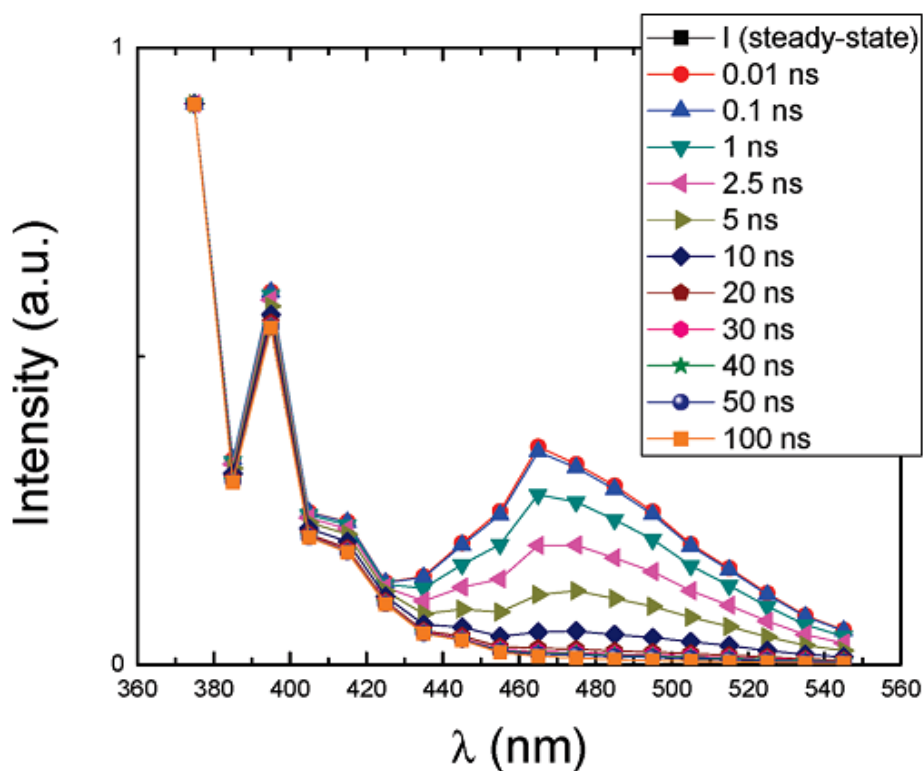
Figure-3.3: Nanosecond time-resolved emission spectra (ns-TRES) of PAAMePy (450). The fluorescence decays were collected in the range from 375 to 545, using $\lambda_{ex} =$ 339 nm. *Adapted from reference 34.*

This chapter focuses on the exploration of self-assembly by photophysical and morphological studies of random copolymers having varying amount of pyrene fluorophore. A series of random copolyurethane methacrylate polymers having varying incorporation of pyrene and 3-pentadecyl phenol (PDP) pendant moieties (**PIHPDP-xPy**) have been synthesized. For the sake of convenience and with relevance to this chapter **PIHP** homopolymer was renamed as **PIHP-100Py**. In this chapter we have relooked the **PIHP-100Py** homopolymer along with the newly synthesized random copolymers using TRES experiments collected at room temperature (25 °C) as well as at 70 °C. A series of random copolyurethane methacrylates having varying pyrene incorporation like 50, 33, 11, 5 and the lowest at 1 mol % were analysed. The other co monomer (**p**enta **d**ecyl **p**henol - PDP) was chosen carefully so as to have similar self assembling properties or at least which would not disrupt the self organizing properties of the pyrene urethane methacrylate polymer. The 100 mol % PDP polyurethane methacrylate polymer had also exhibited similar self assembling tendencies like sphere and vesicle formation from THF and THF/water solvent mixtures.[30] The detailed photophysical properties of the series of copolymers and 100 % pyrene homopolymer were studied using variable temperature steady state emission and decay experiments as well as TRES at different temperatures. This chapter contributes probably the first time where such a detailed study has been undertaken to retrieve information regarding evolution of various emitting species using a series of polymers spanning 1 − 100 % pyrene labeling.

3.3. Experimental Section

3.3.1. Materials

2-Hydroxyethyl methacrylate (HEMA), 1-pyrenemethanol, dibutyltin dilaurate (DBTDL), isophorone diisocyanate (IPDI) and 3-pentadecyl phenol (PDP) and benzoyl peroxide (BPO) were purchased from Aldrich. Benzoyl peroxide (BPO) was recrystallized from methanol before use. Purification of dimethyl formamide (DMF) was carried out by keeping it for 72 h over calcium sulfate followed by decanting and vacuum distilling.

3.3.2. Measurements

200- and 400-MHz Bruker NMR spectrophotometer was used for recording ^{1}H and ^{13}C NMR spectra of monomers and polymers in CDCl$_3$ containing small amounts of tetramethylsilane (TMS) as internal standard. Infrared spectra were recorded using a Bruker Alpha FTIR spectrometer. IR spectra were recorded in the range of 4000–500 cm^{-1}. The molecular weights of the polymers were determined by GPC instrument (Viscotek) provided with Styragel column, VE 1122 pump, Viscotek VE 3580 RI detector and Viscotek VE 3210 UV/Vis detector in tetrahydrofuran (THF). The instrument was calibrated using 12 polystyrene standards in the molecular weight range from 1 x 10^3 to 4 x 10^6. The flow rate of the THF was maintained as 1 mL/min throughout the experiments, and the sample solutions at very dilute concentrations were filtered and injected for recording the GPC chromatograms at 35 ^{o}C. The viscosity of the polymers was measured by using Schott Instrument. The inherent viscosity (η_{inh}) of the polymers was determined in tetrahydrofuran (THF) for 0.5 wt % solution at 30 °C. Thermal gravimetric analysis (TGA) of the polymers was performed using Perkin Elmer Pyris-6 instrument. Differential scanning calorimetry (DSC) measurements were performed on a TA Q20 differential scanning calorimeter at a heating rate of 10°C min^{-1} under nitrogen atmosphere. Typically, 1–2 mg of samples was placed in an aluminium pan, cramped properly, and scanned from -30 to 200 ^{o}C. The instrument was calibrated using indium standards.

Photophysical Studies

Perkin Elmer Lambda 35 UV-spectrophotometer was used for measuring absorption spectrum. Steady-state fluorescence studies and time-resolved fluorescence lifetime measurements were conducted on Horiba Jobin Yvon Fluorolog 3

spectrophotometer having 450-W Xenon lamp. The steady state emission, variable temperature steady state emission and fluorescence lifetime decay analysis were carried out in DMF. The emission and excitation slit width was maintained at 1 nm throughout the experiments, and the data was obtained in ''S1/R1'' mode. Temperature dependent fluorescence was recorded using Peltier sample compartment having Peltier Sample Cooler F-3004 attached with thermoelectric temperature controller (Model No. LFI-3751) supplied by Wavelength Electronics. The temperature was set manually for each reading, and it was equilibrated for 10 min at each temperature before recording the spectrum. The tolerance range for each set temperature was maintained 0.5 $^{\circ}$C. For lifetime measurements, decay curves were obtained by the time-correlated single photon counting (TCSPC) technique.

Lifetime measurements and TRES studies were conducted using TCSPC Fluorohub supplied by Horiba Jobin Yvon and Nano-LED source with wavelength 340 nm was used to excite all the samples. For the lifetime decay profile, data was collected at monomeric (λ_{em}-375 nm) emission as well as excimeric (λ_{em}-500 nm) emission region. The Time-Resolved Emission Spectra (TRES) was procured by incrementing the monochromator on the emission channel of the time-resolved fluorometer in fixed wavelength steps. The time resolved decays were acquired for fixed time intervals at each wavelength. Slices of data were taken in the intensity-wavelength plane to obtain spectra at different times during the decay. Picosecond Time-resolved-emission spectra (TRES) and Fluorescence lifetime decays were collected by a time-correlated single photon counting (TCSPC) setup from IBH Horiba Jobin Yvon (U.S.) using a 405 nm diode laser (IBH, U.K., NanoLED-405 L, with a λ max = 405 nm) as a sample excitation source.

The samples were prepared by making the optical density 0.1 ± 0.05 at excitation wavelength (λ_{ex} ~ 343 nm) in DMF. All samples were purged with gentle flow of nitrogen for 1 hour before carrying out the measurements to ensure complete removal of dissolved oxygen from the DMF solution. All experiments were performed under identical conditions. Fluorescence lifetime values were determined by deconvoluting the data with exponential decay using DAS6 decay analysis software. The quality of fit was judged by fitting parameters such as $\chi2 \approx 1$, as well as the visual inspection of the residuals and autocorrelations.

Scanning Electron Microscopy (SEM)

FEI, QUANTA 200 3D Scanning Electron Microscope with tungsten filament as electron source was used for recording SEM images. The sample preparation method adopted was as follows. 0.65-0.75 mg of polymer was dissolved in 1 mL of solvent resulting in a stable and clear polymer solution. 20 μL of this solution was placed on a glass slide and the solution was allowed to evaporate at room temperature in air for 12 hours. All films were prepared and dried under ambient conditions. Before recording the morphology, films were coated by 5 nm thick gold film by sputtering method.

Transmission Electron Microscopy

JEOL-JEM-3010 instrument operated at 80 KV was used for recording TEM images. For TEM measurements, a drop of the polymer solution (0.65-0.75 mg in 1 ml solvent was deposited directly on carbon coated copper grid. No staining treatment was performed for the measurement. A JEOL JEM-3010 electron microscope operating at 300 kV (Cs=0.6 mm, resolution 1.7 A°) was used for HR-TEM sample observation. A Gatan digital camera (model 794, Gatan 1024 x 1024 pixels, pixel size 24 x 24 μm) at 15 000-80 000 x magnifications was used to record micrographs.

3.3.3. Synthesis of IPDI-HEMA-Pyrene (IHP-monomer)

The IHP-monomer synthesis has been reported in chapter 2. In a 50 mL two necked round bottom flask, isophorone diisocyanate (IPDI) (1 g, 4.5×10^{-3} mol) in 6 mL dry dimethylformamide (DMF) was taken and the contents were cooled with ice. 2-hydroxyethyl methacrylate (0.59 g, 4.5×10^{-3} mol) was added drop wise under nitrogen atmosphere over a period of 0.5 hr. The reaction was allowed to proceed under ice cold conditions for further 0.5 hr and then left stirring at room temperature for 2 hr. 2-3 drops dibutyltin dilaurate (DBTDL) was added as catalyst followed by drop wise addition of 1-pyrenemethanol (1.04 g, 4.5×10^{-3} mol) solution in DMF (5 mL) to the reaction mixture under ice cold conditions within 0.5 hr and then slowly heated to 60 °C for 6 hr. The contents were poured into 300 mL water and extracted with dichloromethane. The extract was washed with plenty of water and then dried over anhydrous sodium sulphate. The solvent was removed under reduced pressure and dried in vacuum oven at 60 °C for 2 hr. Yield: 2.45 g (91 %). ^{1}H NMR (200 MHz, CDCl$_3$) δ ppm: 8.30-8.02 (m, 9H, Ar-**H**), 6.13, 5.58 (2s, 2H, C**H**$_2$=C), 5.78 (s, 2H, OC**H**$_2$ next to pyrene ring), 4.80-4.50 (m, N**H**), 4.29 (s, 4H, O-C**H**$_2$-C**H**$_2$-O of HEMA), 3.24, 2.86 (b,

3H, -C**H**-NH-COO and -C**H$_2$**-NH-COO of IPDI), 1.93 (s, 3H, -C**H**$_3$ of HEMA), 1.65-0.86 (aliphatic protons of IPDI). FT-IR (cm^{-1}): 3331, 3043, 2955, 2916, 1718, 1637, 1530, 1456, 1386, 1307, 1299, 1233, 1168, 1058, 1027, 944, 896, 844, 813, 762, 711.

3.3.4. Synthesis of IPDI-HEMA-pentadecylphenol (IHPDP-monomer)

In a 50 mL two necked round bottom flask, isophorone diisocyanate (IPDI) (1 g, 4.5 x 10^{-3} mol) in 6 mL dry DMF was taken and the contents were cooled with ice. Under nitrogen atmosphere 2-hydroxyethyl methacrylate (HEMA) (0.59 g, 4.5 x 10^{-3} mol) was added drop wise over a period of 0.5 hr. The reaction was allowed to proceed under ice cold conditions for further 0.5 hr and then left stirring at room temperature for 2 hr. 2-3 drops dibutyltin dilaurate (DBTDL) was added as a catalyst followed by drop wise addition of 3-pentadecyl phenol (1.38 g, 4.5 x 10^{-3} mol) solution in DMF (5 mL) to the reaction mixture under ice cold conditions within 0.5 hr followed by further ice-cold condition stirring for 0.5 hr and then the reaction contents were heated at 55 $^{\circ}$C for 48 hr. The contents were poured into ~300 mL water and extracted with dichloromethane thrice. The extract was washed with plenty of water and then dried over anhydrous sodium sulphate. The solvent was removed under reduced pressure and dried in vacuum oven at 60 $^{\circ}$C for 2 hr. Yield: 86 % (2.51 g). ^{1}H NMR (200 MHz, CDCl$_3$) δ ppm: 7.22 (t, 1H, Ar-**H**); 6.99–6.93 (m, 3H, Ar-**H**); 6.12, 5.58 (2s, 2H, C**H$_2$**=C of HEMA); 5.25–4.94 (m, N**H**); 4.31 (s, 4H, -OC**H$_2$**C**H$_2$**O- of HEMA); 3.93 (b, 2H, -C**H$_2$**-NH-COO of IPDI); 2.57 (t, 2H, Ar-C**H$_2$**); 1.93 (s, 3H, C**H$_3$** of HEMA); 1.58 (b, 2H, Ar-CH$_2$-C**H$_2$**-); 1.88–0.83 (other aliphatic protons). FT-IR (cm^{-1}): 3352, 3054, 2924, 2854, 1723, 1632, 1554, 1463, 1386, 1306, 1232, 1155, 1069, 1015, 952, 839, 809, 773.

3.3.5. Synthesis of homopolymer PIHP-100Py

IHP-monomer (1 g, 1.23 x 10^{-3} mol) and benzoyl peroxide (BPO) (0.009 g, 3.69 x 10^{-5} mol) were taken in DMF (5 mL) in a 10 mL round bottom (RB) flask provided with a water condenser. The reaction mixture was purged with nitrogen for 0.5 hr. The polymerization was carried out by stirring the contents at 65 $^{\circ}$C for 20 hr. The viscous liquid was cooled and precipitated in methanol. Yield: 0.67 g (67 %); THF GPC: M$_n$=2.20x10^{4}, Đ=1.43. ^{1}H-NMR (200 MHz, CDCl$_3$) δ ppm: 8.30-7.94 (m, 9H, Ar-**H**), 5.69 (b, 2H, OC**H$_2$** next to pyrene ring), 4.30 (b, N**H**), 4.12-3.71 (b, 4H, O-C**H$_2$**-OC**H$_2$**-O of HEMA), 2.89-0.86 (aliphatic protons of IPDI).

3.3.6. Synthesis of random copolymer PIHPDP-1Py

IHPDP-monomer (1 g, 1.52×10^{-3} mol), IHP-monomer (0.009 g, 1.52×10^{-5} mol) and benzoyl peroxide (BPO) (0.019 g, 2.5×10^{-5} mol) were taken in DMF (3 mL) in a 10 mL round bottom flask. The reaction mixture was purged with nitrogen for 0.5 hr. The polymerization was carried out by stirring the contents at 65 °C for 20 hr. The viscous liquid was cooled and precipitated into methanol. Yield: 0.65 g (65 %). THF GPC: $M_n=3.10 \times 10^4$, Đ=1.16. ^{1}H NMR (200 MHz, CDCl$_3$) δ ppm: 8.35-8.01 (b, 9H, Ar-**H** of pyrene), 7.24 (b, 1H, Ar-**H** of PDP), 6.99-6.69 (3 Ar-**H** of PDP), 5.81 (b, 2H, -OC**H**$_2$ next to pyrene ring) 4.30 (s, N**H**), 3.74 (b, 4H, O-C**H**$_2$-C**H**$_2$-O of HEMA), 3.38 (b, 1H, C**H**NH-COO of IPDI), 2.89 (b, 2H, -C**H**$_2$-NH-COO of IPDI), 1.93-0.88 (other aliphatic protons).

3.3.7. Synthesis of random copolymer PIHPDP-5Py

A similar procedure as that for **PIHPDP-1Py** was followed using (0.47 g, 7.1×10^{-4} mol) IHPDP-monomer, (0.022 g, 3.75×10^{-5} mol) IHP-monomer, and (0.009 g, 5×10^{-5} mol) benzoyl peroxide (BPO) in 3 mL DMF. Yield: 0.31 g (50 %). THF GPC: $M_n=2.10 \times 10^4$, Đ=1.24. ^{1}H NMR (200 MHz, CDCl$_3$) δ ppm: 8.30-8.01 (b, 9H, Ar-**H** of pyrene), 7.24 (b, 1H, Ar-**H** of PDP), 6.99-6.69 (3 Ar-**H** of PDP), 5.81 (b, 2H, -OC**H**$_2$ next to pyrene ring) 4.30 (s, N**H**), 3.74 (b, 4H, O-C**H**$_2$-C**H**$_2$-O of HEMA), 3.38 (b, 1H, C**H**NH-COO of IPDI), 2.89 (b, 2H, -C**H**$_2$-NH-COO of IPDI), 1.93-0.88 (other aliphatic protons).

3.3.8. Synthesis of random copolymer PIHPDP-11Py

A similar procedure as that for **PIHPDP-1Py** was followed using (0.59 g, 1×10^{-4} mol) IHPDP-monomer, (0.06 g, 9×10^{-4} mol) IHP-monomer, and (0.012 g, 5×10^{-5} mol) benzoyl peroxide in 3 mL DMF. Yield: 0.31 g (50 %). THF GPC: $M_n=3.90 \times 10^4$, Đ=1.92. ^{1}H NMR (200 MHz, CDCl$_3$) δ ppm: 8.17-8.05 (b, 9H, Ar-**H** of pyrene), 7.21 (b, 1H, Ar-**H** of PDP), 6.99-6.69 (b, 3 Ar-**H** of PDP), 5.80 (b, 2H, -OC**H**$_2$ next to pyrene ring) 4.22 (s, N**H**), 3.74 (b, 4H, O-C**H**$_2$-C**H**$_2$-O of HEMA), 3.38 (b, 1H, C**H**NH-COO of IPDI), 2.56 (b, 2H, -C**H**$_2$-NH-COO of IPDI), 1.93-0.88 (other aliphatic protons).

3.3.9. Synthesis of random copolymers PIHPDP-33Py

A similar procedure as that for **PIHPDP-1Py** was followed using (0.15 g, 2.5 x 10^{-4} mol) IHPDP-monomer, (0.49 g, 7.5 x 10^{-4} mol) IHP-monomer, and (0.012 g, 5 x 10^{-5} mol) benzoyl peroxide in 3 mL DMF. Yield: 0.32 g (51 %). THF GPC: M_n=3.60x10^4, Đ=1.47. ^{1}H NMR (200 MHz, CDCl$_3$) δ ppm: 8.35-8.01 (b, 9H, Ar-**H** of pyrene), 7.24 (b, 1H, Ar-**H** of PDP), 6.99-6.69 (3 Ar-**H** of PDP), 5.81 (b, 2H, -OC**H**$_2$ next to pyrene ring) 4.30 (s, N**H**), 3.74 (b, 4H, O-C**H**$_2$-C**H**$_2$-O of HEMA), 3.38 (b, 1H, C**H**NH-COO of IPDI), 2.89 (b, 2H, -C**H**$_2$-NH-COO of IPDI), 1.93-0.88 (other aliphatic protons).

3.3.10. Synthesis of random copolymer PIHPDP-50Py

A similar procedure as that for **PIHPDP-1Py** was followed using (0.29 g, 5 x 10^{-4} mol) IHPDP-monomer, (0.33 g, 5 x 10^{-4} mol) IHP-monomer, and (0.012 g, 5 x 10^{-5} mol) benzoyl peroxide in 3 mL DMF. Yield: 0.31 g (50 %). THF GPC: M_n=3.80x10^4, Đ=1.21. ^{1}H NMR (200 MHz, CDCl$_3$) δ ppm: 8.35-8.01 (b, 9H, Ar-**H** of pyrene), 7.24 (b, 1H, Ar-**H** of PDP), 6.99-6.69 (3 Ar-**H** of PDP), 5.81 (b, 2H, -OC**H**$_2$ next to pyrene ring) 4.30 (s, N**H**), 3.74 (b, 4H, O-C**H**$_2$-C**H**$_2$-O of HEMA), 3.38 (b, 1H, C**H**NH-COO of IPDI), 2.89 (b, 2H, -C**H**$_2$-NH-COO of IPDI), 1.93-0.88 (other aliphatic protons).

3.4. Results and Discussions

3.4.1. Synthesis and Characterization

The random copolymers were designed to avoid additional complexities related to structure and these could be explored for their self assembling properties by making use of photophysics of pyrene. For this, two methacrylate monomers incorporating 3-pentadecyl phenol and fluorophore pyrene as the pendants were designed connecting the polymerizable methacrylate through hydrogen bondable urethane linkage. The monomers were named **IHPDP** (**I**PDI-**H**EMA-**P**enta**D**ecyl **P**henol) and **IHP** (**I**PDI-**H**EMA-**P**yrene) respectively, highlighting the varying pendant units. The synthesis of the monomer **IHPDP** and **IHP** involved the one-pot coupling of one equivalent of isophorone diisocyanate (IPDI) with one equivalent respectively of hydroxyethyl methacrylate (HEMA) followed by reacting with one equivalent of 3-pentadecyl phenol and 1-pyrene methanol respectively (scheme-3.1). The monomers were polymerized using 5 mol% benzoyl peroxide (BPO) as initiator in dimethyl formamide (DMF) as solvent as shown in (scheme-3.2). The feed ratio of **IHP** was varied from 1 to 50 percent in the order 1, 5, 10, 25, 50 with respect to **IHPDP** for the random copolymers and they were polymerized under identical conditions as that for the homopolymers.
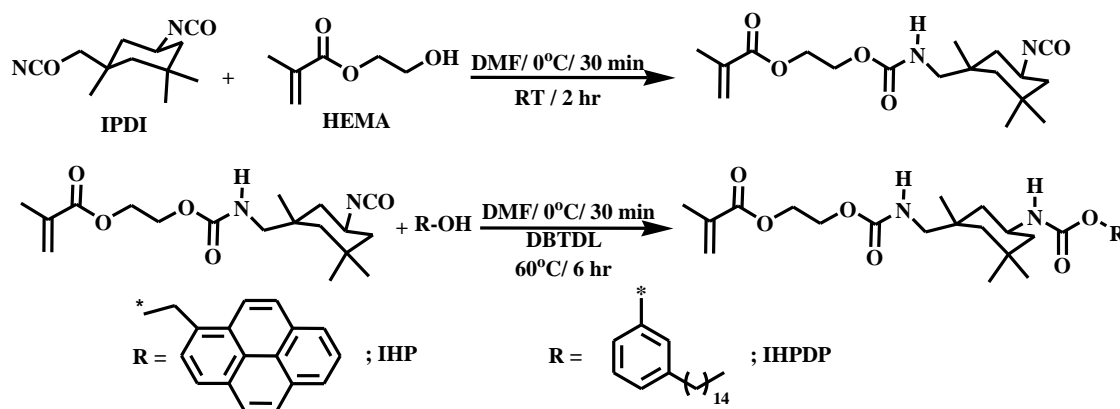
Scheme-3.1: Chemical structure of the monomers **IHP** and **IHPDP**.

R= C$_{15}$ H$_{31}$
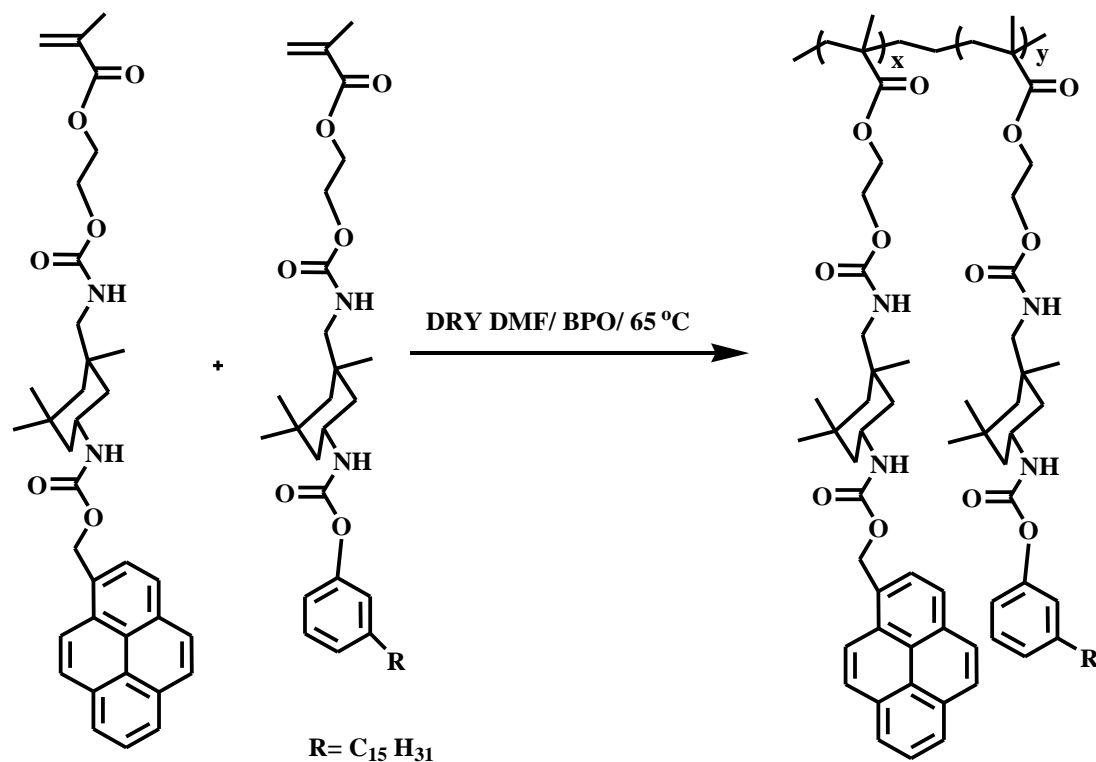
Scheme-3.2: Chemical structure and polymerization scheme for random copolymers.

The monomers were structurally characterized by ^{1}H-NMR and MALDI-TOF MS, whereas the polymers were characterized by ^{1}H-NMR spectroscopy. Figure-3.4 compares the proton NMR spectra of the polymers with varying incorporation of IHP-monomer. The methacrylate double bond peaks at 6.12 and 5.58 ppm in the ^{1}H-NMR spectrum of monomers disappeared on successful completion of polymerization. In all the random copolymers, the aromatic protons of 3-pentadecyl phenol were distinguishable at 7.24-6.69 ppm from the aromatic protons of pyrene at 8.38-8.01 ppm. The incorporation of 3-pentadecyl phenol and pyrene units in the random copolymer was calculated by integrating the peak at 8.38-8.01 corresponding to the 9 aromatic protons of pyrene and the peak at 7.24-6.69 ppm corresponding to the 4 aromatic protons of 3-pentadecyl phenol. From the integration values, the incorporation percentage of pyrene unit was calculated for all the random copolymers. The incorporation percentage along with the feed ratio is given in the table-3.1, from where it can be seen that the feed and incorporation were very similar.Furthermore, the absorption spectra were also used to calculate the amount of pyrene incorporation in the random copolymers, in accordance with literature procedure.[34] The **IHP** monomer was used as a reference to calculate the molar extinction coefficient which was found to be

40598 L M^{-1} cm^{-1}. Using the Beer-Lambert's law to estimate the amount of pyrene in the random copolymers, the amount of pyrene in fixed amount of polymers was found to be 3.49×10^{-6}, 4.28×10^{-5}, 9.81×10^{-5}, 1.66×10^{-4} and 7.91×10^{-4} mol/g for **PIHPDP-1Py**, **PIHPDP-5Py**, **PIHPDP-11Py**, **PIHPDP-33Py** and **PIHPDP-50Py,** respectively. The molecular weight for all the copolymers was recorded by gel permeation chromatography (GPC) in THF and the values are given in table-3.1 and the chromatogram is given in figure-3.5. The number average molecular weight (M_n) was found to be ranging from 2.10×10^{3} to 3.90×10^{3}. The viscosity for all the polymers recorded in THF and the inherent viscosity values are given in table-3.1. The inherent viscosity was obtained in the order of 0.19 to 0.38 dL/g.
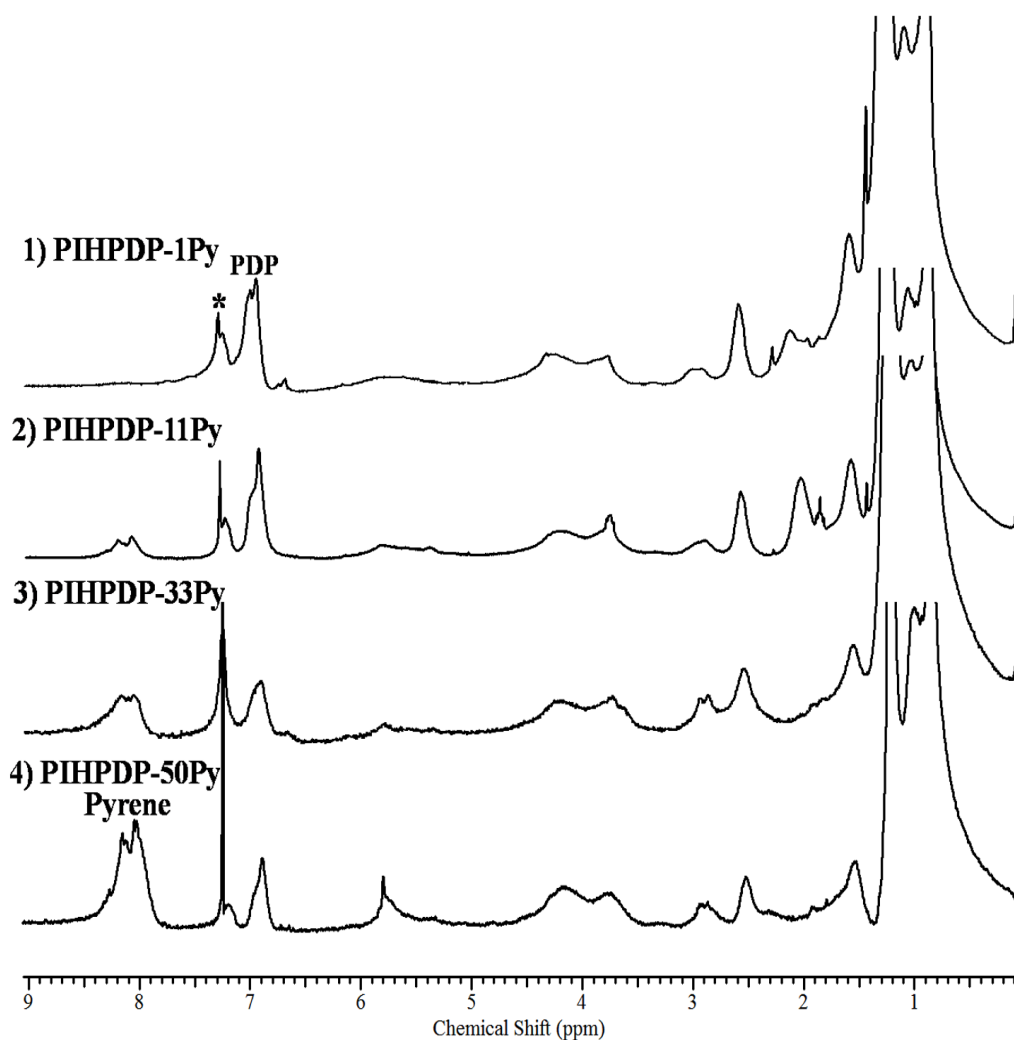
Figure-3.4: ^{1}H NMR spectrum (top to bottom): Copolymers with 1, 11, 33 and 50 mol % pyrene incorporation: **(1) PIHPDP-1Py, (2) PIHPDP-11Py, (3) PIHPDP-33Py** and **(4) PIHPDP-50Py** recorded in CDCl$_3$.
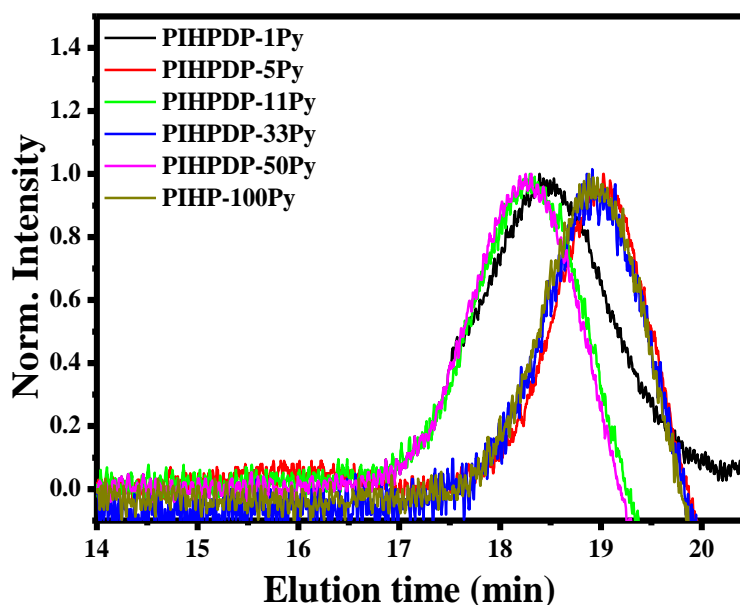
Figure-3.5: The GPC chromatogram of all polymers obtained from RI detector.

The thermal properties of the polymers were studied using TGA and DSC. The 10 weight % loss temperature values are given in the table-3.1. The TGA measurements showed that all the copolymers were thermally stable with the 10 weight % loss temperature around 235-280 $^{\circ}$C (figure-3.6). The T_g of the random copolymers were in between that of the two respective homopolymers (T_g of pyrene homopolymer **PIHP-100Py** = 158 $^{\circ}$C and T_g of PDP homopolymer **PIHPDP-0Py** = 144 °C). The T_g of the random copolymers obtained from the DSC curves were 144, 145, 146, 153, 155 °C for **PIHPDP-1Py**, **PIHPDP-5Py, PIHPDP-11Py, PIHPDP-33Py and PIHPDP-50Py** respectively. The DSC curves of all the polymers are given in the figure-3.7.

Table-3.1: Sample designation, Pyrene incorporation, Number Average Molar Mass (M_n), Weight Average Molar Mass (M_w), Polydispersity indices (Đ), Inherent Viscosity and 10 Wt % loss Temperature of homo and copolymers employed in this study.

Sample Designation	Incorporation of Pyrene (%)		M_n^b	M_w^b	$Đ^b$	Inherent Viscosity (η_{inh}) (dL/g)^c	10 Wt % Loss Temp. (^oC)^d
	In Feed	Actual (from ^1H NMR)^a					
PIHPDP-0Py	0	0	3.80×10^4	4.40×10^4	1.16	0.12	251
PIHPDP-1Py	01	0.9	3.10×10^4	3.60×10^4	1.16	0.20	247
PIHPDP-5Py	05	05	2.10×10^4	2.60×10^4	1.24	0.10	250
PIHPDP-11Py	10	11	3.90×10^4	5.50×10^4	1.41	0.38	251
PIHPDP-33Py	25	33	3.60×10^4	5.30×10^4	1.47	0.37	254
PIHPDP-50Py	50	51	3.80×10^4	4.60×10^4	1.21	0.17	260
PIHP-100Py	100	100	2.20×10^4	3.15×10^4	1.43	0.13	275

a. Calculated from NMR by comparison of integrals.

b. Measured by size exclusion chromatography (SEC) in tetrahydrofuran (THF), calibrated with linear, narrow molecular weight distribution polystyrene standards.

c. Inherent viscosity (η_{inh}) measured in THF.

d. TGA measurements at heating rate of 10 ^oC/ min under nitrogen.
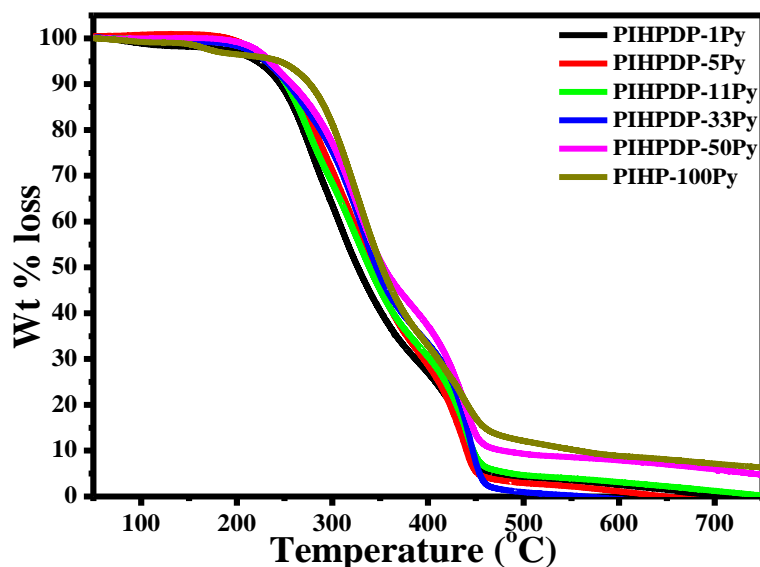
Figure-3.6: TGA Plots of all polymers.
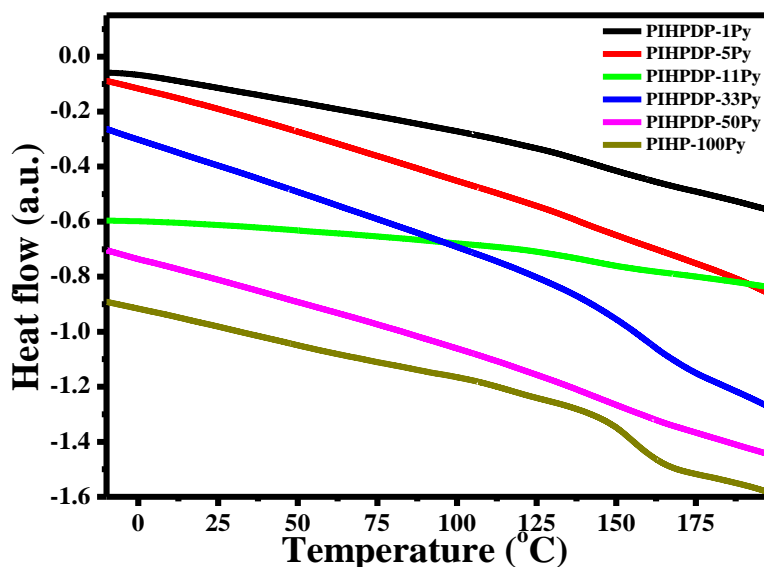
Figure-3.7: DSC curves of all polymers.

3.4.2. Morphology

The side chain urethane methacrylate polymers could self organize in solvents like DMF, $CHCl_3$ and THF. The homopolymers of pyrene and 3-pentadecyl phenol **PIHP-100Py** and **PIHPDP-0Py** self-organised into various architectures such as spheres, vesicles, rods etc. by varying the solvents or solvent combinations.[28, 29, 30] For further studies it was important to establish that the pyrene incorporated as a probe did not have a destructive influence on the self assembling ability of the polymer being probed. The self-organizing tendency of the side chain urethane methacrylate

copolymers were investigated in solvents like DMF, CHCl$_3$ and THF. 0.6-0.8 mg of the copolymers was dissolved in the different solvents and subsequently drop casted onto glass coverslips for the SEM studies.
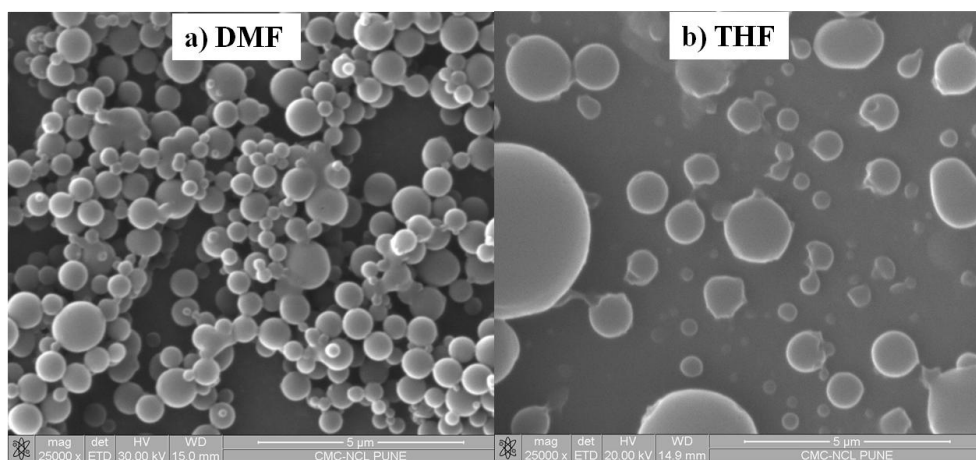
Figure-3.8: SEM image of **PIHPDP-0Py** from DMF and THF dropcasted films.
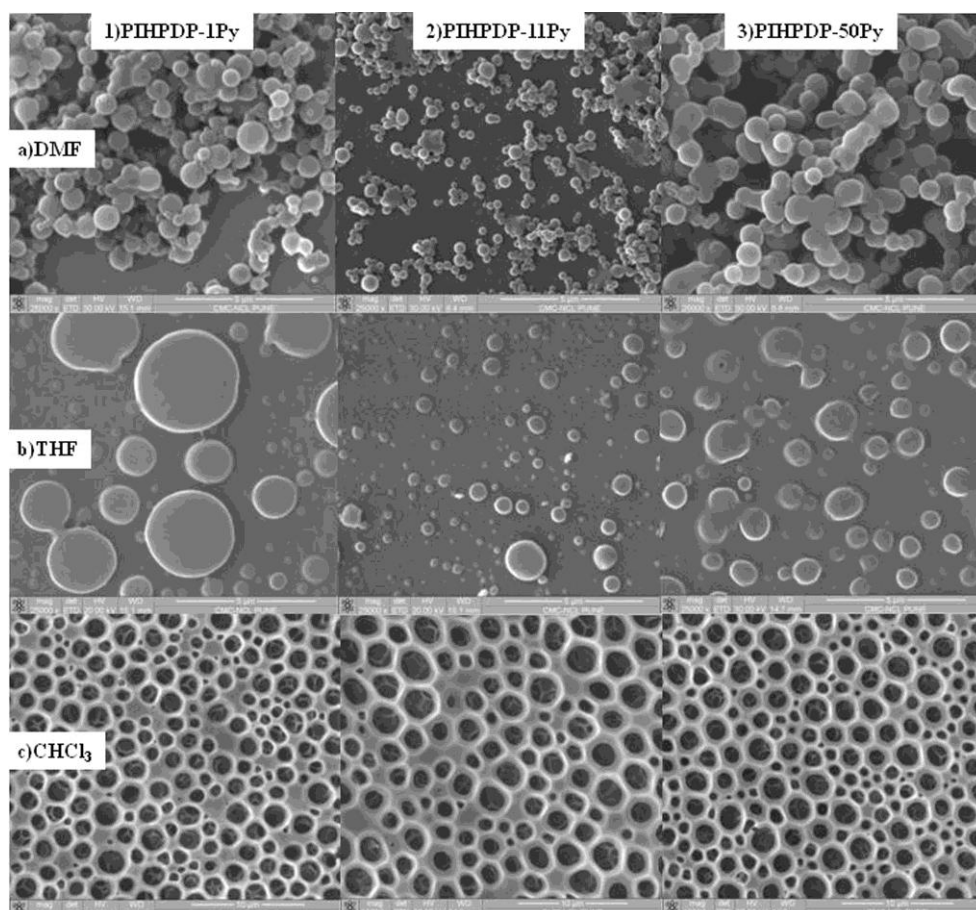
Figure-3.9: SEM image from DMF, THF and CHCl$_3$ drop casted films. **(1a, 2a, 3a)** show images in DMF, **(1b, 2b, 3b)** in THF and **(1c, 2c, 3c)** in CHCl$_3$ for **PIHPDP-1Py**, **PIHPDP-11Py** and **PIHPDP-50Py.**
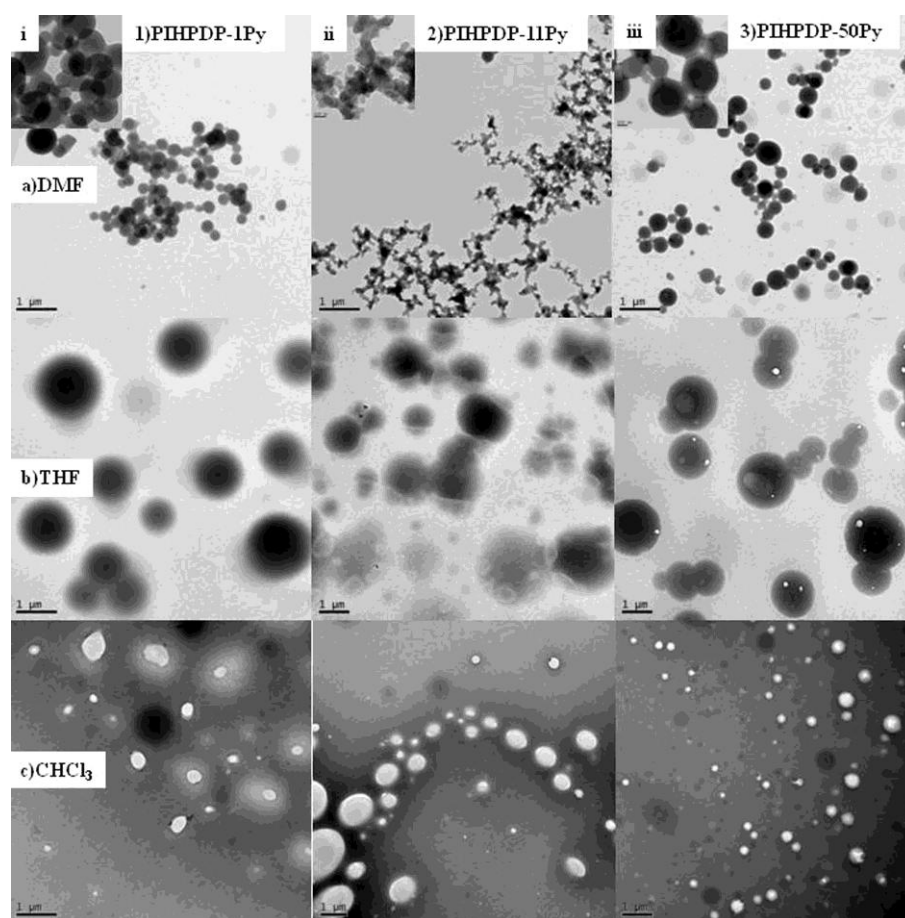
Figure-3.10: TEM images from DMF, THF and CHCl$_3$ drop casted films. **(1a, 2a, 3a)** show images in DMF, **(1b, 2b, 3b)** in THF and **(1c, 2c, 3c)** in CHCl$_3$ for **PIHPDP-1Py**, **PIHPDP-11Py** and **PIHPDP-50Py.**

The solution was evaporated under ambient conditions for 20 hr. It was observed that all the copolymers formed spheres in the size range of 0.4 to 2.5 μm from solvents like DMF and THF. Figure-3.8 shows the SEM images of **PIHPDP-0Py** in DMF and THF. On the other hand, upon drop casting from chloroform, the polymer formed pores. Figure–3.9 shows the SEM images of the three random copolymers**: PIHPDP-1Py**, **PIHPDP-11Py** and **PIHPDP-50Py** drop cast from DMF, CHCl$_3$ and THF as solvent. Figure-3.10 shows the TEM images of these polymers in the respective solvents. From the figure-3.8 and 3.9, it could be noted that the incorporation of varying mole ratios of the bulky pyrene units as pendants into the **PIHPDP** did not disrupt its ability to self-organize.[28, 30] The same morphological features were observed by SEM as well as TEM studies. In chloroform, the polymers formed the honeycomb morphology with the pore size varying from 0.2 to 2.5 μm. The self-organising tendency depends on

various parameters such as sample concentration, molecular weight, polydispersity, various solvents and solvent combinations, solvent viscosity, solvent evaporation, humidity, moisture and specific gravity etc.[36, 37] The variation in self organization for the same sample in different solvents could be due to different rates of drying of the solvent. Since the morphology obtained from DMF solution showed more uniform spheres all further studies were carried out in DMF. The studies were conducted for solutions having pyrene content equivalent to 0.1 OD from absorbance studies.

3.4.3. Photophysical studies

The photophysical studies of all the polymers were carried out for 0.1 OD solution in DMF at a slit width of 1 nm. Figure-3.11 shows the absorption (normalized) and emission spectra (normalised) of all random copolymers along with the **PIHP-100Py** homopolymer recorded by exciting at the λ_{max} of 343 nm for 0.1 OD solutions. The absorption spectra of all the polymers showed the three peaks at 312, 326 and 343 nm corresponding to the characteristic vibronic transitions of pyrene.[1, 38] The emission spectra of the polymers showed characteristic peaks at 375-395 nm regions corresponding to the pyrene monomer emission and a broad red shifted peak around 480 nm corresponding to pyrene excimer emission.[12] The emission parameters such as I_E/I_M ratio and quantum yields values (monomer, excimer and total emission quantum yield) for all the copolymers are compared with the homopolymer **PIHP-100Py** in table-3.2.
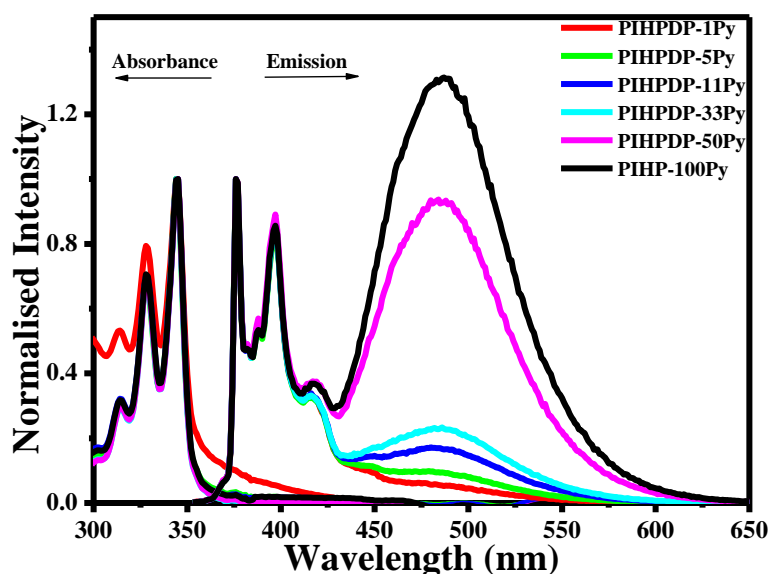
Figure-3.11: Combined UV-VIS Absorption (normalised) and Emission Spectra (normalised) (λ_{ex}-343 nm) for 0.1 OD solution at 343 nm in DMF.

The amplitude of excimer emission expressed by the ratio I_E/I_M (the ratio of the integrated area of excimer region (500-530 nm) and monomer emission region (372-378 nm) was different for all the copolymers.[34] The copolymer **PIHPDP-1Py** had the lowest excimer efficiency ($I_E/I_M = 0.18$) whereas the homopolymer **PIHP-100Py** ($I_E/I_M = 5.68$) exhibited the highest excimer efficiency. Comparing all the copolymers, the excimer efficiency increased with increase in pyrene loading. Table-3.2 also compares the quantum yield for the polymers in DMF which were measured by a relative method using quinine sulfate as the standard ($Q_r = 0.546$ in 0.1M H_2SO_4) for nitrogen purged polymer samples. The quantum yield was calculated using a suitable literature reference.[39]

Table-3.2: The Total Emission Quantum Yield (Q_{Em}), Excimer Emission Efficiency (Q_E) and Monomer Emission Efficiency (Q_M), I_E/I_M ratio, I_1/I_3 ratio and Activation energy (E_a) of the polymers in DMF for 0.1 OD solution at 343 nm.

POLYMER	$Q_{Em}{}^{a}$	$Q_M{}^{a}$	$Q_E{}^{a}$	$I_E/I_M{}^{b}$	$I_1/I_3{}^{c}$	E_a Values (kJ mol^{-1})^{d}
PIHPDP-1Py	0.50 ± 0.04	0.38	0.12	0.18	1.81	1.35 ± 0.41
PIHPDP-5Py	0.48 ± 0.05	0.34	0.14	0.31	1.78	7.59 ± 0.78
PIHPDP-11Py	0.66 ± 0.06	0.39	0.27	0.75	1.80	9.22 ± 0.39
PIHPDP-33Py	0.34 ± 0.03	0.18	0.16	1.05	1.86	9.43 ± 0.35
PIHPDP-50Py	0.31 ± 0.03	0.08	0.23	4.23	1.77	10.5 ± 0.78
PIHP-100Py	0.40 ± 0.04	0.08	0.32	5.68	1.85	8.32 ± 1.05

a. Calculated using 0.1 OD quinine sulphate solution as standard. Excitation wavelength was 343 nm.

b. I_E/I_M determined by taking the ratio of integrated area of excimer (500-530 nm) and monomer (372-378 nm) emission ($\lambda_{ex} = 343$ nm).

c. I_1/I_3 determined by taking the ratio of intensity of I_1 peak (376 nm) and I_3 peak (388 nm) in the monomer emission region emission.

d. Calculated from the Stevens-Ban plot for temperature dependent fluorescence studies for temperature range 10 to 80 ^{o}C.

From table-3.2 it can be seen that, **PIHPDP-11Py** copolymer which had 11% pyrene loading, had the highest overall fluorescence quantum yield of Q = 0.66 ± 0.06. The homopolymer **PIHP-100Py** had overall quantum yield of 0.40 ± 0.04. The quantum efficiency determined separately for the monomer (370-425 nm) and excimer (426-650 nm) region is also given in table-3.2. It can be understood from this tabulation that **PIHPDP-11Py** had the highest monomer quantum efficiency (Q_M = 0.39) whereas the highest excimer quantum efficiency was observed for the homopolymer **PIHP-100Py** (Q_E= 0.32). Thus, the reason for the high total fluorescence quantum yield for the copolymer **PIHPDP-11Py** which was higher than even the 100 % pyrene homopolymer was due to the fact that **PIHPDP-11Py** had high monomer emission but at the same time it also had significant excimer emission which was even higher than **PIHPDP-33Py** and **PIHPDP-50Py**.

Table-3.3: Spectroscopic parameters obtained from Absorption and Fluorescence Excitation Spectra for the copolymers in DMF for 0.1 OD solutions at 343 nm.

POLYMER	$P_A{}^a$	$P_M{}^b$	$P_E{}^c$
PIHPDP-1Py	1.70	2.88	2.75
PIHPDP-5Py	2.69	2.90	2.84
PIHPDP-11Py	2.82	2.94	2.79
PIHPDP-33Py	2.81	2.90	2.69
PIHPDP-50Py	2.81	2.83	2.81
PIHP-100Py	2.79	2.89	2.77

a. Peak-to-valley ratio, P_A, obtained from the Absorption Spectra.
b. Peak-to-valley ratio, obtained from the monomer (P_M) excitation spectrum due to the (0,1) transition.
c. Peak-to-valley ratio, obtained from the Excimer (P_E) excitation spectrum due to the (0,1) transition.

The nature of origin of excimers could be extracted from the absorbance spectrum by comparing the P_A values (which is defined as the peak-to-valley ratio in the first vibronic S2 ←S0 transition)[40] and also from the excitation spectra recorded at the monomer emission (395 nm) and excimer emission (476 nm). P_M can be obtained from the peak-to-valley ratio from the excitation spectrum at the monomer emission wavelength whereas P_E can be extracted from the excitation spectrum at the excimer emission wavelength.[1] A value of ~ 3 for P_A, P_M and P_E indicated absence of ground state aggregates whereas values less than 3 suggested the presence of ground state aggregated species. Table-3.3 compares the P_A, P_M and P_E values for the copolymers extracted from the absorption and excitation spectra recorded in dimethyl formamide (DMF) as solvent. From the P_A values of 1.70, 2.69, 2.82, 2.81, 2.81 and 2.79 respectively for the copolymers with increasing pyrene incorporation, it could be inferred that all the polymers indicated the presence of ground state aggregates (GSA). However, it has to be mentioned here that the absorption spectra of **PIHPDP-1Py** had a sloping baseline making accurate calculation of P_A values difficult. The sloping baseline even after subtracting the blank in the absorption spectrum could be attributed to the larger amounts of sample needed to maintain 0.1 OD for **PIHPDP-1Py**, which could induce polymer aggregation resulting in light scattering.

Another useful parameter that can be extracted from the emission spectra which provides information regarding the microenvironment around the pyrene is the I_1/I_3 ratio. This ratio is dependent on the dielectric constant of the solvent and it provides substantial information regarding the polarity of the medium. I_1/I_3 ratio can be obtained by the intensity ratio between the first (I_1) and the third (I_3) vibronic bands of the monomeric emission.[1] Table-3.2 gives the I_1/I_3 ratio of the random copolymers in DMF, which varied from 1.76 to 1.81 indicating that the pyrene moieties experienced a similar polar environment in all the polymers.

3.4.4. Fluorescence Lifetime decay Profiles

The fluorescence decay was monitored at the monomer region (375 nm) and at the excimer region (500 nm) for nitrogen bubbled solutions in DMF for all the copolymers and compared with homopolymer **PIHP-100Py**. The data was fitted using DAS software. The best fits for the monomer as well as excimer decays for all polymers involved a tri-exponential expression. Fits were good resulting in χ^2 smaller than 1.3 and the residuals and autocorrelation function of the residuals were randomly

distributed around zero. Figure-3.12 compares the decay parameters retrieved from the tri-exponential fits for the copolymers at the monomer (~ 375 nm) and excimer (~ 500 nm) decay. The fluorescence decay times (τ_{M1}, τ_{M2}, τ_{M3}) and pre-exponential factors (α_{M1}, α_{M2}, α_{M3}) obtained by tri-exponential fitting of decay curves at monomer emission (~ 375 nm) were plotted for each polymer in figure-3.12a and b respectively.

Table-3.4 displays the decay times, their pre-exponential contribution and χ^2 values. The long monomer decay time $\tau_{M3,}$ which could be attributed to intrinsic lifetime of pyrene monomer that decayed with it's natural lifetime without undergoing any change, remained similar to that of the IHP monomer, (which was obtained as ~200 ns) for **PIHPDP-1Py** (~188 ns) and **PIHPDP-5Py** (~204 ns) and it decreased with increase in pyrene incorporation in the other random copolymers. **PIHPDP-5Py** had the longest lifetime of 204 ± 4.14 ns and **PIHPDP-33Py** and **PIHPDP-50Py** had the shortest τ_{M3} lifetime value of ~125 ns. The corresponding pre-exponential factor α_{M3} decreased steadily with pyrene incorporation. The decrease in the value of the intrinsic lifetime with increase in pyrene incorporation could be attributed to interaction of 3-pentadecyl phenol with the isolated pyrene species. The monomer decay time τ_{M1} had values ranging from 32 to 72 ns. The short monomer decay time τ_{M2} had values in the range 10-20 ns for all the random polymers except **PIHPDP-1Py** with reasonable pre-exponential contribution. This corresponded to the species which decayed fast to give excimer through dynamic mechanism.From figure-3.12b it can be seen that the change in the pre exponential factors $\alpha_{M1,}$ α_{M2} and α_{M3} as a function of pyrene incorporation was interrelated. For instance, as pyrene incorporation increased, the chances of diffusional encounters among the pyrene increased giving rise to excimer formation and consequent reduction of isolated monomer which could decay with its intrinsic lifetime. Thus α_{M1} and α_{M2} increased with pyrene incorporation whereas α_{M3} decreased with higher pyrene incorporation. Beyond 33 % pyrene incorporation, there was no significant difference in the photophysical properties of the polymers, especially in **PIHPDP-50Py** and **PIHP-100Py**.
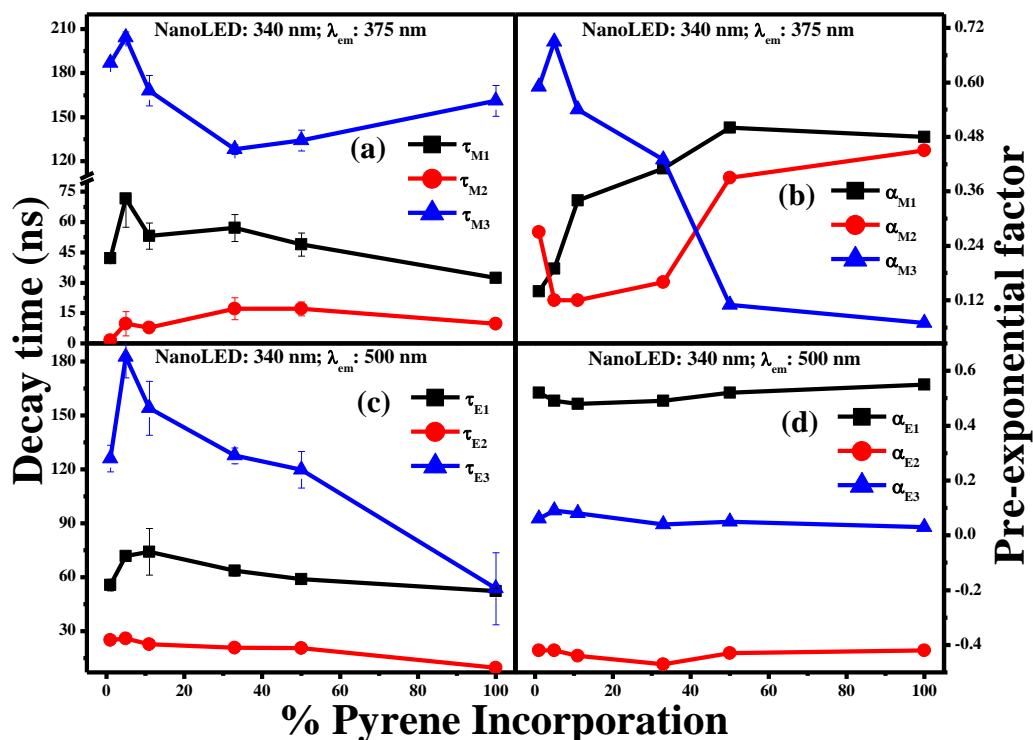
Figure-3.12: Comparison of fluorescence decay times and pre-exponential contribution fitted with tri-exponential parameters for random copolymers for 0.1 OD solution at 343 nm in DMF. **(a and c)** Decay times collected at monomer (~ 375 nm) and excimer emission (~500 nm) respectively. **(b and d)** Pre-exponential factors corresponding to monomer (~ 375 nm) and excimer emission (~500 nm) decay respectively. The nano LED used for excitation was 340 nm. The vertical lines in **(a and c)** shows the error bar.

Table-3.4: Parameters (τ: decay time, α: pre-exponential factor, χ^2: chi-squared value) retrieved from the biexponential fit of the pyrene monomer (375 nm) in DMF obtained by using nano LED 340 nm for excitation.

POLYMER	τ_{M1}	τ_{M2}	τ_{M3}	α_{M1}	α_{M2}	α_{M3}	τ_{Av}	χ^2
PIHPDP-1Py	42.1 ± 1.25	1.45 ± 0.10	187 ± 0.77	0.14	0.27	0.59	119	1.07
PIHPDP-5Py	71.7 ± 14.2	9.72 ± 6.00	204 ± 4.14	0.19	0.12	0.69	165	1.01
PIHPDP-11Py	53.1 ± 6.50	7.80 ± 2.50	168 ± 10.3	0.34	0.12	0.54	119	1.13

PIHPDP-33Py	57.2 ± 6.7 0	17.2 ± 5.50	128 ± 3.25	0.41	0.16	0.43	78.3	1.06
PIHPDP-50Py	48.9 ± 5.70	17.2 ± 3.50	134 ± 7.10	0.50	0.39	0.11	41.2	1.26
PIHP-100Py	32.3 ± 2.20	9.70 ± 1.40	161 ± 10.5	0.48	0.45	0.07	30.7	1.22

Table-3.5: Parameters (τ: decay time, α: pre-exponential factor, $\chi2$: chi-squared value) retrieved from the biexponential fit of the pyrene excimer (500 nm) in DMF obtained by using nano LED 340 nm for excitation.

POLYMER	τ_{E1}	τ_{E2}	τ_{E3}	α_{E1}	α_{E2}	α_{E3}	τ_{av}	$\chi2$
PIHPDP-1Py	55.6 ± 3.20	24.9 ± 1.7	126 ± 7.40	0.52	-0.42	0.06	47.7	1.11
PIHPDP-5Py	71.8 ± 1.50	25.9 ± 1.5	182 ± 11.5	0.49	-0.42	0.09	63.1	1.07
PIHPDP-11Py	74.1 ± 13.0	22.6 ± 0.80	154 ± 15.0	0.48	-0.44	0.08	62.5	1.07
PIHPDP-33Py	63.6 ± 2.80	20.7 ± 1.4	128 ± 4.40	0.49	-0.47	0.04	45.4	1.14
PIHPDP-50Py	58.9 ± 1.50	20.6 ± 1.3	120 ± 10.2	0.52	-0.43	0.05	42.7	1.17
PIHP-100Py	52.3 ± 1.50	9.61 ± 1.45	53.6 ± 20.0	0.55	-0.42	0.03	35.3	1.15

      The fluorescence decay times and pre-exponential factors obtained by tri-exponential fitting of decay curves at excimer emission (~ 500 nm) were plotted for each polymer in figure-3.12c and 3.12d respectively. Table-3.5 displays the decay times, their pre-exponential contribution and χ^2 values. The excimer decay time was obtained between 50-74 ns; the usually reported pyrene normal excimer lifetime being between 40 and 60 ns.[12] All polymers except **PIHPDP-5Py** and **PIHPDP-11Py**

exhibited a typical excimer lifetime within this range. One of the excimer decay had a rise time component which was identified by the negative value of the pre-exponential factors α_{E2}. The negative value of the pre-exponential contribution corresponding to the excimer decay time τ_{E2} i.e. α_{E2} suggested the nature of excimer formation to be through diffusive encounter. The ratio of pre-exponentials i.e. α_{E2}/ α_{E1} corresponding to the excimer emission wavelength provides an insight about the origin of excimer formation.[41] If the ratio is nearly -1, then the excimer formed is through diffusive encounter, and if it deviates from -1, the extent of excimer formed is also contributed by the ground state pyrene aggregates. It can be seen that the ratio of pre-exponentials deviated from -1 for all the polymers (-0.69 to -0.89) indicating the presence of ground state aggregates in all the polymers. The deviation was highest for **PIHPDP-1Py** and **PIHPDP-5Py** at -0.69 which could also be due to the polymer aggregation and light scattering as discussed earlier. The third component was used for the better fitting and its pre-exponential contribution was found to be very small. Due to the complexity of the system having various emitting species of varying lifetimes, it became difficult to carry out a kinetic analysis on the polymers having large pyrene incorporation.

To confirm further the presence of ground state aggregates in the system, the fluorescence decay studies were conducted using the nanoLED of 390 nm as the excitation source, where selectively the ground state aggregates are excited (pyrene monomer absorption is absent)[33] and the decay curves were observed at 440 nm (emission from aggregated species). Figure-3.13 shows the decay curves at 440 nm obtained by exciting at 390 nm. The data was fitted tri-exponentially but it was observed that the pre-exponential contributions: α_2 and α_3 for the two lifetime values: τ_2 and τ_3 were almost negligible for all the polymers. For the copolymer **PIHPDP-1Py** the fitted values were $\tau_1 = 0.75$ ns, $\tau_2 = 3.04$ ns and the corresponding pre-exponentials were $\alpha_1 = 0.84$ and $\alpha_2 = 0.16$. For all other copolymers the τ_1 value remained 0.86 to 0.90 ns with the pre-exponential value (α_1) as 0.94 to 0.99. The τ_2 value also remained around 3.8 to 5.3 ns with small pre-exponential contributions. From the literature, it was found that the pyrene dimers had a decay time of 2 - 3.7 ns with no rise time.[26, 27] Thus, presence of significant amounts of pyrene ground state aggregates were confirmed from the higher contribution ($\alpha_2 = 0.16$) of species with the characteristic decay of 3.0 ns of dimers in **PIHPDP-1Py**.
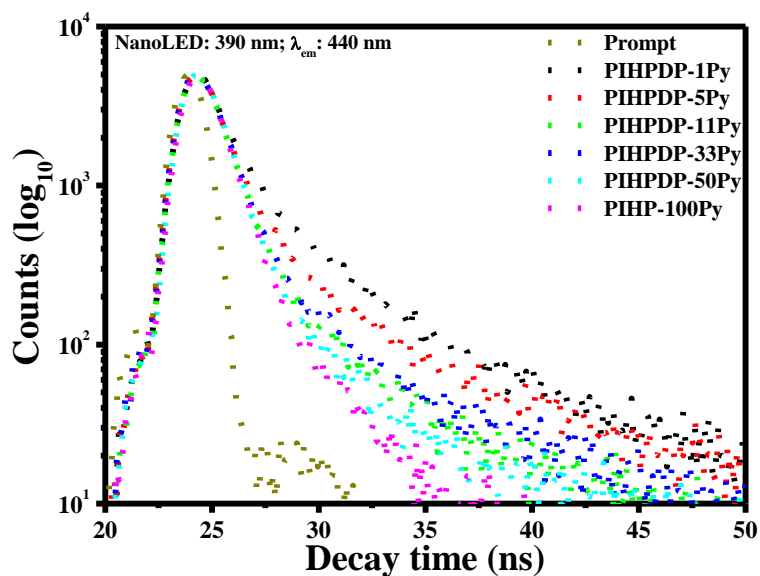
Figure-3.13: Fluorescence decay curves collected at dimer emission wavelength (λ_{em}: 440 nm) by using the nano LED of 390 nm as excitation source in DMF.
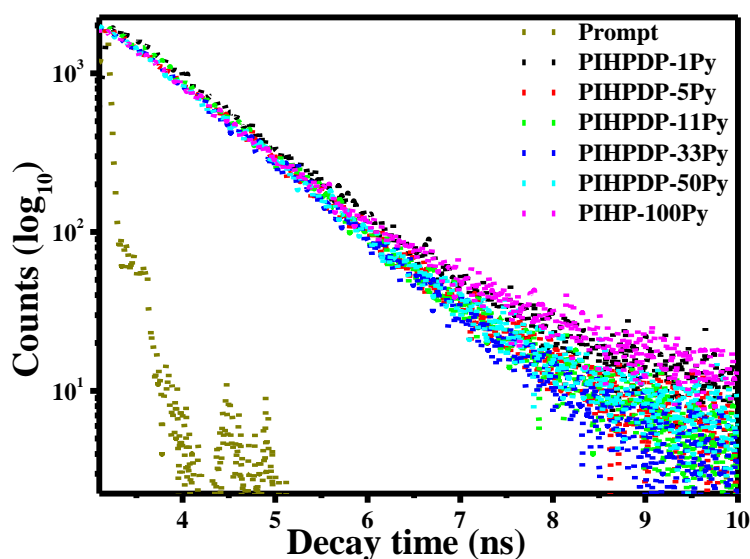
Figure-3.14: Fluorescence decay curves collected at dimer emission wavelength (λ_{em}: 440 nm) by using laser diode of 405 nm as excitation source in DMF.

An attempt was also made to follow the dimer formation using picosecond lifetime studies. Accordingly, 405 ns laser was used to excite the polymer samples and the decay curves were collected at 440 nm. No rise curve was observed and the decay times were observed in the 2-5 ns range for the polymers. The decay curves are given in the figure-3.14. From the figure, it could be clearly seen that the laser is sensitive enough to study the formation of dimer in picoseconds timescale as is evidenced by the

decay curves recorded for the prompt (instrument response function(IRF) values are in ps) and the polymers.

3.4.5. Variable Temperature Studies

3.4.5.1. VT Steady-state emission

Variable temperature emission was recorded in DMF as solvent by varying the temperature from 0 to 85 °C at the excitation wavelength 343 nm. Figure-3.15 demonstrates the steady state emission spectrum obtained upon exciting at 343 nm for the two random copolymers labelled with smallest and highest amount of pyrene i.e **PIHPDP-1Py** and **PIHPDP-50Py**. The lowest and the highest temperature plots are shown in bold lines.
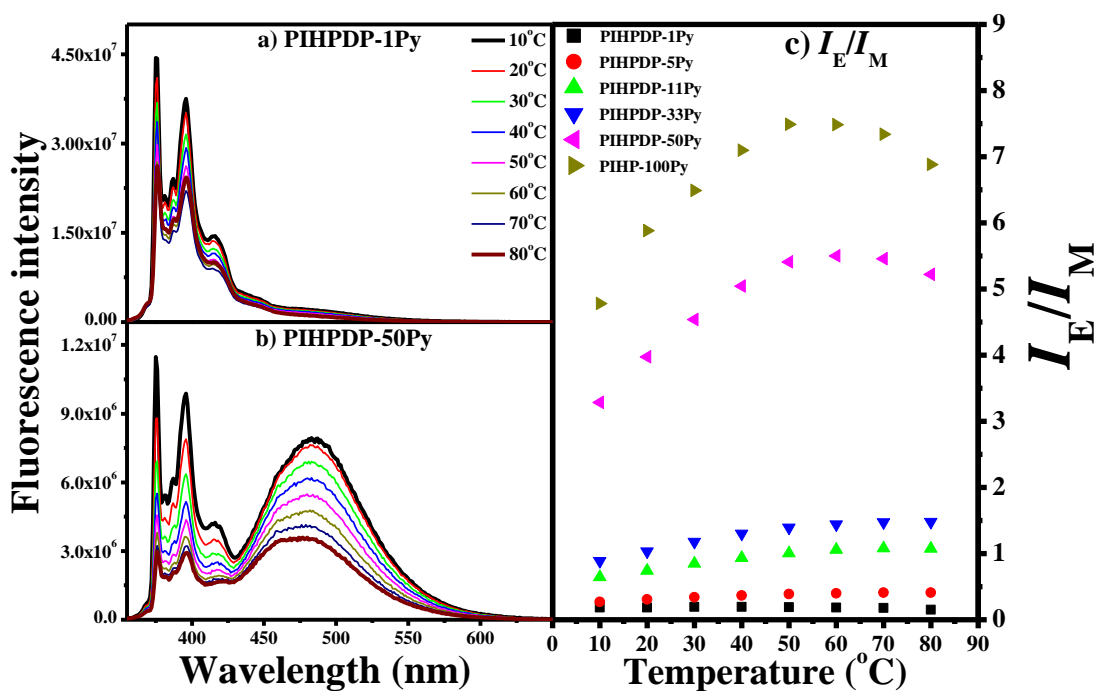
Figure-3.15: **a and b**) Temperature dependent steady state fluorescence for 1 and 50% pyrene incorporated random copolymers and **c**) I_E/I_M ratio as a function of temperature for all polymers for 0.1 OD solution at 343 nm in DMF.

From the figure it can be seen that the total emission (monomer + excimer) decreased for the polymers with increase of temperature. Figure-3.15c compares the excimer emission efficiency of the different polymers as the ratio (I_E/I_M) of the integrated area of excimer region (I_E: 500-530 nm) to that of the integrated area of monomer region (I_M: 372-378 nm) as a function of temperature for the 343 nm

excitation. Although both I_E and I_M values decreased with increase of temperature, their rates were different. The net effect on the I_E/I_M ratio was an initial increase followed by a levelling off at higher temperature (beyond 50 °C). This levelling off temperature varied from 50 °C for **PIHPDP-1Py** to 58 °C for **PIHPDP-50Py** and **PIHP-100Py.** As temperature increased the diffusional encounters of excited pyrene with ground state pyrene also increased resulting in an increase in excimeric emission at the expense of the monomeric emission. However at still higher temperatures the dissociation of pyrene excimer and the domination of non-radiative processes over radiative losses resulted in a levelling-off of the I_E/I_M value.[42]
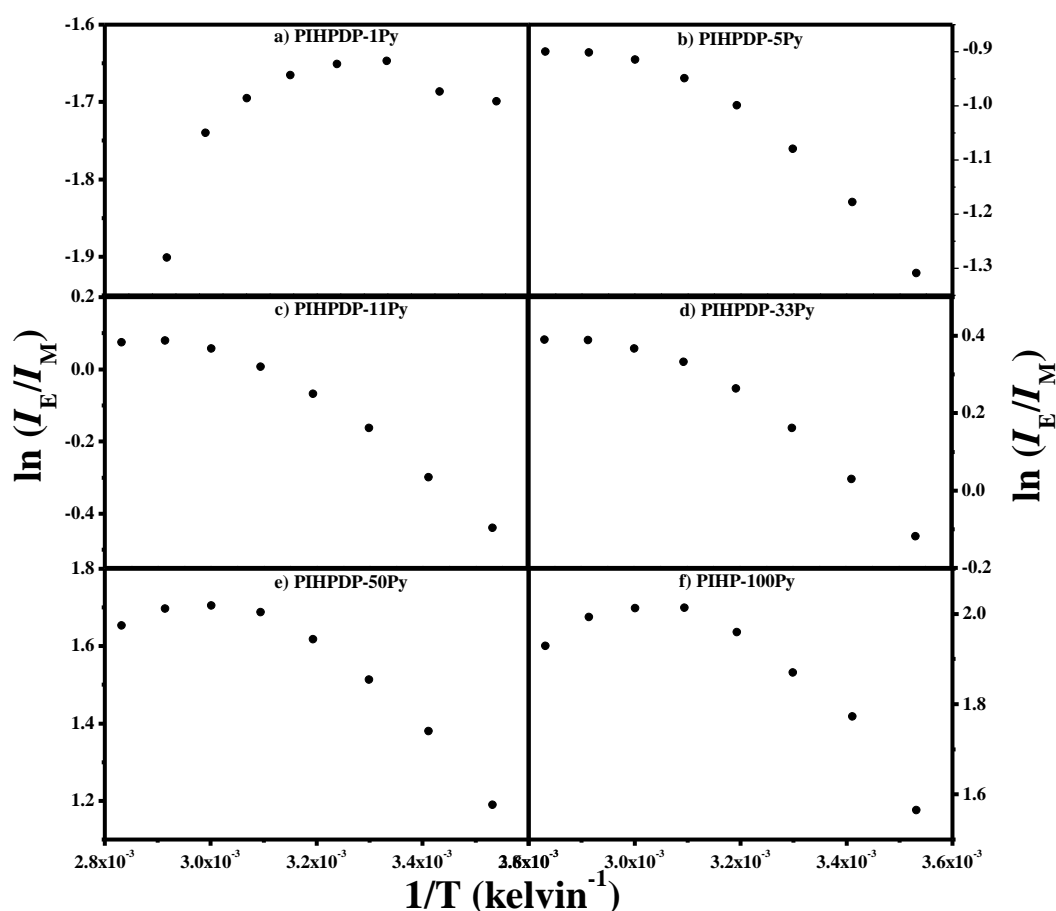
Figure-3.16: Stevens-Ban Plot (Plot of $\ln(I_E/I_M)$ vs $1/T$) for the copolymers for 0.1 OD solution at 343 nm in DMF.

         Stevens-Ban Plot provides significant information of the dependence of the ratio of fluorescence intensity of excimer to monomer (I_E/I_M) as a function of temperature.[43] The complexity of the random copolymers reported here, with various emitting species made it impossible to fit the Stevens-Ban plot in the entire temperature range studied. But the linearity in the I_E/I_M ratio upto a fixed temperature allowed us to

calculate the combined activation energies. Figure-3.16 shows the Stevens-Ban Plot ($\ln(I_E/I_M)$ vs 1/T) for the temperature range 10 to 80 ^{o}C in DMF. The I_E/I_M ratio was found to be proportional to average rate constant of excimer formation at low temperatures and it increased with increasing temperature.[44] On the basis of the Stevens-Ban Plot, activation energy (E_a) of excimer formation below 50 ^{o}C was calculated and given in table-3.2. The activation energies for the polymers were obtained to be 1.35 ± 0.41, 7.59 ± 0.79, 9.22 ± 0.38, 9.43 ± 0.35, 10.5 ± 0.78 and 8.32 ± 1.05 KJ mol^{-1} for **PIHPDP-1PY**, **PIHPDP-5Py**, **PIHPDP-11Py**, **PIHPDP-33Py**, **PIHPDP-50Py** and **PIHP-100Py** respectively. The activation energies of all the polymers with 11% or more pyrene content were almost similar. The deviation of activation energy for **PIHPDP-5Py** could be attributed to slower diffusion due to less excimer formation, whereas the lower value for **PIHPDP-1Py** is due to negligible amount of excimer formation. When the temperature was increased above 50 ^{o}C, the excimer dissociation became non-negligible and the linearity of the $\ln(I_E/I_M)$ versus 1/T was lost. Similar observations have been reported previously for various systems. For instance, the dependence of I_E/I_M on temperature was studied for different pyrene-labeled systems such as Poly(dimethylsiloxane) (Py-PDMS-Py) in ethyl acetate,[42, 45] hydrophobically modified poly(acrylic acid) polymers (PAAMePy)[46] and pyrene and naphthalene labeled EP (Py-EP and Np-EP) in toluene,[44] pyrene labeled PEO chains in toluene,[47] pyrene labeled poly(ε-caprolactone).[48] An activation energy of 8.5 ± 0.3 KJ mol^{-1} was reported for Py-EP-CR in toluene which matched with that of the solvent viscosity activation energy, indicating the diffusion controlled excimer formation process.[44] Similarly activation energy of 8.9 ± 0.7 KJ mol^{-1} for pyrene-labeled poly(dimethylacrylamide) (PDMA05Py) in methanol was nearly the same as the viscosity activation energy of methanol ($E\eta$) 9.5 KJ mol^{-1}, highlighting the excimer formation to be diffusion controlled. The viscosity activation energy of DMF was calculated from the viscosity at different temperatures collected from various literature reports and it was obtained to be 9.1 ± 0.3 KJ mol^{-1}.[49, 50] The activation energy of ~ 9.0 KJ mol^{-1} for the polymers with 11% or more pyrene content matched very well with the solvent activation energy of DMF, thus the excimer formation was found to be diffusion controlled. The polymers having 11% or more pyrene content has no effect on the activation energy of excimer formation, whereas the polymers having <11 % pyrene content deviated from this behavior.

3.4.5.2. VT Fluorescence Decay Studies

To further understand the photophysics of the random copolymers, the fluorescence decay studies were also conducted as a function of temperature in DMF. The fluorescence decay curves of random copolymers were obtained for 0.1 OD solution in DMF at various temperatures ranging from 10 to 70 ^{o}C, by using nanoLED of 340 nm as excitation source and the decays were obtained at pyrene monomer emission (375 nm) and excimer emission (500 nm) wavelengths.
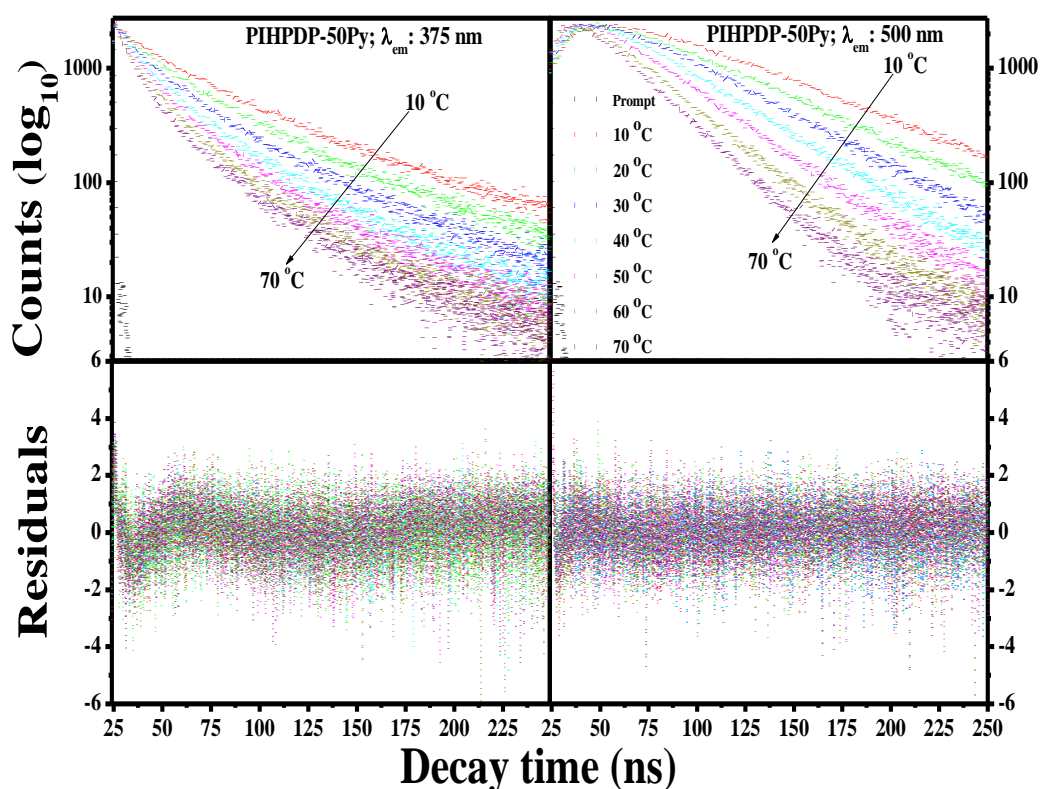
Figure-3.17: Temperature dependent lifetime for **PIHPDP-50Py** and the residuals obtained by triexponential fitting of the decay curves for each temperature for 0.1 OD solution at 343 nm in DMF. NanoLED used: 340 nm and decay collected at monomer (375 nm) and excimer (500 nm) emission as a function of temperature.

Figure-3.17 displays the fluorescence decay curves as a function of temperature for random copolymer **PIHPDP-50Py** as a representative example collected at monomer emission (375 nm) and excimer emission (500 nm) along with the residuals. The DAS software was used for fitting the data with χ^2 values smaller than 1.3 for tri-exponential fits and the residuals and autocorrelation function uniformly spread around zero. There was a decrease in the monomer as well as excimer fluorescence decay time with the

increase in temperature. Figure-3.18 compares the fluorescence decay time values collected at the monomer emission (375 nm) wavelength for all the polymers as a function of temperature. The decay times were obtained by fitting the data tri-exponentially. The corresponding pre-exponential contribution is compared in the figure-3.19.
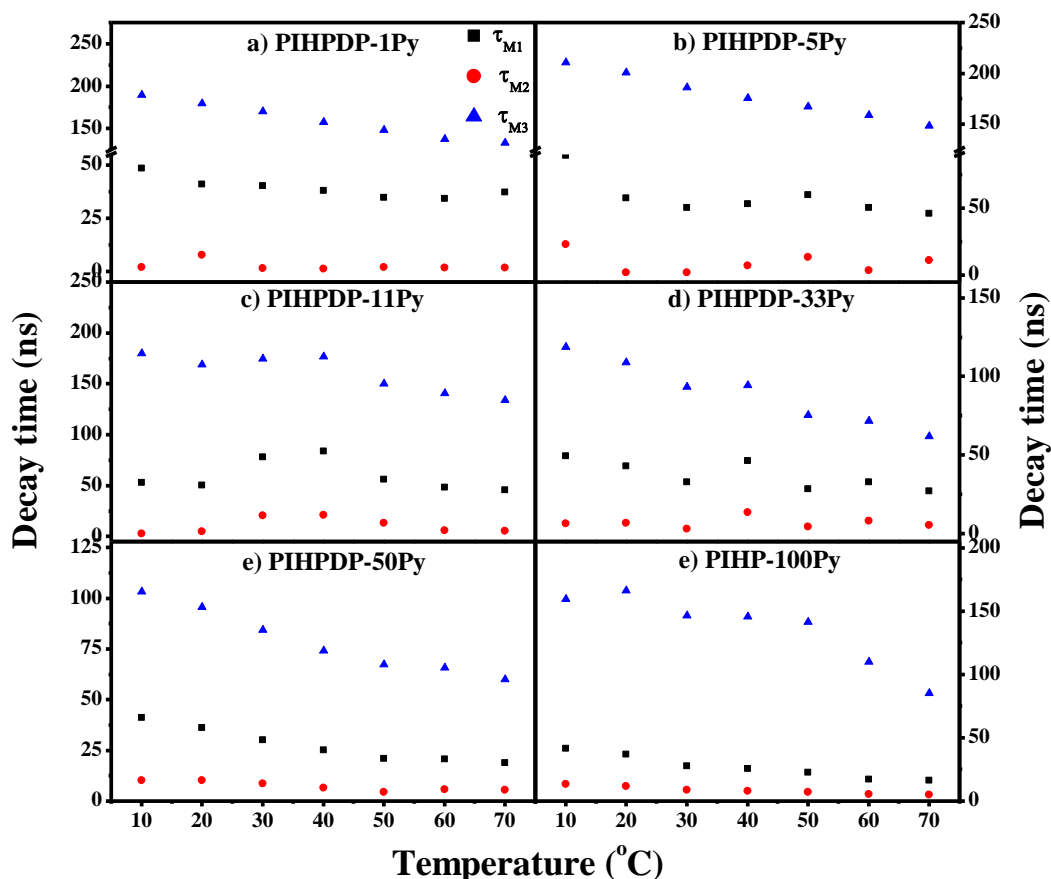
Figure-3.18: Monomer Fluorescence decay times (τ_{M1}, τ_{M2}, τ_{M3}) collected at monomer emission wavelength (λ_{em}: 375 nm) for all the copolymers as a function of temperature in the temperature range 10 to 70 ^{o}C for 0.1 OD solution at 343 nm in DMF.

There was continuous decrease in all the lifetime values due to the increase in the contribution of non-radiative decay processes with the increase in temperature. With the increase in pyrene content, the chances of diffusional encounter increases and the corresponding pre-exponential contribution (α_{M2}) also increases. Upon increase in temperature, the diffusional encounter increases upto a certain temperature, beyond which the dissociation rate constant of the excimer increases, which is observed as a change in pattern of α_{M2}. In the case of copolymer **PIHPDP-50Py** and homopolymer **PIHP-100Py**, the amount of pyrene was more; hence the pre-exponential factor corresponding to the shorter monomer lifetime τ_{M1} was more as more of the species can

give rise to excimer by faster diffusion. The lifetime data exhibited a change of slope around 50-60 $^{\circ}$C mirroring the observation from the variable temperature steady state emission studies indicating changes in the extent of the monomer and excimer emission beyond 50 $^{\circ}$C.
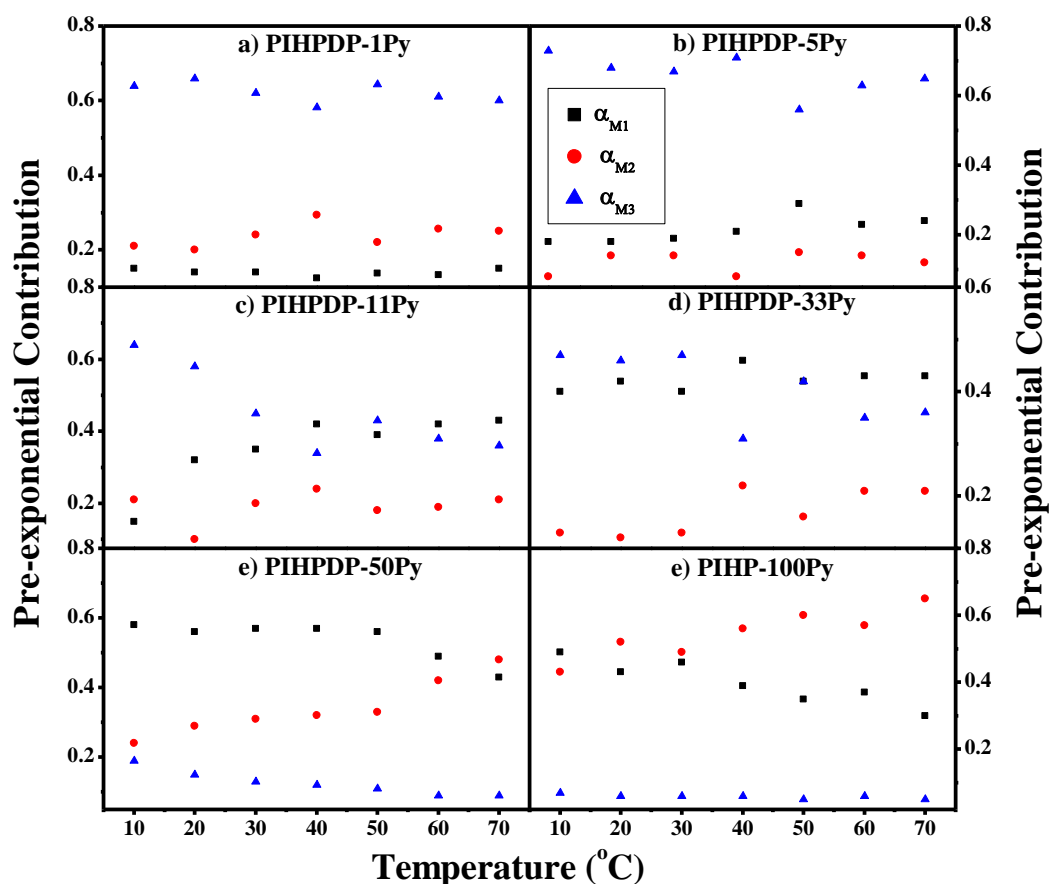
Figure-3.19: Pre-exponential contributions for the respective monomer fluorescence decay times (α_{M1}, α_{M2}, α_{M3}) collected at monomer emission wavelength (λ_{em}: 375 nm) for all the copolymers as a function of temperature in the temperature range 10 to 70 $^{\circ}$C for 0.1 OD solution at 343 nm in DMF.

Figure-3.20 compares the fluorescence decay time values collected at the excimer emission (500 nm) wavelength for all the polymers as a function of temperature. The decay times were obtained by fitting the data tri-exponentially but the pre-exponential contribution corresponding to the largest component τ_{E3} was almost negligible, therefore only τ_{E1} and τ_{E2} are given in the plot. τ_{E1} is a combination of lifetime of excimer and the dissociation rate constant in organic solvents, where as τ_{E2} with negative pre-exponential represent excimer formation through diffusion. From the

figure, it could be clearly seen that the fluorescence decay times decreased linearly with temperature for all the polymers. But another interesting point to be noticed here is that the corresponding pre-exponential contribution remained constant throughout with the increase in temperature.
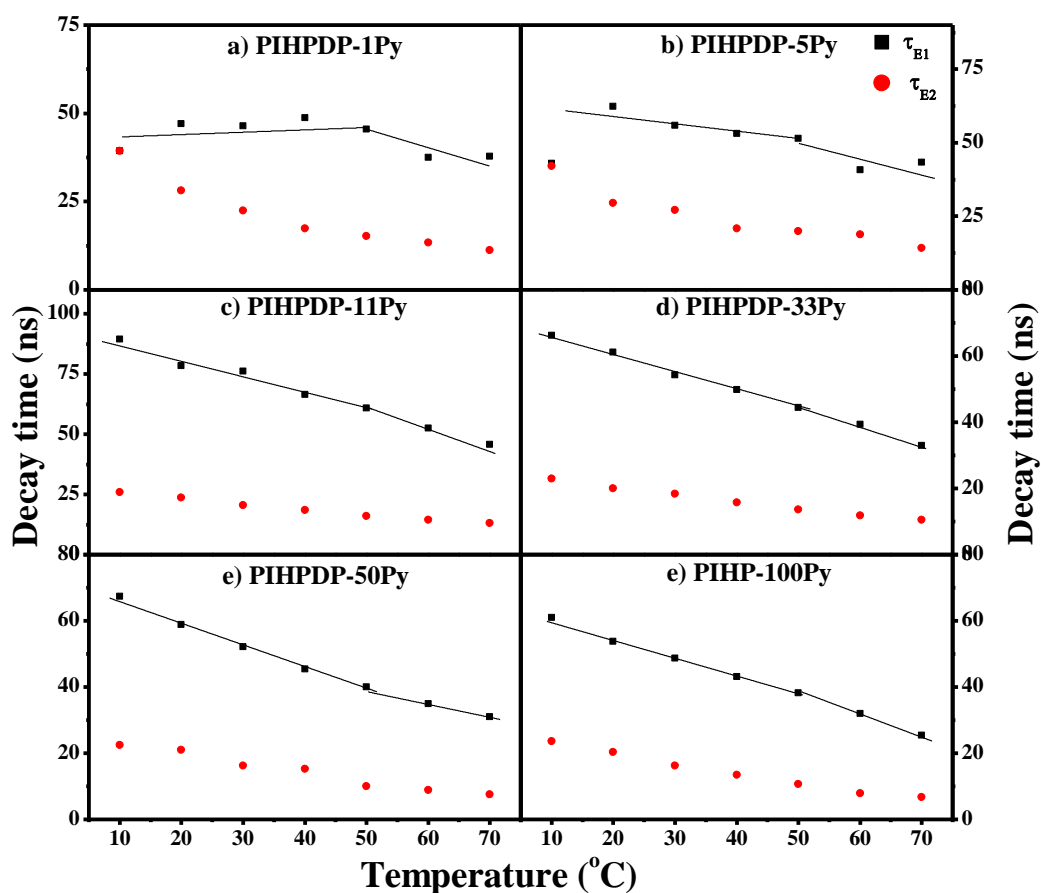
Figure-3.20: Excimer Fluorescence decay times (τ_{E1}, τ_{E2}) collected at monomer emission wavelength (λ_{em}: 375 nm) for all the copolymers as a function of temperature in the temperature range 10 to 70 ^{o}C for 0.1 OD solution at 343 nm in DMF. (τ_{E3} was excluded from the plot since the pre-exponential contribution corresponding to τ_{E3} was negligible.)

3.4.6. Time-resolved emission spectroscopy

The time-dependence of the emission spectra was studied using TRES (time-resolved emission spectra) experiments, which can provide more insight into fluorescence dynamics compared to steady-state based measurements. In this experiment the time-resolved decays at a number of wavelengths (365-545 nm) across the emission spectrum were collected. Figure-3.21 and figure-3.22 show the 3 D contour plots representing the three-dimensional time-intensity-wavelength data

110

recorded at RT (25 °C) and 70 °C respectively for each polymer sample. The decay at each wavelength was then normalized and used to calculate the time-resolved emission spectra (TRES) for any desired time following excitation using the equation.[30, 51]

$$I(\lambda,t) = I_{ss}(\lambda) \left(\sum_j \alpha_j(\lambda) \, e^{-t/\tau_j(\lambda)} \Big/ \sum_j \alpha_j(\lambda) \, \tau_j(\lambda) \right)$$

Where $I_{ss}(\lambda)$ is the steady state fluorescence intensity, $\alpha_j(\lambda)$ is the amplitude pre-exponential factor and $\tau_j(\lambda)$ is the decay times.

Figure-3.21: The 3-D contour plots representing the three-dimensional time-intensity-wavelength data recorded at 25 °C (RT) in the wavelength range 365 to 545 nm using nanoLED of 340 nm for 0.1 OD solution at 343 nm in DMF.

Figure-3.23 also shows the two-dimensional normalized fluorescence emission spectra constructed from intensities sampled at discrete times (0.66 to 32.9 ns) during the fluorescence decay of the sample measured over the wavelength range of 365-545 nm for all the 6 polymers. Although the information regarding the relative difference between the fluorescence intensities for the different time intervals are lost by normalization, information regarding the time evolution of emission can be retrieved. The reconstructed TRES was very similar to the steady-state emission spectra except that the isoemissive points were also observed in the TRES. An isoemissive point in emission spectra is analogous to isosbestic point in the absorption spectrum and is

defined by the wavelength at which the intensity does not vary with time and is indicative of the presence of more than one emitting species in the system.[51] In general, the n number of isoemissive points in the system gives the n+1 emitting species. Another information that could be retrieved from the wavelength dependent decay studies is the kinetic coupledness of the emissive species by observing the negative amplitude of a decay constant at long emission wavelength.
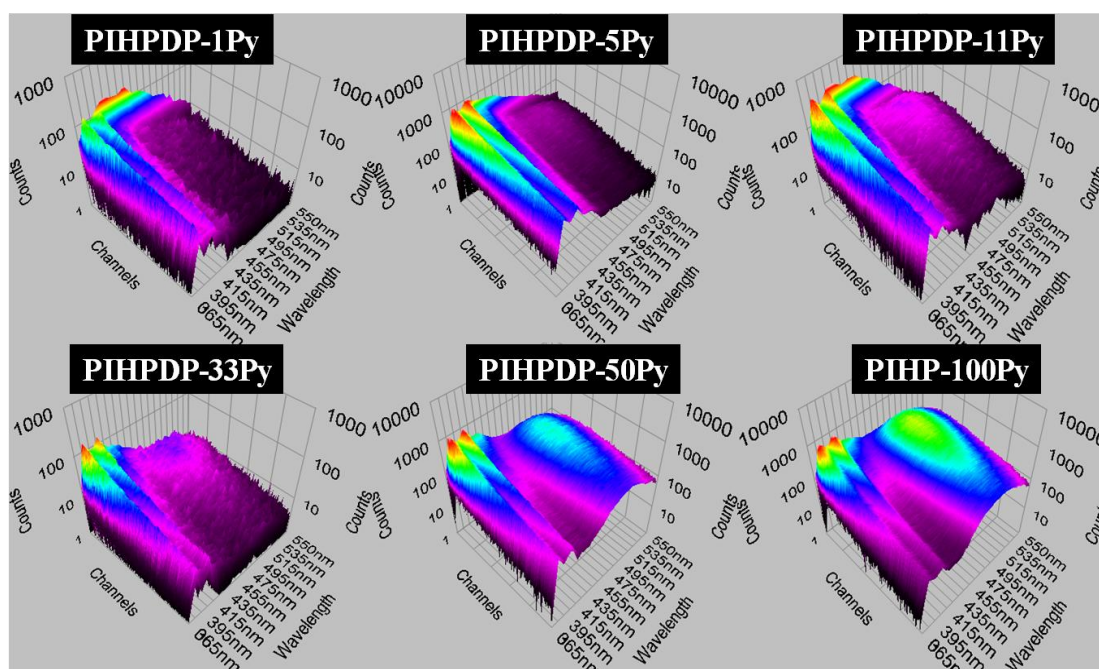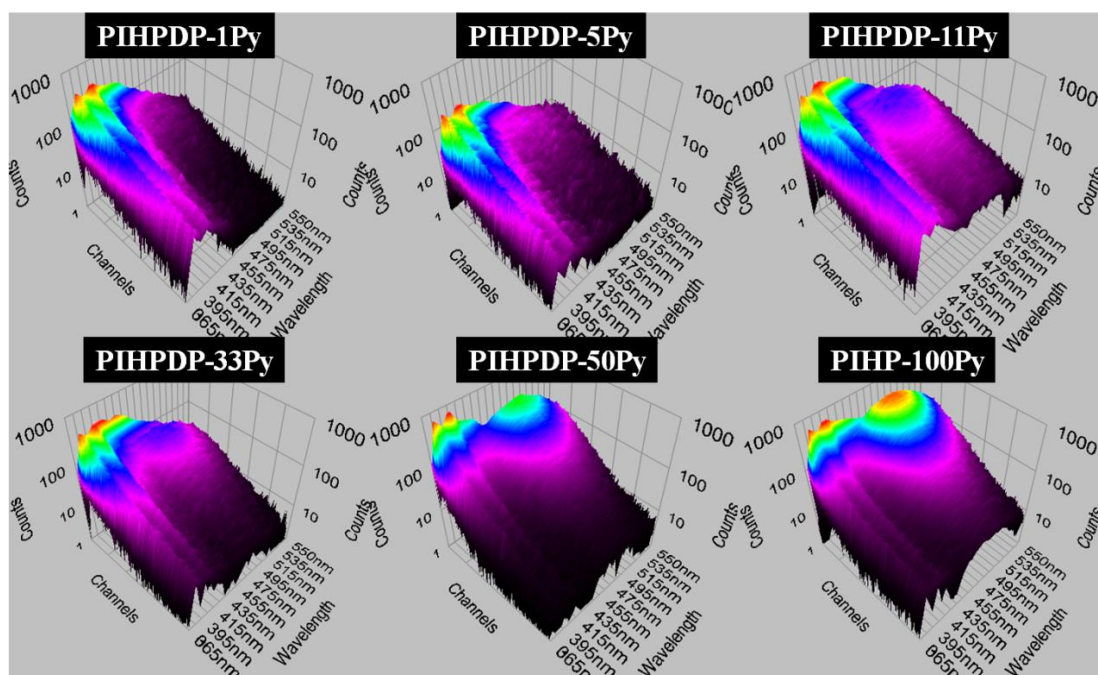

Figure-3.22: The 3-D contour plots representing the three-dimensional time-intensity-wavelength data recorded at 70 ^{o}C in the wavelength range 365 to 545 nm using nano LED of 340 nm for 0.1 OD solution at 343 nm in DMF.

From the plots it can be clearly seen that there was domination of monomer emission in the earlier time gate spectra which gradually red shifted for the higher time gate spectra. This absence of excimer emission in the early spectra and its slow formation in the later time gated spectra indicated dynamic nature of excimer formation. A careful examination of the early time gated spectra indicated emission centred ~430 nm especially in the copolymers with pyrene incorporation greater than 10 %. This emission gave way to two emission peaks centred ~455 to 465 nm and 485 nm respectively in the higher time (>8.58 ns) gated spectra. The emission centred around 435-445 nm has usually been attributed to direct excitation of ground state pyrene dimers or static excimers, whereas the emission ~455 to 465 nm corresponded to emission from partially overlapped or distorted pyrenes. The emission ~455 to 465 nm

is considered due to the more stable excimer having twisted sandwich geometry.[12, 32] The higher wavelength emission ~485 nm have their origin from pyrene which are perfectly oriented with respect to each other and give rise to less stable excimer having parallel sandwich conformation.[32, 52, 53] Therefore, in polymers with higher pyrene incorporation emission from short-lived dimeric pyrene predominated in the early stages whereas at later times (>8 ns) emission from both distorted and perfectly oriented pyrene predominated. In **PIHP-100Py** even in the 8.0 ns time gated spectra the excimer emission intensity was so high compared to the monomeric emission that the peak was broad making it difficult to distinguish the presence of two peaks. For **PIHPDP-1Py** and **PIHPDP-5Py** there was very negligible excimer emission. However, their initial spectra showed broadening in the region from 415-440 nm suggesting presence of ground state aggregates. This was in confirmation with the observation from the steady state fluorescence experiments which also suggested presence of pre formed aggregates in **PIHPDP-1Py** as a consequence of polymer aggregation.

The TRES with time gates from 0.66 to 32.9 ns during the fluorescence decay of the polymer samples measured over the wavelength range of 365-545 nm for the polymers at 70 ^{o}C was also studied. The most prominent difference of these spectra compared to that collected at room temperature (25 °C) was the higher intensity for excimer emission at 70 °C, especially for polymers with >10 % pyrene incorporation. Even for the short time gated spectra, excimer emission centered ~ 455 and 485 nm was visible. The one exception was **PIHPDP-1Py** which did not exhibit much excimer emission at 70 °C even in the 32.9 ns time-gated spectra. The 3-D contour plots of **PIHPDP-1Py** collected at 70 °C showed some excimeric emission in the early time period. This could be seen in the two dimensional reconstructed TRES plot also that the 0.66 ns time gated spectra was broad in the range 435-445 nm with a shoulder clearly visible near 455 nm suggesting distorted pyrene emission. Since this emission was short-lived it was not observed in the higher time-gated spectra. Another important observation was that even at 70 °C, the emission centered around 430-445 nm was observed in all the polymers suggesting the distortion of pyrene excimers brought about by the temperature. The overall picture of the nature of emitting species and their formation time obtained by the TRES experiments have been summarised in the figure-3.24.

Figure-3.23: The normalized (at the wavelength of maximum fluorescence intensity) TRES at RT with a gated time from 0.66 to 32.9 ns for 0.1 OD solution at 343 nm in DMF.

Dimer formation process was followed in the picosecond range using TRES of polymers collected with the excitation at 405 nm (a region where the pyrene monomer is completely absent) and emission collected in the wavelength range 420-550 nm. The regenerated TRES is given in the figure-3.25. The regenerated spectrum of smaller time-gated range (<0.46 ns) showed only peak at around 435 nm (data not shown). It could be clearly seen that the emission peak at 435 nm shifted towards 465 and 485 nm at higher time gated spectra (> 5.78 ns), which clearly indicated that the origin of these species could not be differentiated by steady state emission studies alone. In the polymers having higher pyrene content i.e **PIHPDP-50Py** and **PIHP-100Py** peaks at around 430, 465 and 485 nm were observed even at lowest time-gated spectra (0.46 ns), indicating the presence of various emitting species. Thus the picosecond-TRES experiments clearly highlighted the existence of different emitting species i.e. emission

due to ground state dimers (~430 nm), stable excimers having twisted geometry (~455-465 nm) and less stable excimers having sandwich geometry (~485 nm).

Emitting species / Polymer	Isolated monomer (375-395 nm)	Partially overlapped excimer (455-465 nm)	Sandwich excimer (~485 nm)
PIHPDP-1Py	< 0.66 ns	< 0.66 ns	Almost negligible (even after 8.5 ns)
PIHPDP-5Py	< 0.66 ns	< 0.66 ns	Very small (even after 8.5 ns)
PIHPDP-11Py	< 0.66 ns	< 0.66 ns	Very small (after 8.5 ns)
PIHPDP-33Py	< 0.66 ns	< 0.66 ns	> 1.32 ns
PIHPDP-50Py	< 0.66 ns	< 0.66 ns	> 0.66 ns
PIHP-100Py	< 0.66 ns	< 0.66 ns	> 0.66 ns

Figure-3.24: Tabulated picture representing the nature of emitting species and their formation time on the basis of TRES experiments conducted at room temperature.
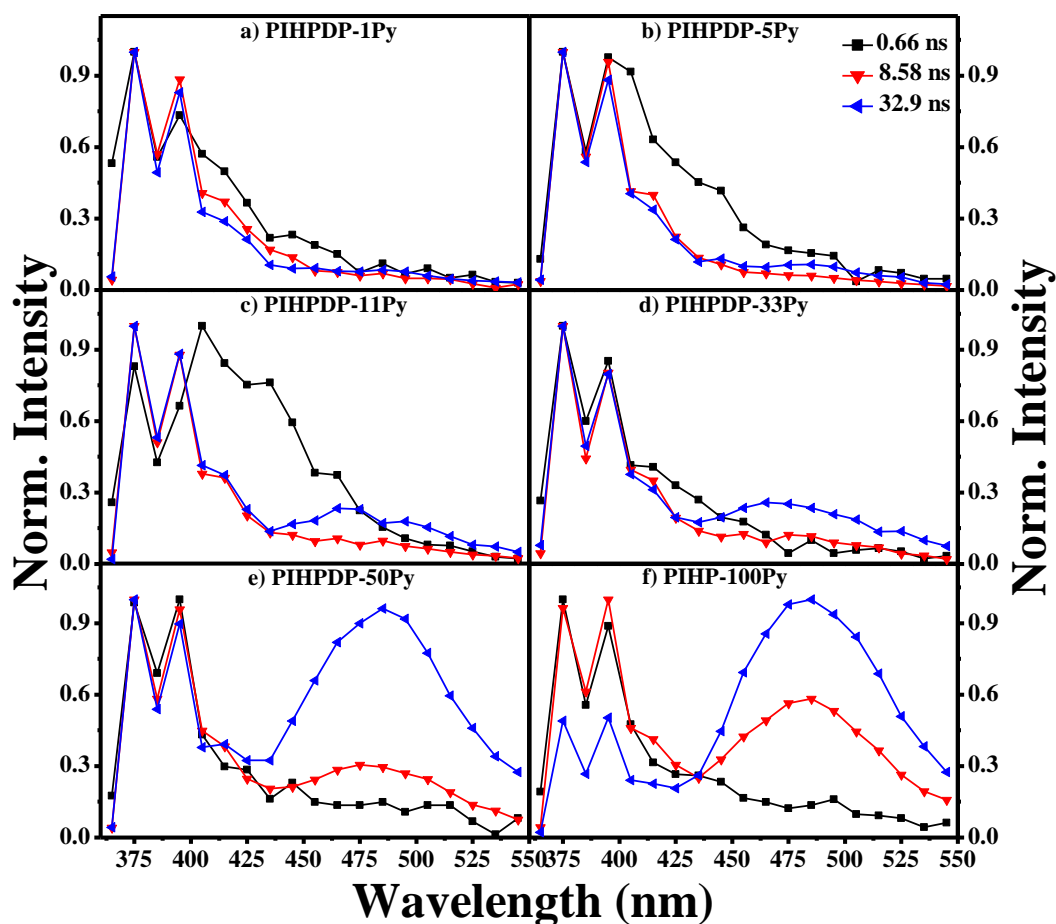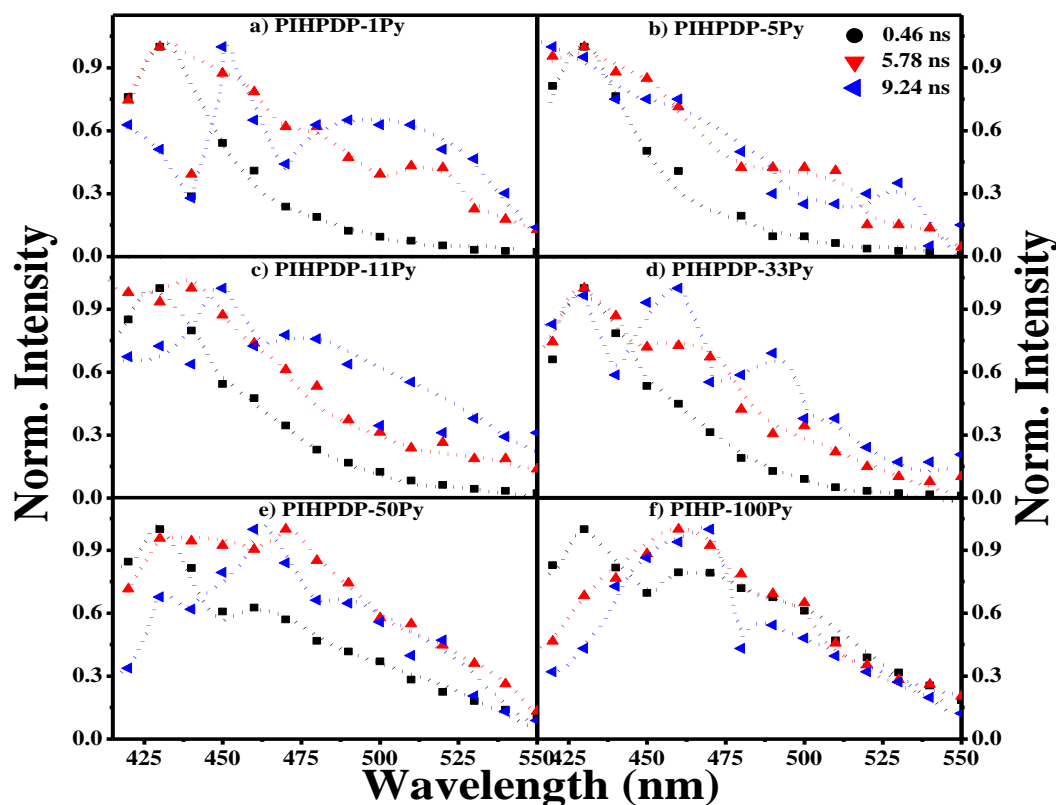
Figure-3.25: The normalized (at the wavelength of maximum fluorescence intensity) picosecond-TRES at RT with a gated time from 0.46 to 9.24 ns for 0.1 OD solution at 343 nm using laser of 405 nm in DMF.

3.5. Conclusions

Steady-state and time-resolved fluorescence studies were used to probe the nature and evolution of various emitting species in randomly pyrene labeled side chain urethane methacrylate polymers with pyrene incorporation varying the entire range from 1 to 100 %. The existence of ground state aggregated pyrenes in all polymers was unequivocally proven by the fluorescence lifetime decay as well as TRES experiments. Fluorescence lifetime decay studies conducted using nanoLED of 390 nm and laser of 405 nm and decay observed at 440 nm showed the existence of significant amounts of short lived (~3 to 5 ns) species in the copolymer with lowest pyrene incorporation i.e **PIHPDP-1Py** and to a lesser extent in all polymers. This was rather unexpected in **PIHPDP-1Py**. TRES experiments showed that the short-lived ground state aggregated species emitting in the 435 nm region dominated the earlier time-gated spectra which then gave way to emission ~465 and 485 nm corresponding to excited pyrene in constrained and perfect orientation respectively. But the copolymers **PIHPDP-1Py** and **PIHPDP-5Py** showed mainly monomer and dimer emission at very short time-gated spectra and the excimer

emission was almost negligible even at higher time. The polymers having higher pyrene i.e. **PIHPDP-50Py** and **PIHP-100Py** content showed the various emitting species which emit in the monomer, dimer and excimer in constrained environment as well as perfect orientation. The TRES carried out at higher temperature surprisingly showed that even at 70 °C, aggregated species emitting in the 435 nm region was present in **PIHPDP-1Py**. The variable temperature steady-state studies showed that a transition from more monomer dominated emission to diffusion-induced excimer emission occurred around 50 °C for copolymers with low pyrene incorporation (>33 %); whereas for the copolymers with 50 and 100% pyrene incorporation this transition occurred at higher temperature ~58 °C. In summary, the series of steady-state emission, fluorescence lifetime decay analysis, variable temperature measurements and TRES experiments performed on these urethane methacrylate random pyrene copolymers has helped to develop an overall picture, albeit qualitative, of the nature and evolution of various types of emitting species as a function of varying pyrene incorporation. These experiments have clearly brought about a perfect picture of nature and time of origin of various emitting species which was reasonably rationalised with the varying amount of pyrene content in the copolymers.

3.6. References

1) Winnik, F. M.; *Chem. Rev.* **1993**, *93*, 587-614.

2) Zachariasse, K.; Kuhnle, W. *Z. Phys. Chem. Neue F* **1976**, *101*, 267-276.

3) Cuniberti, C.; Perico, A. *Eur. Polym. J.* **1977**, *13*, 369-374.

4) Winnik, F. M.; Regismond, S. T. A. *Colloids Surf. A* **1996**, *118*, 1-39.

5) Martinho, J. M. G.; Farinha, J. P.; Berberan-Santos, M. N.; Duhamel, J.; Winnik, M. A. *J. Chem. Phys.* **1992**, *96*, 8143-8149.

6) Selinger, B. K.; Watkins, A. R. *J. Photochem.* **1981**, *16*, 321-330.

8) Birks, J. B.; Lumb, M.D.; Munro, I. H. *Proc. Roy. Soc. Lond. A* **1964***, 280,* 289-297.

9) Birks, J. B.; Alwattar, A. J. H.; Lumb, M. D. *Chem. Phys. Lett.* **1971**, *11*, 89-92.

10) Birks, J. B.; Dyson, D. J.; Munro, I. H. *Proc. Roy. Soc. Lond. A* **1963**, *275*, 575-588.

11) Lakowicz, J. R. *Principles of Fluorescence Spectroscopy*, 2nd ed.; Kluwer Academics/Plenum Publisher: New York, **1999**.

12) Birks, J. B. *Photophysics of Aromatic Molecules*, Wiley/Interscience; New York, **1970**.

13) Conlon, P.; Yang, C. J.; Wu, Y.; Chen, Y.; Martinez, K.; Kim, Y.; Stevens, N.; Marti, A. A.; Jockusch, S.; Turro, N. J.; Tan, W. *J. Am. Chem. Soc.* **2008**, 130, 336-342.

14) Berlman, I. B. Handbook of Fluorescence Spectra of Aromatic Molecules, Academic Press N. Y., **1971**.

15) Kalyanasundaram, K.; Thomas, J. K. *J. Am. Chem. Soc.* **1977**, *99*, 2039-2044.

16) Duhamel, J. *Langmuir* **2012**, *28*, 6527-6538.

17) Yip, J.; Duhamel, J.; Qiu, X. P.; Winnik, F. M. *Macromolecules* **2011**, *44*, 5363-5372.

18) Holappa, S.; Kantonen, L.; Winnik, F. M.; Tenhu, H. *Macromolecules* **2004**, *37*, 7008-7018.

19) Zhao, C.; Wu, D.; Lian, X.; Zhang, Y.; Song, X.; Zhao, H. *J. Phys. Chem. B* **2010**, *114*, 6300-6308.

20) Schillen, K.; Anghel, D. F.; Miguel, M. D.; Lindman, B. *Langmuir* **2000**, *16*, 10528-10539.

21) Arora, K. S.; Hwang, K. C.; Turro, N. J. *Macromolecules* **1986**, *19*, 2806-2810.

22) Nezu, T.; Winnik, F. M. *Biomaterials* **2000**, *21*, 415-419.

23) Kashyap, S.; Jayakannan, M. *J. Phys. Chem. B* **2012**, *116*, 9820-9831.

24) Siu, H.; Duhamel, J. *J. Phys. Chem. B* **2008**, *112*, 15301-15312.

25) Siu, H.; Duhamel, J. *J. Phys. Chem. B* **2012**, *116*, 1226-1233.

26) Gago, S.; Costa, T.; de Melo, J. S.; Goncalves, I. S.; Pillinger, M. *J. Mater. Chem.* **2008**, *18*, 894-904.

27) Reynders, P.; Kuhnle, W.; Zachariasse, K. A. *J. Am. Chem. Soc.* **1990**, *112*, 3929-3939.

28) Deepak, V. D.; Asha, S. K. *J. Phys. Chem. B* **2009**, *113*, 11887-11897.

29) Kaushlendra, K.; Deepak, V. D.; Asha, S. K. *J. Polym. Sci., Part A: Polym. Chem.* **2011**, *49*, 1678-1690.

30) Rekha, N.; Asha, S. K. *J. Polym. Sci., Part A: Polym. Chem.* **2009**, *47*, 2996-3009.

31) Lakowicz, J. R. *Principles of Fluorescence Spectroscopy*, Plenum Press: New York, 1983; Chapters 8 and 12.

32) Yamazaki, I.; Winnik, F. M.; Winnik, M. A.; Tazuke, S. *J. Phys. Chem.* **1987**, *91*, 4213-4216.

33) Gao, L.; Fang, Y.; Wen, X.; Li, Y.; Hu, D. *J. Phys. Chem. B* **2004**, *108*, 1207−1213.

34) Costa, T.; de Melo, J. S. S.; Castro, C. S.; Gago, S.; Pillinger, M.; Goncalves, I. S. *J. Phys. Chem. B* **2010**, *114*, 12439-12447.

35) Duhamel, J.; Kanagalingam, S.; O'Brien, T. J.; Ingratta, M. W. *J. Am. Chem. Soc.* **2003**, *125*, 12810-12822.

36) Stenzel, M. H. *Aust. J. Chem.* **2002**, 55, 239-243.

37) Bormashenko, E.; Pogreb, R.; Stanevsky, O.; Bormashenko, Y.; Stein, T.; Gendelman, O. *Langmuir* **2005**, *21*, 9604-9609.

38) Prado, E. A.; Yamaki, S. B.; Atvars, T. D. Z.; Zimerman, O. E.; Weiss, R. G. *J. Phys. Chem. B* **2000**, *104*, 5905−5914.

39) Eaton, D. F. *Pure Appl. Chem.* **1988**, *60*, 1107-1114.

40) De Melo, J. S. S.; Costa, T.; Miguel, M. G.; Lindman, B.; Schillen, K. *J. Phys. Chem. B* **2003**, *107*, 12605−12621.

41) Mathew, A. K.; Duhamel, J.; Gao, J. *Macromolecules* **2001**, *34*, 1454−1469.

42) Gardinier, W. E.; Bright, F. V. *J. Phys. Chem. B* **2005**, *109*, 14824-14829.

43) Stevens, B.; Ban, M. I. *Trans. Faraday Soc.* **1964**, *60*, 1515−1523.

44) Zhang, M.; Duhamel, J. *Macromolecules* **2007**, *40*, 661−669.

45) Gardinier, W. E.; Bright, F. V. *Macromolecules* **2005**, *38*, 8574-8582.

46) De Melo, J. S.; Costa, T.; Francisco, A.; Macanita, A. L.; Gago, S.; Goncalves, I. S. *Phys. Chem. Chem. Phys.* **2007**, *9*, 1370-1385.

47) Farinha, J. P. S.; Picarra, S.; Miesel, K.; Martinho, J. M. G. *J. Phys. Chem. B* **2001**, *105*, 10536-10545.

48) Picarra, S.; Gomes, P. T.; Martinho, J. M. G. *Macromolecules* **2000**, *33*, 3947−3950.

49) Lide, D. R. Ed. CRC Handbook of Chemistry and Physics, Internet Version 2005; CRC Press: Boca Raton, FL, 2005; http://www.hbcpnetbase.com.

50) Marchetti, A.; Preti, C.; Tagilazucchi, M.; Tassi, L.; Tosi, G. *J. Chem. Eng. Data* **1991**, *36*, 365−368.

51) Koti, A. S. R.; Krishna, M. M. G.; Periasamy, N. *J. Phys. Chem. A* **2001**, *105*, 1767-1771.

52) Zachariasse, K. A.; Duveneck, G.; Kuhnle, W. *Chem. Phys. Lett.* **1985**, 113, 337-343.

53) Winnik, F. M.; Tamai, N.; Yonezawa, J.; Nishimura, Y.; Yamazaki, I. *J. Phys. Chem.* **1992**, *96*, 1967−1972.

Chapter 4:

Microstructural Reorganization and Cargo Release
from Dye Encapsulated Pyrene Urethane
Methacrylate Copolymer Hollow Capsule

4.1. Abstract

From chapter 3 it was observed that the pyrene urethane methacrylate copolymers and homopolymers formed spheres upon drop casting from THF or DMF. Interestingly, when a hydrophilic oligoethyleneoxy unit was incorporated into the monomer design, no morphology was observed when dropcast from a variety of solvents, although excimer emission was still observed under dilute conditions also. This study clearly highlighted the difficulty in correlating self-assembly in solution to the observed organized structures in solvent dried films using SEM, TEM, AFM techniques and prompted us to design an experiment where we could bridge this gap in distinguishing the truly molecular structure driven self-organization from a solvent evaporation driven process. The two pyrene urethane methacrylate random copolymers with 1% and 50% pyrene incorporation and homopolymer were chosen to address this issue.

The objective was to exploit the heterogeneity of the pyrene incorporation in the random copolymers to understand the mechanism of self-assembly which was driven by the different chemical microstructure of the copolymers. The ambiguity of self organized structures being present in solution or formed during the solvent drying process was avoided by carrying out the studies on water dispersed polymer samples which ensured that the polymers were self-organized in solution also. The copolymers in a good solvent like THF were dialyzed against water to obtain polymer microspheres. One of the best ways to probe the microstructure of a polymer microcapsule is to encapsulate suitable probe molecules inside the cavity. The water soluble fluorescent dye rhodamine B (RhB) was chosen for encapsulation studies and the structural changes happening to the comb polymer as a function of temperature was probed by changes in FRET induced RhB emission. The sensitivity of the pyrene I_1/I_3 ratio to changes in the environment as a function of temperature was used to probe the changes in the microenvironment occurring during the RhB release. Dynamic Light Scattering (DLS) studies, steady state fluorescence, fluorescence lifetime decay analysis and microscopic techniques like SEM, TEM, and fluorescence microscopy were used to understand the mechanism of self assembly in these polymer capsules.

4.2. Introduction

The self-assembly of block copolymers with blocks having different solubility parameters have been intensely investigated due to their ability to form nanostructures like micelles, vesicles, capsules etc.[1-9] In the recent years there has been increasing interest in the self assembly exhibited by random copolymers also since these are comparatively easier to synthesize.[10-16] In one such example, an amphiphilic random copolymer was shown to form vesicles and a thermo-responsive vesicle-to-micelle transition also took place resulting in triggered release of encapsulated hydrophilic guest molecules.[16] Figure-4.1 shows the spontaneous vesicle formation from an amphiphilic random copolymer, which could undergo vesicle-to-micelle transition thermo-responsively.
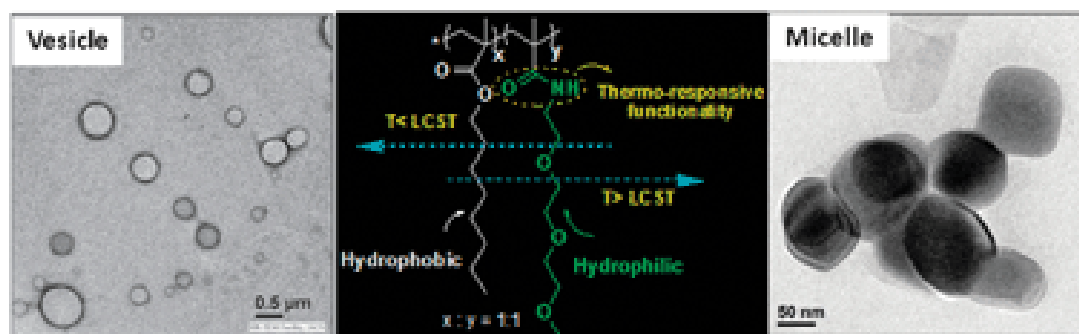
Figure-4.1: Schematic representation of amphiphilic thermo-responsible random copolymer which undergoes vesicle-to-micelle transition. Adapted from *reference 16.*

The common structural criteria in all these systems, whether block copolymer or random copolymer is to have blocks or units of varying chemical composition, for example a hydrophilic unit and a hydrophobic unit so as to enable microphase separation. Seldom has there been an investigation into the mechanism of self assembly in systems which are either fully hydrophilic or fully hydrophobic.[17, 18] An example of fully hydrophobic block copolymer of poly(styrene)-block-poly(methyl methacrylate) [PS-b-PMMA] was explored for their self-assembly in a hydrophilic solvent mixture.[17] Figure-4.2 shows schematically the micellization and thermoresponsive gellation in a double hydrophobic block copolymer namely poly(styrene)-block-poly(methyl methacrylate) [PS-b-PMMA] in a water/ethanol solvent mixture. In this article, authors have made use of the already known reports of the enhanced solubility of poly(methyl methacrylate) in ethanol-water mixtures with maximum solubility at 20% water.[17,19, 20]
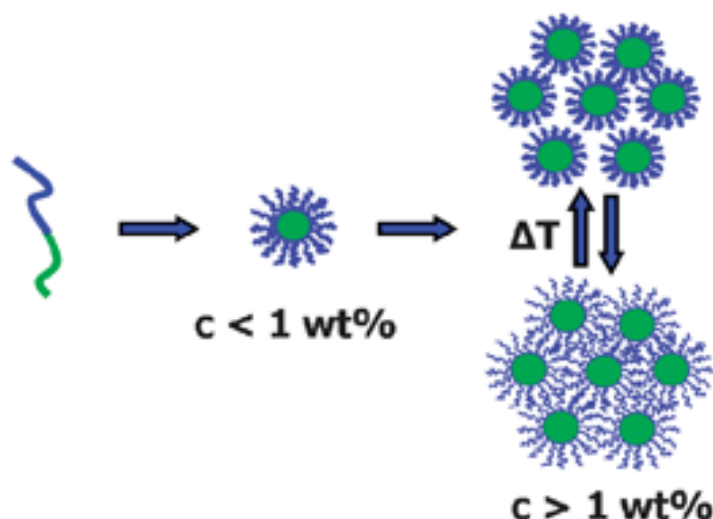
Figure-4.2: Micellization and thermoresponsive gel formation of double hydrophobic block copolymer in a water/ethanol solvent mixture. Adapted from *reference 17.*

The spontaneous formation of self-assembled structures based on simple polymer structure design in a one-pot free radical polymerization process is very rare.[21-23] Most often, complicated structures involving multistep synthetic procedures are required to produce self-assembled polymeric structures. Using pyrene as a fluorescent handle, the self-assembly could be probed under very dilute conditions and it could be established that the intramolecular pyrene excimer emission occur even at very dilute concentrations (10^{-6} M).[24]

In this chapter, the copolyurethane methacrylate polymers having 1, 50, and 100% pyrene namely **PIHPDP-1Py**, **PIHPDP-50Py** and **PIHP-100Py** respectively were chosen to address the self-assembly brought about by the heterogeneity of pyrene incorporation. The synthesis and characterization of these polymers have been discussed in chapter 3. The copolymers in a good solvent like THF were dialysed against water to obtain polymer microspheres. One of the best ways to probe the microstructure of a polymer microcapsule is to encapsulate suitable probe molecules inside the cavity. The water soluble fluorescent dye rhodamine B (RhB) was chosen for encapsulation studies and the structural changes happening to the comb polymer as a function of temperature was probed by changes in FRET induced RhB emission. The sensitivity of the pyrene I_1/I_3 ratio to changes in the environment as a function of temperature was used to probe the changes in the microenvironment occurring during the RhB release. The homopolymer **PIHP-100Py** (pyrene homopolymer) microcapsules as a control sample were also produced adopting the same procedure. Dynamic light scattering (DLS)

studies, steady state fluorescence, fluorescence lifetime decay analysis and microscopic techniques like SEM, TEM and fluorescence microscopy were used to understand the mechanism of self assembly in these polymer capsules.

4.3. Experimental Section

4.3.1. Measurements

Photophysical Studies

Absorption spectra were recorded using Perkin Elmer Lambda 35 UV-spectrophotometer. Steady-state fluorescence studies and time-resolved fluorescence lifetime measurements were performed using Horiba Jobin Yvon Fluorolog 3 spectrophotometer having 450-W Xenon lamp for steady-state fluorescence and nanoLED of 560 nm for fluorescence decay time. For steady state emission as well as excitation and variable temperature fluorescence, samples were dissolved in THF and dialyzed against distilled water for 3 days and the water dispersed solution was used for the studies. The emission and excitation slit width was maintained at 1 nm throughout the experiments, and the data was obtained in ''S1/R1'' mode (to account for the variations in lamp intensity). Temperature dependent fluorescence was recorded using Peltier sample compartment having Peltier Sample Cooler F-3004 attached with thermoelectric temperature controller (Model No. LFI-3751) with autotune PID supplied by wavelength electronics. The temperature was set manually for each reading, and it was equilibrated for 10 min at each temperature before recording the spectrum. The tolerance range for each set temperature was maintained 0.5 ^{o}C. For lifetime measurements, decay curves were obtained by the time-correlated single photon counting (TCSPC) technique.

Rhodamine B encapsulation Studies

The polymer (25 mg) and rhodamine B (3.5 mg) were codissolved in tetrahydrofuran (THF) and kept stirring for 4 hours to ensure encapsulation. The THF solution was then taken in dialysis membrane with molecular weight cut off 2000, sealed off at the ends and subjected to dialysis against deionized water for 3 days. The water was removed several times till it became colourless to ensure complete removal of unencapsulated rhodamine B.

Scanning Electron Microscopy

SEM images were recorded using FEI, QUANTA 200 3D Scanning Electron Microscope with tungsten filament as electron source. The sample preparation method adopted was as follows. The encapsulated samples and dialyzed blank samples were drop-casted as water dispersion taken out from the dialysis bag and the solvent was allowed to evaporate at room temperature in air for 12 hours. All films were prepared at atmospheric pressure without air flow. Before recording the morphology, films were coated by 5 nm thick gold film by spluttering method.

Transmission Electron Microscopy

TEM images were recorded using a JEOL-JEM-3010 instrument at 80 KV. For TEM measurements, the encapsulated samples in water dispersion were deposited directly on carbon coated copper grid. No staining treatment was performed for the measurement. A JEOL JEM-3010 electron microscope operating at 300 kV (Cs=0.6 mm, resolution 1.7 A°) was used for HR-TEM sample observation. A Gatan digital camera (model 794, Gatan 1024 x 1024 pixels, pixel size 24 x 24 μm) at 15 000-80 000 x magnifications was used to record micrographs.

Atomic Force Microscopy

AFM images were taken by a Multimode scanning probe microscope equipped with a Nanoscope IV controller from Veeco Instruments, Inc. in the contact mode using an SiN probe, with a maximum scan size of 10 mm x10 mm and with a vertical range of 2.5 mm. For the AFM studies, samples were prepared by drop casting dialyzed water solution of the polymers onto the glass slide and allowed to dry at ambient temperature before being subjected to AFM analysis.

Fluorescence Microscopy

The fluorescence microscopic images were taken from Carl Zeiss Axiovert 200 instrument. The samples were prepared by dropcasting 60 μl of water dialysed polymers on to the glass slide and covering by coverslip. For imaging rhodamine B, RFP (Red Fluorescent Protein) (excitation wavelength: 502- 547 nm) filter was used and for pyrene DAPI (4'-6-Diamidino-2-phenylindole) (excitation wavelength: 358 nm) filter was used.

Dynamic Light Scattering (DLS)

DLS measurements were carried out on Malvern Zetasizer ZS 90. The dialyzed polymer capsules in water were subjected to DLS measurements.

4.3.2. Synthesis of monomers and Polymerization

The synthesis of IHP- monomer (**I**PDI-**H**EMA-**P**yrene) and IHPDP-monomer (**I**PDI-**H**EMA-**P**enta**D**ecyl**P**henol) and polymers- **PIHP-100Py**, **PIHPDP-1Py,** and **PIHPDP-50Py** is already discussed in chapter-3.

4.4. Results and Discussions

The three polymers namely **PIHPDP-1Py**, **PIHPDP-50Py** and **PIHP-100Py** were chosen for the encapsulation and release studies to address the self-assembly and heterogeneity brought about by pyrene incorporation. The details of the structural characterization have already been discussed in chapter-3.

4.4.1. Polymer Microcapsules and dye encapsulation

The pyrene homopolymer **PIHP-100Py** and PDP homopolymer **PIHPDP-0Py** formed self-organized structures like spheres and rods upon drop casting from various solvents.[23, 25] Small amount of added water was shown to promote microphase separation. Thus, the observed morphology of solvent cast films changed from pores in THF to spheres from THF/water combination for **PIHP-100Py**. The methacrylate backbone with the polar ester linkages are known to have affinity towards water and PMMA is miscible with water at 20%.[17, 19, 20] For the present work, the entire studies were carried out in water. A THF solution of the different copolymers was dialyzed against deionized water in dialysis membranes with a molecular weight cut off ~2000. The water dispersed polymer particles were analyzed for particle size and their distribution using dynamic light scattering (DLS) studies. Figure-4.3 shows the DLS measurement of the three polymers **PIHPDP-1Py**, **PIHPDP-50Py** and **PIHP-100Py** in water which indicated that the polymers formed particles of almost uniform size with average size 300-400 nm.
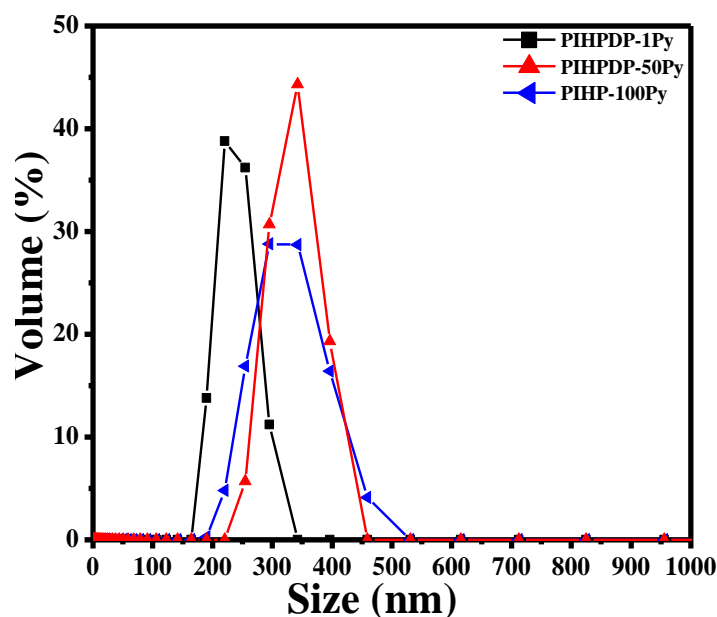
Figure-4.3: Volume – average size distribution of the polymer blank capsules in water obtained by dynamic light scattering (DLS) analysis.

In 100% labeled pyrene polymers the possibility of simultaneous existence of various emitting species like the isolated monomers which decay by monomer emission, monomers that can give rise to excimer emission and those which are held in conformation that are unfavourable for excimer formation can complicate the analysis of time resolved fluorescence data. For instance, the possibility of ground state pyrene association is very high when they are incorporated on every pendant chain of a side chain polymer. Analysing the photophysical data, which is rich in information regarding orientation, distribution etc., can lead to a better understanding of the polymer self organization.

The nature of the particles formed was investigated using SEM and TEM making use of the same solution that was used for the DLS studies. The water dispersion was dropcast on to glass slides for SEM and copper grids for TEM analysis and dried. Figure-4.4 shows the SEM and TEM images of the copolymer **PIHPDP-50Py**. The SEM images showed uniform spheres in the size range of 1.8 to 2.2 μm. The TEM image clearly showed collapsed spheres (50-500 nm) indicating they were solvent filled cavities which collapsed during the application of vacuum. The difference in size observed for the particles using SEM, TEM and DLS are due to the differences in the methods of sample preparation as well as instrumentation techniques used. For instance, the samples for microscopic techniques undergo chain collapse, deformation etc during

solvent evaporation and application of vacuum on the substrate. Therefore such discrepancies between particle sizes measured using DLS and microscopic techniques have been generally reported in literature.[16, 26] The reason for the large particle size observed could be understood if we analyzed the process of polymer diffusion and precipitation occurring during rapid solvent exchange into aqueous phase. When a polymer is taken in a highly water miscible organic solvent, and dialyzed against a poor solvent like water, large polymer agglomerates are formed due to rapid rate of diffusion followed by emulsification due to rapid solvent exchange.
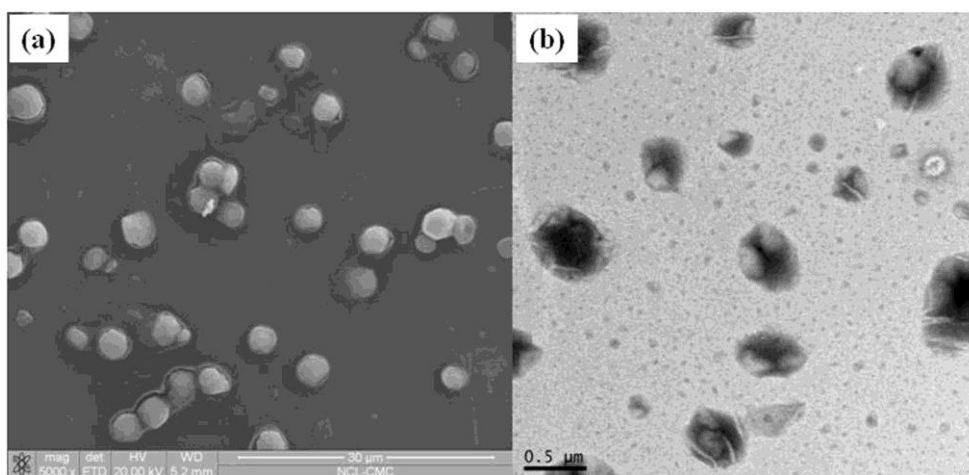
Figure-4.4: (a) SEM and (b) TEM images of **PIHPDP-50Py** blank capsules in water.
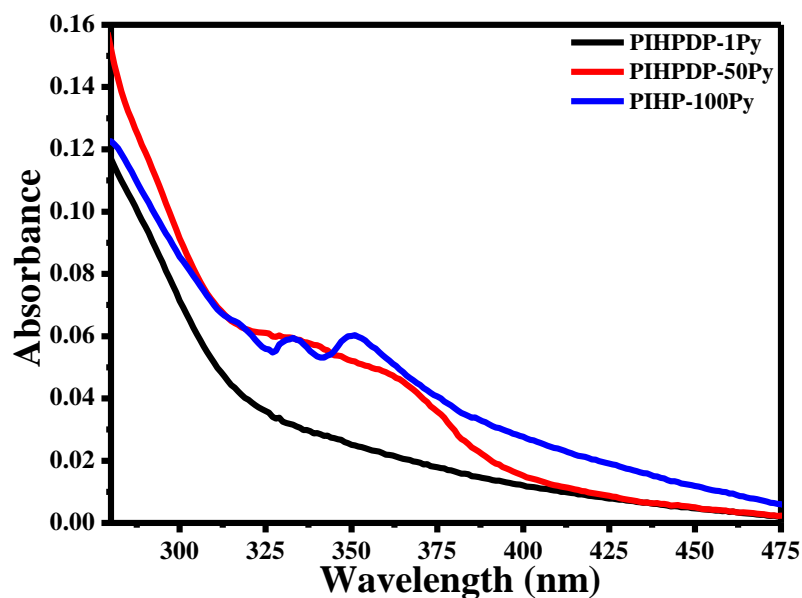
Figure-4.5: Absorption spectra of blank copolymer capsules in water.
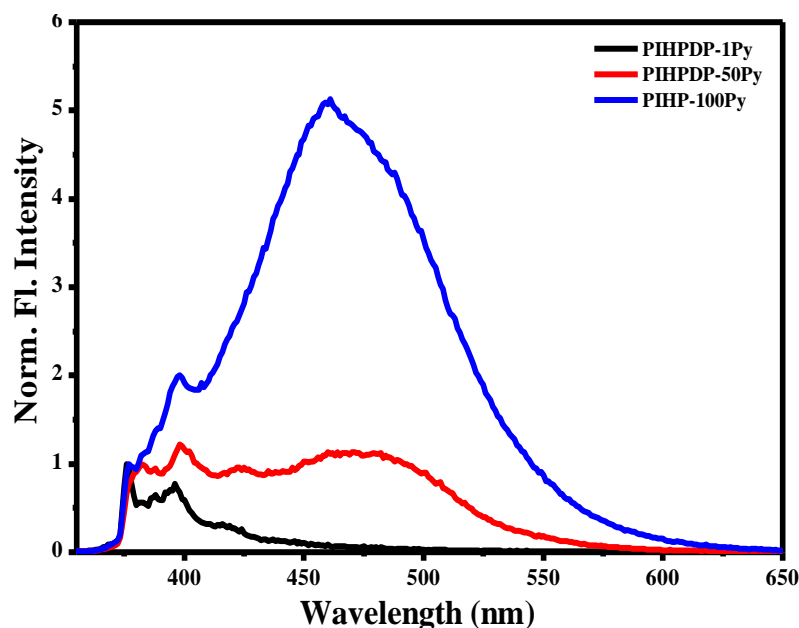
Figure-4.6: Normalized fluorescence emission spectra of the water dispersed blank polymer capsules upon excitation at 343 nm.

Table-4.1: The I_E/I_M ratio of the blank copolymer capsules in water and the I_1/I_3 ratio of the polymer capsules in water before and after the rhodamine B (RhB) encapsulation.

Sample	$I_E/I_M{}^a$ (20 °C)	$I_1/I_3{}^b$ (20 °C)	I_1/I_3 (after RhB encapsulation) (20 °C)
PIHPDP-1Py	0.26	1.58	1.61
PIHPDP-50Py	2.23	0.85	0.99
PIHP-100Py	5.53	0.76	0.90

a. I_E/I_M determined by taking the ratio of integrated area of excimer (425-550 nm) and monomer (370-420 nm) emission (λ_{ex} = 343 nm).

b. I_1/I_3 determined by taking the ratio of the intensity at 377 nm and 388 nm in the emission spectrum.

      The photophysical properties of the particles were studied using absorption and emission. Figure-4.5 shows the absorption spectra and the Figure-4.6 compares the normalized emission spectra of the water dispersed polymer particles upon excitation at 343 nm. Table-4.1 compares relative efficiency of excimer fluorescence emission - the I_E/I_M values (the ratio of integrated area of excimer (430-600 nm) and monomer (370-

420 nm) emission) for the blank polymer capsules in water. The low pyrene incorporated polymer showed only emission characteristic of pyrene monomer in the range 370-420 nm whereas the **PIHPDP-50Py** and **PIHP-100Py** showed both pyrene monomer as well as excimer emission at 375 and 470 nm respectively. The I_E/I_M ratio for **PIHPDP-1Py**, **PIHPDP-50Py** and **PIHP-100Py** were 0.26, 2.23 and 5.53 respectively which showed that higher extent of excimer formation was directly related to the amount of pyrene incorporated in the polymer. Information regarding the pyrene local environment can be obtained from the ratio of the first and third vibronic band of monomer emission. These fine structures are very sensitive to the solvent microenvironment and generally the intensity ratio of peak I/peak III (I_1/I_3: 377 nm/388 nm) serves as a measure of solvent polarity.[27, 28] This peak ratio can be qualitatively taken as a measure of the extent of interaction between the pyrene system and the solvent. A value above 1.5 is an indication of pyrene experiencing a hydrophilic environment whereas a value of ~ 0.6 suggested a hydrophobic environment.[24, 29] Table-2 also shows the I_1/I_3 values for the blank polymer capsules recorded at 20 °C. The values of peak I/peak III for the two copolymers **PIHPDP-1Py** and **PIHPDP-50Py** and the homopolymer **PIHP-100Py** were 1.58, 0.85 and 0.76 respectively. This information throws insight into the microenvironment in the water filled polymer capsules as sensed by the pyrene in the three different polymers. The pentadecyl phenol as well as the pyrene units are hydrophobic in nature and prefer to be away from hydrophilic environment. In the respective homopolymers **PIHPDP-0Py** and **PIHP-100Py**, the PDP and pyrene units would be packed with the bulky pendant units shielded from water. For the low pyrene incorporated copolymer, the chain packing is dominated by the PDP units which can pack very effectively making use of the π stacking of the aromatic core as well as the interdigitation of the C15 alkyl side chain.[30] The bulky pyrene units hinder this packing and to reduce the damage the pyrene units are thrown out resulting in them sensing the hydrophilic environment inside the capsules (this is shown in the schematic representation in figure 1). This is indicated by the value of 1.58 for I_1/I_3 in **PIHPDP-1Py**. As the pyrene incorporation increases in the random copolymer, the pyrene units also end up shielded away from the hydrophilic surroundings which is reflected in the lower values for I_1/I_3.
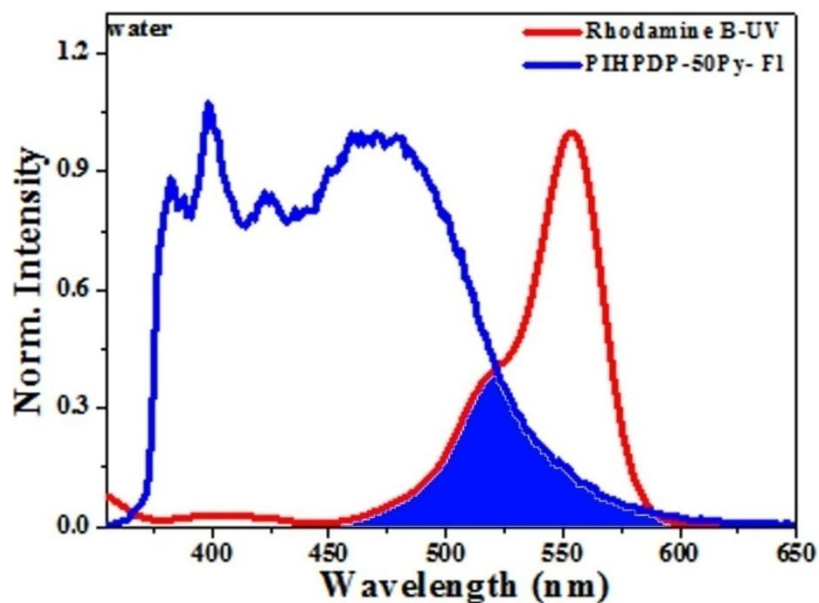
Figure-4.7: Spectral overlap (shaded blue region) between the normalised emission spectrum of **PIDPDP-50Py** and the normalised absorption spectrum of rhodamine B.

The hollow nature of the spherical particles was tested by encapsulation studies using rhodamine B (RhB) as the encapsulating dye. The Figure-4.7 shows the emission spectra of **PIHPDP-50Py** upon excitation at 343 nm stack plotted with the absorption spectra of RhB in water. The shaded region shows the overlap of pyrene excimer emission with RhB absorption suggesting that pyrene and RhB could form a nice donor-acceptor (Förster resonance energy transfer) FRET pair.[31, 32] For encapsulation, a fixed w/w ratio of the polymer and RhB were codissolved in THF and kept stirring for 4 hours.[33] The THF solution was then transferred to dialysis membrane with a molecular weight cut off ~2000, sealed off at the ends and subjected to dialysis against deionized water. The water outside was replaced and dialysis continued until the water became colourless. Figure-4.8 compares the sizes of the polymer capsules both before (dotted line) and after (solid line) RhB encapsulation as measured using DLS studies. The particle size increased from ~ 300-400 nm before encapsulation to ~1000 nm after encapsulation.
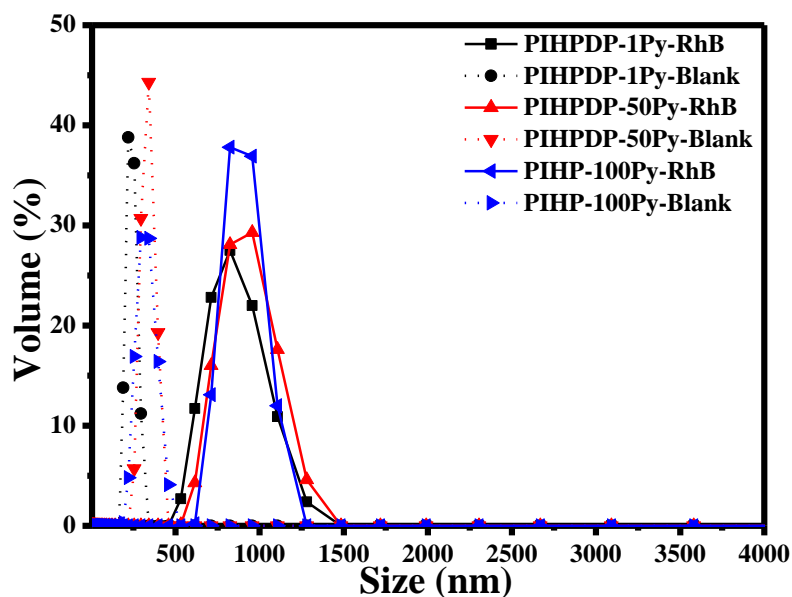
Figure-4.8: Volume – average size distribution of the copolymer capsules in water before (dotted lines) and after (solid lines) rhodamine B encapsulation.

Figure-4.9 shows the SEM images of the three polymer capsules after RhB encapsulation. Figure-4.10 compares the TEM images of the polymers **PIHPDP-50Py** and **PIHP-100Py** both before and after RhB encapsulation. The TEM images showed dark spots inside the capsules due to dye encapsulation. The spheres also became more uniformly spherical and larger after RhB encapsulation which indicated that encapsulation gave it more strength and the capsules did not collapse during the evacuation process. An increase in size of the capsules after encapsulation was clearly evident from the SEM and TEM images. The average particle size increased from 50-500 nm to 800-1000 nm after RhB encapsulation as observed from TEM. AFM images (Figure-4.11) also showed smooth spherical particles after RhB encapsulation.
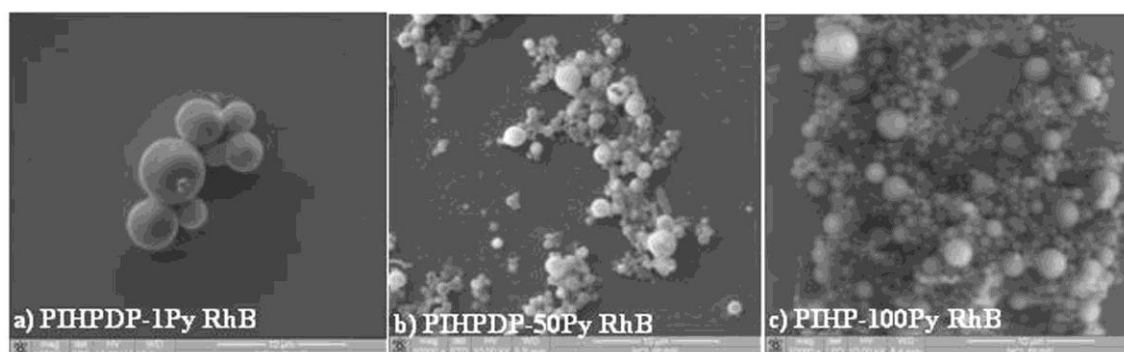
Figure-4.9: SEM images of rhodamine B encapsulated copolymers drop cast from water.
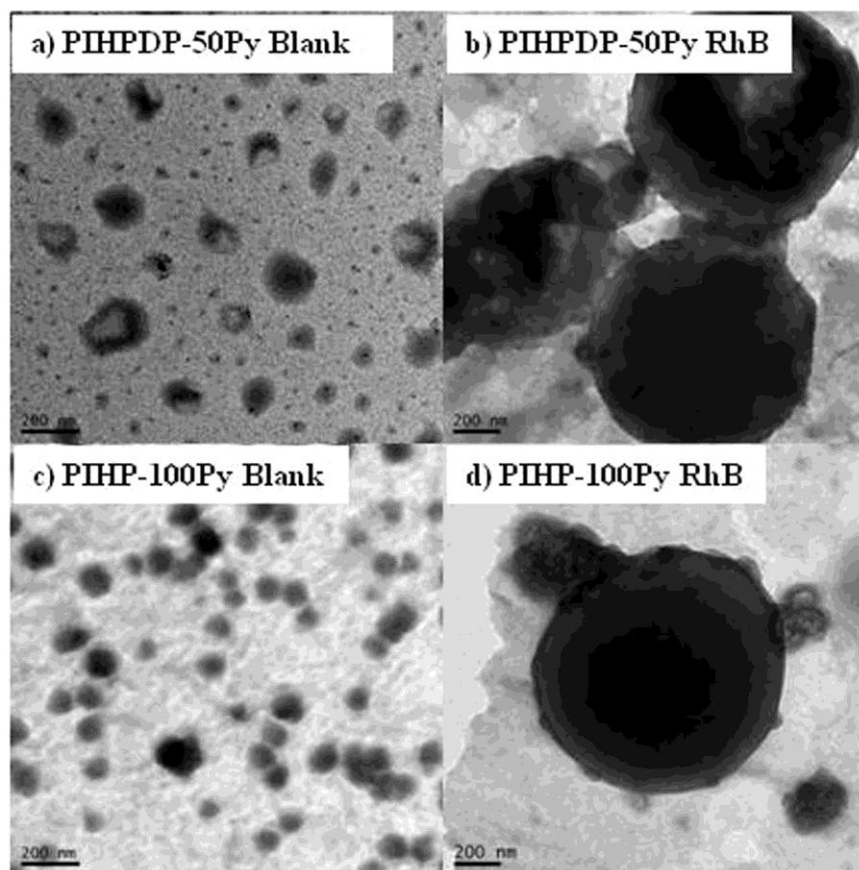
Figure-4.10: Comparison of the TEM images of the polymers **PIHPDP-50Py** and **PIHP-100Py** before and after rhodamine B encapsulation, drop cast from water.
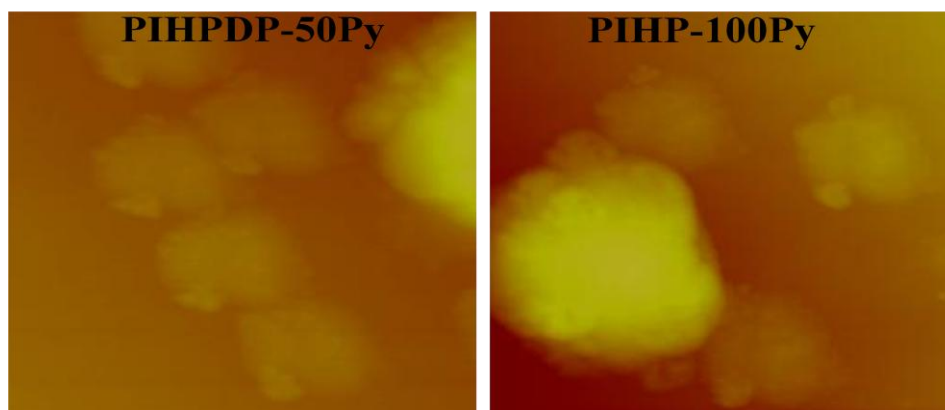
Figure-4.11: Tapping mode AFM height images of the Rhodamine B encapsulated polymer capsules (2 μM x 2 μM).

Figure-4.12 (a-c) compares the fluorescence microscopy images of **PIHPDP-50Py** after RhB encapsulation. Image (a) shows the blue spheres using DAPI filter highlighting the pyrene region, whereas the same upon using RFP filter highlights the red spheres (b) indicating RhB encapsulation. The dark background indicated that the

RhB was present as encapsulated in the spheres only. The merged image (c) shows the pink spheres where the blue and red have combined indicating that the location of the red of RhB was same as the blue of pyrene. The stability of the encapsulated polymer capsules were checked by subjecting it to lyophilisation and then dispersing the dry powder in solvents like THF, DMF and water. Figure-4.12 (d-f) shows the fluorescence microscopy images of the lyophilized sample dissolved in DMF. The images clearly showed that the spherical particles retained their shape as well as their cargo intact in DMF.
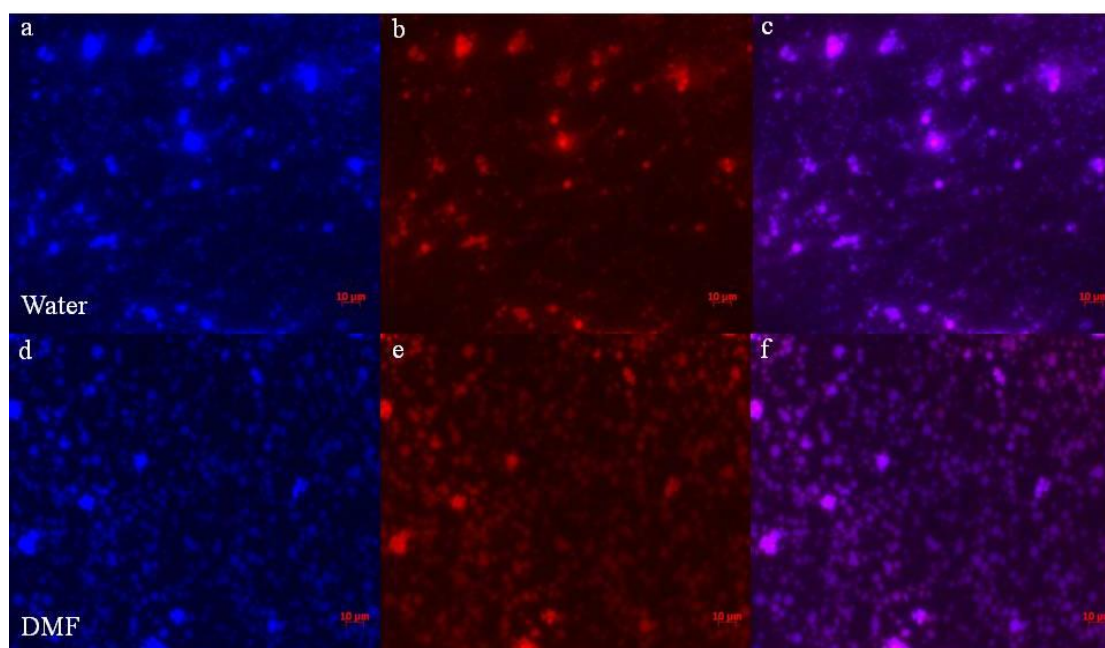
Figure-4.12: Fluorescence optical microscopy images of encapsulated polymer **PIHPDP-50Py** (a) pyrene emission (blue) observed using DAPI filters, (b) rhodamine B emission (red) observed using RFP filters and (c) merged image (purple) indicating the location of the pyrene and rhodamine B; (d-f) lyophilized samples of rhodamine B encapsulated **PIHPDP-50Py** dissolved in DMF and observed for pyrene emission (blue), rhodamine B emission (red) and merged image (purple) respectively.

Figure–4.13a shows the UV-Vis absorption spectra of the RhB encapsulated **PIHPDP-1Py** dispersed in water. The characteristic peaks of RhB could be observed ~554 nm. For the copolymer with 50% pyrene incorporation and the pyrene homopolymer the RhB absorption peak was suppressed due to the high coefficient of absorption of pyrene. Therefore, the quantification of encapsulated RhB could not be determined for these polymers. The RhB percentage encapsulation efficiency determined from the absorption spectra for **PIHPDP-1Py** was 6.43 %. The

encapsulation efficiency was determined as EE = w_1/w_2 x 100 where w_1 was the amount of RhB encapsulated and w_2 was the amount of RhB taken in the feed.[34] The value of w_1 was calculated using Beer-Lambert's equation (with the molar absorption coefficient of RhB determined in water as 90825 L M^{-1} cm^{-1}) taking the optical density at 554 nm. Figure-4.13b compares the normalized emission spectra of the polymer capsules before and after RhB encapsulation for **PIHPDP-50Py**. The FRET induced emission from RhB at 570 nm gave conclusive proof of RhB encapsulation inside the pyrene containing methacrylic polymers.
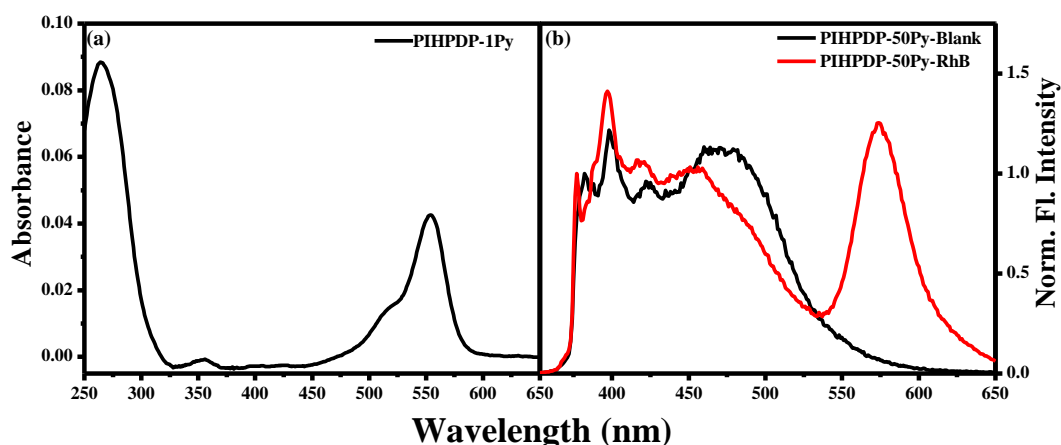
Figure-4.13: (**a**) UV-Vis absorption spectra of **PIHPDP-1Py** in water after RhB encapsulation. (**b**) Comparison of fluorescence emission spectra of polymer capsules of **PIHPDP-50Py** before and after rhodamine B encapsulation, (excitation at 343 nm).

Figure-4.14 compares the emission spectra of the three copolymers upon excitation at various wavelengths. Excitation at 343 nm resulted in pyrene monomer emission (375-420 nm) as well as rhodamine emission at 570 nm in the case of **PIHPDP-1Py**. For the copolymers with higher pyrene content i.e **PIHPDP-50 Py** and homopolymer **PIHP-100Py**, excitation at 343 nm resulted in both pyrene monomer and excimer emission in the wavelength range 375-420 nm and 425-550 nm range respectively along with RhB emission at 570 nm. In **PIHP-100Py**, the pyrene excimer emission at 425-550 nm dominated the monomer emission. The intensity of the RhB emission at 570 nm also was very significant indicating energy transfer from pyrene to RhB. Although no pyrene excimer emission was observed for **PIHPDP-1Py**, emission of RhB at 570 nm was still observed. This could be due to some extent of direct excitation of RhB upon 343 nm excitation since 100 % selective excitation was not

possible.[35] Another important point of observation was the high intensity of RhB emission at 570 nm from **PIHPDP-1Py** upon direct excitation at the RhB absorption λ_{max} of 545 nm. This gave direct proof of the fact that RhB was effectively encapsulated in **PIHPDP-1Py** also and the reduced RhB emission via FRET mechanism was only because of reduced pyrene excimer emission and not due to less efficiency of RhB encapsulation. More information on the energy transfer could be obtained by analyzing the excitation spectra collected while observing the RhB emission at 570 nm. The excitation spectra of the polymers with high pyrene incorporation showed both pyrene and RhB components indicating the occurrence of FRET in these cases.[35, 36] In **PIHPDP-50Py** and **PIHP-100Py** the pyrene peaks dominated the excitation spectra. Also noticeable was the presence of a peak at 375 nm (indicated by arrow) which was a characteristic of ground state pyrene aggregates.

Fluorescence lifetime decay analyses were performed on the RhB encapsulated polymer capsules in water. The fluorescence decay of the bare RhB in water also was collected for comparison. The nano-LED of 560 nm was used as the exciting source and the decay profile was collected towards the red edge of RhB emission wavelength at 600 nm to eliminate the contribution from pyrene species. Figure-4.14d shows the fluorescence lifetime decay curves for the RhB encapsulated polymers along with that for bare RhB in water. The fluorescence decay of RhB in water could be fitted using a single exponential decay and the lifetime was obtained as 1.67 nm which matched with the literature reports.[37] The decay curves for the RhB encapsulated polymers were analyzed as biexponential decay with the χ^2 values < 1.3.

The fluorescence decay parameters are given in table-2. The biexponential decay indicated the presence of two species.[32] The shorter lifetime τ_1 for the polymers at 1.58, 1.59 and 1.95 ns for **PIHPDP-1Py**, **PIHPDP-50Py** and **PIHP-100Py** respectively, indicated RhB molecules without any interaction with the pyrene. The longer lifetime component τ_2 for the polymers at 2.83, 3.37, 3.83 ns for **PIHPDP-1Py**, **PIHPDP-50Py and PIHP-100Py** respectively, corresponded to the lifetime of rhodamine B which were in close proximity of the pyrene units.[38] Table also shows the relative amplitude (α_1, α_2) of these two lifetime components. The pyrene homopolymer **PIHP-100Py** had higher contribution from the long lived species compared to the other polymers and also it had the longest lifetime at 3.83 ns compared to the shortest lifetime for **PIHPDP-1Py** at 2.83 ns. This was direct proof for the strong interaction between pyrene and RhB

molecules through spatial interaction resulting in transfer of energy through FRET in **PIHP-100Py**.[38] The copolymer **PIHPDP-50Py** had intermediate values for the lifetime of long lived excited species which correlated well with the extent of pyrene incorporation in these polymers.
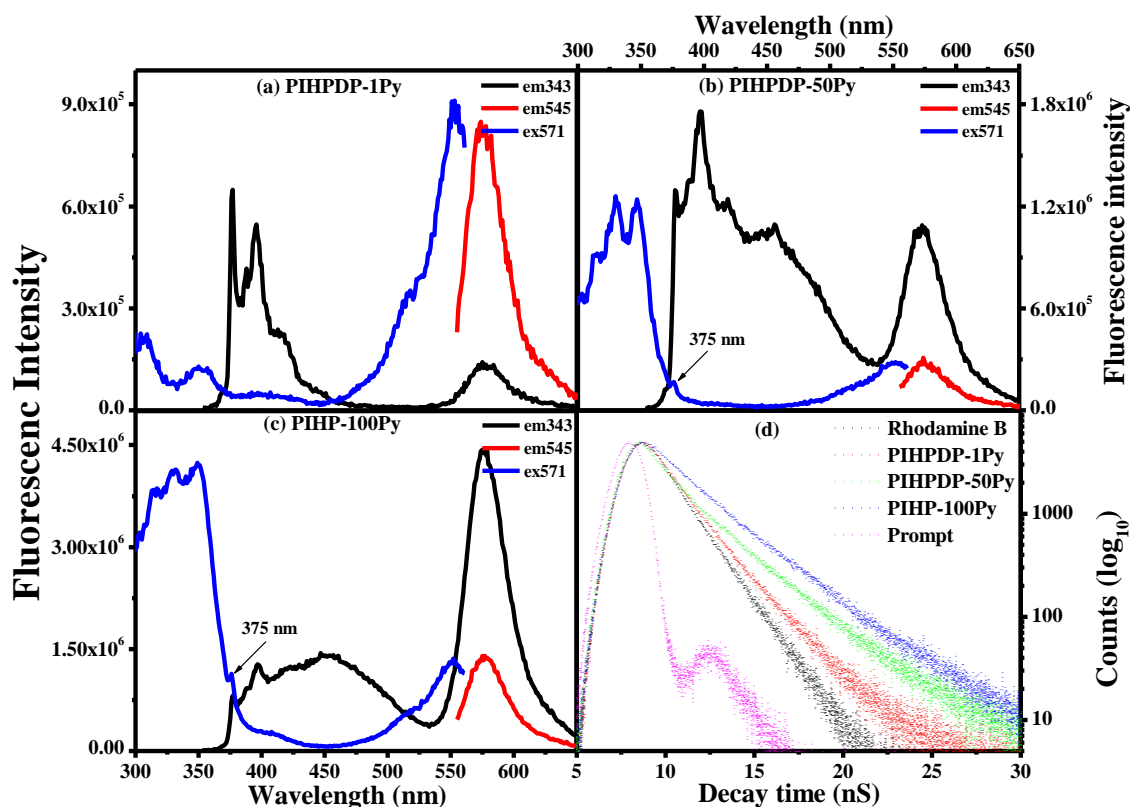
Figure-4.14: Fluorescence emission spectra of (a) **PIHPDP-1Py** (b) **PIHPDP-50Py** and (c) **PIHP-100Py** recorded by exciting at 343 nm and 545 nm and their respective excitation spectra recorded for the emission of 571 nm. (d) Fluorescence lifetime of the rhodamine B encapsulated copolymers observed for rhodamine B emission at 600 nm by using nano LED of 560 nm.

Another conclusive proof for the existence of energy transfer between pyrene and RhB was obtained by analyzing the fluorescence lifetime decay upon excitation at the pyrene excitation wavelength ~340 nm. The **PIHP-100Py** and **PIHPDP-50Py** polymers were excited using 339 nm nanoLED and the fluorescence decay was monitored for RhB emission at 600 nm. The decay could be fit biexponentially and one of the lifetime had a negative pre exponential factor. The values were τ_1: 0.74 ns (α_1: -0.5) and τ_2: 7.49 ns (α_2: 0.5) for **PIHPDP-50Py** and τ_1: 0.77 ns (α_1 -0.41) and τ_2: 6.24 ns (α_2 0.59) for **PIHP-100Py** respectively. The negative pre exponential term indicated

a rise time of RhB emission which was conclusive proof of energy transfer from pyrene.[32]

Table-4.2: Parameters (τ: decay time, α: pre-exponential factor, $\chi 2$: chi-squared value) retrieved from the biexponential fit for rhodamine B encapsulated copolymers. The decay time was collected for rhodamine B emission at 600 nm by using nano LED 560 nm for excitation.

Sample	τ_1 (ns)	τ_2 (ns)	α_1	α_2	χ^2
RHODAMINE B	1.67	-	1	-	1.15
PIHPDP-1Py	1.58	2.83	0.76	0.24	1.15
PIHPDP-50Py	1.59	3.37	0.57	0.43	1.29
PIHP-100Py	1.95	3.83	0.44	0.56	1.16

4.4.2. RhB release and Microstructure change probed by Variable Temperature Studies

The RhB encapsulated polymer capsules were heated from 0 °C to 85 °C and the emission spectra (λ_{ex}: 343 nm) were recorded both in the forward (heating) and backward (cooling) cycles. Figure-4.15a compares the emission spectra of RhB encapsulated **PIHPDP-50Py** in water upon excitation at 343 nm as a function of increasing temperature. At 20 °C, pyrene excimer emission at 470 nm and FRET induced RhB emission at 570 nm were prominent. Upon increasing the temperature, reduction in both pyrene emission and FRET based RhB emission was observed. As temperature was increased both pyrene monomer and excimer emission decreased; though at different rates. Reduction in pyrene fluorescence occurs due to increase in non-radiative pathways which are increasingly favoured at higher temperatures.[39, 40] The decrease in RhB emission is due to two reasons – (1) decrease in FRET based RhB emission due to reduced pyrene excimer emission (2) leaching out of RhB at higher temperature. Thus, at the highest recorded temperature of 85 °C, the RhB emission at

570 nm was drastically reduced. The stack plot also shows the emission spectrum recorded at 20 °C after cooling back from 85 °C (dotted line). The pyrene emission had recovered almost completely and the spectrum was nearly same as that before heating, but RhB emission did not increase, which suggested that the leached out RhB was not re-encapsulated upon cooling. For the 100 % pyrene polymer **PIHP-100Py** (figure-4.15b) also, pyrene excimer emission at 470 nm and RhB emission at 570 nm were very prominent at 20 $^{\circ}$C. Upon increasing the temperature, pyrene excimer emission decreased with the consequent reduction in the FRET based RhB emission also. However, even at the highest recorded temperature of 85 °C, significant RhB emission was still retained, which suggested incomplete leaching out of RhB from the polymer capsules.

While cooling, pyrene regained its original emission intensities and RhB emission also increased slightly more. In fact, the pyrene monomer emission was slightly higher compared to its original intensity before the temperature was increased. Figure-4.15c shows the emission spectra of RhB encapsulated **PIHPDP-1Py** dispersion in water upon excitation at 343 nm as a function of increasing temperature. The pyrene monomer as well as RhB emission decreased with increase in temperature and the RhB emission almost disappeared completely at higher temperature. Upon cooling, the pyrene emission increased and almost recovered its original intensity before heating (dotted line). Figure-4.15 (d-f) shows the variation in the ratio of the integrated area of the RhB emission in the region 525–650 nm to that of the integrated area of the combined pyrene monomer and excimer emission from 350–525 nm as a function of temperature for the three polymers. The dotted lines are for guidance of eye only. For all the three polymers a clear break was observed ~50-60 °C when the RhB emission reduced drastically.
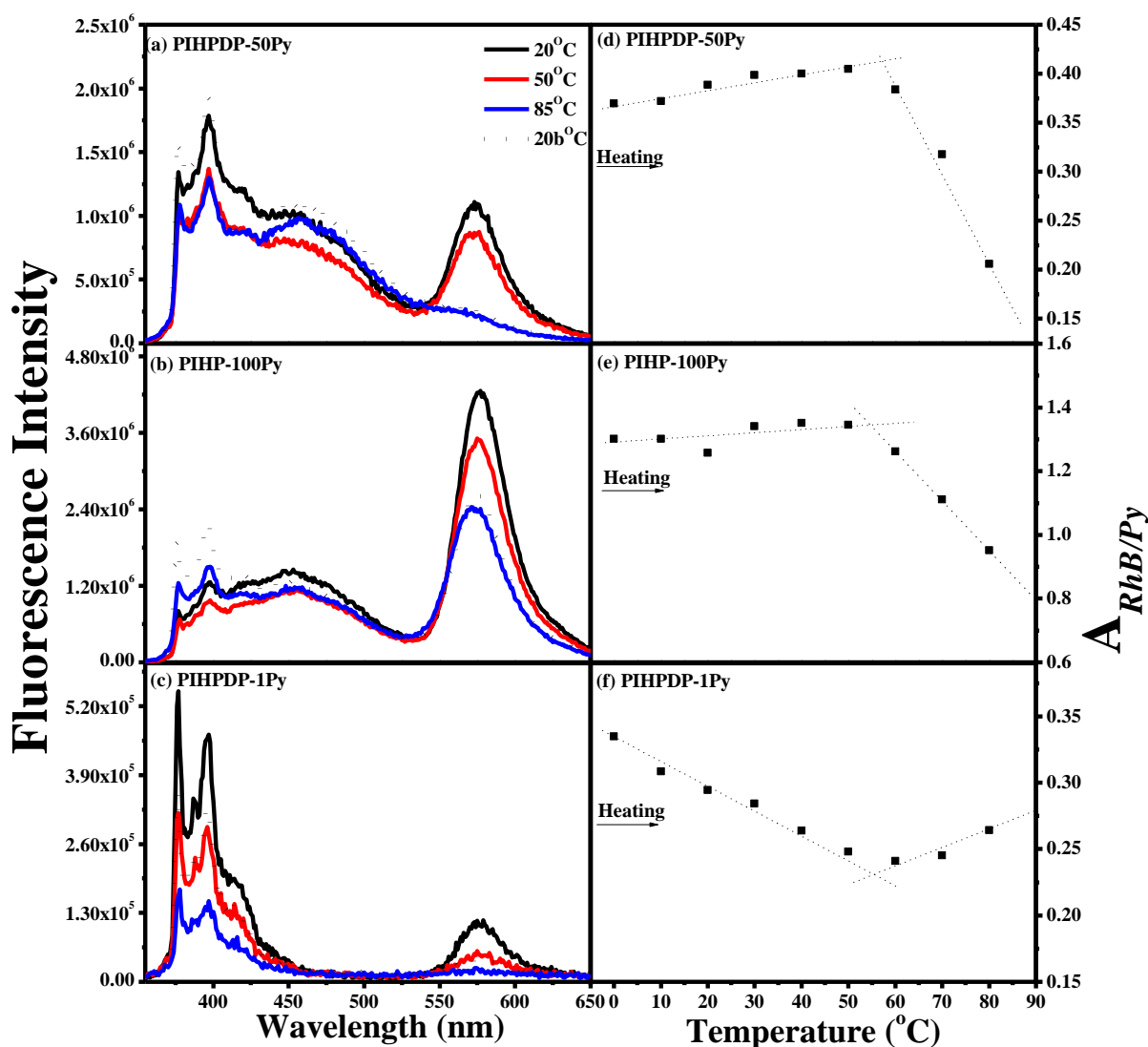
Figure-4.15: Fluorescence emission spectra of (a) **PIHPDP-50Py**, (b) **PIHP-100Py** and (c) **PIHPDP-1Py** collected at selected temperature while heating and while cooling. Plot of ratio of rhodamine B to pyrene emission areas ($A_{RhB/Py}$) for (d) **PIHPDP-50Py**, (e) **PIHP-100Py** and (f) **PIHPDP-1Py** as a function of temperature. Dotted lines are for guidance of eye only.

It is interesting to analyze the changes in the pattern of the I_1/I_3 ratio also as a function of temperature and pyrene incorporation for the RhB encapsulated polymer (figure-4.16). Change in I_1/I_3 ratio as a function of temperature has been correlated to the changes in solvent dipolarity/polarizability.[41] In thin films of pyrene labeled polymers, temperature dependence of I_1/I_3 ratio has been shown to correspond to the polymer T_g.[42] Lodge et. al recently correlated the changes in the I_1/I_3 ratio to the changes in the micelle core as a function of temperature in pyrene containing PS block

copolymer micelles.[40] Unlike reports where pyrene was used as a probe to trace the critical micelle concentration this report used pyrene to trace reorganizations related to glass transition temperature of the PS micelle core. In a similar way, in the present study changes in I_1/I_3 ratio was correlated to microstructural reorganization as a function of temperature. Table-4.1 compares the I_1/I_3 ratio of the three polymers at 20 °C for both the blank as well as RhB encapsulated forms. The I_1/I_3 values for the three RhB encapsulated polymers were 1.61, 0.99 and 0.9 for **PIHPDP-1Py**, **PIHPDP-50Py** and **PIHP-100Py** respectively. It can be seen from the table that this value was very similar for the empty capsules in the case of **PIHPDP-1Py** suggesting that RhB encapsulation had not affected the packing of the pyrene in this polymer and pyrene sensed similar environment. However for the copolymer **PIHPDP-50Py** and homopolymer **PIHP-100Py**, RhB encapsulation resulted in the pyrene moieties experiencing more hydrophilic environment compared to the corresponding blank capsules. The strong donor-acceptor interaction of pyrene-RhB in the higher pyrene incorporated polymers could be expected to result in pyrene getting more exposed to hydrophilic environment in the presence of RhB.
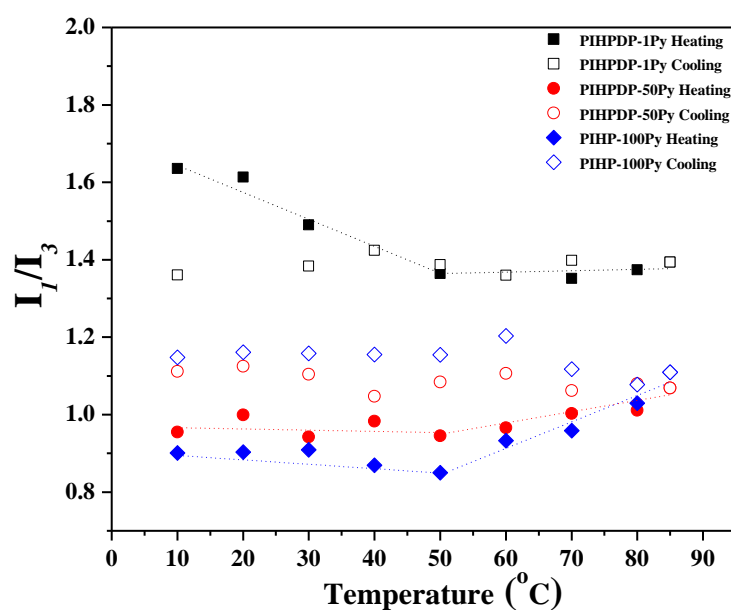
Figure-4.16: Change in the I_1/I_3 ratio as a function of temperature while heating (filled symbols) and cooling (hollow symbols) for the rhodamine B encapsulated polymer capsules. Dotted lines are for guidance of eye only.

Figure-4.16 compares the change in the I_1/I_3 ratio for the three RhB encapsulated polymer capsules plotted against temperature on heating (filled symbols) as well as

cooling (hollow symbols) for λ_{ex} = 343 nm. The I_1/I_3 ratio varied from 1.64 at 10 °C to 1.39 at 85 °C for **PDP-1Py** with a transition point at ~50 °C on heating, which matched very well with the transition observed in the area ratio of RhB to pyrene as a function of temperature. While cooling back to 10 °C, the I_1/I_3 ratio did not go back to its original value before heating (1.64) but remained ~1.36. For **PIHPDP-50Py**, the I_1/I_3 ratio varied from 0.95 at 10 °C to 1.07 at 85 °C on heating with a transition point ~50 °C and remained constant (1.07 to 1.11) on cooling. Similarly for **PIHP-100Py**, the I_1/I_3 ratio changed from 0.90 at 10 °C to 1.11 on heating with a transition ~50 °C and remained constant (1.11 to 1.15) on cooling. The I_1/I_3 ratio for blank capsules of **PIHPDP-50Py** as a function of temperature for heating (black squares) as well as cooling (red circles) decreased from 0.95 at 10 °C to 0.87 at 40 °C, followed by a steady increase to 1.06 at 85 °C. The value remained steady ~ 1.06 upon cooling back to 10 °C.

It can be ruled out that these changes in the I_1/I_3 ratio observed in water as a function of temperature were due to the changes in the solvent dipolarity/polarizability. The effect of temperature on the static dielectric constant of water has been reported to be observed only around 100 °C.[41, 43] In these polymers the change in the I_1/I_3 ratio happened around 50-60 °C and around 40-50 °C for the blank capsule. The trend in the blank capsule suggested that the observed change upon heating was inherent to the polymer. This change in the I_1/I_3 ratio during the temperature change confirmed that the microenvironment of the pyrene changed from a more hydrophilic to less hydrophilic one for **PIHPDP-1Py** whereas for **PIHPDP-50Py** and **PIHP-100Py** it changed from a more hydrophobic to a less hydrophobic one and these changes in environment coincided with the release of the encapsulated RhB. Thus although the total pyrene emission (monomer + excimer) recovered its original intensities upon heating followed by cooling, the microenvironment changed irreversibly upon heating and exhibited an averaged value of I_1/I_3 ~1.1 to 1.4 for all the polymers. This probably reflected a thermodynamically stabilized organization of pyrene and PDP compared to the kinetically trapped one formed during dialysis. The heated RhB encapsulated samples were immediately drop cast and analysed using SEM, which showed that the spherical structure was intact. Figure-4.17 shows the SEM image of the heated particles immediately drop casted after heating at 85 °C.

a) PIHPDP-1Py   **b) PIHPDP-50Py**   **c) PIHP-100Py**
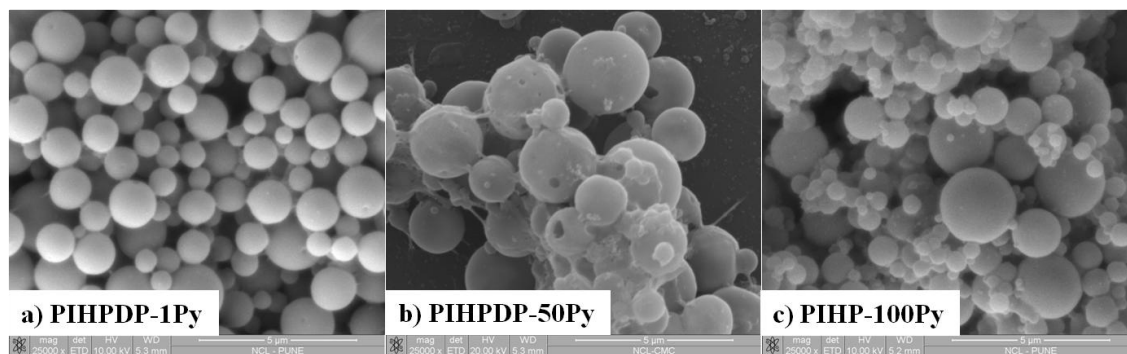
Figure-4.17: SEM images of the rhodamine B encapsulated copolymers after heating at 85 ^{o}C and immediately dropcasting the solution on the glass slide.

It could be assumed that heating resulted in an expansion of the polymer capsules with consequent release of the entrapped RhB followed by reorganization of the polymer chains to a more thermodynamically stabilized one. Upon cooling, the capsules contract back again, but the released RhB does not get entrapped again as there is no driving force to do so. Unlike block copolymers, which have a well-defined core/shell structure where one can imagine a core or shell selective expansion/contraction happening as a function of temperature due to solvent reorganization, it is hard to speculate the origin of the transition occurring in these random copolymer capsules in water as a function of temperature. FRET induced RhB emission from the polymer capsules and the release of RhB as a function of temperature is shown schematically in figure-4.18 for the two extreme cases of 100 % pyrene and 1% pyrene incorporation.
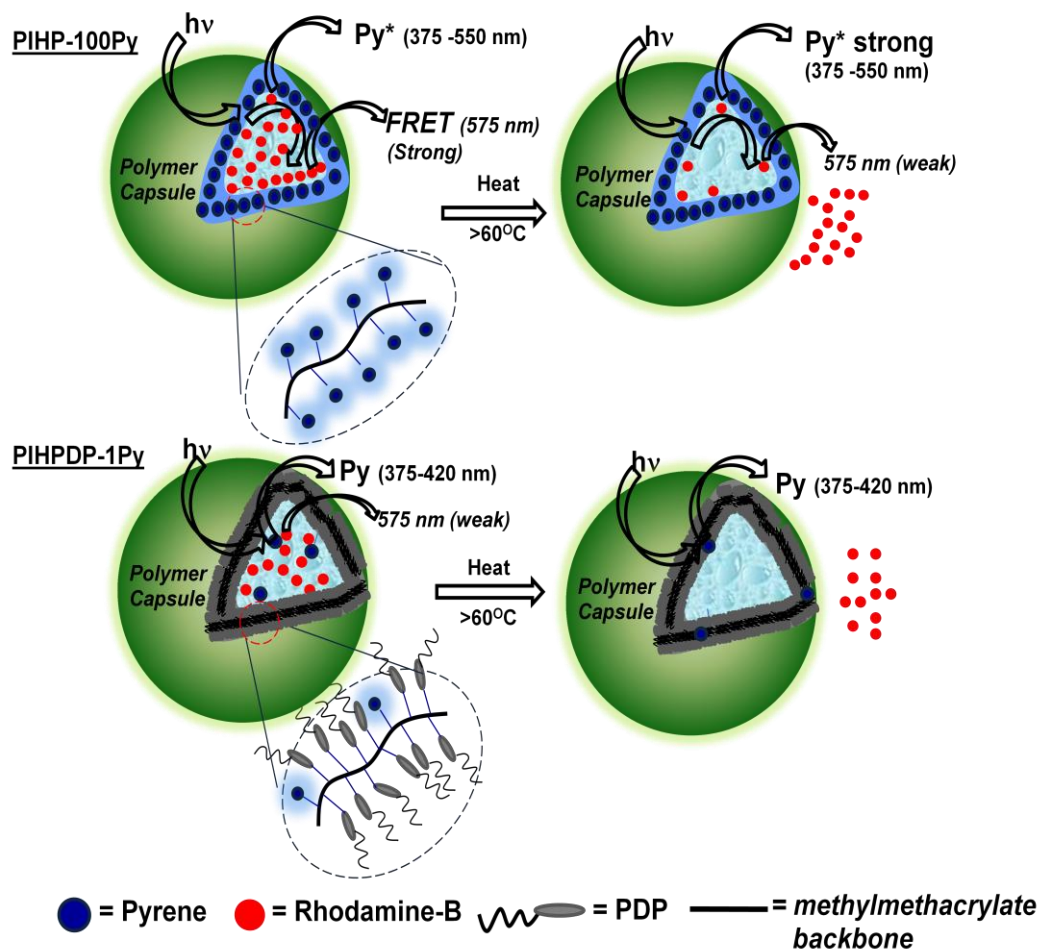
Figure-4.18: Schematic representation of rhodamine B encapsulation and release upon heating for the two copolymers **PIHP-100Py** and **PIHPDP-1Py**.

4.5. Conclusion

In this chapter, the applicative aspects of random urethane methacrylate polymers were extensively explored, where the microstructural analysis of the polymeric architecture was studied by rhodamine encapsulation and its release as a function of temperature. A simple approach to polymer hollow capsule fabrication which involved free radical polymerization of urethane methcarylate monomers was presented. Polymer capsules were obtained by dialyzing the polymer solution in THF against water in a dialysis bag. The driving force for formation of spherical particles in these polymers is assumed to be the phase separation between polar ester linkages and hydrophobic bulky terminal units pyrene/PDP which was assisted by the urethane units which could form hydrogen bonds with water. The hollow nature of the capsules was proved by RhB encapsulation. Dynamic light scattering (DLS) studies in solution and microscopic studies of dried, drop cast samples showed an increase in size upon RhB encapsulation. Pyrene and RhB formed a good donor-acceptor pair with fluorescence emission occurring from RhB upon excitation of pyrene via the förster resonance energy transfer (FRET) mechanism. Fluorescence lifetime data of encapsulated sample collected at RhB emission (600 nm) was fitted to biexponential decay which clearly indicated presence of both short lived RhB emission as well as long-lived emission from RhB which were associated with pyrene. A comparison of the I_1/I_3 ratio of the pyrene emission for the polymers before and after RhB encapsulation indicated that the pyrene moieties in the polymers with low pyrene incorporation were more exposed to the water inside the capsules. For polymers with higher pyrene incorporation, pyrene moieties were more shielded from water compared to **PIHPDP-1Py**; but after RhB encapsulation their surroundings changed towards more hydrophilic one. Upon increasing the temperature, the RhB leached out beyond 50 °C – almost completely for all polymers, except for the pyrene homopolymer **PIHP-100Py** where the interaction between pyrene and RhB was so strong that even at the highest recorded temperature of 85 °C, some amount of RhB was still retained. The polymers underwent some irreversible microstructural reorganization upon heating beyond 50 °C which was reflected in the shift in the I_1/I_3 values which did not recover the original value before heating. The random nature of the copolymers did not affect their ability of capsule formation or RhB encapsulation and the temperature at which the capsules underwent structural reorganization with consequent release of encapsulated dye also remained roughly the same for the **PIHPDP-1Py** to **PIHP-100Py**. The studies

presented here is an attempt to probe the microstructure variation in random polymer capsules as a function of temperature making use of the donor acceptor interaction of pyrene/ RhB. Such studies have rarely been undertaken before and it helps give more insight into microstructural reorganization occurring in drug loaded polymer capsules.

4.6. References

1) Deepak, V. D.; Sundararajan, P. R. *J. Phys. Chem. B* **2011**, *115*, 8458-8464.

2) Discher, D. E.; Eisenberg, A. *Science* **2002**, *297*, 967-973.

3) Jenekhe, S. A.; Chen, X. L. *Science* **1998**, *279*, 1903-1907.

4) Sugihara, S.; Blanazs, A.; Armes, S. P.; Ryan, A. J.; Lewis, A. L. *J. Am. Chem. Soc.* **2011**, *133*, 15707-15713.

5) Walther, A.; Goldmann, A. S.; Yelamanchili, R. S.; Drechsler, M.; Schmalz, H.; Eisenberg, A.; Müller, A. H. E. *Macromolecules* **2008**, *41*, 3254-3260.

6) Yu,Y.; Zhang, L.; Eisenberg, A. *Macromolecules* **1998**, *31,* 1144-1154.

7) Marsat, J. N.; Heydenreich, M.; Kleinpeter, E.; Berlepsch, H. V.; Bottcher, C.; Laschewsky, A. *Macromolecules* **2011**, *44*, 2092-2105.

8) Maiez-Tribut, S.; Pascault, J. P.; Soule, E. R.; Borrajo, J.; Williams, R. J. J. *Macromolecules* **2007**, *40,* 1268-1273.

9) Ho, R. M.; Chiang, Y. W.; Lin, C. C.; Bai, S. J. *Macromolecules* **2002**, *35,* 1299-1306.

10) Wit, J. D.; Ekenstein, G. A. V.; Polushkin, E.; Korhonen, J.; Zuokolainen, J.; Brinke, G. T. *Macromolecules* **2009**, *42*, 2009-2014.

11) McHale, R.; Patterson, J. P.; Zetterlund, P. B.; O'Reilly, R. K. *Nature Chem.***2012**, 4, 1-6.

12) Mansky, P.; Liu, Y.; Huang, E.; Russell, T. P.; Hawker, C. *Science* **1997***, 275*, 1458-1460.

13) In, I.; La, Y. H.; Park, S. M.; Nealey, P. F.; Gopalan, P. *Langmuir* **2006**, *22,* 7855-7860.

14) Peng, B.; Grishkewich, N.; Yao, Z.; Han, X.; Liu, H.; Tam, K. C. *ACS Macro Lett*. **2012**, *1*, 632-635.

15) Guo, P.; Guan, W.; Liang, L.; Yao, P. *J. Colloid Interface Sci*. **2008**, *323*, 229-234.

16) Dan, K.; Bose, N.; Ghosh, S. *Chem. Commun*. **2011**, *47*, 12491-12493.

17) Hoogenboom, R.; Rogers, S.; Can, A.; Becer, C. R.; Guerrero-Sanchez, C.; Wouters, D.; Hoeppener, S.; Schubert, U. S. *Chem. Commun*. **2009**, *37*, 5582-5584.

18) Sedlak, M.; Colfen, H. *Macromol. Chem. Phys*. **2001**, *202*, 587-597.

19) Brandrup, J.; Immergut, E. H.; Grulke, E. A. *Polymer Handbook*, Wiley-Interscience, New York, 4th Ed., **1999.**

20) Piccarolo, S.; Titomanlio, G. *Makromol. Chem. Rapid Commun*. **1982**, *3*, 383-387.

21) Deepak, V. D.; Asha, S. K. *J. Polym. Sci.: Part A: Polym. Chem.* **2008**, *46*, 1278-1288.

22) Deepak, V. D.; Asha, S. K. *J. Phys. Chem. B* **2006**, *110,* 21450-21459.

23) Rekha, N.; Asha, S. K. *J. Polym. Sci.: Part A: Polym. Chem.* **2009**, *47*, 2996-3009.

24) Winnik, F. M.; *Chem. Rev.* **1993**, *93*, 587-614.

25) Deepak, V. D.; Asha, S. K. *J. Phys. Chem. B* **2009**, *113,* 11887-11897.

26) Wang, M.; Zhang, G.; Chen, D.; Jiang, M.; Liu, S. *Macromolecules* **2001**, *34*, 7172−7178.

27) Acree, W. E., Jr. *Absorption and Luminescence Probes. In Encyclopedia of Analytical Chemistry: Theory and Instrumentation*; Meyer, R. A., Ed.; John Wiley & Sons, Ltd.: Chichester, U.K., **2000**.

28) Lakowicz, J. R. *Principles of Fluorescence Spectroscopy*, 3rd ed.; Kluwer Academics/Plenum Publisher: New York, **2006**.

29) Kalyanasundaram, K.; Thomas, J. K. *J. Am. Chem. Soc.* **19**77, *99*, 2039-2044.

30) Bhavsar, G. A.; Asha, S. K. *Chem. Eur. J.* **2011**, *17*, 12646-12658.

31) Othman, A. B.; Lee, J. W.; Wu, J.-S.; Kim, J. S.; Abidi, R.; Thuery, P.; Strub, J. M.; Dorsselaer, A. V.; Vicens, J. *J. Org. Chem.* **2007**, *72*, 7634-7640.

32) Pevenage, D.; Auweraer, M.V. D.; Schryver, F. C. D. *Chem. Phys. Lett.* **2000**, *319*, 512-520.

33) Xiao, Z. Y.; Zhao, X.; Jiang, X. K.; Li, Z. T.; *Chem. Mater.* **2011**, *23*, 1505–1511.

34) Liang, X. F.; Wang, H. J.; Luo, H.; Tian, H.; Zhang, B. B.; Hao, Li J.; Teng, J. I.; Chang, J. *Langmuir* **2008**, *24*, 7147–7153.

35) Ribou, A.-C.; Vigo, J.; Salmon, J.-M. *Photochem. and Photobiol.* **2002**, *151*, 49-55.

36) Masuko, M.; Ohuchi, S.; Sode, K.; Ohtani, H.; Shimadzu, A. *Nucl. Ac. Res.* **2000,** *28*, 1-8.

37) Magdel, D.; Rojas, G. E.; Seybold, P. G.; *Photochem. and Photobiol.* **1999**, *70*, 737-744.

38) Paira, T. K.; Banerjee, S.; Raula, M.; Kotal, A.; Si, S.; Mandal, T. K. *Macromolecules* **2010**, *43,* 4050-4061.

39) Zhang, M.; Duhamel, J. *Macromolecules* **2007**, *40,* 661-669.

40) Mok, M. M.; Lodge, T. P. *J. Polym. Sci. Part B: Polym. Phys.* **2012**, *50*, 500-515.

41) Trivedi, S.; Malek, N. I.; Behera, K.; Pandey, S. *J. Phys. Chem. B* **2010**, *114*, 8118-8125.

42) Kim, S.; Roth, C. B.; Torkelson, J. M. *J. Polym. Sci. Part B: Polym. Phys.* **2008**, *46*, 2754-2764.

43) Lide, D. R. (ed.) *CRC Handbook of Chemistry and Physics*, 87th ed.; CRC Press: Boca Raton, FL, **2006**.

Chapter 5:

H-bonding vs Non H-bonding in 100% Pyrene Labeled Methacrylate Comb Polymers: TRES and Temperature Dependent Fluorescence

5.1. Abstract

This chapter brings forth the fundamental studies of a class of homopolymers which were designed to highlight the importance of small structural variations on the self organization by pyrene photophysics. A series of side chain methacrylate polymers having pendant pyrene units in every repeat unit was designed, which differed from one another by presence or absence of hydrogen bondable linkages and the length as well as nature (linear vs kink) of the spacer segment linking the pendant pyrene units from the methacrylate backbone. The importance of hydrogen bonding interactions provided by the urethane linkage in directing the self organization of these polymers were compared with analogous 100 % pyrene polymers lacking the hydrogen bonding interaction. The effect of these subtle structural variations on the fluorescence characteristics was analyzed using extensive photophysical measurements. The nature of excimer emission was analyzed to obtain information regarding the chain organization in each of the polymers. The absence of rise curve in the excimer decay profile of non-H-bonded **Poly(PBH)** showed the excimer emission through static pathways. Variable temperature (heating & cooling) emission studies significantly showed the difference in the chain interactions of H-bonded vs non-H-bonded polymers. On cooling, the fluorescence emission recovered completely for non-H-bonded **Poly(PBH)** while the restrictive hydrogen bonds of urethane linkage in the polymers **Poly(PIC)**, **Poly(PHH)** and **PIHP** restricted the complete recovery of fluorescence emission. The TRES studies for non-H-bonded **Poly(PBH)** showed the absence of monomeric emission at the earliest time gated spectra (0.42 ns) while the extent of monomeric emission in H-bondable polymers **Poly(PIC)**, **Poly(PHH)** and **PIHP** was varying**.** Thus, it was proved the small changes in the architecture of the polymer had a profound influence on the nature and extent of excimer formation.

5.2. Introduction

Significant progress has been made in the understanding of the photophysics of various simple as well as complex molecules labeled with pyrene at specified positions and complex polymers randomly labeled with pyrenes.[1-10] The various photophysical techniques such as steady-state emission studies, fluorescence decay studies, fluorescence quenching studies and time resolved emission spectra (TRES) etc. have strongly contributed to the evolution of this area. The chain dynamics of randomly labeled pyrene polymers with the help of advanced techniques have significantly contributed to the development of this area. [11-15] Infact, this area has evolved upto an extent where the quantitative information regarding the chain dynamics and structure could be obtained if the excimer formation process in the macromolecules occurs via diffusional encounters.[15] Recently, the more complex architectures such as dendrimers, lipids, peptides or other poly amino acids labeled with pyrenes etc have attracted the attention of researchers.[16-22] The photophysical properties of dendrimers are very interesting and are highly dependent on the complex architectures of these macromolecules. The fluorophores can be attached to dendrimers at three different locations: periphery, branches, or core. In one such recent example, a pyrene-labeled dendrimer was covalently linked to trimesitylphenylporphyrin and the energy transfer between the porphyrin and pyrene was studied.[22] Figure-5.1 shows the schematic representation of pyrene dendronized porphyrins and the nature of excimer formation and the FRET between pyrene and porphyrins. The photophysical investigations have contributed significantly in bringing about the difference and the similarities among the various architectures.

Even though complex architectures with pyrene labeling have been examined recently, there is a dearth of research on 100% pyrene labeled polymers where every repeat unit has pyrene incorporation. It is very challenging to study 100% pyrene labeled polymers because of presence of various emitting species like monomers, dimers and excimers in proper orientation (sandwitched excimers) or partially overlapped excimers etc. Previous chapters reported randomly pyrene labeled side chain urethane methacrylate polymers where the pyrene loading was varied from 1 to 100%.[23, 24] The existence of ground state aggregated pyrenes in all polymers was proven by the fluorescence lifetime decay as well as TRES experiments. TRES experiments showed that the short-lived ground state aggregated species emitting in the 435 nm region

dominated the earlier time-gated spectra which then gave way to emission ~465 and 485 nm corresponding to excited pyrene in constrained and perfect orientation respectively.[24, 25]
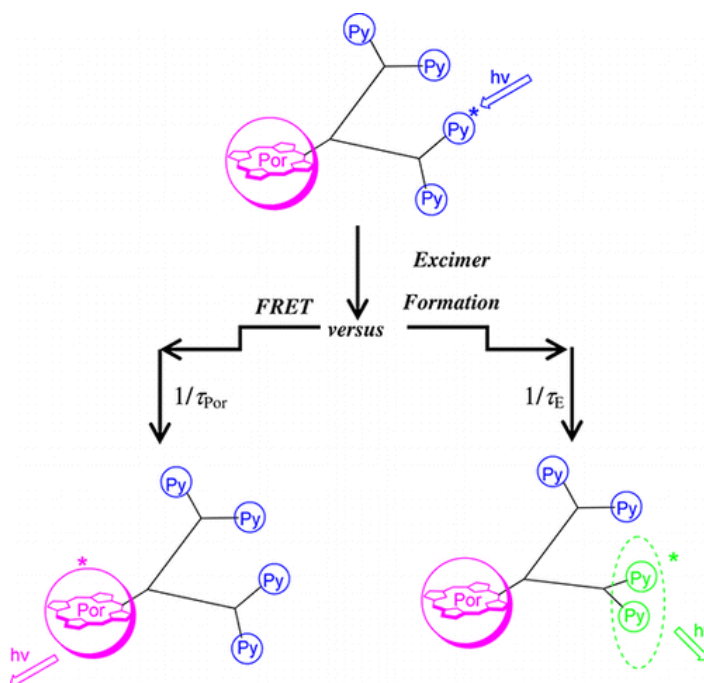
Figure-5.1: Schematic representation of pyrene-labeled dendrimer linked to trimesitylphenylporphyrin. *Adapted from reference 22.*

In this chapter, we have examined the importance of the hydrogen bonding interaction provided by the urethane linkage in directing the self assembly of pendant pyrenes and compared it with analogous 100 % pyrene polymers lacking the hydrogen bonding interaction. Hydrogen bonding is a directional interaction which can introduce constraints on the self-assembled architecture. It becomes very crucial while designing molecules for applications like Field Effect Transistors (FET) where charge carrier mobility plays a very important role. There is ample evidence in literature that the presence of restrictive directional hydrogen bonding interactions is not very favourable for efficient charge transport compared to the freedom in charge transport pathways offered by a three dimensional crystalline organization.[26] It is important to understand the influence of these restrictive hydrogen bonding interactions on the self assembly in solution state as well. Towards this end, we have designed a series of side chain methacrylate polymers having pendant pyrene units in every repeat unit, but differing

from one another in terms of presence or absence of hydrogen bondable units in the form of urethane linkages, or the length as well as nature (linear vs kink) of the spacer segment linking the pendant pyrene units from the methacrylate backbone. The effect of these subtle structural variations on the fluorescence characteristics was analyzed using steady-state and lifetime decay studies, variable temperature emission and time resolved emission spectra (TRES) experiments. The fluorescence properties were analyzed as regards to the nature of excimer emission – dimer vs static or dynamic excimer, to obtain information regarding the chain organization in each of the polymers with differing architecture.

5.3. Experimental Section

5.3.1. Materials

2-Hydroxyethyl methacrylate (HEMA), 2-isocyanatoethyl methacrylate (IEMA), hexamethylene diisocyanate (HMDI), 1-Ethyl-3-(3-dimethylaminopropyl)carbodiimide hydrochloride (EDCl), dibutyltin dilaurate (DBTDL), 1-pyrene butyric acid and 1-pyrenemethanol were purchased from Aldrich and used as such. Benzoyl peroxide was recrystallised from methanol. DCM and THF were purchase from Merck, India. Dimethyl formamide was dried by stirring with calcium sulphate for 72 hr followed by vacuum distillation.

5.3.2. Measurements

^{1}H NMR spectra of monomer and polymers were recorded using 200-MHz Bruker NMR spectrophotometer in CDCl$_3$ containing small amounts of tetramethylsilane (TMS) as internal standard. The gel permeation chromatography (GPC) instrument (Viscotek) provided with a Styragel column, VE 1122 pump, Viscotek VE 3580 RI detector were used for molecular weight calculations. The instrument was calibrated using 12 polystyrene standards in the molecular weight range from 1 x 10^3 to 4 x 10^6. The flow rate of the THF was maintained as 1 mL throughout the experiments, and the sample solutions at very dilute concentrations were filtered and injected for recording the GPC chromatograms at 30 ^{o}C. Bruker Alpha Fourier transform infrared (FTIR) spectrometer was used to record Infrared (IR) spectra. The powder samples were mixed with KBr and KBr pellets were made to record IR spectra and it was recorded in the range of 4000-500 cm^{-1}. Perkin Elmer Pyris-6 instrument was used for thermal

gravimetric analysis (TGA) of the polymers. TA Q20 differential scanning calorimeter was used for differential scanning calorimetry (DSC) measurements at a heating rate of 10 ^{o}C min^{-1} under nitrogen atmosphere. Typically, 1–2 mg of samples was placed in an aluminium pan, cramped properly, and scanned from -30 to 200 ^{o}C. The instrument was calibrated using indium standards.

Photophysical Studies

The absorption spectrum was recorded with Perkin Elmer Lambda 35 UV-spectrophotometer. Horiba Jobin Yvon Fluorolog 3 spectrophotometer having 450-W Xenon lamp was used for steady state fluorescence studies. The steady state emission, variable temperature steady state emission and fluorescence lifetime decay analysis were carried out in DMF. The emission and excitation slit width was maintained at 1 nm throughout the experiments, and the data was obtained in ''S1/R1'' mode. Peltier sample compartment with Peltier Sample Cooler F-3004 was attached with thermoelectric temperature controller (Model No. LFI-3751) (Wavelength Electronics), which was attached to the fluorometer for temperature dependent fluorescence. The temperature was set manually for each reading, and it was equilibrated for 10 min at each temperature before recording the spectrum. The tolerance range for each set temperature was maintained 0.5 ^{o}C.

Lifetime studies and TRES measurements were conducted using TCSPC Fluorohub supplied by Horiba Jobin Yvon and Nano-LED source of wavelength 340 nm was used to excite all the samples. For the lifetime decay profile, data was collected at monomeric (λ_{em}-375 nm) emission as well as excimeric (λ_{em}-500 nm) emission region. The Time-Resolved Emission Spectra (TRES) was procured by incrementing the monochromator on the emission channel of the time-resolved fluorometer in fixed wavelength steps. Slices of data were taken in the intensity-wavelength plane to obtain spectra at different times during the decay. Picosecond Time-resolved-emission spectra (TRES) and Fluorescence lifetime decays were collected by a time-correlated single photon counting (TCSPC) setup from IBH Horiba Jobin Yvon (U.S.) using a 405 nm diode laser (IBH, U.K., NanoLED-405 L, with a λ max = 405 nm) as a sample excitation source.

The samples were prepared by making the optical density 0.1 $\pm$ 0.05 at excitation wavelength (λ_{ex} ~ 343 nm) in DMF. All samples were purged with gentle

flow of nitrogen for 1 hour before carrying out the measurements to ensure complete removal of dissolved oxygen from the DMF solution. All experiments were performed under identical conditions. DAS6 decay analysis software was used to obtain fluorescence lifetime values. The quality of fit was judged by fitting parameters such as $\chi^2 < 1.3$, and the residuals and autocorrelations are distributed around zero.

5.3.3. Synthesis of monomer PBH by esterification of 1-pyrene butyric acid with 2-hydroxyethyl methacrylate[27]

A mixture of 1-pyrene butyric acid (1 g, 3.47×10^{-3} mol) and dimethyl amino pyridine (DMAP) (0.08 g, 6.24×10^{-4} mol) was taken in 100 ml of distilled dichloromethane (DCM) and cooled to $0^{o}C$ under nitrogen environment followed by addition of 1-ethyl-3-(3-dimethylaminopropyl)carbodiimide hydrochloride (EDCL) (0.73 g, 3.81×10^{-3} mol). The reaction was brought to room temperature (RT) and stirring continued for 1 hr. Thereafter 2-hydroxyethyl methacrylate (0.45 g, 3.47×10^{-3} mol) was added drop wise under ice-cold condition. The reaction contents were allowed to come to RT and the stirring continued for 40 hr. After the completion, the contents were diluted with DCM and extracted thrice with 0.02 M aqueous hydrochloric acid (HCl). The aqueous layer was again extracted with 50 ml DCM and then the organic layers were combined to extract them further with saturated sodium bicarbonate solution followed by extraction with brine. The organic layer was dried over sodium sulphate, filtered and the solvent removed by vacuum oven. The product was recrystallized from methanol and dried in vacuum oven at 60 ^{o}C overnight. Yield: 1.2 gm (83%). ^{1}H NMR (200 MHz, CDCl$_3$) δ ppm: 8.31-7.82 (m, 9H, Ar-**H**), 6.11, 5.53 (2s, 2H, **CH**$_2$=C), 2.48 (t, 2H, O**CH**$_2$ next to pyrene ring), 3.39 (t, O=C-C**H-** of pyrene butyric acid), 4.36 (s, 4H, O-**CH**$_2$-**CH**$_2$- of HEMA), 2.19 (m, O=C-CH$_2$-**CH**$_2$ of pyrene butyric acid)), 1.91 (s, 3H, -**CH**$_3$ of HEMA). FTIR: 3041, 2953, 2886, 1726, 1634, 1597, 1452, 1372, 1318, 1297, 1245, 1158, 1045, 946, 895, 845, 816, 759, 715. Theoretical mass (m/z): 400.17 and MALDI-TOF mass (m/z): 400.12.

5.3.4. Synthesis of short chain PIC monomer by coupling of 2-isocyanatoethyl methacrylate and 1-pyrene methanol

In a 2-necked round bottom flask, 2-isocyanatoethyl methacrylate (IEMA) (0.33 g, 2×10^{-4} mol) and 3 ml dry tetrahydrofuran (THF) was taken under nitrogen atmosphere. 1-pyrene methanol (0.5 g, 2×10^{-4} mol) was dissolved in 3 ml dry THF and added drop

wise to the round bottom flask under ice cold condition with constant stirring. 2-3 drops of dibutyltin dilaurate (DBTDL) was added as catalyst. The reaction was allowed to proceed under ice-cold condition for 30 min followed by RT stirring for 20 hr. After the completion of reaction, THF was removed under reduced pressure. Then methanol was added to the solid residue and filtered to remove unreacted 1-pyrene methanol. The solid was collected and dried under vacuum oven at 60 ^{o}C over night. Yield: 75 %. ^{1}H NMR (200 MHz, CDCl$_3$) δ ppm: 8.41-7.98 (m, 9H, Ar-**H**), 6.05, 5.51 (2s, 2H, C**H**$_2$=C), 5.83 (s, 2H, OC**H**$_2$ next to pyrene ring), 5.04 (b, N**H**), 4.23 (t, 2H, O-C**H**$_2$-CH$_2$- of HEMA), 3.52 (m, 2H, N-C**H**$_2$-CH$_2$- of IEMA), 1.88 (s, 3H, -C**H**$_3$ of HEMA). FTIR: 3299, 3080, 3047, 2955, 2922, 1714, 1695, 1637, 1597, 1553, 1459, 1401, 1368, 1323, 1273, 1179, 1118, 1048, 1016, 947, 917, 844, 817, 780, 746, 709. Theoretical mass (m/z): 387.15, MALDI-TOF mass (m/z): 387.096.

5.3.5. Synthesis of PHH monomer by coupling of hexamethylene diisocyanate with 2-hydroxyethyl methacrylate and 1-pyrene methanol[28]

Hexamethylene diisocyanate (HMDI) (1 g, 6 x 10^{-3} mol) in 6 ml dry dimethylformamide (DMF) was taken in a 100 ml two necked round bottom flask under nitrogen environment and the contents were cooled with ice. 2-hydroxyethyl methacrylate (0.78 g, 6 x 10^{-3} mol) was added drop wise under nitrogen atmosphere over a period of 0.5 hr. The reaction contents were allowed to stir under ice cold conditions for further 0.5 hr and then left stirring at room temperature for further 2 hr. 3-4 drops of dibutyltin dilaurate (DBTDL) was added as catalyst followed by drop wise addition of 1-pyrenemethanol (1.58 g, 6 x 10^{-3} mol) solution in DMF to the reaction mixture under ice cold conditions within 0.5 hr. The reaction contents were allowed to stir under ice cold conditions for further 0.5 hr and then left stirring at room temperature for further 1.5 hr. The contents were poured into 300 ml water and extracted with dichloromethane. The extract was washed with plenty of water and then dried over anhydrous sodium sulphate. The solvent was removed under reduced pressure. The product was purified by column chromatography using silica (200 mesh) column and pet ether/ethyl acetate (70/30) as solvent combination. The solvent was removed under reduced pressure and dried in vacuum oven at 60 ^{0}C overnight. Yield: 2.25 g (70 %). ^{1}H NMR (200 MHz, CDCl$_3$) δ ppm: 8.39-7.98 (m, 9H, Ar-**H**), 6.11, 5.58 (2s, 2H, C**H**$_2$=C), 5.80 (s, 2H, OC**H**$_2$ next to pyrene ring), 4.80-4.50 (b, N**H**), 4.30 (s, 4H, O-C**H**$_2$-C**H**$_2$-O of HEMA), 3.13 (t, 4H, -C**H**$_2$-NH-COO of HMDI), 1.93 (s, 3H, -C**H**$_3$ of HEMA), 1.65-

0.86 (aliphatic protons of HMDI). FTIR: 3317, 3040, 2923, 2854, 1717, 1683, 1637, 1535, 1464, 1401, 1368, 1263, 1176, 1136, 1045, 972, 842, 810, 746, 711, 630. Theoretical mass (m/z): 530.24 and MALDI-TOF mass (m/z): 530.18

5.3.6. Synthesis of IHP-monomer by coupling of isophorone diisocyanate with 2-hydroxyethyl methacrylate and 1-pyrene methanol

The IHP-monomer was synthesized as reported in chapter 2. In a 50 mL two necked round bottom flask, isophorone diisocyanate (IPDI) (1 g, 4.5×10^{-3} mol) in 6 mL dry dimethylformamide (DMF) was taken and the contents were cooled with ice. 2-hydroxyethyl methacrylate (0.59 g, 4.5×10^{-3} mol) was added drop wise under nitrogen atmosphere over a period of 0.5 hr. The reaction was allowed to proceed under ice cold conditions for further 0.5 hr and then left stirring at room temperature for 2 hr. 2-3 drops dibutyltin dilaurate (DBTDL) was added as catalyst followed by drop wise addition of 1-pyrenemethanol (1.04 g, 4.5×10^{-3} mol) solution in DMF (5 mL) to the reaction mixture under ice cold conditions within 0.5 hr and then slowly heated to 60 °C for 6 hr. The contents were poured into 300 mL water and extracted with dichloromethane. The extract was washed with plenty of water and then dried over anhydrous sodium sulphate. The solvent was removed under reduced pressure and dried in vacuum oven at 60 °C for 2 hr. Yield: 2.35 g (90 %). ^{1}H NMR (200 MHz, CDCl$_3$) δ ppm: 8.30-8.02 (m, 9H, Ar-**H**), 6.13, 5.58 (2s, 2H, C**H$_2$**=C), 5.78 (s, 2H, OC**H$_2$** next to pyrene ring), 4.80-4.50 (m, N**H**), 4.29 (s, 4H, O-C**H$_2$**-C**H$_2$**-O of HEMA), 3.24, 2.86 (b, 3H, -C**H**-NH-COO and -C**H$_2$**-NH-COO of IPDI), 1.93 (s, 3H, -C**H$_3$** of HEMA), 1.65-0.86 (aliphatic protons of IPDI). FT-IR (cm^{-1}): 3331, 3043, 2955, 2916, 1718, 1637, 1530, 1456, 1386, 1307, 1299, 1233, 1168, 1058, 1027, 944, 896, 844, 813, 762, 711. Theoretical mass (m/z): 584.29 and MALDI-TOF mass (m/z): 584.21

5.3.7. Synthesis of homopolymer Poly(PBH)

PBH (0.50 g, 1.25×10^{-3} mol) and benzoyl peroxide (0.015 g, 6.24×10^{-5} mol) were taken in DMF (2 ml) in a 10 ml round bottom flask. The reaction mixture was purged with nitrogen for 30 min. The polymerization was carried out by stirring the contents at 65 °C for 24 hr. The viscous liquid was cooled and precipitated in methanol. Polymer was dissolved in small amount of THF and reprecipitated in acetone. Yield: 0.31 g (62 %), THF GPC: $M_n=1.70 \times 10^5$, Đ=1.47. ^{1}H NMR (200 MHz, CDCl$_3$) δ ppm: 8.02-7.4 (b, 9H, Ar-**H**), 2.20 (b, 2H, OC**H$_2$** next to pyrene ring), 3.04(b, O=C-C**H-** of pyrene butyric

acid), 3.98 (b, 4H, O-C**H**$_2$-C**H**$_2$- of HEMA), 1.88 (b, O=C-CH$_2$-**CH**$_2$- of pyrene butyric acid), (1.15-0.75 (b, aliphatic protons). FTIR: 3037, 2926, 2860, 1924, 1731, 1595, 1483, 1453, 1373, 1241, 1139, 1062, 960, 882, 843, 753, 714, 620.

5.3.8. Synthesis of homopolymer Poly(PIC)

PIC (0.75 g, 1.94 x 10^{-3} mol) and benzoyl peroxide (0.023 g, 9.68 x 10^{-5} mol) were taken in DMF (3 ml) in a 10 ml round bottom flask. The reaction mixture was purged with nitrogen for 30 min. The polymerization was carried out by stirring the contents at 65 $^{\circ}$C for 20 hr. The viscous liquid was cooled and precipitated in methanol. It was purified by soxhlet extraction in 20% chloroform / methanol mixture for 48 hr. Yield: 0.55 g (73 %). THF GPC: M$_n$=2.10x10^4, Đ=1.76. ^{1}H NMR (200 MHz, CDCl$_3$) δ ppm: 7.68 (b, 9H, Ar-**H**), 5.41(b, 2H, OC**H**$_2$ next to pyrene ring), 3.83 (b, 2H, O-C**H**$_2$-CH$_2$- of HEMA), 3.17 (b, 2H, N-C**H**$_2$-CH$_2$- of HEMA), 1.80 (b, 3H, -C**H**$_3$ of HEMA), 0.79 (b, aliphatic protons). FTIR: 3334, 3040, 2950, 2889, 1723, 1597, 1522, 1456, 1401, 1366, 1329, 1252, 1148, 1064, 1034, 966, 845, 754, 710.

5.3.9. Synthesis of homopolymer Poly(PHH)

PHH (1.0 g, 1.89 x 10^{-3} mol) and benzoyl peroxide (0.016 g, 5.64 x 10^{-5} mol) were taken in DMF (3 ml) in a 10 ml round bottom flask. The reaction mixture was purged with nitrogen for 30 min. The polymerization was carried out by stirring the contents at 65 $^{\circ}$C for 20 hr. The viscous liquid was cooled and precipitated in methanol. Yield: 0.61 g (61 %). THF GPC: M$_n$=4.90x10^4, Đ=1.2. ^{1}H NMR (200 MHz, CDCl$_3$) δ ppm: 8.34-7.64 (b, 9H, Ar-**H**), 5.87 (b, 2H, OC**H**$_2$ next to pyrene ring), 4.3 (b, N**H**), 4.15 (b, 4H, O-C**H**$_2$-C**H**$_2$-O of HEMA), 3.10 (b, 4H, -C**H**$_2$-NH-COO of HMDI), 1.83-0.86 (b, aliphatic protons). FTIR: 3350, 3044, 2935, 2860, 1721, 1688, 1530, 1455, 1401, 1367, 1245, 1141, 1061, 967, 890, 847, 772, 712, 624.

5.3.10. Synthesis of homopolymer PIHP

IHP-monomer (1 g, 1.23 x 10^{-3} mol) and benzoyl peroxide (BPO) (0.009 g, 3.69 x 10^{-5} mol) were taken in DMF (5 mL) in a 10 mL round bottom (RB) flask provided with a water condenser. The reaction mixture was purged with nitrogen for 0.5 hr. The polymerization was carried out by stirring the contents at 65 $^{\circ}$C for 20 hr. The viscous liquid was cooled and precipitated in methanol. Yield: 0.67 g (67 %). THF GPC: M$_n$=2.20x10^4, Đ=1.59. ^{1}H-NMR (200 MHz, CDCl$_3$) δ ppm: 8.01-7.94 (m, 9H, Ar-**H**), 5.69 (b, 2H, OC**H**$_2$ next to pyrene ring), 4.30 (b, N**H**), 4.12-3.71 (b, 4H, O-C**H**$_2$-OC**H**$_2$-

O of HEMA), 2.89-0.86 (aliphatic protons of IPDI). FTIR (cm^{-1}): 3379, 3043, 2955, 1718, 1530, 1465, 1386, 1356, 1302, 1237, 1137, 1110, 1058, 1023, 896, 844, 800, 770, 708, 682.


5.4. Results and Discussions

5.4.1. Synthesis and Characterization

Three structurally different pyrene monomers were designed and synthesized as shown in scheme-5.1. One monomer had an alkyl spacer segment consisting of five carbon atoms and an ester link in between, separating the pendant pyrene unit from the polymerizable methacrylate moiety. This was synthesized by coupling 2-hydroxyethyl methacrylate (HEMA) with 1-pyrene butyric acid and was named as **PBH** (**P**yrene-**B**utyric acid **H**EMA).[27] Two pendant pyrene monomers, one with short linear spacer segment and another with long linear spacer segment were also designed which were capable of hydrogen bonding via urethane linkages. The short spacer pyrene monomer was developed by coupling 2-isocyanatoethyl methacrylate with 1-pyrene methanol and was named **PIC** (**P**yrene-**ICEMA**). The linear long chain pyrene monomer was synthesized in a step wise manner by first coupling hexamethylene diisocyanate (HMDI) with one equivalent of 2-hydroxyethyl methacrylate (HEMA) followed by subsequent coupling with pyrene methanol to obtain **PHH** (**P**yrene-**H**MDI-**H**EMA).[28] The monomers were all structurally characterized by ^{1}H and ^{13}C NMR spectroscopies and MALDI-TOF mass spectrometry. The monomers were polymerized using 5 mol% benzoyl peroxide (BPO) as initiator in dimethyl formamide (DMF) as solvent. The polymers were compared with 100% pyrene urethane methacrylate with a kinked spacer- **PIHP**. The structures of the 100% pyrene labeled polymers used in the study are shown in schemes-5.2. The polymers were structurally characterized by ^{1}H and molecular weight was determined using Gel Permeation Chromatography (GPC) in THF. Figure-5.2 compares the proton NMR spectra (recorded in CDCl$_3$) of the three monomers with their respective polymers. The complete disappearance of the methacrylic double bonds (shown by the dotted lines) and the overall broadening of the peaks indicated the completion of polymerization. The molecular weight details and the dispersity of the homopolymers are given in table-5.1. From the table, the number of repeat unit was calculated to be more than 40 for the three polymers with **poly(PBH)**

exhibiting very high molecular weight with repeat unit ~425. For comparative study a kinked hydrogen bondable urethane methacrylate pyrene polymer - **PIHP** (synthesis and characterization described previously in chapter-2) was also included in the study.

Scheme-5.1: Synthesis of linear pyrene monomers.
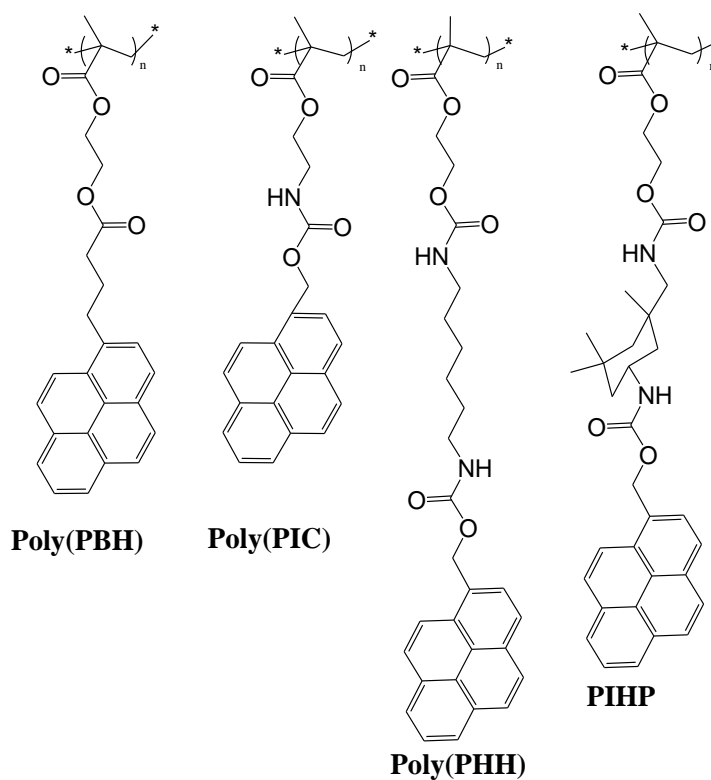
Scheme-5.2: Structure of 100 % Pyrene labeled polymers.
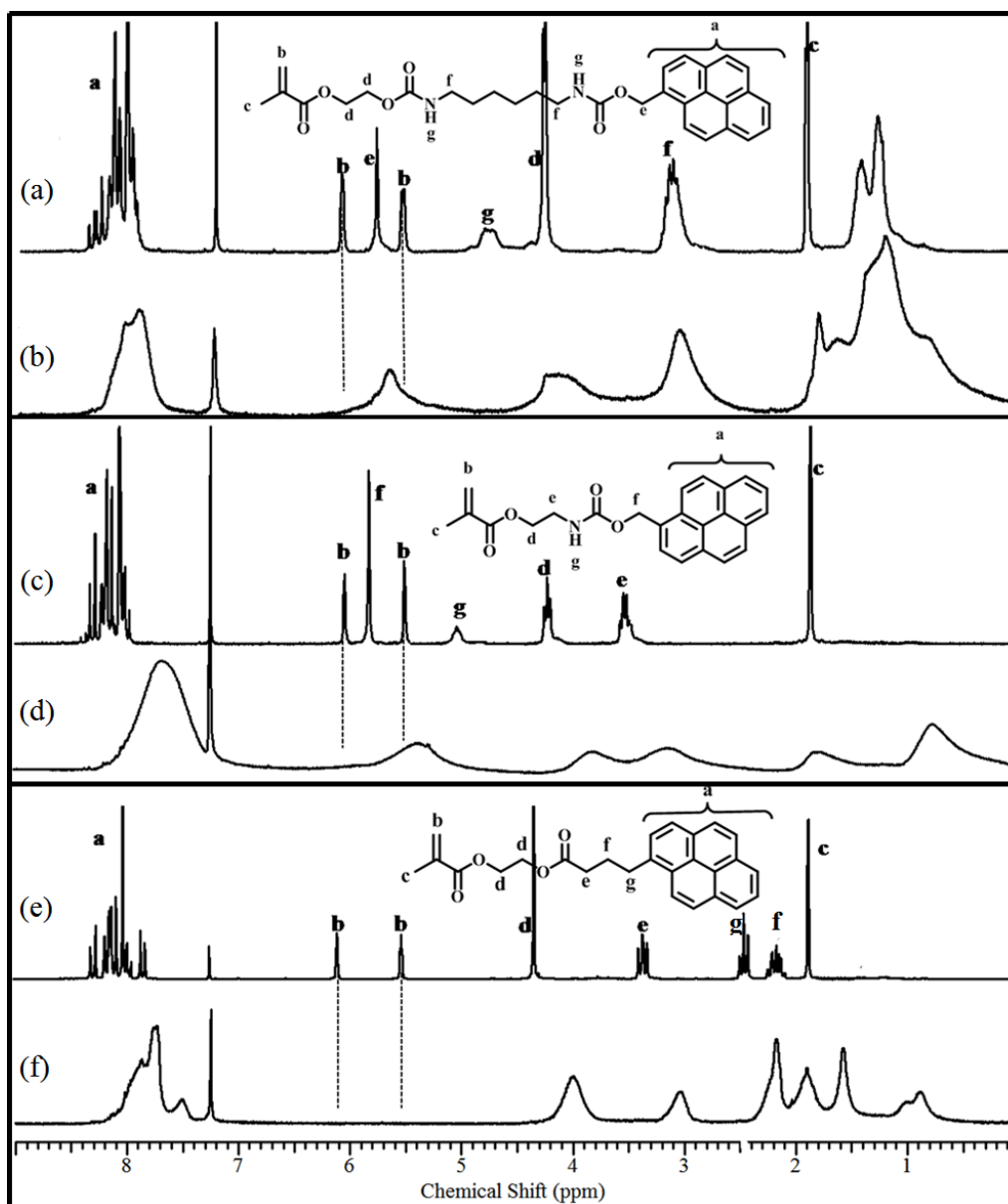
Figure-5.2: ^{1}H NMR spectrum (top to bottom) in CDCl$_3$. (a) Monomer **PHH** and (b) **Poly(PHH)** (c) Monomer **PIC** and (d) **Poly(PIC)** (e) Monomer **PHH** and (f) **Poly(PHH)**.

       The thermal properties of the homopolymers were studied using TGA and DSC and the thermal data is given in the table-1. The TGA plots for all the polymers are given in the figure-5.3. From the TGA measurements, it was found that the polymers were thermally stable with the 10 weight % loss temperature around 280-330 ^{o}C. Figure-5.4 shows the DSC curves of all homopolymers obtained by third heating cycle. The glass transition temperature (T_g) values obtained from the DSC studies (given in table 1) reflected the varying rigidity of the polymers afforded by the different structural designs. The lowest T_g value of 67 ^{o}C was exhibited by the non-hydrogen bonded

162

polymer **Poly(PBH)**, whereas the highest T_g value of 158 ^{o}C was exhibited by the hydrogen bonded polymer with the kinked urethane linkage **PIHP**. The other two linear hydrogen bonded short and long chain urethane methacrylate polymers **Poly(PIC)** and **Poly(PHH)** had T_g values of 90 and 72 ^{o}C respectively. Hydrogen bonding afforded rigidity and consequently higher glass transition temperatures while comparing the hydrogen bonded versus non-hydrogen bonded polymers.[29, 30] On the other hand, comparing among short and long side chain polymers the increased flexibility of the long alkyl chain resulted in lower T_g values for **Poly(PHH)** compared to **Poly(PIC)**.
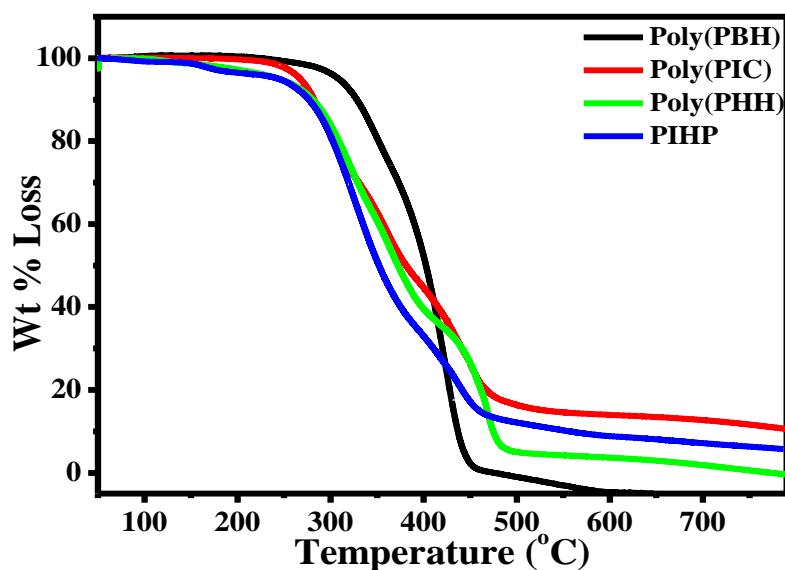

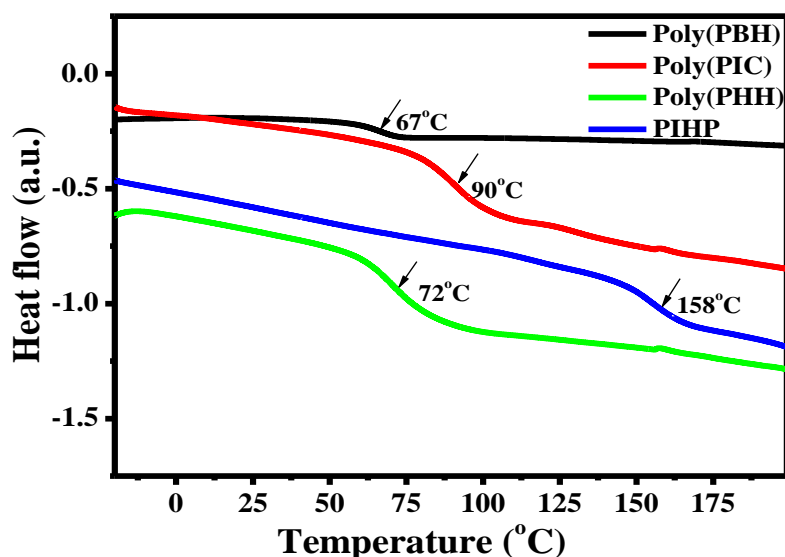*Figure-5.3:* TGA Plots of the homopolymers.

Figure-5.4: DSC thermograms of the homopolymers obtained from third heating cycle.

Table-5.1: Polymer designation, Number Average Molar Mass, Weight Average Molar, Polydispersity indices and 10 Wt % loss Temperature and T_g of polymers.

POLYMER	$M_n{}^a$	$M_w{}^a$	Đ[a]	10 Wt. % Loss (^oC)[b]	$T_g{}^c$
Poly(PBH)	1.70×10^5	2.50×10^5	1.47	330	67
Poly(PIC)	2.10×10^4	3.70×10^4	1.76	282	90
Poly(PHH)	4.90×10^4	5.90×10^4	1.20	280	72
PIHP	2.20×10^4	3.49×10^4	1.59	282	158

a. Measured by size exclusion chromatography (SEC) in tetrahydrofuran (THF), calibrated with linear, narrow molecular weight distribution polystyrene standards.

b. TGA measurements at heating rate of 10 ^oC/ min under nitrogen.

c. Determined by DSC analysis.

5.4.2. Photophysical studies

5.4.2.1. Steady State emission Studies

The photophysical properties of the four 100% pyrene loaded polymers were studied in dimethyl formamide (DMF). Figure-5.6 compares the absorbance and the emission spectra of 0.1 OD solutions of the four polymers upon excitation at 343 nm. All emission were recorded at a slit width of 1 nm for both the emission and excitation for nitrogen bubbled solutions in DMF. The normalized emission spectra of the polymers showed peaks in the 375-395 nm region corresponding to pyrene monomer emission and a broad red shifted peak at ~480 nm corresponding to pyrene excimer emission.[31] The most significant difference among the four polymers was the almost negligible pyrene monomer emission in the 375-395 nm region for the two polymers **Poly(PBH)** and **Poly(PIC)** compared to the other two polymers which had highly intense pyrene monomer emission also along with excimeric emission.
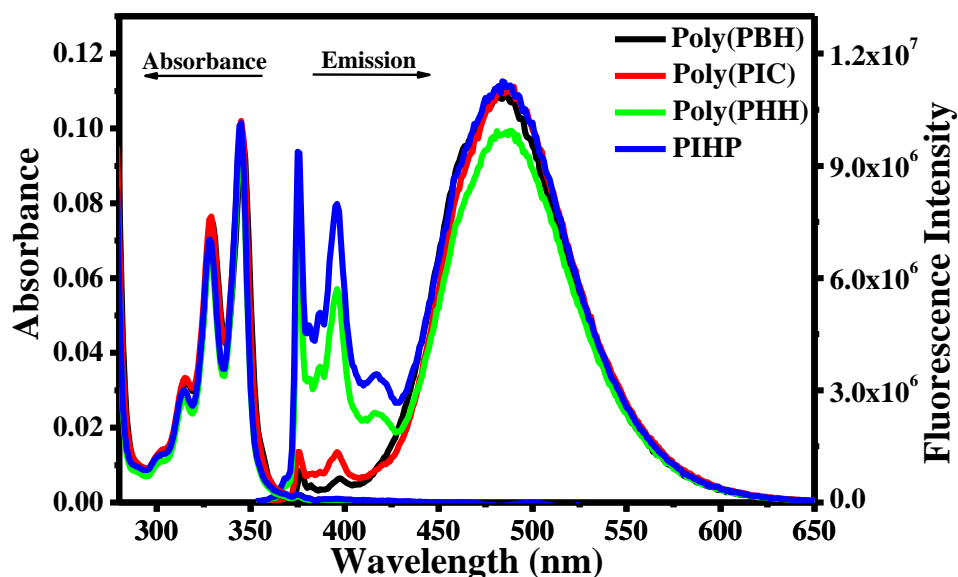
Figure-5.5: Absorbance and Steady State Emission Spectra (λ_{ex}-343 nm) of the polymers for 0.1 OD solutions in DMF.

Table-5.2: The total emission quantum yield (Q_{Em}), excimer emission quantum yield (Q_E) and monomer emission quantum yield (Q_M), I_E/I_M ratio and spectroscopic parameters obtained from Absorption and Fluorescence Excitation Spectra for the polymers in DMF.

POLYMER	Q_{Em} [a]	Q_M [a]	Q_E [a]	I_E/I_M [b]	P_A [c]	P_M [d]	P_E [e]
Poly(PBH)	0.40	0.01	0.39	72.96	2.31	2.12	2.16
Poly(PIC)	0.36	0.02	0.34	38.95	2.30	2.80	2.25
Poly(PHH)	0.39	0.07	0.32	7.20	2.83	2.80	2.70
PIHP	0.44	0.09	0.35	5.52	2.82	2.80	2.70

a. Calculated using 0.1 OD quinine sulphate solution as standard. Excitation wavelength was 343 nm.

b. I_E/I_M determined by taking the ratio of integrated area of excimer (500 -530 nm) and monomer (372-378 nm) emission ($\lambda_{ex} = 343$ nm).

c. Peak-to-valley ratio, P_A, obtained from the Absorption Spectra.

d. Peak-to-valley ratio, obtained from the monomer (P_M) excitation spectrum due to the (0,1) transition.

e. Peak-to-valley ratio, obtained from the Excimer (P_E) excitation spectrum due to the (0,1) transition.

The excimer emission efficiency measured as the I_E/I_M ratio (the ratio of the integrated area of excimer region (500-530 nm) and monomer emission region (372-378 nm))[17] for the four polymers is given in table-5.2. The values were respectively 72.96, 38.95, 7.20, 5.52 for the polymers **Poly(PBH), Poly(PIC), Poly(PHH)** and **PIHP** respectively. Information regarding the nature of the excimeric species - whether static or dynamic, can be obtained by comparing the P_A, P_M and P_E values. As described in chapter 3, a value ~3 for the P_A, P_M and P_E is taken to be indicative of absence of ground state aggregates.[31] The P_A, P_M and P_E values for the polymers in DMF are given in table-5.2. From the table it can be seen that for the two polymers **Poly(PBH)** and **Poly(PIC)** indicated significant presence of ground state aggregates based on the low P_A, P_M and P_E values. For the polymers **Poly(PHH)** and **PIHP** also the values of P_A, P_M and P_E were lower than 3, although the extent of deviation was lesser compared to **Poly(PBH)** and **Poly(PIC),** which suggested the presence of ground state aggregates, albeit to a lesser extent. Table-5.2 also compares the total emission quantum yields along with the quantum yields for the monomer and excimer emission individually. The relative quantum yields were measured using quinine sulfate as the standard (ϕ_r =0.546 in 0.1M H_2SO_4) for nitrogen purged polymer samples and calculated using the equation followed in chapter-2.[32]

The total emission quantum yields for the polymers **Poly(PBH), Poly(PIC), Poly(PHH)** and **PIHP** were 0.40, 0.36, 0.39, 0.44 respectively. The emission intensity for monomer as well as excimer was highest for **PIHP** thus giving the highest quantum yield but low I_E/I_M ratio. The major difference between the quantum yield and the I_E/I_M ratio was that the former gave the coefficient of emission where as the latter provided the extent of excimer formation (self organization behavior).

5.4.2.2. Fluorescence lifetime studies

Fluorescence lifetime decay studies were conducted for the polymers by exciting using a 340 nm nanoLED source and monitoring at the monomer (375 nm) and excimer (500 nm) region. DAS software was used for fitting the retrieved data. For all polymers, the best fits for the monomer and excimer decays were obtained to be triexponential. The fitted data had χ^2 values lower than 1.3 with the residuals and autocorrelation function of the residuals randomly distributed around zero. The monomeric lifetime of the H-bondable monomer species **PIC**, **PHH** and **IHP** was ~200 ns which matched very well with the lifetime of 1-pyrene methanol (~200 ns) in DMF.[33] This clearly

highlighted the fact that the lifetime remained unchanged after urethane linkage formation during synthesis of monomer species. For the non H-bondable **PBH** monomer, the monomeric lifetime was found to be ~175 ns, which was higher than the reported value of another ester 1-pyrenebutyl derivative i.e ~160 ns in DMF.[34] It may be due to reduced mobility of pyrene units of **PBH** monomer as compared with the literature report. Figure-5.6 compares the decay curves along with the residuals obtained for the polymers at the monomer (~ 375 nm) and excimer (~ 500 nm) emission region.
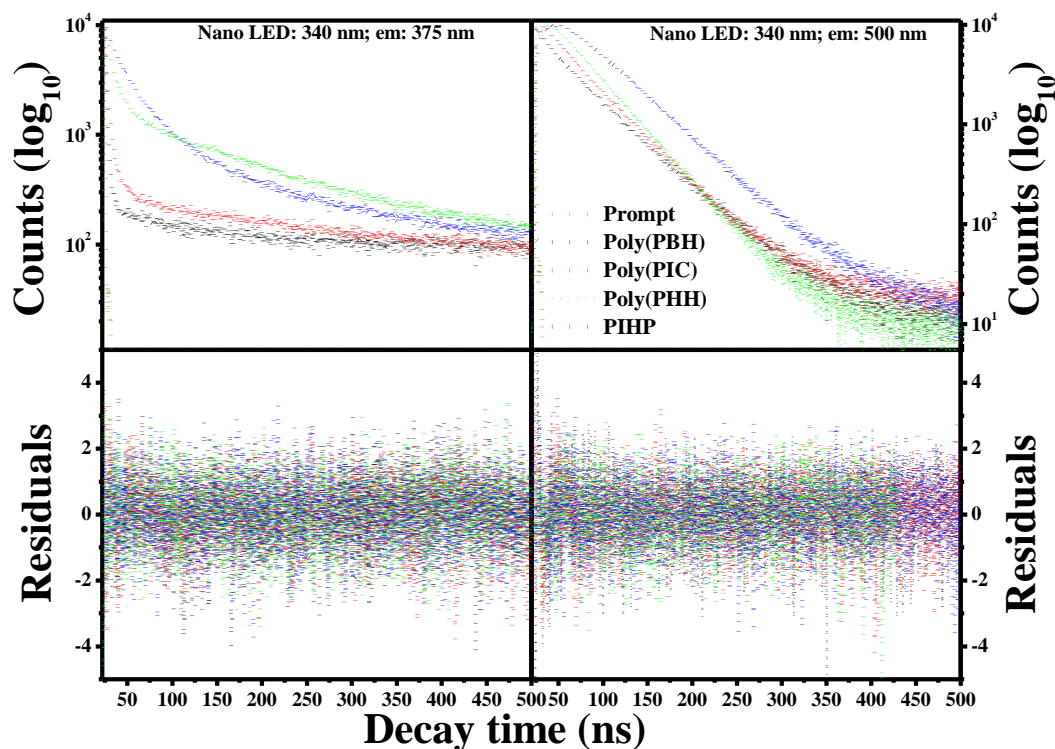

Figure-5.6: Fluorescence Decay curves of the polymers in DMF for 0.1 OD solution, collected at monomer (375 nm) and excimer (500 nm) emission wavelength along with the residuals obtained by tri-exponential fitting of monomer excimer emission curves. The nano LED used as excitation wavelength was 340 nm.

Table-5.3 shows the fluorescence lifetime values retrieved from the decay curves. From the table it could be seen that although the monomer decay was best fitted with tri-exponentials, the contribution of the third exponential component (τ_{M3}) was almost negligible, especially for **Poly(PBH)** and **Poly(PIC)**. The contribution from the higher lifetime component (τ_{M3}) could be attributed to the species which decay with the intrinsic lifetime of the monomeric species. The shorter lifetime (τ_{M2}) values for the polymers **Poly(PBH)**, **Poly(PIC)**, **Poly(PHH)** and **PIHP** was 1.15, 1.57, 4.86, 10.7 ns respectively with the corresponding pre-exponential contributions (α_{M2}) of 0.92, 0.85,

0.63 and 0.50. This lifetime is attributed to the species which were aggregated in ground-state and decayed on a faster time scale. A careful observation of the decay curves at excimer emission (~ 500 nm) revealed the absence of a rise time signified by a negative value of pre-exponential α_{E2} in the case of **Poly(PBH)**. The absence of rising curve signified excimer formation through static mechanism from pre-formed aggregates. The polymers **Poly(PHH)** and **PIHP** showed two rise curves signifying the excimers having different pathways of origin.[35, 36] The excimer lifetime varied between 44 ns and 60 ns which is the typical lifetime of excimer in organic solvents.[37, 38]

Table-5.3: Parameters (τ: decay time, α: pre-exponential factor, $\chi2$: chi-squared value) retrieved from the triexponential fit of the pyrene monomer (375 nm) and excimer (500 nm) in DMF obtained by using nano LED 340 nm for excitation.

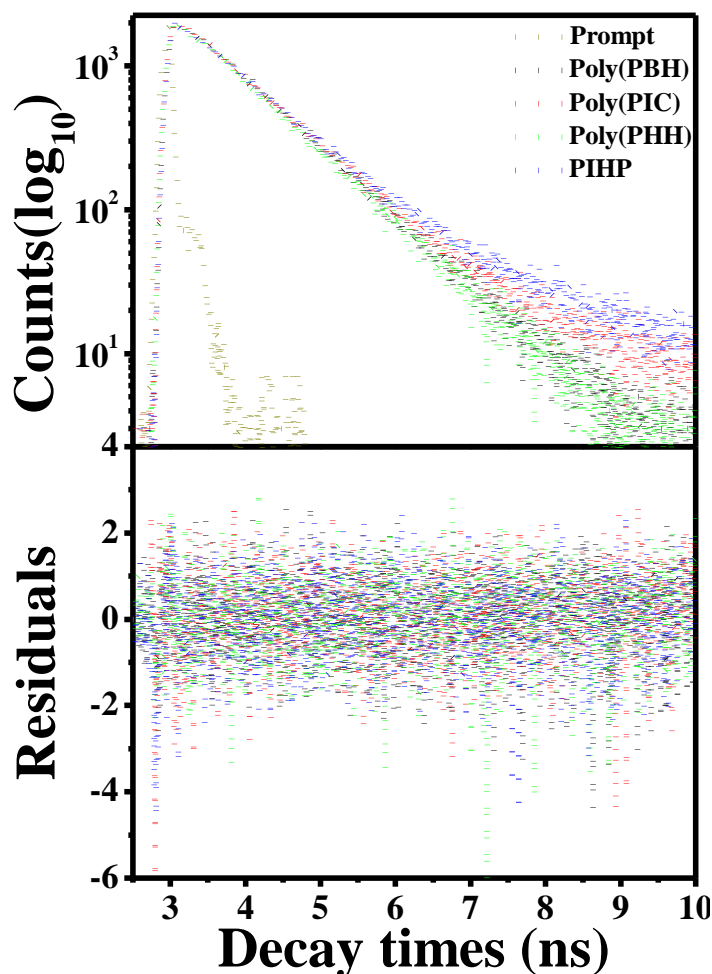| Polymer	λ_{em}: 375 nm				λ_{em}: 500 nm			
	$\tau_1(\alpha_1)$ ns	$\tau_2(\alpha_2)$ ns	$\tau_3(\alpha_3)$ ns	χ^2	$\tau_1(\alpha_1)$ ns	$\tau_2(\alpha_2)$ ns	$\tau_3(\alpha_3)$ ns	χ^2
Poly(PBH)	4.09 (0.07)	1.15 (0.92)	176.9 (0.00)	1.13	59.7 (0.39)	4.38 (0.31)	34.9 (0.30)	1.08
Poly(PIC)	8.23 (0.14)	1.57 (0.85)	188.8 (0.01)	1.13	53.9 (0.24)	2.40 (-0.36)	38.44 (0.39)	1.11
Poly(PHH)	15.4 (0.25)	4.86 (0.63)	198.3 (0.12)	1.13	44.1 (0.54)	9.72 (-0.20)	4.91 (-0.26)	1.05
PIHP	34.42 (0.44)	10.76 (0.50)	177.6 (0.06)	1.22	53.3 (0.52)	18.3 (-0.35)	8.29 (-0.13)	1.15

Figure-5.7: The fluorescence Decay curves of the polymers in DMF for 0.1 OD solution, collected at dimer (445 nm) emission wavelength along with the residuals obtained by tri-exponential fitting of dimer emission curves. The Laser diode used as excitation wavelength was 405 nm.

The existence of dimeric species was also investigated by picosecond lifetime studies by exciting at 405 nm (which selectively excites the ground state aggregated species)[39] and decay curves were recorded at 445 nm. Figure-5.7 displays the fluorescence decay curves recorded at 445 nm by exciting at 405 nm. When the decay times were observed at 445 nm (a typical dimer peak) by exciting at 405 nm, the tri-exponential fits were applied to get the better residuals and the χ^2 smaller than 1.3. But the third component had almost negligible contribution. From the literature reports, decay time of pyrene dimers has a value of 2 - 3.7 ns with no rise time.[39, 40, 41] For the polymers **Poly(PBH)**, **Poly(PIC)**, **Poly(PHH)** and **PIHP** the decay time values were 3.35, 3.56, 2.85, 2.62 respectively with the corresponding pre-exponential contributions as 0.11, 0.06, 0.05 and 0.17. These values are very well in sync with the literature

reported values. The detailed understanding of the mechanism and origin of excimer formation was confirmed by wavelength dependent decay studies.

5.4.2.3. Nanosecond Time-resolved emission Studies (ns-TRES)

The wavelength dependent lifetime studies were conducted to understand the heterogeneity of the emissive species in the system and also to study the excited state kinetics. A time-resolved emission spectrum (TRES) was constructed by plotting the intensity vs wavelength $I(\lambda,t)$ using the following equation.[39, 42]

$$I(\lambda,t) = I_{ss}(\lambda) \left(\sum_j \alpha_j(\lambda)\, e^{-t/\tau_j(\lambda)} / \sum_j \alpha_j(\lambda)\, \tau_j(\lambda) \right)$$

Where $I_{ss}(\lambda)$ - steady state fluorescence intensity, $\alpha_j(\lambda)$ - amplitude pre-exponential factor and $\tau_j(\lambda)$ - decay times.

Figure-5.8 shows the three dimensional contours showing time-intensity-wavelength dependence plots obtained by the wavelength dependent lifetime studies collected in the wavelength range 365 to 545 nm with the interval of 10 nm with the decay curves collected for 2 minutes at each wavelength. A nanoLED of 340 nm was used as excitation source. For the polymers **Poly(PBH)** and **Poly(PIC)**, the decay curves at the lower wavelength region had negligible intensity as compared to that at higher wavelength region. The rise curve was absent at higher wavelength for **Poly(PBH)**, giving ample proof of excimer formation by static route. For the **Poly(PIC)**, rise curve with very small negative amplitude was present at higher wavelength. From the decay studies carried out at different wavelength, a reconstructed time-resolved emission spectrum was created by using the above equation.
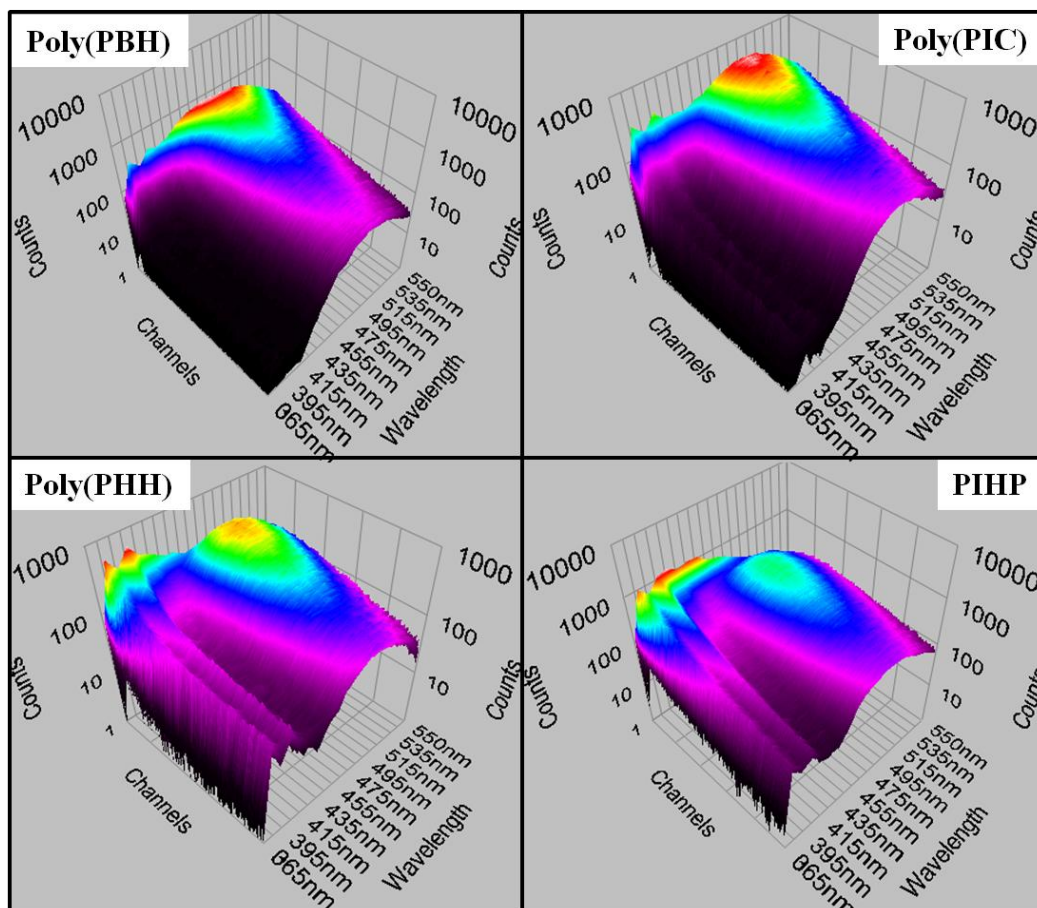
Figure-5.8: The three dimensional time resolved emission spectrum (3D-TRES) for all the polymers. The emission decays were collected in the range 365 to 545 nm, using Nano LED of 340 nm.

Figure-5.9 presents the reconstructed time resolved emission spectrum (TRES) for the polymers in the wavelength range 365- 545 nm by using the nanoLED of 340 nm as the excitation source. From the figure it was evident that **Poly(PBH)** lacked significant monomer emission even at the very onset i.e. 0.42 ns. On the other hand a broad peak centered at 440 nm was noticeable in the early time-gated spectra, whose maxima shifted towards 485 nm within very short time. A shoulder ~460 nm was also clearly observable in these later time-gated spectra. **Poly(PIC)** contained both monomer as well as excimer emission peak even at the onset time i.e 0.42 ns, which indicated that along with the monomer species some ground state aggregated species were also present in the system. The absence of an isoemissive point in the TRES pointed to the presence of ground state aggregated species as the source of static excimer emission, rather than excimer emission through diffusive interactions. On the other hand, **Poly(PHH)** showed mostly monomer emission with very small amount of

excimer emission at the onset time i.e 0.42 ns. With time the monomer emission reduced and excimer emission increased with the presence of an isoemissve point at ~445 nm, indicating the presence of two emissive species and the formation of excimer through diffusive encounters. In the case of the polymer **PIHP** upto 1.26 ns, only monomer emission was present. At 2.5 ns, monomer emission was still very intense and excimer emission was very less. As time increased, excimer emission started increasing and monomer emission decreased with an isoemissive point ~445 nm. The presence of an isoemissive point along with the excimer increase clearly indicated that there were two emissive species and the excimer formation was mostly diffusion controlled. The TRES studies thus proved beyond doubt that small changes in the architecture of the polymer had a profound influence on the nature and extent of excimer formation.

Figure-5.9: The reconstructed time resolved emission spectrum (TRES) for all the polymers. The emission decays were collected in the range 365 to 545 nm, using nano LED of 340 nm.

To follow the presence of ground state aggregates in the polymers in more detail, the TRES studies were also conducted for 2 minutes each in the wavelength range of 420-550 nm at an interval of 10 nm by using the excitation source of 390 nm (which selectively excites the dimer species). The 3D contour plot obtained by wavelength dependent lifetime studies is shown in the figure-5.10. Figure-5.11 shows

the normalized TRES spectrum for all the polymers conducted at the above parameters. From the figure it was clearly evident that the ground state aggregated species were present in all the polymers, whose maxima shifted towards higher wavelength region as the time increased. Clearly noticeable was the absence of the rise curve at higher wavelength region in any of the polymers, clearly ruling out the possibility of dynamic encounters. This also proved that the steady state emission spectrum alone could not differentiate the origin of excimer species whether they were formed through the static mechanism or dynamic encounters as the peak position remained the same for both. From the figure it was clearly visible that all the polymers possessed ground state aggregated species although the extent was different as proven by the TRES conducted by 340 nm excitation.

Figure-5.10: The three dimensional time resolved emission spectrum (3D-TRES) for all the polymers. The emission decays were collected in the range 410 to 550 nm, using Nano LED of 390 nm.
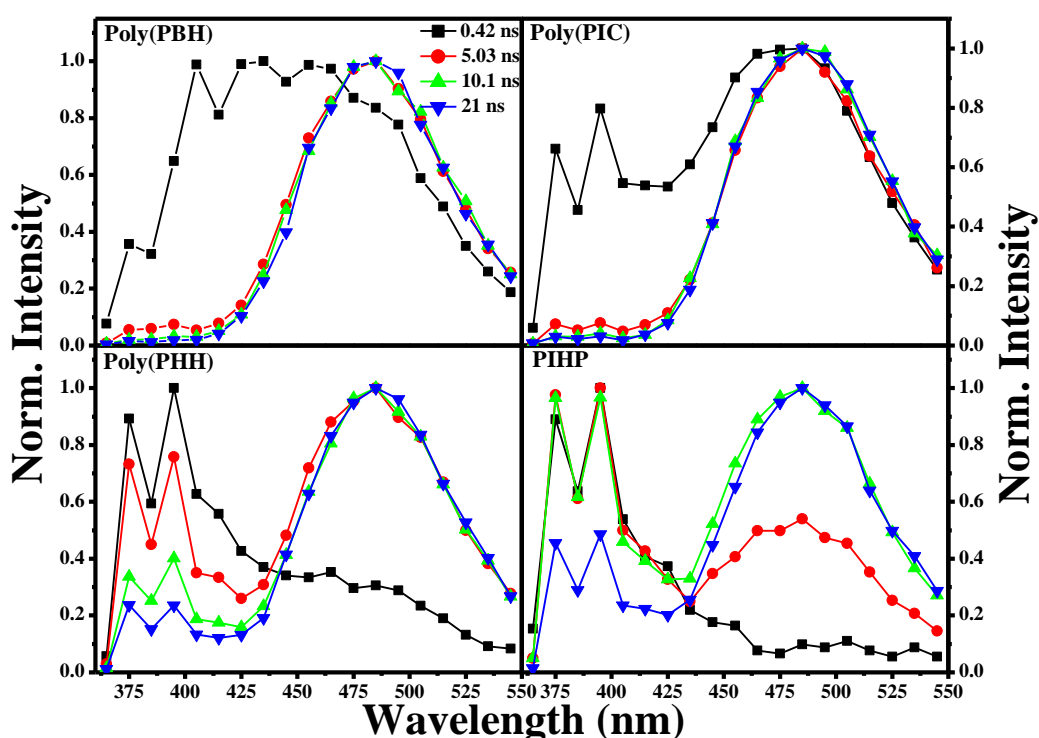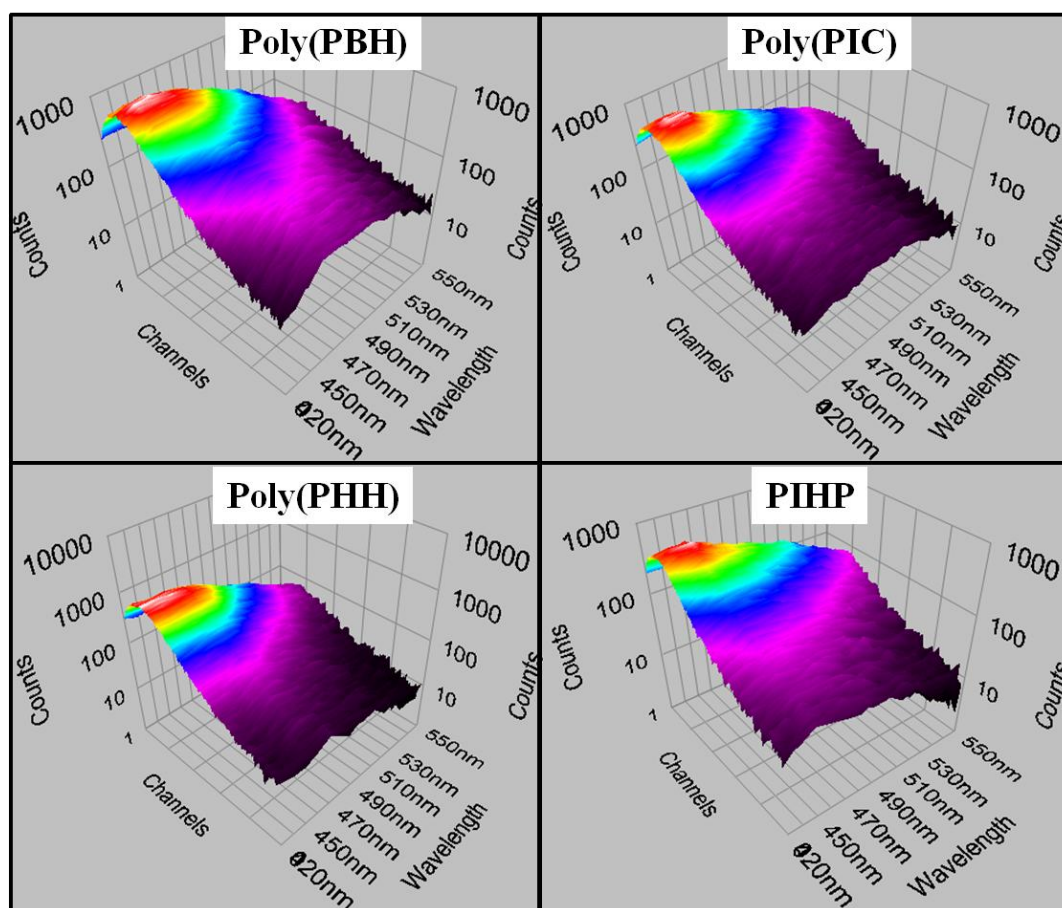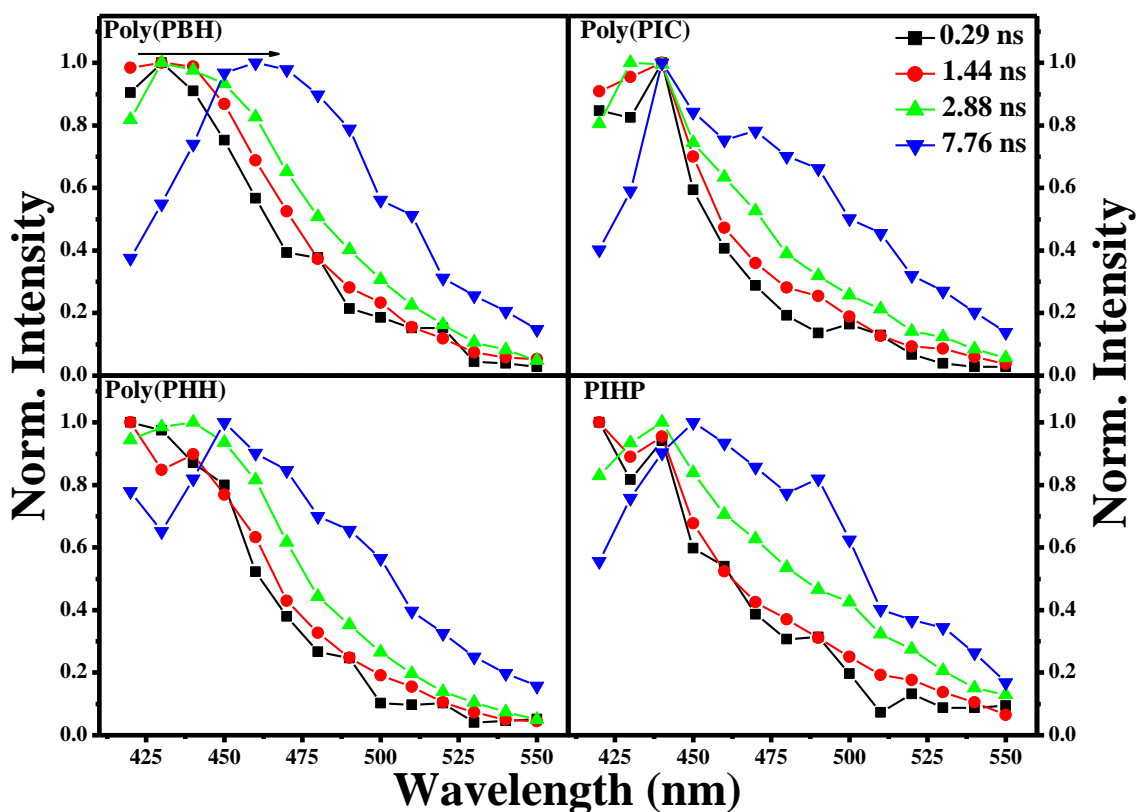
Figure-5.11: Reconstructed Normalised time resolved emission spectrum (nTRES) for all the polymers. The emission decays were collected in the wavelength range 420 to 550 nm, using nano LED of 390 nm.

5.4.2.4. Variable temperature emission studies

Variable temperature emission studies are helpful in analyzing the origin of excimer formation; whether the excimers were formed by dynamic mechanism through diffusional encounters or by static mechanism through the direct excitation of ground state aggregates.[43] The temperature-dependent emission studies were conducted for 0.1 OD solution of all polymers in DMF at the excitation wavelengths of 343 and 395 nm. The emission were recorded in the temperature range from 0 to 85 ^{o}C while heating and cooled back to 0 ^{o}C (0 → 85 → 0 ^{o}C) at an interval of 10 ^{o}C. At each temperature the samples were equilibrated for 10 minutes before recording the emission.

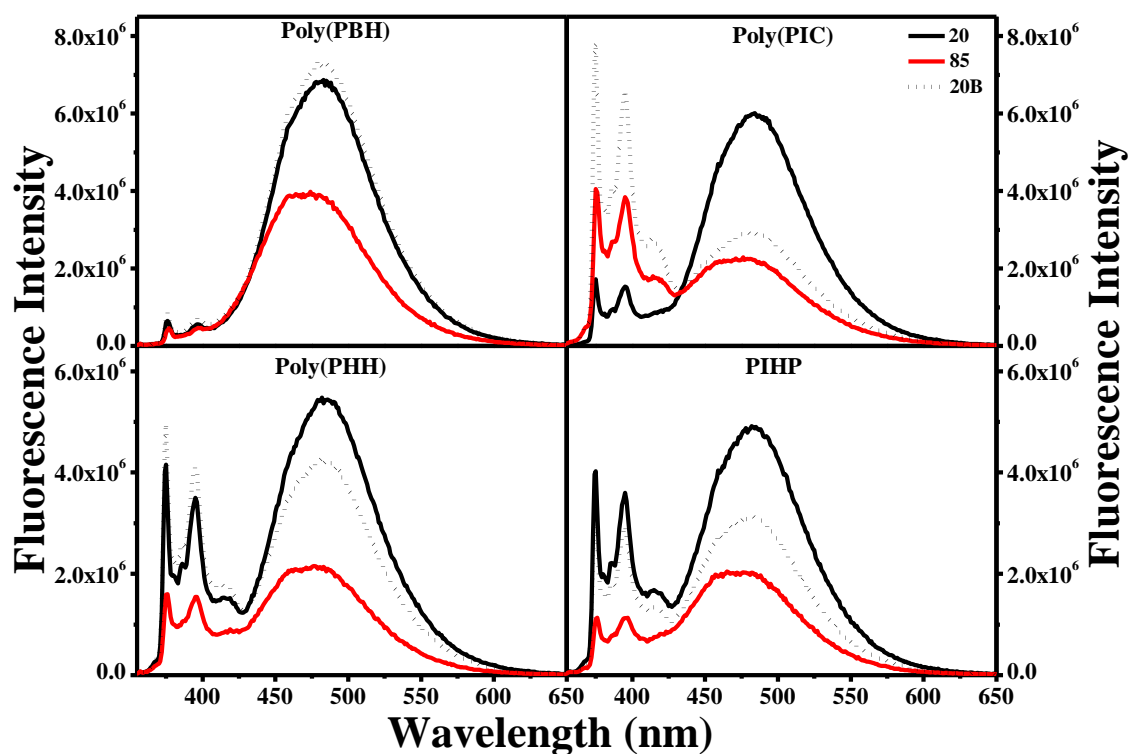***Figure-5.12:*** Temperature dependent steady state emission spectrum in DMF for the heating temperature range of 20 to 85 $^{\circ}$C and cooling back to 20 $^{\circ}$C (20B) for **Poly(PBH)**, **Poly(PIC)**, **Poly(PHH)** and **PIHP**.

Figure-5.12 compares the emission spectra by exciting at 343 nm for the polymers **Poly(PBH)**, **Poly(PIC)**, **Poly(PHH)** and **PIHP** at 25 $^{\circ}$C, 85 $^{\circ}$C during heating and 25 $^{\circ}$C while cooling (dotted line). The total emission intensity of both pyrene monomer and excimer emission decreased with increase of temperature for all polymers with a pronounced broadening of the excimer wavelength maxima. While cooling, an almost complete recovery of the total emission intensity to the original value was observed only in the case of **Poly(PBH)**. In all the other cases, the excimer emission observed at 25 $^{\circ}$C while cooling was much lower compared to that at 25 $^{\circ}$C during heating. The excimer emission wavelength also exhibited a clear shoulder peak ~460 nm in addition to the peak maxima at 480 nm as the temperature was increased. The emission around 455 to 465 nm is usually attributed to emission from partially overlapped or distorted pyrenes, while emission around 485 nm have their origin from pyrene which are perfectly oriented with respect to each other.[25, 44, 45] Therefore, an increase in temperature resulted in an increase in population of pyrenes in distorted orientations. A clear difference in behaviour between the non-hydrogen bonded pyrene

polymer – **Poly(PBH)** and the other three hydrogen bonded pyrene polymers was obvious from this variable temperature (heating & cooling) studies. For the dilute solutions used in the study, the excimer emission could be attributed to intrachain pyrene interactions. The hydrogen bonding introduced by the urethane linkage in the polymers **Poly(PIC)**, **Poly(PHH)** and **PIHP** served as a constraining hold arresting the pyrenes in unfavourable conformations. Providing thermal energy enables the polymer chains to break out of these constraints and adopt the most favourable conformation. In **Poly(PBH)** there is no gain or loss attained by different conformations and therefore heating followed by cooling does not produce any pronounced change in overall average conformation of the polymer chains. In the short side chain pyrene urethane methacrylate polymer **Poly(PIC)**, an isoemissive point was observed ~ 445 nm indicating the presence of only two species – the pyrene monomer and pyrene excimer whose amounts varied as a function of temperature. Upon heating the polymer to 80 ^{o}C followed by cooling to 20 ^{o}C, the pyrene monomer emission increased in intensity while the pyrene excimer emission reduced considerably.

5.5. Conclusions

Four side chain methacrylate polymers having 100 % pendant pyrene units with structural variations like presence or absence of hydrogen bonding interactions in the form of urethane linkages, short or long alkyl spacer segments separating the pyrene units from the polymer backbone, linear versus kinked urethane linkage etc. were compared and contrasted for their excimer forming abilities. Steady-state and fluorescence lifetime decay studies as well as variable temperature emission and time-resolved emission spectra (TRES) studies were carried out in DMF to understand their self organization behaviour in very dilute solutions (0.1 OD). The non-hydrogen bonded polymer **Poly(PBH)** exhibited mostly excimer emission with almost negligible monomeric emission and the excimer emission was through static route with the direct excitation of ground state aggregated species. It is evidenced by the absence of rise curve in the decay curve collected in the excimer region (500 nm) as well as TRES studies. The hydrogen bonded polymers exhibited excimer formation via static as well as dynamic route. Variable temperature emission studies collected both while heating and cooling helped to establish the conformational differences adopted by the hydrogen bonded versus non-hydrogen bonded side chain pyrene methacrylate polymers. The overall outcome of this chapter is mentioned below.

a) The excimer formation by the non-H-bonded polymer and H-bonded polymers brought out the differences in their architecture as the H-bonded polymers **Poly(PIC), Poly(PHH)** and **PIHP** formed excimer through dynamic as well as static mechanism whereas the non-H-bonded polymer **poly(PBH)** formed excimer exclusively via static mechanism.

b) TRES studies conducted on the polymers showed that with the small changes in the architecture the excimer formation greatly varied and the mechanism of excimer formation followed was different among the polymers.

c) The hydrogen bonding introduced by the urethane linkage in the polymers **Poly(PIC)**, **Poly(PHH)** and **PIHP** servedas a constraining hold arresting the pyrenes in unfavourable conformations, which was evidenced by the variable temperature fluorescence emission. For non-H-bonded polymer **poly(PBH)** the emission recovered fully on cooling whereas for the H-bonded polymers **Poly(PIC), Poly(PHH)** and **PIHP**, the emission was not recovered completely.

5.6. References

1) Zachariasse, K.; Kühnle, W. *Phys. Chem. Neue F* **1976**, *101*, 267−276.

2) Snare, M. J.; Thistlethwaite, P. J.; Ghiggino, K. P. *J. Am. Chem. Soc.* **1983**, *105*, 3328-3332.

3) Winnik, M. A. *Acc. Chem. Res.* **1985**, *18*, 73-79.

4) Ringsdorf, H.; Venzmer, J.; Winnik, F. M. *Macromolecules* **1991**, *24*, 1678-1686.

5) Winnik, M. A.; Redpath, T.; Richards, D. H. *Macromolecules* **1980**, *13*, 328-335.

6) Collart, P.; Toppet, S.; Zhou, Q. F.; Boens, N.; De Schryver, F. C. *Macromolecules* **1985**, *18,* 1026-1030.

7) De Melo, S. J.; Costa,T.; Francisco, A.; Macanita, A. L.; Gago, S.; Goncalves, I. S. *Phys. Chem. Chem. Phys.* **2007**, *9*, 1370-1385.

8) Picarra, S.; Relogio, P.; Afonso, C. A. M.; Martinho, J. M. G.; Farinha, J. P. S. *Macromolecules*, **2003**, *36*, 8119-8129.

9) Ingratta, M.; Hollinger, J.; Duhamel, J. *J. Am. Chem. Soc.* **2008**, *130*, 9420-9428.

10) Zhao, C.; Wu, D.; Lian, X.; Zhang, Y.; Song, X.; Zhao, H. *J. Phys. Chem. B* **2010**, *114*, 6300–6308.

11) Yekta, A.; Xu, B.; Duhamel, J.; Adiwidjaja, H.; Winnik, M. A. *Macromolecules* **1995**, *28*, 956-966.

12) Picarra, S.; Duhamel, J.; Fedorov, A.; Martinho, J. M. G. *J. Phys. Chem. B* **2004**, *108*, 12009-12015.

13) Duhamel, J. *Acc. Chem. Res.* **2006**, *39*, 953−960.

14) De Melo, J. S. S.; Costa, T.; Miguel, M. d. G.; Lindman, B.; Schillen, K. *J. Phys. Chem. B* 2003, *107*, 12605−12621.

15) Duhamel, J. *Langmuir* **2012**, *28*, 6527-6538.

16) Duhamel, J. *Polymers* **2012**, *4*, 211−239.

17) Duhamel, J.; Kanagalingam, S.; O'Brien, T.; Ingratta, M. *J. Am. Chem. Soc.* **2003**, *125,* 12810−12822.

18) Bondurant, B.; Last, J. A.; Waggoner, T. A.; Slade, A.; Sasaki, D. Y. *Langmuir* **2003**, *19*, 1829−1837.

19) Arora, K. S.; Hwang, K. C.; Turro, N. J. *Macromolecules* **1986**, *19*, 2806-2810.

20) Hudgins, R. R.; Huang, F.; Gramlich, G.; Nau, W. M. A. *J. Am. Chem. Soc.* **2002**, *124*, 556−564.

21) Graceffa, P.; Lehrer, S. S. *J. Biol. Chem.* **1980**, *255*, 11296-11300.

22) Zaragoza-Galán, G.; Fowler, M. A.; Duhamel, J.; Rein, R., Solladié, N.; Rivera, E. *Langmuir* **2012**, *28*, 11195-11205.

23) Kaushlendra, K.; Asha, S. K. *Langmuir* **2012**, 28, 12731-12743.

24) Kaushlendra, K.; Asha, S. K. *J. Phys. Chem. B* **2013**, *117*, 11863-11876.

25) Gao, L.; Fang, Y.; Wen, X.; Li, Y.; Hu, D. *J. Phys. Chem. B* **2004,** *108,* 1207-1213.

26) Kolhe, N. B.; Devi, R. N.; Senanayak, S. P.; Jancy, B.; Narayan, K. S.; Asha, S. K. *J. Mater. Chem.* **2012**, *22*, 15235–15246.

27) Greef, T, F, A.; Ercolani, G.; Ligthart, G. B. W. L.; Meijer, E. W.; Sijbesma, R. P. *J. Am. Chem. Soc.* **2008**, *130*, 13755–13764.

28) Deepak, V. D.; Asha, S. K. *J. Phys. Chem. B* **2009**, *113,* 11887-11897.

29) Hadjichristidis, N.; Touloupis, C.; Fetters, L. *Macromolecules* **981**, *14*, 128–130.

30) Matsumoto, A.; Mizuta, K.; Otsu, K. J. *J. Polym. Sci. Part A: Polym. Chem.* **1993**, *31*, 2531–2539.

31) Winnik, F. M. *Chem. Rev.* **1993**, *93*, 587-614.

32) Eaton, D. F. *Pure & Appl. Chem.* **1988**, *60*, 1107-1114.

33) Chen, S.; Duhamel, J. *J. Phys. Chem. B* **2011**, *115*, 3289–3302.

34) Ingratta, M.; Mathew, M.; Duhamel, J. *Can. J. Chem.* **2010**, *88*, 217-227.

35) Ilharco, L. M.; Martinho, J. M. G. *Langmuir* **1999**, *15*, 7490–7494.

36) Lehrer, S. S. *Methods Enzymol* **1997**, *278*, 286–295.

37) Birks, J. B. *Photophysics of Aromatic Molecules*; Wiley/Interscience; New York, 1970.

38) Winnik, M. A.; Redpath, A. E. C.; Paton, K.; Danhelka, J. *Polymer* **1984**, *25*, 91–99.

39) Costa,T.; de Melo, J. S. S.; Castro, C. S.; Gago, S.; Pillinger, M.; Goncalves, I. S. *J. Phys. Chem. B* **2010**, *114,* 12439-12447.

40) Gago, S.; Costa, T.; de Melo, J. S.; Goncalves, I. S.; Pillinger, M. *J. Mater. Chem.* **2008**, *18*, 894–904.

41) Reynders, P.; Kuhnle, W.; Zachariasse, K. A. *J. Am. Chem. Soc.* **1990***, 112*, 3929-3939.

42) Koti, A. S. R.; Krishna, M. M. G.; Periasamy, N. *J. Phys. Chem. A* **2001**, *105,* 1767-1771.

43) Zilberstein, J.; Bromberg, A.; Berkovic, G. *Photochem. Photobiol. A* **1994**, 77, 69–81.

44) Zachariasse, K. A.; Duveneck, G.; Kuhnle, W. *Chem. Phys. Lett.* **1985**, *113*, 337–343.

45) Winnik, F. M.; Tamai, N.; Yonezawa, J.; Nishimura, Y.; Yamazaki, I. *J. Phys. Chem.* **1992**, *96*, 1967-1972.

Chapter 6:

Conclusions and Thesis Essence

Abstract

This chapter summarizes the results and the overall outcome based on the work reported in the thesis. The importance of photophysical studies in understanding the self assembly of the pyrene containing methacrylate polymers have been proved unequivocally. The hierarchical architectures such as homopolymers, random copolymers, block copolymers were studied for their self organization. Furthermore these studies were extended to the random copolymers by varying the incorporation of pyrene from 1 to 100%. The applicative aspects of these random copolymers were explored by dye encapsulation and release using rhodamine B as a model compound. These studies also helped in understanding the microstructure of these polymers. Finally a series of homopolymers with different structural design were explored to throw insight into the importance of non-covalent interactions such as H-bonding versus π-π interactions.

Thesis Essence and Overall Outcome

The thesis entitled "**Fluorescence as a Probe to Study Self-organization in Methacrylate Polymers and the Design of Novel Hierarchical Architectures**" explores the self-assembly in urethane methacrylate polymers by photophysical studies. The self-assembly of polymers in selective solvents to produce polymeric micelles and aggregates is a very interesting area of research. By controlling the composition and architecture of block copolymer segments these copolymers can self assemble into one, two or three-dimensional structures leading to different morphologies like spheres, vesicles etc.

The focus of this thesis lies in understanding the self organization of polymers by extensive photophysical investigations. Initially a series of hierarchical side chain urethane based methacrylate polymers with pyrene as pendant unit were embedded in different architectures. Pyrene was incorporated as pendant unit to side-chain urethane methacrylate polymers having a short ethyleneoxy or a long polyethyleneoxy spacer segment. The short-spacer pyrene urethane methacrylate was also incorporated either as block or random copolymer (1:9) along with polystyrene. The polymerization techniques adopted in this work are free radical and atom transfer radical polymerization (ATRP). The extent of excimer formation brought about by these polymers was thoroughly analyzed to find the self-assembling nature of these polymers. The excimer emission was observed to be different for different polymers with the random copolymer exhibiting the lowest efficiency due to less than 10% random labeling of pyrene. The styrene block in the block copolymer led to enhanced aggregation of the pyrene as evidenced by higher excimer efficiency in the block copolymer compared to short chain homopolymer. The higher excimer efficiency in long chain homopolymer compared to short chain homopolymer showed that the oligoethyleneoxy segment in long chain homopolymer afforded better segregation of pyrene compared to short chain homopolymer.

Among the various architectures studied initially, the random copolymers with varying amount of pyrene were explored for detailed investigation of the self organization. The second unit in the random system was carefully selected so that the self-assembly did not get disrupted and hence 3-pentadecyl phenol (PDP) was chosen as the other suitable comonomer and a series of random copolyurethane methacrylate comb polymers with pyrene (Py) and 3-pentadecyl phenol (PDP) as pendant units were

prepared by free radical polymerization. It was observed that all the polymers had a tendency to form spheres in DMF irrespective of the varying pyrene incorporation. The self-assembly in these polymers at very low concentrations have been explored by photophysical techniques. The nature of emitting species of the random copolymers has been extensively explored by the time- resolved emission spectra (TRES) studies conducted at room temperature as well as higher temperature. The existence of ground state aggregated pyrenes in all polymers was unequivocally proven by the fluorescence lifetime decay as well as TRES experiments. TRES experiments showed that the short-lived ground state aggregated species emitting in the 435 nm region dominated the earlier time-gated spectra which then gave way to emission ~465 and 485 nm corresponding to excited pyrene in constrained and perfect orientation respectively.

The applicative aspects of these random copolymers have been explored by making use of their nice self-organizing behavior by rhodamine encapsulation and release studies. A new approach to bridge the gap between solid and solution phase morphology was presented. This issue was clearly addressed by a simple approach to polymer hollow capsule fabrication involving free radical polymerization of urethane methacrylate monomers. One of the best ways to probe the microstructure of a polymer microcapsule is to encapsulate suitable probe molecules inside the cavity. The water soluble fluorescent dye rhodamine B (RhB) was chosen for encapsulation studies and the structural changes happening to the comb polymer as a function of temperature was probed by changes in FRET induced RhB emission. The variable temperature emission studies showed that the dye was released from the microcapsules upon heating beyond 50 ^{o}C and the polymers underwent irreversible microstructural reorganization. These studies helped in understanding the microstructural variations in the random copolymers.

Finally, a fundamentally challenging task was addressed using photophysical investigations. The fundamental studies of an important set of homopolymers which were different from each other by small structural variations were explored by photophysical studies. The importance of the non-covalent interactions such as hydrogen bonding interactions provided by the urethane linkage in directing the self assembly of pendant pyrenes were compared to analogous 100 % pyrene polymers lacking the hydrogen bonding interaction. A series of side chain methacrylate polymers having pendant pyrene units in every repeat unit, but differing from one another in

terms of presence or absence of hydrogen bondable units in the form of urethane linkages, or the length as well as nature (linear vs kink) of the spacer segment linking the pendant pyrene units from the methacrylate backbone was developed and studied. Hydrogen bonding is a very directional interaction which can introduce constraints on the self-assembled architecture. The photophysical properties were analyzed as regards to the nature of excimer emission –static vs dynamic excimer, to obtain information regarding the chain organization in each of the polymers. The variable temperature (heating & cooling) emission studies significantly showed the difference in the chain interactions of H-bonded vs non-H-bonded polymers. The fluorescence emission recovered completely for non-H-bonded polymer on cooling while the complete recovery of fluorescence could not be attained by H-bondable polymers due to the constraining hold brought about by the H-bonding.

Thus, the self-organization in urethane methacylate polymers were explored in 100% pyrene loaded homopolymers, random copolymers or block copolymers. Understanding the dynamics of polymer chains and the quantitative analysis in 100% pyrene loaded polymers still remains a very challenging task and it could be addressed with proper analysis of photophysical studies using advanced techniques. Another significant challenge that needs attention is the self-assembly in various complex architectures such as star shaped polymers, dendrimers etc., which could be addressed by synthesizing urethane methacrylate star shaped polymers by controlled polymerization techniques such as atom transfer radical polymerization (ATRP). The extensive organizational behavior could be explored by fluorescence. Using this concept along with the broad understanding of structure-property relationship in urethane methacrylate system, the pyrene moieties could be replaced by bulky biocompatible units such a cyclodextrins, disaccharide sugars and it could be used for drug delivery applications.

LIST OF PUBLICATIONS

1. Kaushlendra, K.; Deepak, V. D.; Asha, S. K. Correlation of Architecture with Excimer Emission in 100% Pyrene-Labeled Self-Assembled Polymers. *J. Polym. Sci. Part A: Polym. Chem.* **2011**, *49*, 1678-1690.

2. Kaushlendra, K.; Asha, S. K. Microstructural Reorganization and Cargo Release in Pyrene Urethane Methacrylate Random Copolymer Hollow Capsules. *Langmuir* **2012**, *28*, 12731-12743.

3. Kaushlendra, K.; Asha, S. K. Variable Temperature Time-Resolved Emission Spectra (TRES) studies of Random Pyrene Urethane Methacrylate Copolymers with high Pyrene Incorporation. *Journal of Physical Chemistry B*, **2013,** *117*, 11863-11876.

4. Kaushlendra, K.; Asha, S. K.; Duhamel, J. Probing the Tubular Volume Defined by the Side-Chains of Polymethacrylates in Solution by Using Pyrene Excimer Formation. (Manuscript submitted for publication).

5. Kaushlendra, K.; Asha, S. K. Fundamental insights into the 100 % dimer emission from a novel pyrene based methacrylate comb polymers: TRES and temperature dependent fluorescence. (Manuscript submitted for publication)

6. Kaushlendra, K.; Bhaumik, S.; Janardanan, J.; S. K. Asha. Fluorescent Tagging of Silk Fibroin by Grafting Approach and it's conformational studies. (Manuscript under preparation).

Patent

1. Kaushlendra, K.; Asha, S. K. Fluorescent grafting and chemical modification of silk for optoelectronic application. (Ref. No.0095NF2012 : 1502DEL201.

Papers Presented in Conferences

1. Kaushlendra Kumar, Deepak Vishnu D. and S. K. Asha "Probing the Self-organization in Pyrene-labeled Homo and Block Copolymers", **National Science Day**, CSIR-NCL, Pune, **2010.**

2. Kaushlendra Kumar and S. K. Asha "Photophysical Studies to Probe Self-Assembly in Structurally Modified Polymeric Architecture," **MACRO 2010 - International Conference on Frontiers of Polymers and Advanced Materials,** Indian Institute of Technology, New Delhi, **2010**.

3. Kaushlendra Kumar and S. K. Asha "Photophysical and Morphological Investigation into the Self-Organization Behaviour of Urethane Methacrylate Random Copolymers", **PSNDS-11, National Conference on Advances in Polymer Science and Nanotechnology: Design and Structure,** Vadodara, **2011**.

4. Kaushlendra Kumar and S. K. Asha "Microstructural Organization Studies by Dye Encapsulation and FRET in Urethane Methacrylate Random Copolymers", **National Science Day**, CSIR-NCL, Pune, **2013**.

5. **Kaushlendra Kumar**, S. K. Asha "Fundamental Insights into Dimer Emission from 100 % Pyrene loaded Methacrylate Comb Polymers: TRES and Temperature dependent Fluorescence." 3rd FAPS Conference and MACRO 2013 (**FAPS-MACRO, 2013)- International Conference on Polymers,** Indian Institute of Science, Bangalore, **2013**.